Homogeneous palladium-catalyzed defunctionalizations of oxygen-containing feedstocks

Dissertation

der Mathematisch-Naturwissenschaftlichen Fakultät

der Eberhard Karls Universität Tübingen

zur Erlangung des Grades eines

Doktors der Naturwissenschaften

(Dr. rer. nat.)

vorgelegt von

Benjamin Ciszek

aus Ingolstadt

Tübingen

2019

Gedruckt mit Genehmigung der Mathematisch-Naturwissenschaftlichen Fakultät der Eberhard Karls Universität Tübingen.

Tag der mündlichen Qualifikation:	24.05.2019
Dekan:	Prof. Dr. Wolfgang Rosenstiel
1. Berichterstatter:	Jun.-Prof. Dr. Ivana Fleischer
2. Berichterstatter:	Prof. Dr. Doris Kunz

The experimental work discussed in this thesis was performed from December 2015 to July 2017 at the University of Regensburg, as from August 2017 to January 2019 at the University of Tübingen under supervision of Prof. Dr. Ivana Fleischer.

Table of contents

1 Introduction

The work discussed in this thesis covers three central topics: the catalytic deoxygenation of alcohols, the characterization of the applied transition metal catalyst to determine the active catalytic species and the transfer of the system to the defunctionalization of lignin model compounds. This chapter gives an introduction to all three parts, summing up the state of the art for these fields of chemistry.

1.1 Deoxygenation in organic synthesis

The reduction of C–O bonds to C–H bonds is one of the fundamental transformations in organic chemistry, e.g. in the deoxygenation of oxygen-containing feedstocks.[1] Herein, the most well-known textbook methods for the deoxygenation of ketones or aldehydes are the Clemmensen reduction, which proceeds on a metallic zinc surface,[2] or the Wolff-Kishner reduction, which makes use of the condensation of carbonyls to hydrazones and a subsequent decomposition to the corresponding alkane.[3] In the case of alcohols, the most popular protocol is the Barton-McCombie-deoxygenation, which constitutes in a radical substitution of the corresponding thionoester.[4] However, these methods suffer from disadvantages like harsh reaction conditions, i.e. high reaction temperatures or strongly acidic or basic reaction media. Also, overstoichiometric amounts of toxic or hazardous reactants, e.g. amalgamated zinc, hydrazines or organic hydrostannanes, need to be used. Additionally, derivatization of the substrates is necessary in some cases (Scheme 1.1). These conditions not only make the transformations hard to handle, but also lead to a decreased reaction selectivity and high amounts of waste products which results in a poor atom-economy of the overall processes.

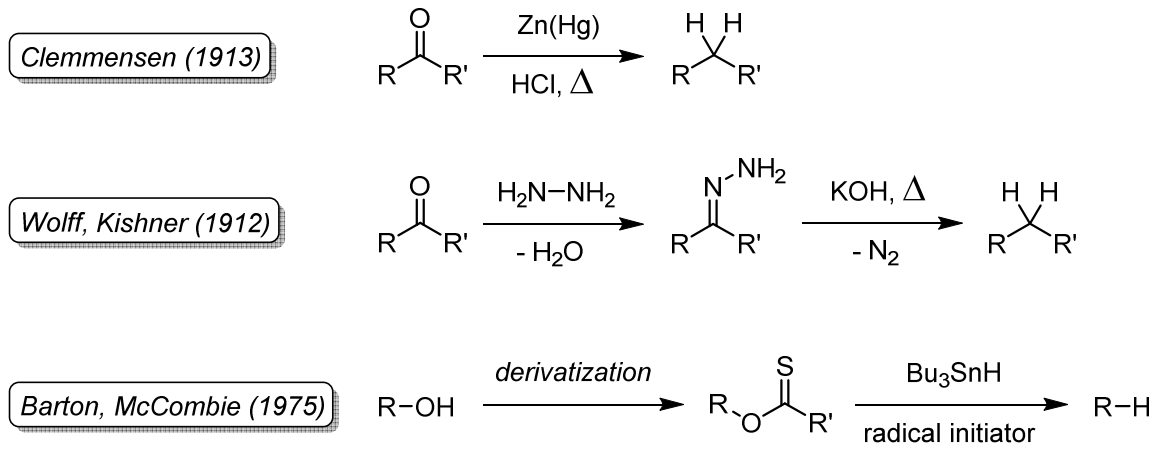

Scheme 1.1 General conditions for traditional deoxygenation methods.

From today's point of view, the mentioned deoxygenation protocols do not meet the standards of modern green chemistry as they were defined at the end of the 20th century. These include the prevention of derivatization steps to reduce waste products, the design of highly atom economic transformations which bear less danger to human health and the environment as well as the application of catalysts for increased reaction selectivity and decreased energy demand.[5-7]

1.2 Catalytic approaches for C–O bond cleavage

In order to take up the challenge for "greener" deoxygenation methods, an exceptionally broad field of research has been explored in the last decades from which a vast number of methodologies arose. This led to a great number of procedures converting a variety of oxygenated substrates like alcohols,[8-12] phenols,[13-15] carbonyl compounds,[16-21] or ethers[14,15,22,23] into the respective deoxygenated, reduced products. The still growing manifold of described protocols accounts for the importance and the need of organic chemists for these kinds of transformations, both in synthetic laboratories and in industrial setups. As mentioned before, these newly developed processes aim to meet the requirements of green chemistry methodologies, especially with respect to the avoidance of harmful waste and the application of more efficient catalytic systems.

For the latter, late transition metals were found as suitable catalysts, both in homogeneous as in heterogeneous fashion (Scheme 1.2). As a general concept, these catalytic methods share the hydrogenolysis approach as common reducing step, i.e. the cleavage of the C–O bond is accomplished *via* the actual or formal addition of a molecule of H_2. This represents a highly atom efficient mode of reduction that proceeds in less synthetic steps and produces less waste than the discussed traditional deoxygenation methods.

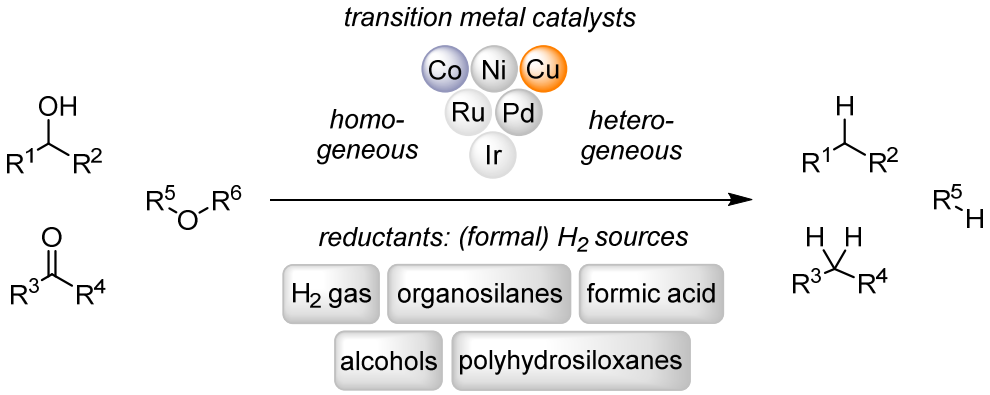

Scheme 1.2 Selected transition metal catalysts and reductants for the hydrogenolysis of C–O bonds.

The concept of hydrogenolysis originates from a report on the transition metal-catalyzed scission of C–O bonds first being published by Padoa and Ponti in 1908.[24] In their approach

a heterogeneous nickel catalyst and hydrogen gas as reductant were used to deoxygenate furfural through furfuryl alcohol as intermediate to produce 2-methylfurane and further reduction products. Later on, Connor and Adkins conducted a more comprehensive study on a broader range of substrates to demonstrate the effect of a heterogeneous copper-chromium oxide catalyst in the hydrogenolysis of C–O and C–C bonds also using hydrogen gas.[25] Since these seminal works were reported at the beginning of the 20th century, many variations concerning the catalyst, the reaction conditions, additives and the reducing agents were shown to be successful in the hydrogenolysis of C–O bonds. Compounds with alcohol or carbonyl functionalities in benzylic position play a special role in the scope of possible substrates for hydrogenolysis. Due to their higher reactivity towards reductive C–O bond cleavage, benzyl ethers are traditionally introduced as protecting groups in organic synthesis as they can be removed again under mild conditions.[26] Furthermore, benzylic alcohols are a common structural motif in organic feedstock originating from biomass. This attractive feature brings these substrates back into today's focus of research.[27-30] As the practical work described in this thesis will concern the transformation of benzylic alcohols as substrates, a brief introduction will be given showing selected examples from previous works of the last decade in the field of hydrogenolysis of benzylic alcohols and carbonyl compounds. Therein an overview of the applied transition metal catalysts is given with a special focus put on the used reducing agents. Additionally the modes of substrate and reductant activation are discussed.

Nishikawa *et al.*[31] showed that co-precipitation of Au(III) and Ni(II) precursors followed by calcination and reduction under hydrogen atmosphere generates a gold/nickel alloy, which exhibits catalytic activity in the hydrogenolysis of benzylic alcohols **1** to the respective hydrocarbons **2** under the use of hydrogen gas as reductant (Scheme 1.3). Through hydrogen temperature programmed reduction (H_2-TPR) and X-ray absorption near edge structure (XANES) analysis they found that the mixing of the two metal precursors led to a facilitated reduction to the alloy at lower temperatures. This presumably is enabled through hydrogen dissociation mediated by generated Au(0) particles towards the non-reduced nickel atoms. The obtained catalyst material was further characterized *via* X-ray diffraction (XRD), X-ray absorption fine structure (XAFS) measurements as well as *via* transmission electron microscopy (TEM) and X-ray photoelectron spectroscopy (XPS).

The hydrogenolysis of 1-phenylethanol (**3**) over the Au/Ni catalyst was optimized with respect to reaction time and solvent. The alloy was found to outperform heterogeneous benchmark catalysts for hydrogenolysis as Pd/C and Raney Ni concerning product yield and selectivity. Catalyst isolation from the reaction mixture can be achieved in an easy manner as the material did stick to the stirring bar due to its magnetic properties.

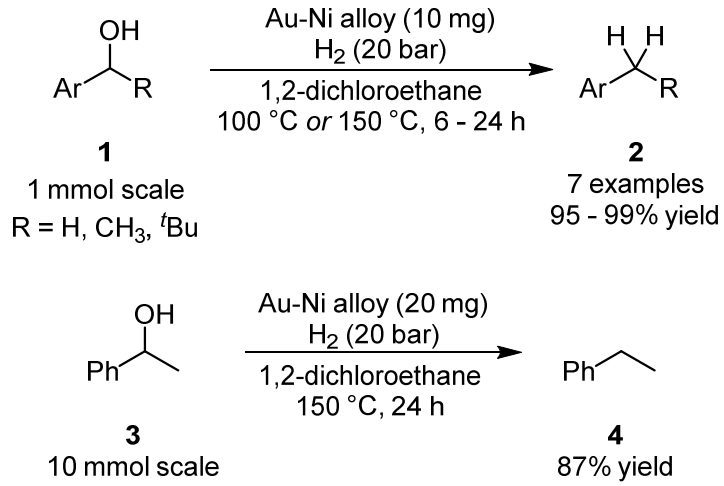

Scheme 1.3 **Hydrogenolysis of benzylic alcohols over a heterogeneous Au/Ni catalysts reported by Nishikawa *et al.*[31]**

The Au/Ni alloy could be reused without further hydrogen activation in three consecutive runs although a slight decrease in activity was observed, possibly caused by passivation of the nickel surface. Exclusion experiments showed that none of the metal components alone is the active catalyst and that hydrogen gas is needed for the reduction. Based on their results, the authors propose a reaction pathway leading through the formation of a benzylic carbocation followed by reduction. Furthermore, benzylic alcohols bearing different substituents either on the aromatic ring or in homobenzylic position were subjected to the transformation. Electronically activated as deactivated substrates were successfully deoxygenated, although for the latter higher reaction temperatures and prolonged reaction times were necessary. Also a sterically hindered substrate and benzyl alcohol were transformed into the respective alkylarenes in excellent yields. In addition, the reaction was shown to be scalable to a 10 mmol batch using a lower relative amount of Au/Ni alloy. Notwithstanding, the desired product was still obtained in a very good yield.

The aforementioned catalyst shows high activity in the heterogeneous hydrogenolysis of benzylic alcohols. Nonetheless, the preparation of the catalyst involves several steps which make special equipment necessary, e.g. for calcination and metal oxide reduction. Moreover, the characterization and the determination of the composition of the catalyst is only achieved under the use of specialized machinery. Despite the high yields obtained in the conversion of several alcohols, the substrate scope is narrow and no thorough mechanistic studies were performed.

In contrast to the method discussed above, Kalutharage *et al.*[18] investigated homogeneously catalyzed hydrogenolysis reactions using hydrogen gas. They found that a well defined cationic ruthenium complex **7**, upon addition of a phenol derived ligand, showed catalytic activity for the direct deoxygenation of benzylic ketones **5** through a benzylic alcohol

intermediate (Scheme 1.4). They could also show that 2-propanol can be applied as a hydride source for the reduction, further expanding the substrate scope of the transformation to aliphatic and aromatic ketones and aldehydes. Furthermore, the group conducted mechanistic and kinetic investigations by varying the electronic properties of the added phenol type ligand. They carried out rate measurements using eight different *para*-substituted phenols as ligands for the catalytically active ruthenium complex. This led to a Hammett plot of the relative reaction rate *versus* the respective substituent constant which exhibits a minimum. The reversal in the sign of the Hammett slope indicates a change in reaction mechanism. Subsequent investigations by the group allowed to correlate the substituent constants and the found isotope effects obtained from experiments using H_2 or D_2 gas, respectively.

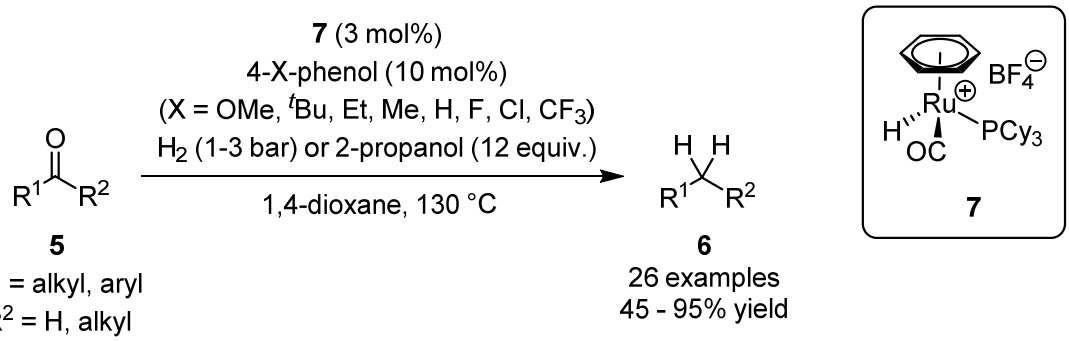

Scheme 1.4 **General reaction conditions for the ruthenium-catalyzed hydrogenolysis of carbonyl compounds developed by Kalutharage *et al*.**[18]

After further isotope labelling studies and investigations of the reaction rate dependence on several reaction parameters as well as kinetic isotope effects concerning hydrogen and carbon atoms participating in the reaction, they proposed two mechanistic pathways sharing the first step of ketone substrate reduction by the ruthenium hydride catalyst **8** (Scheme 1.5). Thereafter, two different modes of hydrogen activation on the catalyst species **9** are thought to occur, depending on the electronic properties of the complex. An electron-releasing phenol ligand like 4-methoxyphenol in species **12** enhances the nucleophilicity of the ruthenium center, which in return facilitates a concerted hydrogen activation and deoxygenation of the coordinated alcohol substrate. On the other hand, this electron-rich ruthenium complex is also prone to competitive inhibition by H_2 when exposed to high pressures. In case of an electron-poor phenol ligand like the investigated 4-trifluoromethylphenol in complex **10**, the metal center would gain rather electrophilic properties, which leads to a stepwise activation of H_2. Subsequently, the binding of the reaction substrate is also favored over the hydrogen molecule, preventing catalyst inhibition as it occurs on the electron-rich ruthenium complex.

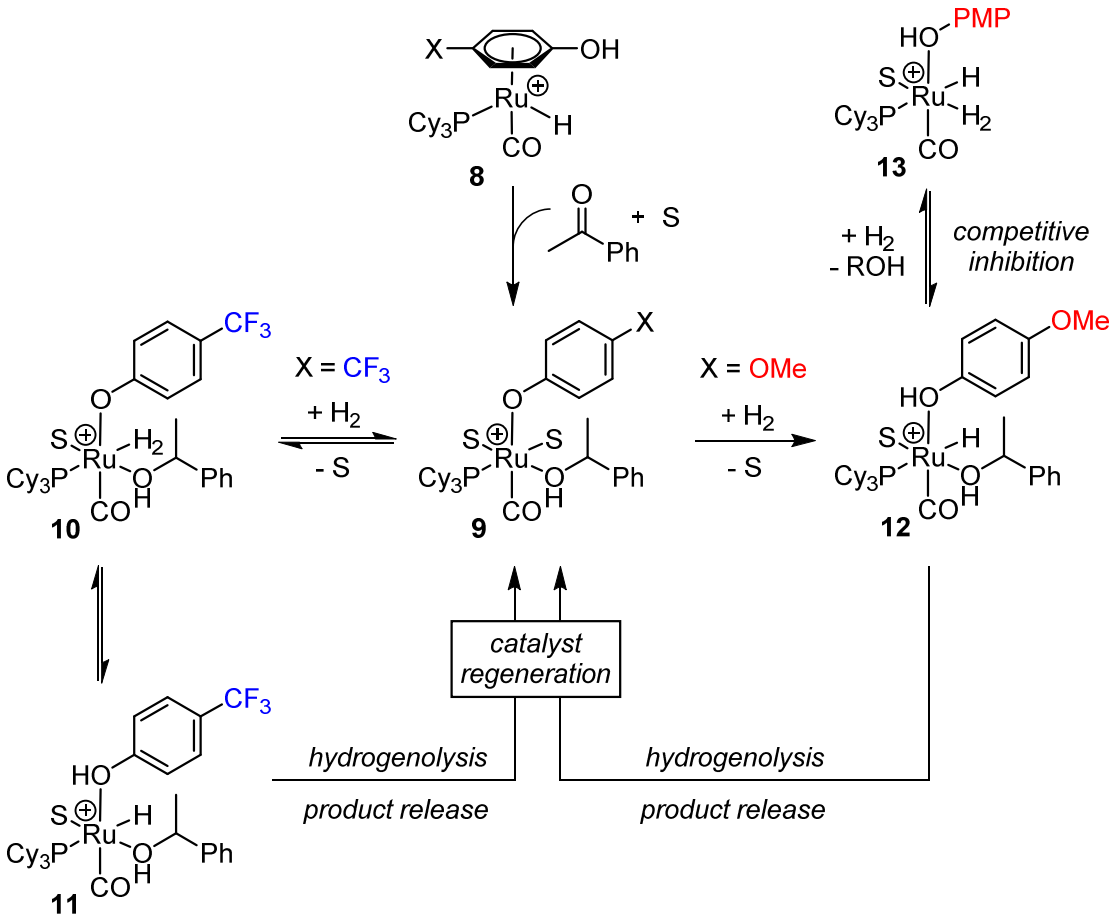

Scheme 1.5 **Proposed mechanistic pathways for the ruthenium-catalyzed hydrogenolysis of acetophenone developed by Kalutharage *et al.* (S: solvent or water, PMP: *para*-methoxyphenyl. Adapted from the original publication).[18]**

The authors presented a tunable homogeneous transition metal catalyst for the hydrogenolysis of carbonyl compounds to the corresponding alkanes. They argue that hydrogen gas is available at low cost and that the only by-product formed is non-problematic water; additionally it can be produced from sustainable sources. Nonetheless, the use of pressurized hydrogen is challenging, as it constitutes a highly flammable and explosive gas and makes further precautions necessary. Furthermore, special pressure equipment is needed for this kind of chemistry. To avoid the disadvantages that arise from pressurized gases as reactants, alternative hydride sources were investigated for their use in deoxygenation processes. These can be compiled under the term of transfer hydrogenolysis, which indicates that no gaseous hydrogen is present in the reaction or just evolves *in situ*. The exemplary works showed in the following should give an insight in possible alternative hydride sources in transfer hydrogenolysis reactions of benzylic substrates.

One of the most popular alternative hydride sources for reduction is 2-propanol, which is already well-known for its application in transfer hydrogenation reactions, e.g. for the reduction of carbonyl compounds with soluble ruthenium and iridium complexes as predominant catalysts.[32-38] The group of Mebane[12] showed that heterogeneous Raney

nickel and cobalt can be applied for the transfer hydrogenolysis of aromatic alcohols using 2-propanol as reductant (Scheme 1.6). A variety of alcohols **14** bearing aromatic structures could be transformed into the corresponding alkylarene products **15** with both catalysts, although Raney cobalt showed lower activity for the transfer hydrogenolysis. The high catalytic activity of Raney nickel in the reaction led to very short reaction times from several minutes to a few hours. After too long reaction periods side reactions like the overreduction of aromatic structures or dehydromethylation of primary alcohols occurred. These selectivity issues could be avoided for benzylic alcohols when Raney cobalt was applied, although prolonged reaction times were necessary to obtain comparable product yields.

Additionally to the convenient reaction setup, in which substrate and catalyst were just refluxed on air in 2-propanol, reaction workup and product isolation was performed more easily. To regain the catalyst particles, filtration over filter aid is sufficient. It was shown that the recovered catalyst can be reused for at least seven further runs. Evaporation of the solvent in the filtrate yielded the pure products. Notwithstanding, the authors conducted no mechanistic investigations, they remark that only substrates containing an aromatic structure are converted, with different chain lengths between arene and alcohol group being tolerated. They speculate that a delocalized π-system is needed for successful adsorption of the substrate to the metal surface of the catalyst. The finding that substrates containing sterically hindered or no aromatic systems perform worse or are not converted at all in the transformation supports this assumption.

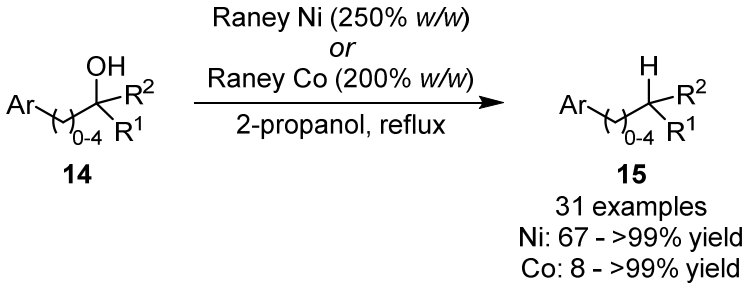

Scheme 1.6 Transfer hydrogenolysis of aromatic alcohols using Raney nickel or cobalt catalysts and 2-propanol as reductant reported by Mebane and co-workers.[12]

Despite the simple and effective protocol, the method developed by Mebane and co-workers suffers from some drawbacks due to the highly pyrophoric nature of Raney metals.[12] For that reason, the catalysts need to be kept wet or stored in a glovebox under inert conditions and handled with care. Furthermore, the high loading of 250 or 200 percent in mass of metal relative to the alcohol substrate, respectively, has to be mentioned, which is a common disadvantage of heterogeneous catalysts. As mentioned before, no mechanistic studies were performed on the Raney metal catalyst systems. The heterogeneous nature of the catalyst impedes variations on the catalytic system. This makes it difficult to achieve a deeper understanding of the underlying reaction mechanism. Another disadvantage of the

Raney transfer hydrogenation catalysts is the observed low selectivity or activity for certain substrate structures, sometimes leading to unwanted overreduction or unsatisfactory conversion in the catalytic reaction, both diminishing the product yield.

A more typical catalyst for the transfer hydrogenolysis of benzylic alcohols and carbonyl compounds is heterogeneous palladium on solid support. This catalyst was shown to be active for this transformation with several alternative hydride sources of which some will be discussed in the following.

Bäckvall, Adolfsson and co-workers[17] introduced a method for the transfer hydrogenolysis of benzylic ketones and aldehydes **16** using palladium on activated charcoal as catalyst, together with polymethylhydrosiloxane (PMHS) as reducing agent (Scheme 1.7). The choice of reductant was justified by PMHS being an inexpensive, readily available reagent, which is obtained as waste product from the silicon industry. Furthermore, it shows high air and moisture stability and thereby is a convenient alternative to conventionally used organosilanes, some of which PMHS did outperform under the given reaction conditions. Investigations concerning the course of the reaction showed that the corresponding benzylic alcohols are formed as intermediary species; follow-up deoxygenation leads to the saturated hydrogenolysis products.

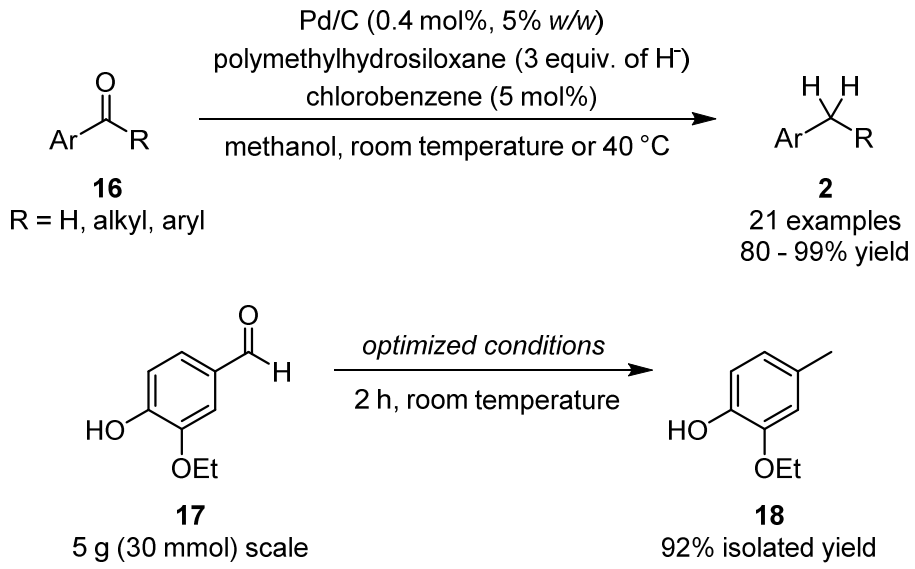

Scheme 1.7 **Transfer hydrogenolysis of aryl ketones over a heterogeneous Pd/C catalyst applying polymethylhydrosiloxane (PHMS) as reducing agent. Optimized reaction conditions and upscaled transformation of ethyl vanillin (13).[17]**

To facilitate the reaction, acidic additives were tested. Chlorobenzene, which releases hydrogen chloride *in situ* through palladium-mediated reduction, was found optimal for this transformation. The found optimized conditions allowed for the conversion of a broad scope of substrates applying low loadings in catalyst, additive and reductant. Only minor changes in the reaction conditions were needed for more sterically challenging substrates. The reaction

was shown to be scalable up to a 30 mmol batch for ethyl vanillin (**17**) as substrate, still yielding the desired product **18** in excellent amount (Scheme 1.7). Studies on catalyst recyclability showed no loss of activity for seven runs, even though agglomeration of the catalyst particles was observed *via* transmission electron microscopy. After comparing the reaction efficiency with PMHS or hydrogen gas as reductants under otherwise unchanged conditions it was stated that after identical reaction times the hydrosilylation protocol performed superior. However, the reaction conditions for the reduction with hydrogen gas were not further specified. Attempts to elucidate the catalytically active species and thereby the mode of activation of the reductant using spectroscopic methods remained without success.

Compared to similar works based on homogeneous palladium catalysts and polymethylhydrosiloxane as reductant,[9,39] the methodology developed by the groups of Bäckvall and Adolfsson applies significantly lower loadings of catalyst with similar amounts of siloxane and chlorobenzene as additive. Although the three mentioned transformations run smoothly under very mild reaction conditions and use an industrial waste product as reagent, which would be in accordance with some of the principles of green chemistry,[5] the formation of oxidized polymethylhydrosiloxane as polymeric waste is to be expected, making separation and purification of the product necessary. Depending on the available methods of product purification, this process could be cost- and resource-intensive.

To avoid the formation of unwanted waste products or to simplify the purification of the products, formic acid was found a valuable alternative hydride source in palladium-catalyzed transfer hydrogenation reactions.[40,41] Formic acid as an inexpensive, readily available chemical is easy to handle, air and moisture stable and can be transported and stored easily.[42] Upon use as reductant in the transfer hydrogenolysis of benzylic alcohols, formic acid shows excellent chemoselectivity, as no overreduction of unsaturated systems occurs.[40,41] Only CO_2 and water are obtained as by-products, both can be easily removed from the reaction mixture. Carbon dioxide can be recycled in a reduction step using hydrogen, regenerating formic acid and thereby making the whole process very atom-efficient and potentially sustainable.[43-46] For these advantages, Samec and co-workers[8] chose formic acid as reducing agent in the transfer hydrogenolysis of benzylic alcohols catalyzed by heterogeneous palladium on activated charcoal (Scheme 1.8). Initial optimization studies showed that the use of formate salts as base additive plays a crucial role for a fast transformation. Without base only the disproportionation of the substrate was detected, while too high concentrations of base additive led to a breakdown of the desired reactivity. The reason for this will be discussed below in this section. Applying only formates as reductant without formic acid led to no reactivity at all, only starting material was recovered. Optimization of the reaction conditions showed that water is needed in the

reaction as a co-solvent in mixture with methanol, presumably for reasons of solubility of the applied formate salts. Under the optimized reaction conditions, a range of benzylic alcohols **19** could be converted into the respective hydrocarbons **20**.

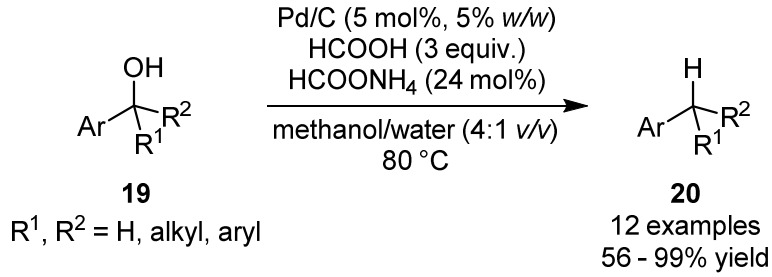

Scheme 1.8 **Formic acid as reducing agent in the transfer hydrogenolysis of benzylic alcohols catalyzed by Pd/C as reported by Samec and co-workers (several other formate salts were tested with no significant difference in the reaction outcome).[8]**

In previous studies investigating the catalytic transfer hydrogenolysis of benzylic alcohols with formic acid, several possible intermediates were observed or proposed (Scheme 1.9). Esterification between the alcohol and the acid can activate the substrate by improving the leaving group character of the hydroxyl group.[47,48] A similar effect can be obtained by the formation of a symmetrical ether from the alcohol that can be converted in the hydrogenolysis reaction.[49,50] Other groups found that the formate ester can decompose to form the desired deoxygenated product or undergo elimination to form an alkene or a carbenium ion, respectively, which are then reduced.[47,51,52] As mentioned before, disproportionation is also a possible reaction pathway, leading to a yield of 50% of the desired product in a short period of time, along with the residual starting material being used as hydrogen source for the reduction.[40] The group of Samec observed that the initially oxidized substrate is converted to the product by the catalyst in a much slower two-step reaction sequence.

To elucidate the reaction mechanism and to exclude or confirm possible intermediates, a series of mechanistic investigations was conducted. The addition of triphenylphosphine (1.0 or 10 equivalents relative to palladium) to a great extent or completely shut down the reaction. In contrast to this finding, polymer-bound PPh_3 had no effect on the outcome of the reaction compared to a non-affected standard run. This was interpreted as proof for an active heterogeneous catalyst.[53] Next, initial rates for the disappearance of possible intermediates under transfer hydrogenolysis conditions were determined. In contrast to the optimized reaction conditions, these measurements were performed at room temperature. Comparison with the initial rate for the model substrate 1-phenylethanol showed that some intermediates would either be converted too fast to be detected in kinetic studies, or others were consumed too slowly, which would lead to their accumulation in the reaction mixture. As the latter was not observed in the reaction, intermediates generated *via* esterification or ether formation

were excluded while the disproportionation and elimination pathways were investigated further.

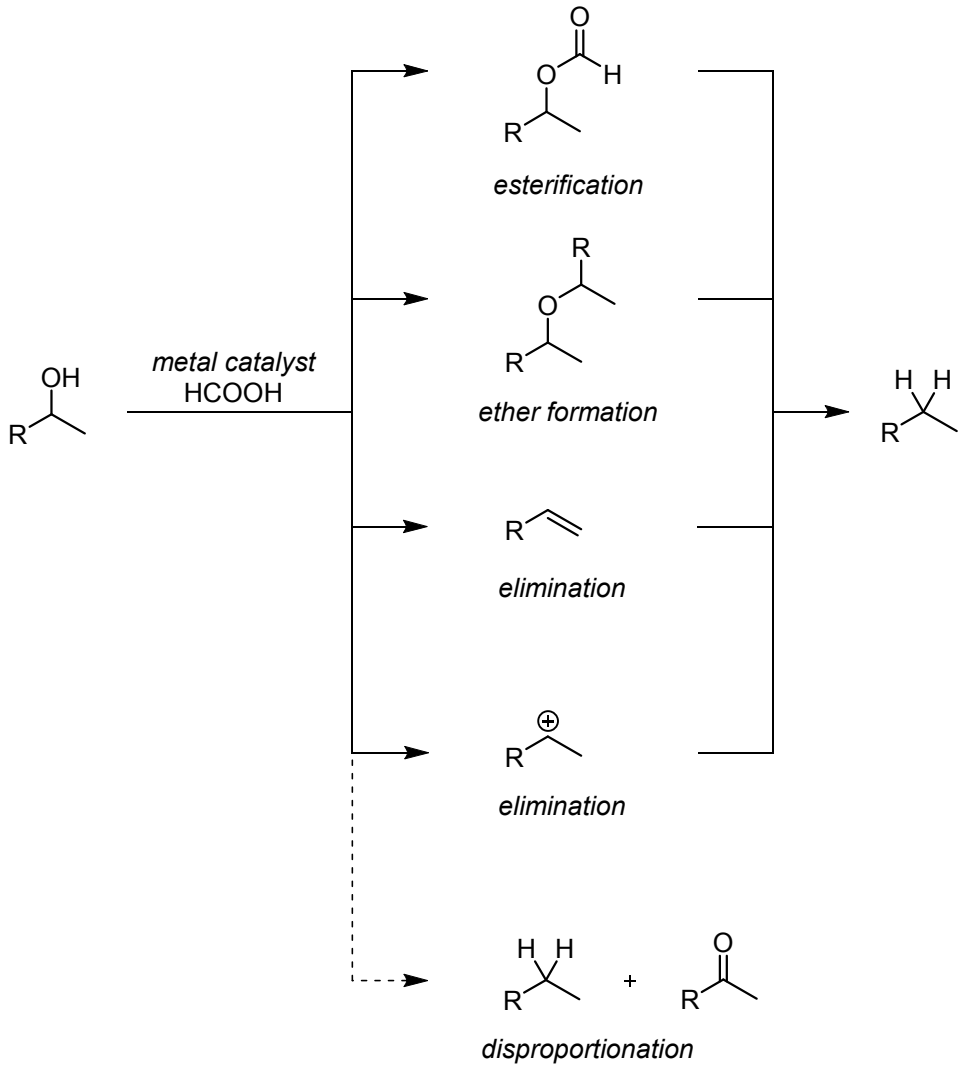

Scheme 1.9 Possible intermediates of the transfer hydrogenolysis of benzylic alcohols using formic acid as reductant (adapted from the original publication).[8]

Elimination on the substrate to form styrene derivatives was not consistent with the findings from the substrate screening, in which substrates not able to undergo that pathway, e.g. primary alcohols or secondary substrates not containing β-hydrogen atoms, were successfully transformed. For a possible formation of an intermediate carbenium ion it was stated by the authors that the methanol being present in great excess would trap the cation to form an unsymmetrical ether. As this trapping product was not observed and its rate of disappearance was lower than for the original substrate, this pathway was also excluded.

Kinetic measurements showed that the reaction is zero order in substrate, but a first order dependence of the initial reaction rate on palladium catalyst and formic acid concentration was found. For the base additive, a range in concentration without effect on the initial rate was determined, while too low or too high concentrations of formate salt inhibited the transfer hydrogenolysis. From these findings and experiments concerning

kinetic isotope effects, a reaction pathway consisting of disproportionation and subsequent reduction of the oxidized substrate was excluded and another mode of catalyst activation and substrate hydrogenolysis was proposed (Scheme 1.10): Adsorption of formate anions partially blocks the active sites of the palladium catalyst, thereby the disproportionation of the substrate is inhibited. The formed formato-palladium intermediate A can enter a protolysis equilibrium with formic acid (B) to generate palladium with chemisorbed dihydrogen (C) while releasing CO_2. From this stage direct reduction of the substrate through concerted hydride and proton transfer occurs, regenerating the catalyst and releasing the hydrogenolysis product.

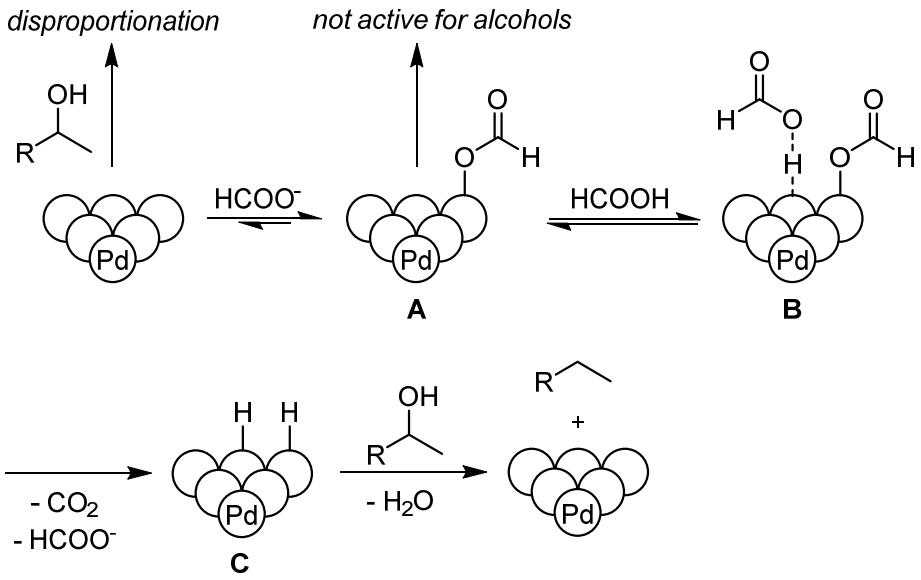

Scheme 1.10 Proposed reaction mechanism for the heterogeneously palladium-catalyzed transfer hydrogenolysis developed by Samec and co-workers (adapted from the original publication).[8]

The method presented by Samec and co-workers allows for the transfer hydrogenolysis of primary, secondary and tertiary benzylic alcohols using formic acid as reducing agent. The heterogeneous character of the catalyst and the formation of only carbon dioxide and water as by-products facilitates an easy product isolation. In addition to the substrate scope given, thorough studies concerning catalyst and substrate activation, including a proposed mechanism for the hydride transfer based on experimental data, are described.

Another methodology for the deoxygenation of benzylic alcohols that makes use of formic acid as hydride source was described by Yang *et al.*[54] The group demonstrated that very low loadings of the preformed iridium complex **23** catalyze the transformation of substituted (4-dialkylaminophenyl)methanols **21** to the respective hydrocarbons **22** under relatively mild conditions (Scheme 1.11). The introduction of the aminoaryl moiety as a directing group was found necessary to establish a high chemoselectivity in the reaction. The applicability of this transformation was presented in a very broad substrate scope containing

primary, secondary and tertiary benzylic alcohols as well as derivatives of natural compounds or drug precursors in very good to excellent yields. For some substrates a change of the solvent from water to a mixture of water and trifluoroethanol or hexafluoroisopropanol was necessary. Furthermore, the reaction could be performed on one gram scale. Remarkably, extremely high substrate to catalyst ratios could be successfully applied in this transformation. Values up to 1,000,000 were observed to still mediate the reaction.

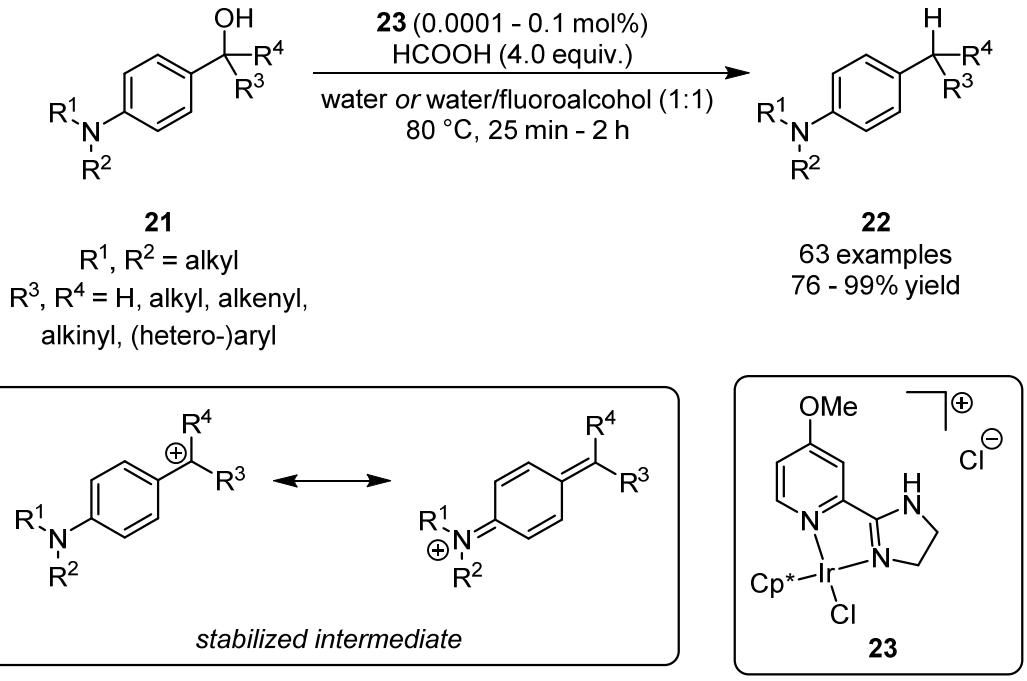

Scheme 1.11 Deoxygenation of amino-substituted phenylmethanol derivatives reported by Yang *et al.*[54]

Mechanistic studies propose an activation of the precatalyst through decomposition of an *in situ* formed iridium formato complex to give a homogeneous iridium hydride catalyst. The alcohol substrates are thought to react through an S_N1 pathway under the acidic reaction conditions. The resulting benzylic carbocation is stabilized by the electron donating effect of the tertiary amino group. Nonetheless, these intermediates possess a high reactivity towards the iridium hydride complex, resulting in the reduction of the substrate. Investigations involving deuterium labelling and the determination of kinetic isotope effects identified the formyl hydrogen of formic acid as source of the introduced hydride, with the rate determining step consisting in the formation of the active catalyst. Conclusively, the authors could show that after successful deoxygenation the introduced directing group can be modified to open the synthetic route to valuable products *via* cross-coupling reactions.

Despite the substantially low catalyst loading and the high number of successfully transformed compounds, it has to be mentioned that the reaction is limited to substrates which feature a (dialkylamino)phenyl group. To obtain structurally different products, the

applied directing group either has to be removed or transformed into another desirable moiety. This involves further synthetic steps.

It could be shown in this section that for the hydrogenolysis of alcohols and carbonyl compounds, especially in benzylic position, a wide range of methods exists. While late transition metal catalysts like palladium or ruthenium dominate the field, a variety of reducing agents, e.g. hydrogen gas, silanes, alcohols or formic acid, was successfully applied for this kind of transformation. Nonetheless, some efforts should still be put in this research area, especially concerning the formation of the active catalysts, both in heterogeneous or homogeneous fashion, as well as in the clarification of substrate activation modes and reaction mechanisms. Part of the work covered in this thesis treats these topics; a newly developed homogeneously catalyzed method for the transfer hydrogenolysis of benzylic alcohols will be presented in section 3.3.

1.3 References

[1] J. M. Herrmann, B. König, *Eur. J. Org. Chem.* **2013**, *2013*, 7017-7027.
[2] E. Clemmensen, *Ber. Dtsch. Chem. Ges.* **1913**, *46*, 1837-1843.
[3] L. Wolff, *Liebigs Ann.* **1912**, *394*, 86-108.
[4] D. H. R. Barton, S. W. McCombie, *J. Chem. Soc., Perkin Trans. 1* **1975**, 1574-1585.
[5] P. T. Anastas, J. C. Warner, *Green Chemistry: Theory and Practice*, Oxford University Press, Oxford, **1998**.
[6] R. A. Sheldon, *Chem. Soc. Rev.* **2012**, *41*, 1437-1451.
[7] R. A. Sheldon, *Green Chem.* **2017**, *19*, 18-43.
[8] S. Sawadjoon, A. Lundstedt, J. S. M. Samec, *ACS Catal.* **2013**, *3*, 635-642.
[9] H. Wang, L. Li, X.-F. Bai, J.-Y. Shang, K.-F. Yang, L.-W. Xu, *Adv. Synth. Catal.* **2013**, *355*, 341-347.
[10] M. Yasuda, Y. Onishi, M. Ueba, T. Miyai, A. Baba, *J. Org. Chem* **2001**, *66*, 7741-7744.
[11] C.-B. Yu, Y.-G. Zhou, *Angew. Chem. Int. Ed.* **2013**, *52*, 13365-13368.
[12] B. H. Gross, R. C. Mebane, D. L. Armstrong, *Appl. Catal., A* **2001**, *219*, 281-289.
[13] A. Ohgi, Y. Nakao, *Chem. Lett.* **2016**, *45*, 45-47.
[14] S. Kusumoto, K. Nozaki, *Nat. Commun.* **2015**, *6*.
[15] Y.-B. Huang, L. Yan, M.-Y. Chen, Q.-X. Guo, Y. Fu, *Green Chem.* **2015**, *17*, 3010-3017.
[16] L. Petitjean, R. Gagne, E. S. Beach, D. Xiao, P. T. Anastas, *Green Chem.* **2016**, *18*, 150-156.
[17] A. Volkov, K. P. J. Gustafson, C.-W. Tai, O. Verho, J.-E. Bäckvall, H. Adolfsson, *Angew. Chem. Int. Ed.* **2015**, *54*, 5122-5126.
[18] N. Kalutharage, C. S. Yi, *J. Am. Chem. Soc.* **2015**, *137*, 11105-11114.
[19] R. J. Rahaim, Jr., R. E. Maleczka, Jr., *Org. Lett.* **2011**, *13*, 584-587.
[20] D. R. Zuidema, S. L. Williams, K. J. Wert, K. J. Bosma, A. L. Smith, R. C. Mebane, *Synth. Commun.* **2011**, *41*, 2927-2931.
[21] S. C. A. Sousa, T. A. Fernandes, A. C. Fernandes, *Eur. J. Org. Chem.* **2016**, *2016*, 3109-3112.

[22] A. G. Sergeev, J. F. Hartwig, *Science* **2011**, *332*, 439-443.
[23] J. M. Nichols, L. M. Bishop, R. G. Bergman, J. A. Ellman, *J. Am. Chem. Soc.* **2010**, *132*, 12554-12555.
[24] M. Padoa, V. Ponti, *Gazz. Chim. Ital.* **1908**, *37*, 105-110.
[25] R. Connor, H. Adkins, *J. Am. Chem. Soc.* **1932**, *54*, 4678-4690.
[26] P. G. M. Wuts in *Greene's Protective Groups in Organic Synthesis*, Wiley, Hoboken, NJ, **2014**, pp. 120-140.
[27] M. V. Galkin, J. S. M. Samec, *ChemSusChem* **2014**, *7*, 2154-2158.
[28] T. L. Lohr, Z. Li, R. S. Assary, L. A. Curtiss, T. J. Marks, *ACS Catal.* **2015**, *5*, 3675-3679.
[29] T. L. Lohr, Z. Li, R. S. Assary, L. A. Curtiss, T. J. Marks, *Energy Environ. Sci.* **2016**, *9*, 550-564.
[30] M. J. Gilkey, B. Xu, *ACS Catal.* **2016**, *6*, 1420-1436.
[31] H. Nishikawa, D. Kawamoto, Y. Yamamoto, T. Ishida, H. Ohashi, T. Akita, T. Honma, H. Oji, Y. Kobayashi, A. Hamasaki, T. Yokoyama, M. Tokunaga, *J. Catal.* **2013**, *307*, 254-264.
[32] H. Meerwein, R. Schmidt, *Liebigs Ann.* **1925**, *444*, 221-238.
[33] H. B. Henbest, T. R. B. Mitchell, *J. Chem. Soc. C* **1970**, 785-791.
[34] S. Hashiguchi, A. Fujii, J. Takehara, T. Ikariya, R. Noyori, *J. Am. Chem. Soc.* **1995**, *117*, 7562-7563.
[35] R. J. Lundgren, M. A. Rankin, R. McDonald, G. Schatte, M. Stradiotto, *Angew. Chem. Int. Ed.* **2007**, *46*, 4732-4735.
[36] Y. Zhang, X. Li, S. H. Hong, *Adv. Synth. Catal.* **2010**, *352*, 1779-1783.
[37] W. Jin, L. Wang, Z. Yu, *Organometallics* **2012**, *31*, 5664-5667.
[38] A. Ruff, C. Kirby, B. C. Chan, A. R. O'Connor, *Organometallics* **2016**, *35*, 327-335.
[39] R. J. Rahaim, R. E. Maleczka, *Org. Lett.* **2011**, *13*, 584-587.
[40] J. Feng, C. Yang, D. Zhang, J. Wang, H. Fu, H. Chen, X. Li, *Appl. Catal., A* **2009**, *354*, 38-43.
[41] X. Liu, G. Lu, Y. Guo, Y. Guo, Y. Wang, X. Wang, *J. Mol. Catal. A: Chem.* **2006**, *252*, 176-180.
[42] P. G. Jessop, F. Joó, C.-C. Tai, *Coord. Chem. Rev.* **2004**, *248*, 2425-2442.
[43] C. Federsel, R. Jackstell, M. Beller, *Angew. Chem. Int. Ed.* **2010**, *49*, 6254-6257.
[44] D. Mellmann, P. Sponholz, H. Junge, M. Beller, *Chem. Soc. Rev.* **2016**, *45*, 3954-3988.
[45] A. Álvarez, A. Bansode, A. Urakawa, A. V. Bavykina, T. A. Wezendonk, M. Makkee, J. Gascon, F. Kapteijn, *Chem. Rev.* **2017**, *117*, 9804-9838.
[46] A. K. Singh, S. Singh, A. Kumar, *Catal. Sci. Technol.* **2016**, *6*, 12-40.
[47] E. Arceo, P. Marsden, R. G. Bergman, J. A. Ellman, *Chem. Commun.* **2009**, 3357-3359.
[48] S. Rajagopal, A. F. Spatola, *Appl. Catal., A* **1997**, *152*, 69-81.
[49] K. J. Miller, M. M. Abu-Omar, *Eur. J. Org. Chem.* **2003**, *2003*, 1294-1299.
[50] M. G. Saulnier, M. Dodier, D. B. Frennesson, D. R. Langley, D. M. Vyas, *Org. Lett.* **2009**, *11*, 5154-5157.
[51] S. T. Bowden, T. F. Watkins, D. L. Clarke, A. R. Kon, H. R. Soper, *J. Chem. Soc.* **1940**, 1333-1335.
[52] A. P. G. Kieboom, J. F. De Kreuk, H. Van Bekkum, *J. Catal.* **1971**, *20*, 58-66.
[53] J. A. Widegren, M. A. Bennett, R. G. Finke, *J. Am. Chem. Soc.* **2003**, *125*, 10301-10310.
[54] S. Yang, W. Tang, Z. Yang, J. Xu, *ACS Catal.* **2018**, *8*, 9320-9326.

1.4 Chemical valorization of lignin

1.4.1 Lignocellulose - a promising renewable carbon source

Facing the continuing global population growth and the related increase in energy demand, a depletion of the fossil resources used for the generation of energy and the production of chemicals is to be expected in the next decades. As a possible solution for the energy sector, alternative technologies are already applied, e.g. for bio-based fuels.[1] The chemical sector, however, still heavily relies on fossil carbon sources. To reduce this dependence, the use of biomass offers an attractive approach for sustainable chemical production. Biomass is inexpensive and globally accessible, the available amounts should be sufficient to cover a great part of the carbon-containing raw materials required by the chemical industry.[2] To make this resource accessible in an efficient manner, the development of new technologies has to be promoted.[3-6] In this context, especially non-edible biomass should be taken into account as the usage of this feedstock evades a possible competition between food and chemical production.[3]

An attractive example for this class of biomass is lignocellulose, which can be obtained in large quantities from forestry and agriculture[3] or food waste.[7] In recent years, more efficient processes for the fractionation of lignocellulose in biorefineries were developed, which allow for the separation of the material in its three main components: cellulose, hemicellulose and lignin.[8] While the cellulose fractions are used for paper production, lignin is widely considered a waste product and put in thermal utilization.[3] Considering this from a chemical point of view, lignin is a highly interesting compound as its structure comprises of aromatic subunits (Figure 1.1). These structural motifs could be transformed into renewable substitutes for aromatic bulk chemicals from fossil resources like the BTX solvents.[9,10] Lignin is formed in plants from three monomers, coumaryl (**24**), coniferyl (**25**) and sinapyl alcohol (**26**). It possesses an amorphous, three-dimensional polymeric structure with high molecular weight in which repeating structural motifs are connected by strong C–C and C–O bonds, with the most abundant linkage being the β-O-4 motif.[11] Therefore, selective cleavage by chemical means proved difficult initially. Nonetheless, the depolymerization of lignin into simple product mixtures has been subject to a great number of fundamental research approaches from several fields like homogeneous[11-13] or heterogeneous catalysis,[10,14,15] to the use of oxidative methods[16,17] or alternative, functional solvents[18] to photocatalytical,[19] thermochemical,[20-22] or biochemical[23] methodologies.

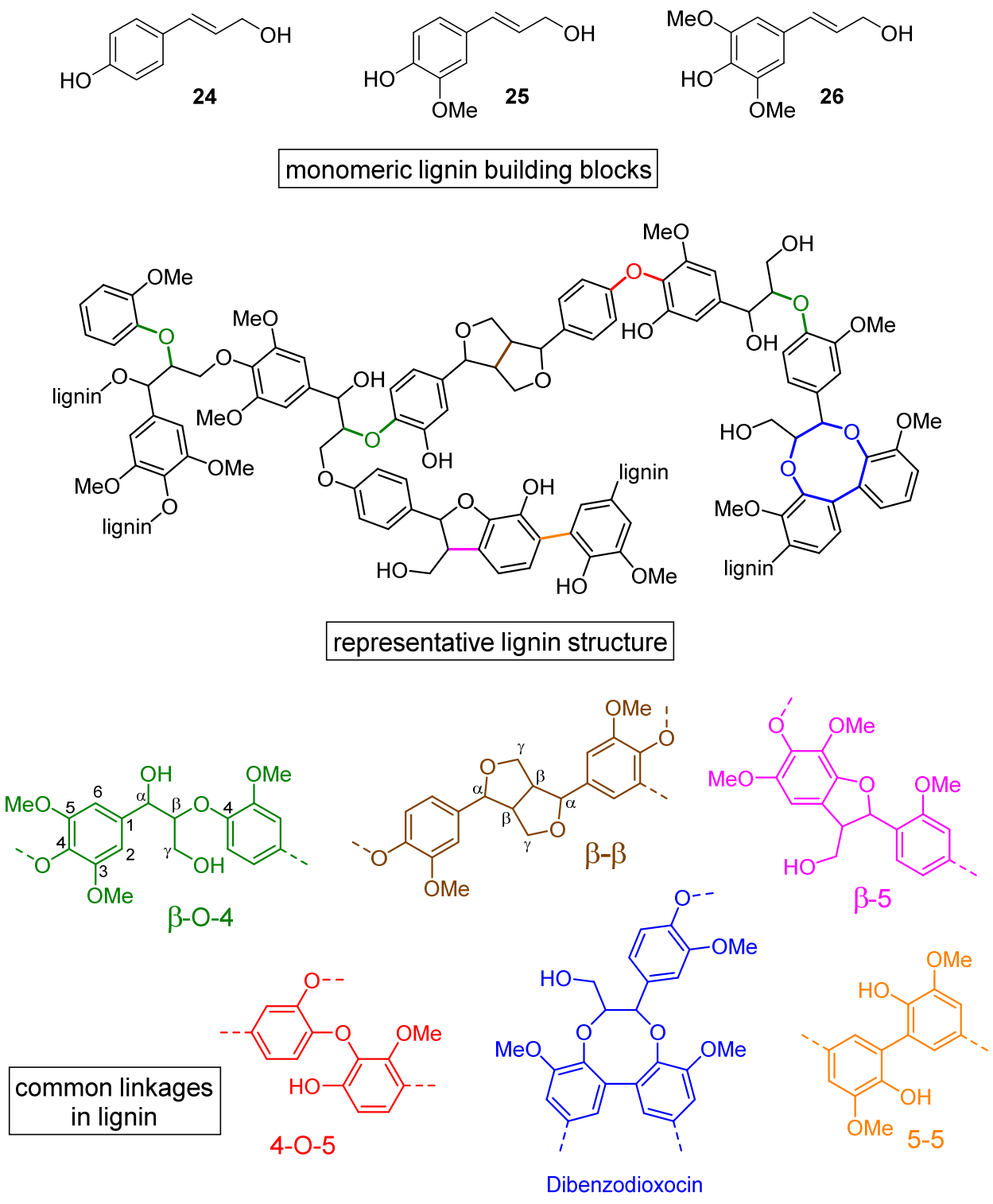

Figure 1.1 **Monomeric building blocks for lignin synthesis in plants, a representative lignin structure with typical linkages marked, common linkages in lignin (adapted from the original publication).[24]**

This section will cover the main laboratory and large-scale processes for lignin isolation as well as its separation from the cellulosic components of raw plant material to give an overview of the developed strategies for the depolymerization of isolated lignins to simple fragments. Only chemical methods relying on relatively mild conditions (low pressures, temperatures below 250 °C) will be discussed together with methods applying only

pretreated, non-native lignin since a full review of the developments in the field is beyond the scope of this introduction.

1.4.2 Lignin isolation from lignocellulosic biomass *via* fractionation

Conventional producers of lignin are the pulp and paper industry or sites fermenting biomass to gain ethanol from cellulose. In both cases great amounts of lignin are obtained in the processes as by-product, e.g. 50 million tons per year in the paper industry, of which less than 2% are utilized for the production of chemicals. From an economic point of view, the valorization of lignin for chemicals should be intensified as one kilogram of lignin used as fuel reaches a monetary equivalent of 0.18 US$/kg while lignin used for chemicals holds a much higher value of 1.08 US$/kg.[25]

The methods applied to isolate lignin from lignocellulose can be separated in two categories, which differ in the extent of modification of the lignin structure during the isolation process (Scheme 1.12, top). Pulping methods as the Kraft,[26] Klason,[27] sulfite[28] or alkaline[29] process apply harsh conditions like the use of strongly acidic or basic media or the introduction of inorganic salts.[8] This leads to high quality cellulose fractions, however, strong structural modification of the extracted lignin occurs. In the Kraft process, which is globally dominant for lignin removal, wood is treated with an aqueous solution of sodium hydroxide and sodium sulfide at 170 °C which leads to the predominant cleavage of β-O-4 and α-O-4 linkages and the formation of free phenolic hydroxyl groups, increasing the solubility of the fragments in the aqueous medium. In addition to recondensation reactions of the cleaved polymer, the application of sulfides in the process leads to lignin fractions containing significant amounts of sulfur (1.5–3%).[26] As sulfides can act as poisons for transition metal catalysts, the downstream processing of Kraft lignin in further catalytic transformations may be problematic. Similar to Kraft lignin, sulfite pulping yields depolymerized lignin with a sulfur incorporation of 4–8%, although it is present in sulfonate groups added to the lignin under the pulping conditions (acidic or basic aqueous medium, treatment with sulfite or bisulfite salts, 140–170 °C). This makes the fragments water soluble and prevents recondensation. To remove the introduced sulfur from processed lignin, a method based on a heterogeneous nickel hydrogenolysis catalyst was developed by Song *et al.*, which additionally allows for the cleavage of the polymeric structure in monomeric phenol derivatives.[30]

The Klason process, which was originally developed for the determination of the lignin content in wood, consists of a total hydrolysis step of the carbohydrates contained in the wood by 72% sulfuric acid. Subsequent dilution with water, washing out the acid and drying yields Klason lignin, which is significantly damaged in its native structure.[27] Alkaline processing or so-called soda pulping applies hydroxide salts for the delignification. Thereby,

ether linkages like alkyl-aryl ethers or β-O-4 linkages are cleaved while less structural modification is observed in the obtained lignin fraction.[15]

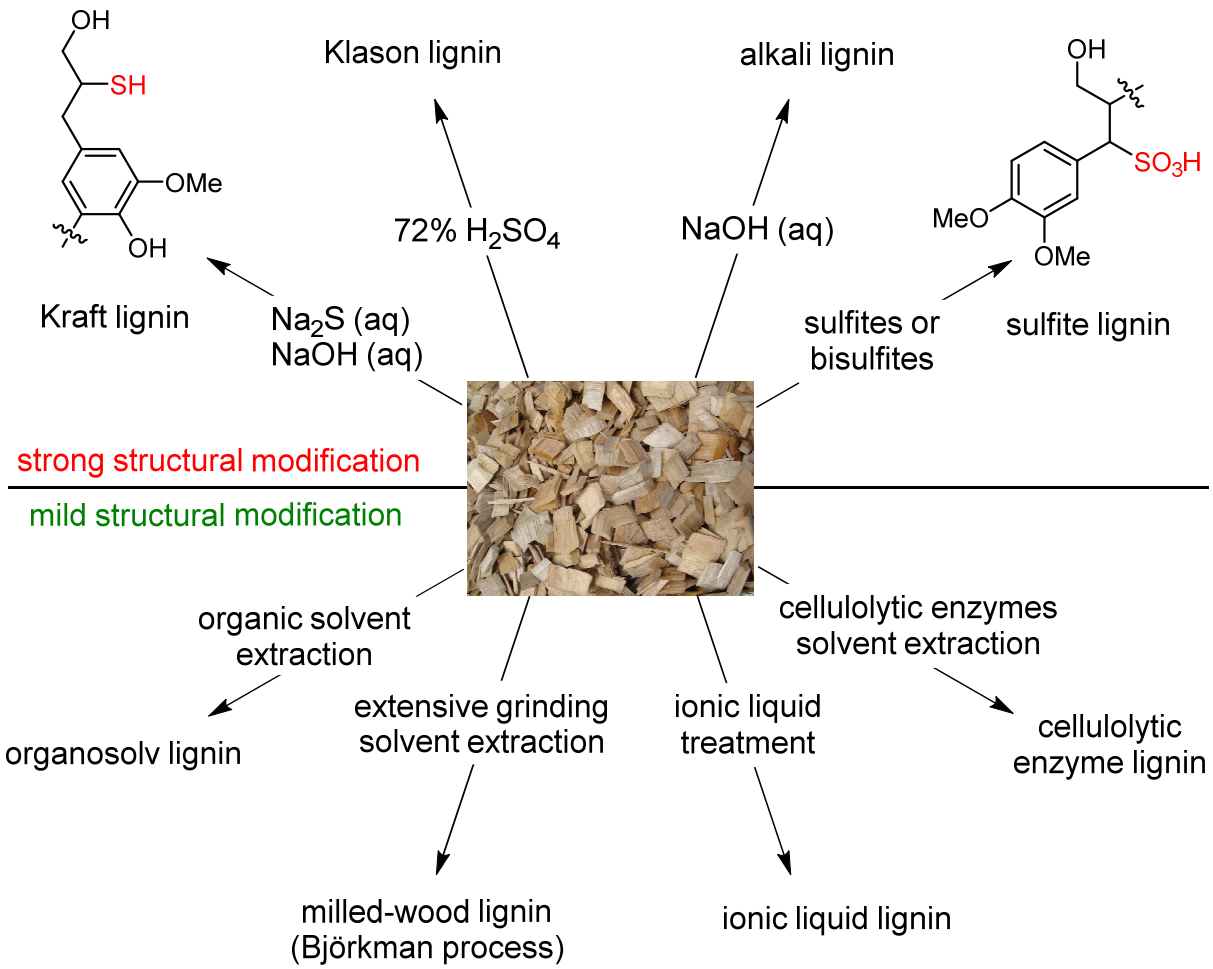

Scheme 1.12 **Methods for lignin isolation *via* strong or mild structural modification (adapted from the original publication).[24]**

To sustain the native structure of lignin during the isolation as far as possible, milder extraction methods were developed (Scheme 1.12, bottom). These rely on less harsh conditions concerning isolation techniques, *p*H and temperature. One of these newer methods is the so-called Björkman process, in which lignin is isolated from the crude wood material *via* extensive grinding using a ball mill under neutral conditions, followed by an extraction with an organic/aqueous solvent mixture, e.g. dioxane/water. The obtained milled-wood lignin resembles more the native lignin in terms of molecular structure. Nevertheless, ball milling can still lead to additional functionalization, introducing hydroxyl or carbonyl groups.[31] The yields of obtained lignin range from 20 to 40%.[28]

An even milder method for the isolation of lignin is the use of cellulolytic enzymes. Herein, finely ground wood is treated with enzymes that catalyze the partial hydrolysis of the contained cellulose and hemicellulose. Extraction of the lignin fraction is performed and the cellulolytic enzyme lignin is precipitated in water. A drawback of this procedure is the long

time needed for the delignification (up to several days) compared to conventional methods which take several hours to one day. Moreover, the obtained lignin may contain protein and carbohydrate impurities. An advancement was achieved by combining enzymatic hydrolysis with mild acidolysis.[32] Yields obtained from this procedure are two to five times higher than from ball-milling or enzymatic hydrolysis alone.[33]

Another specialized approach for lignin isolation consists in the application of ionic liquids.[18] These exhibit special properties concerning solubilizing power, boiling temperatures and thermal stability, which are tunable to adapt the applied system to the conditions of the respective process. Often, the low solvent recyclability, the hard-to-perform separation of the product from the extraction medium and the high costs for the synthesis of ionic liquids are stated as disadvantages of this methodology.[34,35] However, first synthesis routes for ionic liquids starting from fractionated biomass were developed, decreasing the all-over production costs.[36]

A more environmentally benign process compared to the conventional Kraft or sulfite methods, which introduce sulfur-containing groups into the desired lignin product as well as into the residual pulp, is the treatment of lignocellulose with organic solvents like acetone, ethanol, acetic acid or methanol, often as mixtures with water. The so-called organosolv process involves cooking of the raw material at relatively low temperatures (140–220 °C), which leads to the cleavage of α-O-4 linkages in the polymeric structure, while the generated fragments dissolve in the organic solvent.[37]

1.4.3 Catalytic approaches for the production of aromatics from lignin

After discussing methods for the isolation of lignin from raw lignocellulosic biomass, this section will focus on the cleavage of lignin model compounds (Figure 1.2) or isolated lignin to afford monomeric aromatics by using catalytic strategies. Processes to transform native lignin still bound in the lignocellulosic network into simple arenes like alkyl phenols are also known in the literature.[24] Nonetheless, this introduction will focus on the conversion of lignin models or isolated lignin as these allow a better mechanistic understanding of the cleavage reactions and are not disturbed by other lignocellulosic components like carbohydrates. For the cleavage of bonds in known lignin structural motifs, e.g. the β-O-4 linkage, methodologies derived from different basic chemical transformations were applied. In the following, oxidative, reductive and redox neutral catalyst systems will be briefly discussed for their effects in the depolymerization of lignin networks and corresponding model compounds by introducing selected examples from the recent literature. Performing initial studies on model substrates holds the advantage that these are easier to obtain by synthetic means and that their conversion leads to simpler product mixtures. After optimization, the found conditions

can then be directly transferred or adapted to authentic lignin samples to show their applicability.

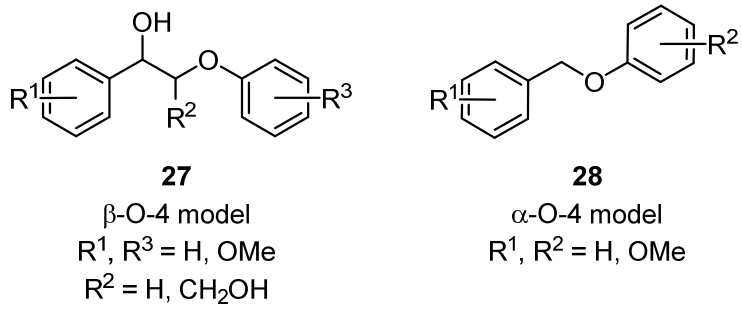

27
β-O-4 model
R^1, R^3 = H, OMe
R^2 = H, CH_2OH

28
α-O-4 model
R^1, R^2 = H, OMe

Figure 1.2 **General structures of selected dimeric lignin model compounds.**

Oxidative approaches

Among the oxidative transformations of lignin, the production of vanillin from lignin is the oldest known valorization process, which was already industrialized in the second half of the 19th century. The mechanism of this reaction was extensively studied,[16,38] but is still under debate. It is assumed that lignin fragments **29** obtained from basic depolymerization undergo several subsequent oxidation steps and a final *retro*-aldol cleavage in an alkaline aerobic medium leads to the vanillin structure **34** (Scheme 1.13).[39,40]

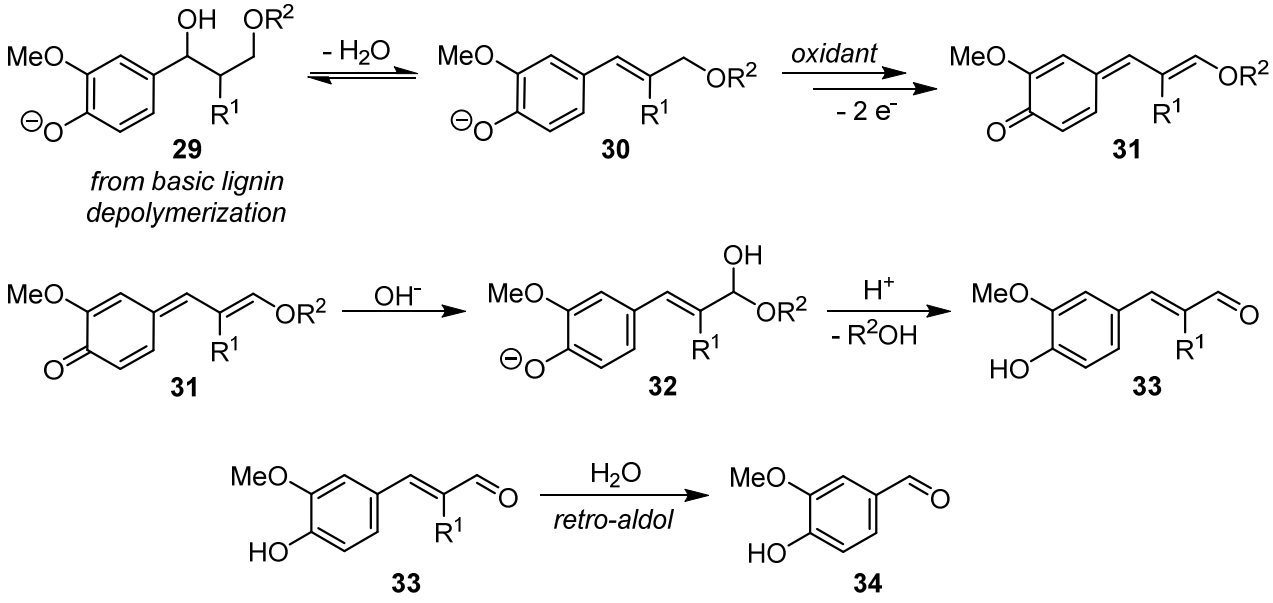

Scheme 1.13 **Proposed reaction pathway for the formation of vanillin from lignin fragmentation products (adapted from the original publication).[40]**

To broaden the scope of products yielded *via* oxidative lignin depolymerization, new electrochemical[41] and photocatalytical[19] methods were developed. Furthermore, heterogeneous catalysts[17] or ionic liquids[18] were applied, as were metal catalysts like

manganese,[42] vanadium,[43,44] iron,[45] copper,[44,46,47] cobalt[48,49] or palladium.[50] As oxidizing agents oxygen, hydrogen peroxide, ozone, peroxyacids and even chlorine have been used, with the latter opening the possibility to synthesize chlorinated substituted arenes. These oxidative methods hold a great potential as they operate under mild conditions.[16] Additionally, DFT calculations showed that oxidation of the alcohol moieties, e.g. in the β-O-4 linkage, weakens the ether C–O bond by 40–80 kJ/mol depending on the extent of oxidation.[51] In this context, large-scale oxidative treatment of biomass and related material is a well-known process in the paper industry, e.g. in pulp bleaching.[16] On the other hand, selectivity is needed for this kind of transformations as overoxidation leads to the formation of gaseous products and thereby the loss of material. The non-selective introduction of functional groups affords more complex product mixtures. Also the formation of radicals and following repolymerization decreases product yields.[16-18]

The group of Wang[50] developed a method for the oxidative conversion of lignin model compounds and authentic lignin using palladium nanoparticles (NPs) on a solid support of cerium(IV) oxide and molecular oxygen as oxidant in an autoclave setup (Scheme 1.14). First studies on 2-phenoxy-1-phenylethanol showed that certain metal oxides, amongst them CeO_2, are able to perform an oxidation of the benzylic alcohol moiety contained in the substrate under atmospheric pressure of oxygen, although conversion was low in all cases (9% for CeO_2).

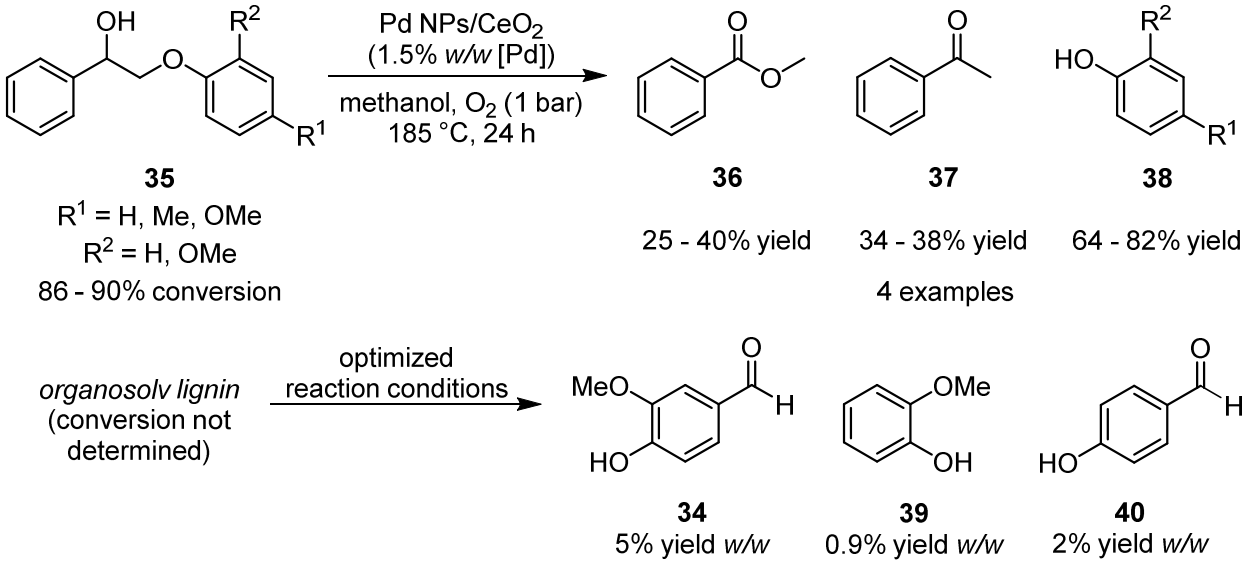

Scheme 1.14 **Oxidative cleavage of lignin models and organosolv lignin *via* β-O-4 or C_α–C_β scission using palladium on solid cerium oxide support as catalyst and oxygen as oxidizing agent.[50]**

When starting from 2-phenoxy-1-phenylethanone, comprising the oxidation product of 2-phenoxy-1-phenylethanol, which features a benzylic ketone instead of an alcohol, conversion drastically improved (over 90% for CeO_2) and β-O-4 cleavage as well as oxidative

C–C bond cleavage was observed which gave rise to several products: benzoic acid, methyl benzoate, acetophenone and phenol. Deposition of palladium nanoparticles on the cerium oxide support proved beneficial for the transformation of benzylic alcohols **35**, it was stated that palladium facilitated the oxidation of the alcohol moiety, while the cerium oxide support promoted the cleavage reactions. It was shown that the catalyst could be recycled for four more runs without significant change in activity. Through the synergistic effect of both applied metals, a good selectivity towards the desired cleavage products could be achieved and the applicability of the catalyst system could not only be shown for several lignin model structures, but also for authentic organosolv lignin. Cleavage of the latter led to three main products **34**, **39** and **40** in good yields of 0.9% to 5% *w/w*. In addition, the catalyst was characterized using X-ray photolelectron spectroscopy and H_2 chemisorption measurements.

Liu and co-workers[42,48] showed that heterogeneous manganese- or cobalt-based catalysts prepared through a sol-gel-process are able to oxidatively depolymerize cellulolytic enzyme lignin under moderate oxygen pressure (Scheme 1.15). The perovskite-type oxides $LaMnO_3$ and $LaCoO_3$ were characterized using X-ray diffraction, temperature programmed reduction and X-ray photoelectron spectroscopy. The catalysts were applied in loadings of 5% *w/w* in an alkaline aqueous lignin solution in a high pressure reactor. The partial oxygen pressure was found sufficient at 5 bar, the total pressure in the reactor was set to 20 bar. As reaction products of the wet aerobic oxidation of lignin obtained from cornstalk, *para*-hydroxybenzaldehyde (**40**), vanillin (**34**) and syringaldehyde (**41**) were found in yields of 2%, 4% or 9% *w/w*, respectively, while only incomplete conversion of lignin was observed. The catalysts could be reused in 5 runs without significant loss of activity. For each product a different optimal reaction time was found, overoxidation to the corresponding carboxylic acids or CO_2 were stated as side reactions diminishing yields.

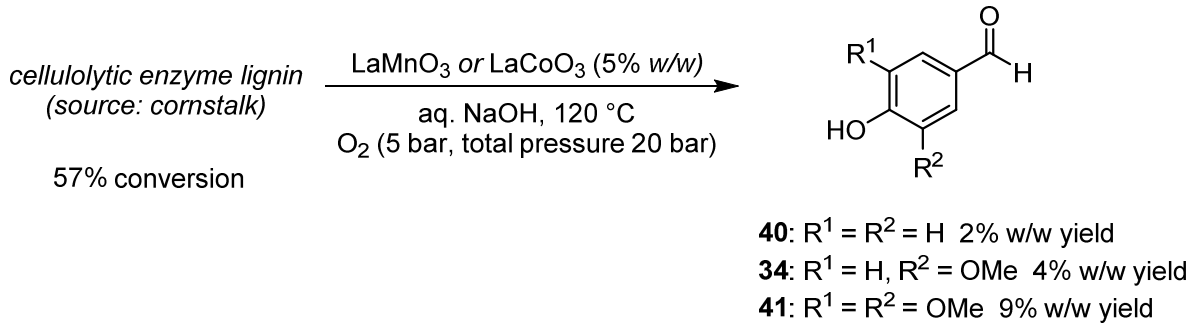

Scheme 1.15 **Wet aerobic oxidative depolymerization of cornstalk lignin reported by Liu and co-workers using heterogeneous $LaMnO_3$ or $LaCoO_3$.[42,48]**

Luo *et al.*[52] reported on a photocatalytic oxidation-hydrogenolysis sequence mediated by two heterogeneous metal-based photocatalysts (Scheme 1.16). Their strategy consisted of a selective oxidation of the benzylic alcohol moiety in β-O-4 linkages using $Pd/ZnIn_2S_4$ as catalyst under irradiation with light of 455 nm wavelength, followed by a TiO_2-catalyzed

hydrogenolysis of the C–O ether bond under 365 nm light irradiation, using ethanol as hydrogen source. In the latter step, sodium acetate was found beneficial in the reaction, presumably as proton transfer reagent from ethanol to the newly formed phenolate. After optimizing the individual reaction steps, a one-pot-setup for the conversion of lignin models was tested, in which switching the applied wavelength as well as simultaneous irradiation with both wavelengths led to very good yields of the cleavage products, even under aerobic conditions. Mechanistic investigations and electron paramagnetic resonance measurements of a suspension of TiO_2 showed that superficial Ti^{3+} is the active catalytic site in the hydrogenolysis reaction which arises from single electron transfer from ethanol to the photocatalyst. Several lignin model compounds **42** could be cleaved in mostly good yields. Substrates bearing methoxy groups showed lower product yields, it was suggested that the electronic activation of the formed phenols makes them prone to oxidation. Direct transfer of the reaction conditions on the conversion of organosolv lignin, however, was not successful, probably due to the dark color of the lignin in the batch reaction preventing the activation of the photocatalyst. The authors propose the use of a flow reactor setup to evade this problem.

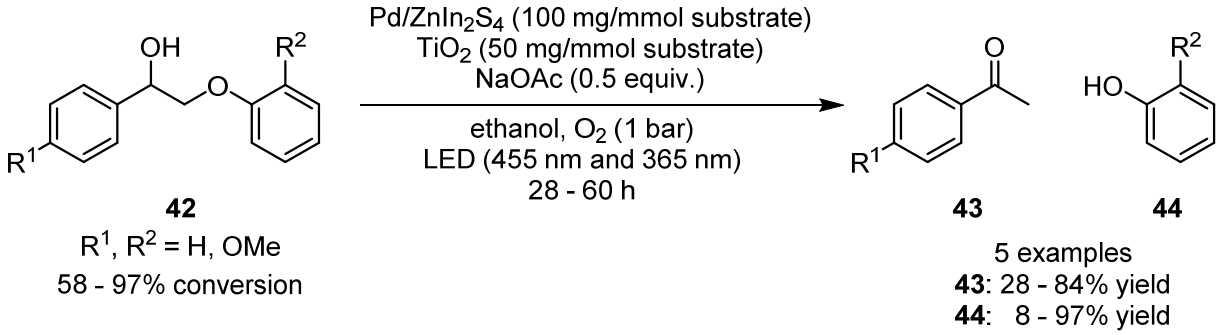

Scheme 1.16 **Photocatalytical oxidation/hydrogenolysis of lignin model compounds developed by Luo *et al.*[52]**

A transition metal-free transformation for the cleavage of lignin models and isolated lignin was developed by the group of Westwood[53] to obtain functionalized benzylic ketone monomers, i.a. bearing phenolic hydroxy groups. The one-pot procedure consists of two steps, first an oxidation of the benzylic alcohol moiety mediated by 2,3-dichloro-5,6-dicyano-1,4-benzoquinone (DDQ) and *tert*-butyl nitrite using oxygen as oxidant, followed by a cleavage induced by zinc and ammonium chloride. Both steps were optimized separately on dimeric or polymeric lignin models, proceeding smoothly under relatively mild reaction conditions and low catalyst loadings (Scheme 1.17). Organosolv lignin recovered from birch sawdust was converted successfully to obtain functionalized ketone **50** in a good yield next to two minor products **49** and **51** (Scheme 1.18).

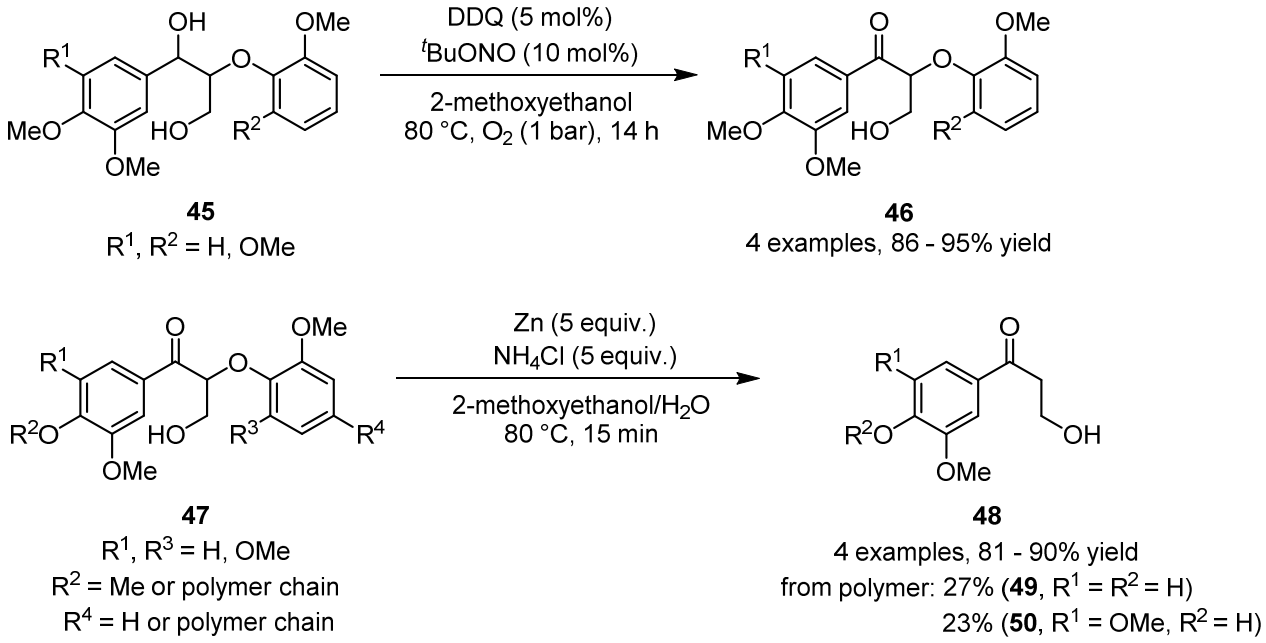

Scheme 1.17 **Optimized reaction conditions of the single steps for the transition metal free oxidative cleavage of lignin model compounds reported by Westwood *et al.*[53]**

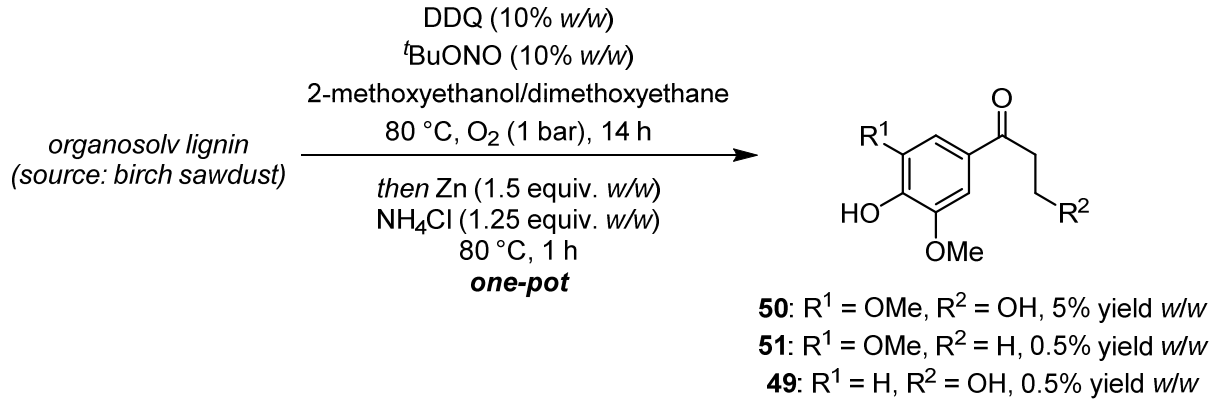

Scheme 1.18 **One-pot methodology for the oxidation and cleavage of lignin model and organosolv lignin developed by Westwood *et al.*[53]**

Reductive approaches

The use of reducing reaction conditions for depolymerization is already known from early studies on the structure elucidation of lignin wherein hydrogenation under high hydrogen pressures and temperatures (240 bar, 260 °C) applying a copper chromite catalyst yielded fully reduced *n*-propyl-cyclohexanols.[54-56]

For an actual valorization of lignin material far more selective catalytic methods are needed, giving the opportunity to maintain desired functionalities or to reductively eliminate non-wanted moieties, e.g. different types of C–O bonds.[57,58] In contrast to oxidative methods, which introduce additional functionalities into the lignin degradation products and thereby aim at the direct production of fine chemicals, reductive methods open the possibility to generate low-functionalized platform chemicals. These can then be further converted to

value-added compounds using already known conventional processes from the petroleum-based chemical industry.[10] For the selective breakage of C–O bonds in lignin, hydrogenolysis can be a useful tool. However, the hydrogenation of the aromatic systems found in lignin is a competitive reaction which has to be avoided by the careful choice of catalyst and reducing agent.[58] Systems which were already successfully applied in the hydrogenolytic cleavage of alkyl aryl ether bonds in lignin models are based on nickel,[30,59,60] ruthenium,[61-63] iron[64] or palladium[65-67] as metal catalysts, but also metal-free, organocatalytic methods[68] were reported. As reductants, hydrogen gas,[59,65,69] hydrosilanes,[68] formates,[67] metal hydrides,[64,66] alcohols[60] or hydrogen generated *via in situ* oxidation of the substrate[61] were used. The latter case of redox neutral cleavage will be discussed in the next section.

Hartwig and co-workers[59] reported that complexes of nickel with *N*–heterocyclic carbenes (NHC) generated *in situ* are active in the reductive cleavage of diaryl or alkyl aryl ethers in presence of a hydride source like metal hydrides or hydrogen gas. They found a suitable catalyst system which showed sufficient stability to prevent deactivation through the formation of heterogeneous species. Under moderate reaction conditions and catalyst loadings, the conversion of a variety of ethers was found possible including two successfully transformed substrates representing models for α-O-4 and β-O-4 linkages in lignin (Scheme 1.19). While the α-O-4 model **52** was converted at already low catalyst loadings, the β-O-4 structure **54** was found to be cleaved under metal-free conditions, both in high yields.

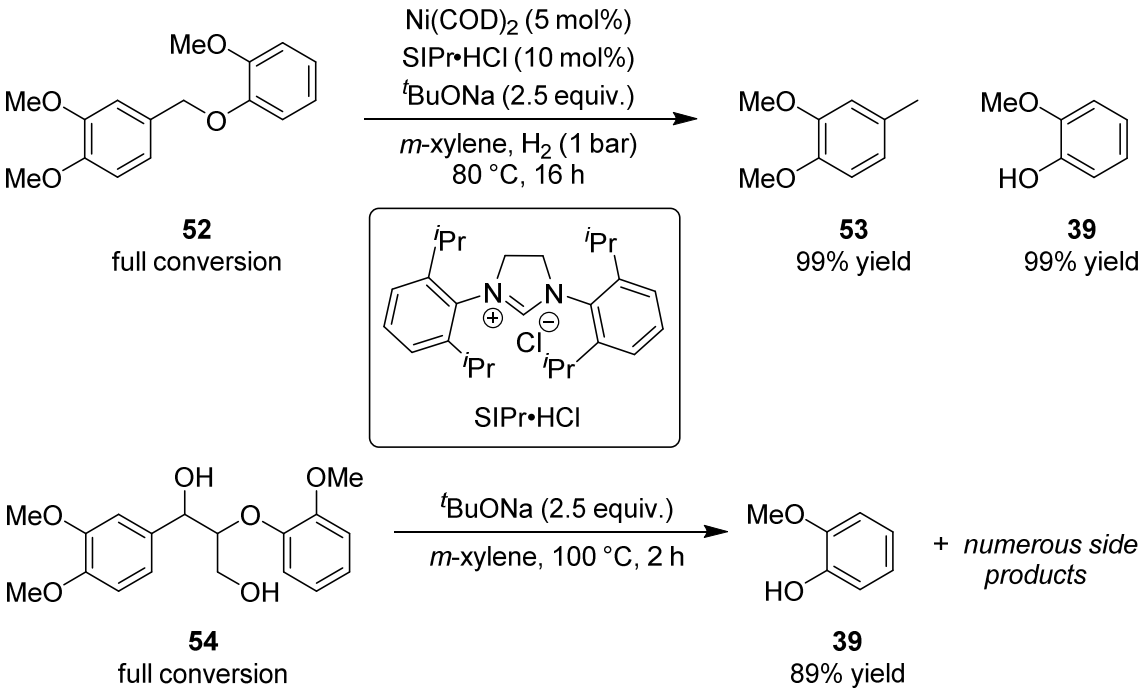

Scheme 1.19 **Reductive cleavage of an α-O-4 lignin linkage model using a homogeneous Ni-NHC catalyst and hydrogen as reductant, non-catalyzed cleavage of a β-O-4 lignin linkage model reported by Hartwig and co-workers.[59]**

The first metal-free, organocatalytic method for the reductive cleavage of lignin models was developed by Feghali *et al*.[68] They showed that several α-O-4 and β-O-4 model compounds can be converted to the silyl ethers of the respective phenols and phenylethanols in very high yields using tris(pentafluorophenyl)borane as catalyst in low to moderate loading and Et_3SiH as reductant under mild conditions (Scheme 1.20). DFT calculations and labelling studies gave an insight into the reaction mechanism, the obtained results propose an activation of the ether moieties in the substrate through silyl coordination, followed by cleavage of the respective aryl alkyl ether bond *via* a semipinacol-type rearrangement. The formed silyl-activated aldehyde is then reduced by the catalytically active triarylborohyride species formed from the introduced borane *via* hydride transfer from the silane. Furthermore, the cleavage of methoxy groups attached to the aromatic ring was also observed.

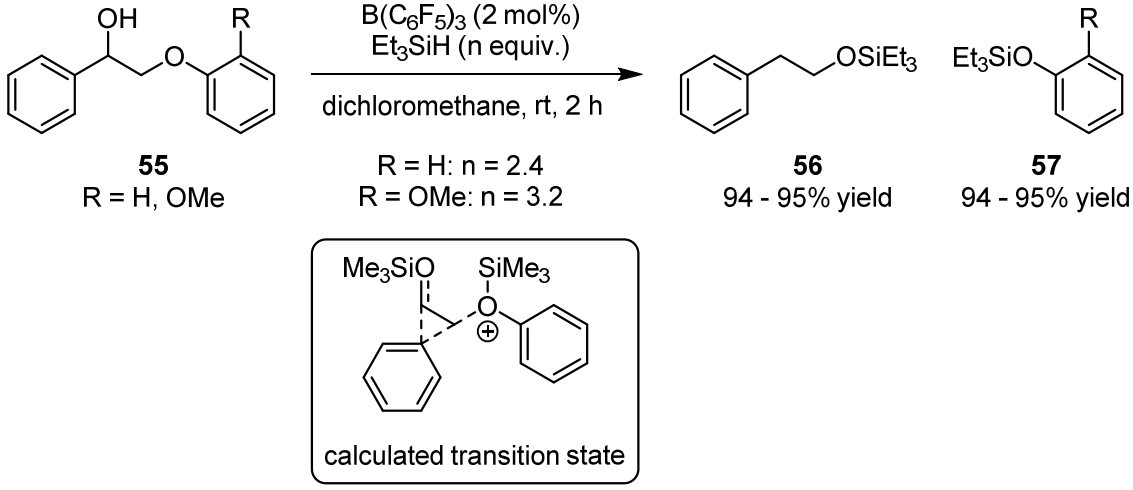

Scheme 1.20 **Metal-free organocatalytic cleavage of lignin model compounds *via* a rearrangement-reduction sequence catalyzed by $B(C_6F_5)_3$ reported by Feghali *et al.*[68]**

In a subsequent work from the same group[70] the deoxygenative cleavage of more complex lignin models as well as the depolymerization of lignin isolated from a range of wood types could be realized using the same catalytic system with only minor changes in the loadings of catalyst and reductant (Scheme 1.21). Herein, a different reaction mechanism was presumed as no semipinacol-type rearrangement was evident from labelling studies. Additionally, it was observed that the reactivity towards primary and secondary alcohol moieties could be influenced by changing reaction times and the amounts of reductant applied. With this strategy, a narrow product range of four monoaromatic lignin fragments **58**, **59**, **61** and **62** could be obtained from the depolymerization of isolated lignin, each in good to very good yields. Nevertheless, differences in product yields were found depending on the lignin source and the chosen extraction process.

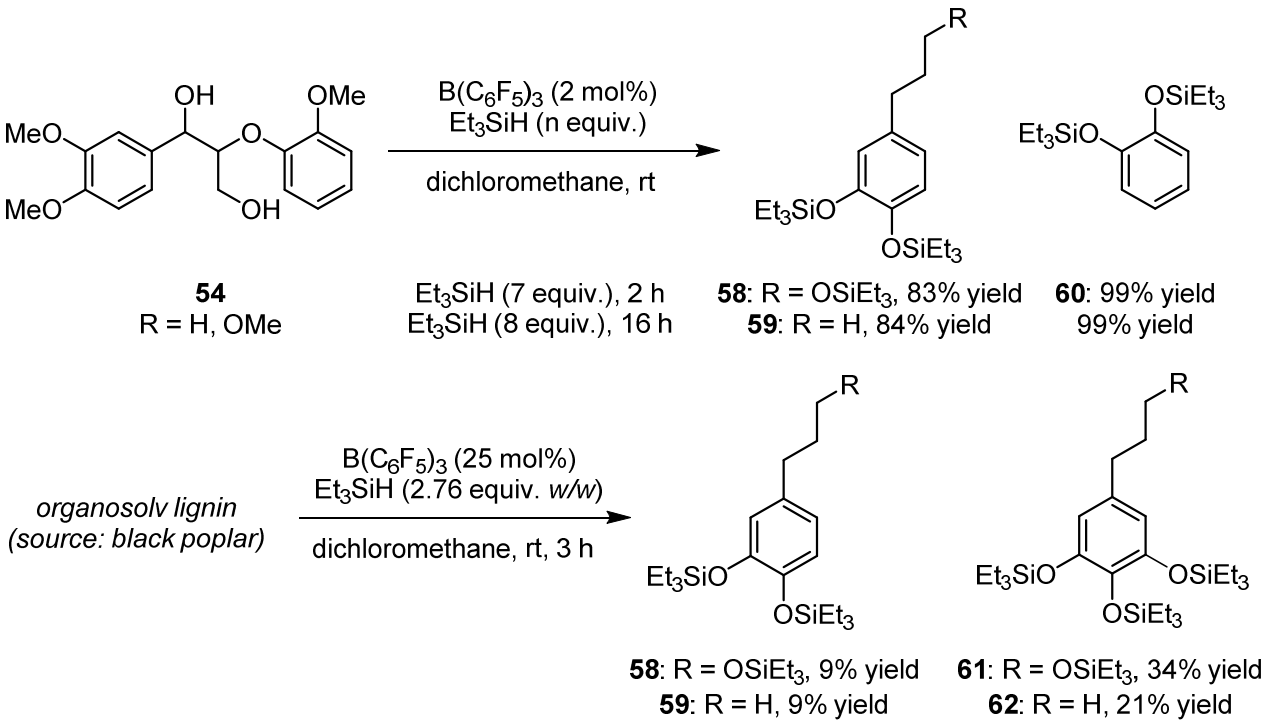

Scheme 1.21 **Adaption of the $B(C_6F_5)_3$ catalyst system for the cleavage of more complex lignin models and isolated lignin using Et_3SiH as reductant.[68,70]**

The group of Samec[67] reported on a reductive method for the cleavage of β-O-4 linkages in lignin model compounds and native lignin under relatively mild conditions under air. As catalyst, palladium on activated charcoal was applied together with formic acid as reducing agent, both in low loadings (Scheme 1.22). The addition of equimolar amounts of an amine base was found necessary for high conversion and selectivity towards the cleavage products. In the substrate screening, formic acid and amine could be added in a combined manner as ammonium formate. The transformation could be shown to be applicable to eleven structurally simple lignin model substrates **63**, in all cases excellent product yields were obtained. Adjustment of the reaction procedure allowed for selective production of several aromatic products differing in their degree of deoxygenation. Attempts to apply the developed protocol on organosolv lignin did not lead to depolymerization, but fragmentation due to the cleavage of several different ether bonds, which was detected *via* gel permeation chromatography and 2D NMR. Furthermore, the heterogeneous character of the catalyst was shown through poisoning and kinetic experiments. Structural modification of the substrate and kinetic isotope effect determinations provided an insight into a possible reaction mechanism which is thought to first proceed through a dehydrogenation of the benzylic alcohol group followed by reductive ether cleavage on the catalyst surface.

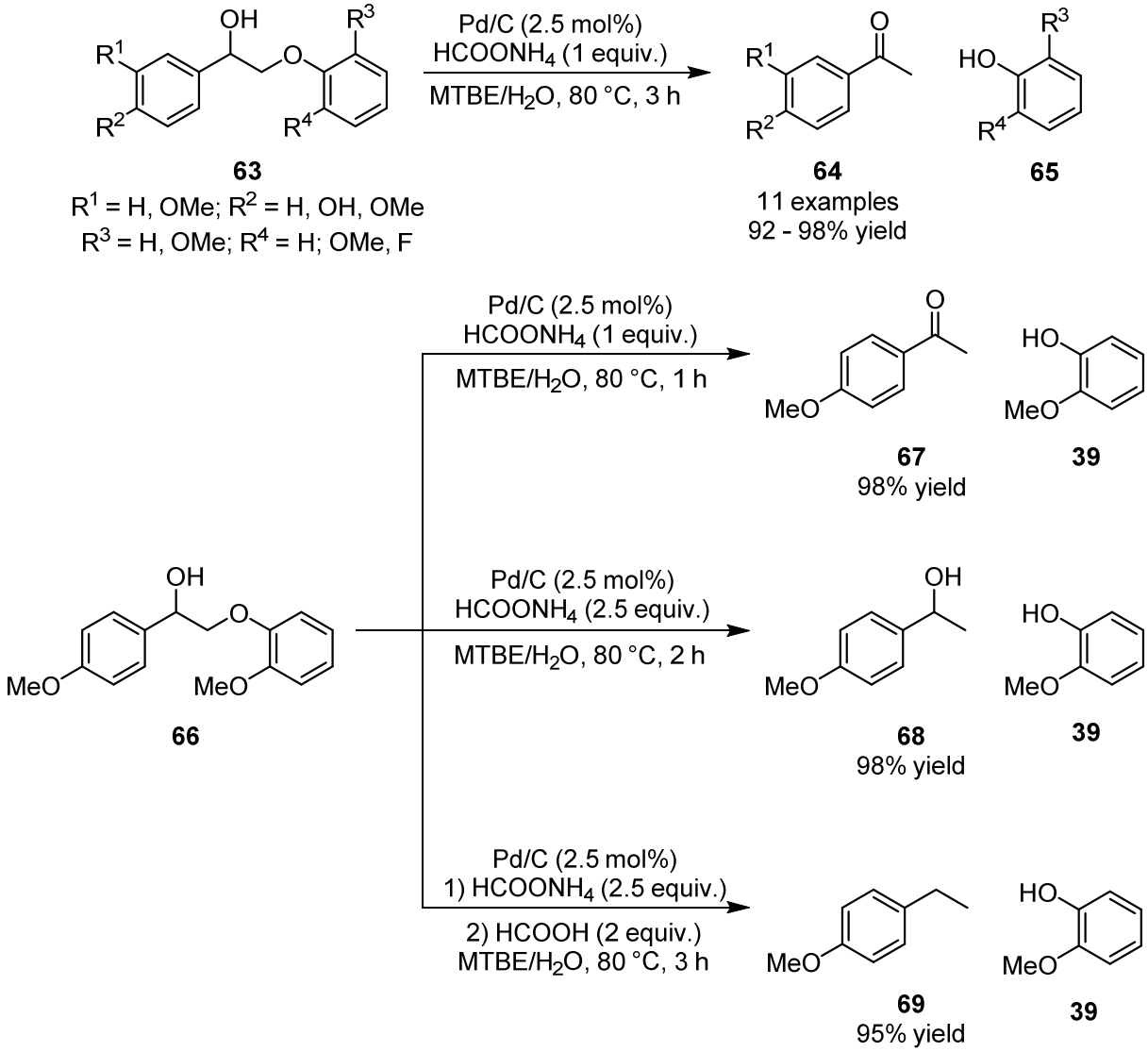

Scheme 1.22 **Reductive cleavage of lignin models reported by Samec and co-workers. Optimized reaction conditions, changed product selectivity with altered reaction conditions.[67]**

Although there is a large number of reductive methods for lignin depolymerization and defunctionalization, the obtained products still contain oxygenated moieties like methoxy or aromatic hydroxyl groups. Yet, a complete deoxygenation for the production of aromatic platform chemicals like benzene would be desirable. Wang, Yang, Ramirez-Cuesta and co-workers[71] investigated a catalytic system for the simultaneous depolymerization of organosolv lignin and deoxygenation of the resulting phenolic products in one process. They applied heterogeneous ruthenium on solid niobium oxide support in low loading and hydrogen gas as reductant under moderate pressure and elevated temperature in a pressure reactor setup (Scheme 1.23). Initial studies on the phenolic model substrate **70** showed promising results in product selectivity and yield. Lignin from different wood sources could also be converted, for birch wood a very good total mass yield of 36% *w/w* was achieved. The selectivity for aromatic deoxygenated products **73** was very high despite the use of a heterogeneous catalyst and the problem of arene overreduction related to it. No residual

phenolic monomers were found in the product mixture. Over several reaction runs, only slight deactivation of the catalyst was observed, while arene selectivity remained high. Inelastic neutron scattering measurements and DFT calculations granted an insight into the adsorption behavior of phenols towards the catalyst surface and the synergistic effects in the Ru/Ni_2O_5 system. The latter was found as an explanation for the selectivity of the system for hydrodeoxygenation over arene hydrogenation.

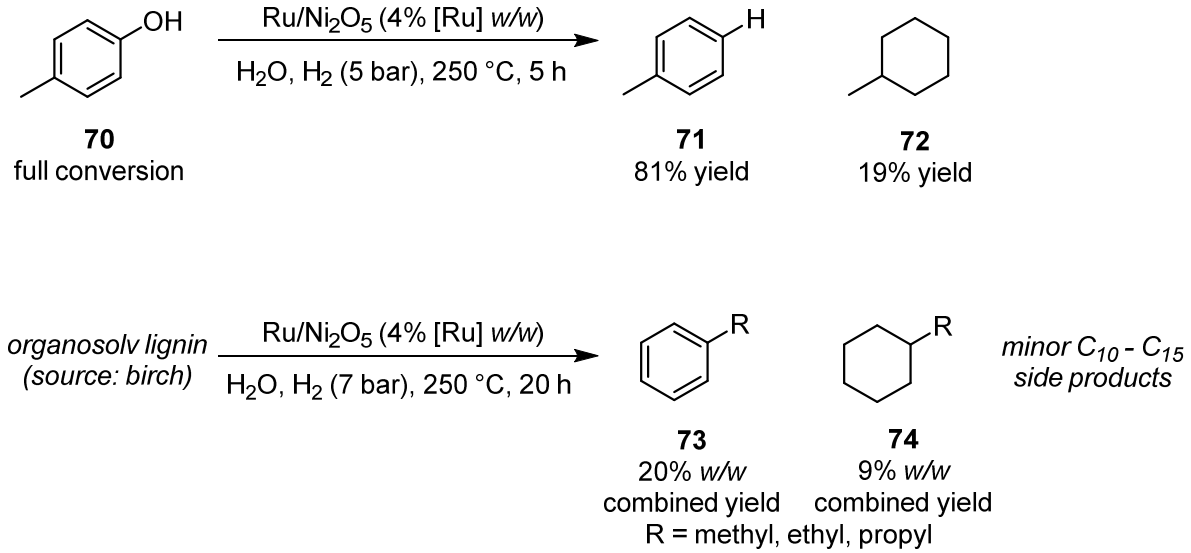

Scheme 1.23 **Reductive lignin depolymerization and phenol hydrodeoxygenation reported by Wang, Yang, Ramirez-Cuesta and co-workers. Conversion of phenol model substrate and organosolv lignin under optimized reaction conditions.[71]**

Redox neutral approaches

As an alternative to the use of external oxidizing or reducing agents for the cleavage of lignin, the idea of applying redox neutral methodologies was developed. This elegant approach is feasible for lignin as the substrate structure features secondary benzylic alcohols as well as alkyl-aryl ethers. While the first can serve as hydrogen donor for a suitable catalyst, the latter can be reduced with the equivalent of hydrogen produced *in situ* from the substrate itself. This constitutes a highly atom-economic pathway for the reductive depolymerization of lignin, which would be feasible under the principles of green chemistry. To pursue this strategy, bifunctional catalysts for transfer hydrogenation are needed. For the case of transition metals, examples based on ruthenium,[72-74] palladium,[65,66,75] vanadium,[76] rhenium,[77] nickel[78] or indium[79] were realized. Selected reports on metal-catalyzed redox neutral cleavage reactions of lignin models and isolated lignin will be briefly discussed in the following.

Seminal work in the field was done by Bergman, Ellman and co-workers[72] who used an *in situ* formed ruthenium 4,5–bis(diphenylphosphino)–9,9–dimethylxanthene (xantphos)

complex to perform the redox neutral cleavage of models for the β-O-4 linkage in lignin and a lignin-related polymer to the respective aryl ketones and phenol derivatives (Scheme 1.24). They found that for the simple model compound **75** under use of the metal precursor $RuH_2(CO)(PPh_3)_3$ only xantphos led to the desired reactivity from a range of mono- and bidentate phosphine ligands with different bite angles. Under optimized reaction conditions, five differently substituted lignin models could be converted in high to excellent yields. In addition to this, a polymer **78** similar to lignin was completely degraded to the respective monomer **79** in quantitative yield.

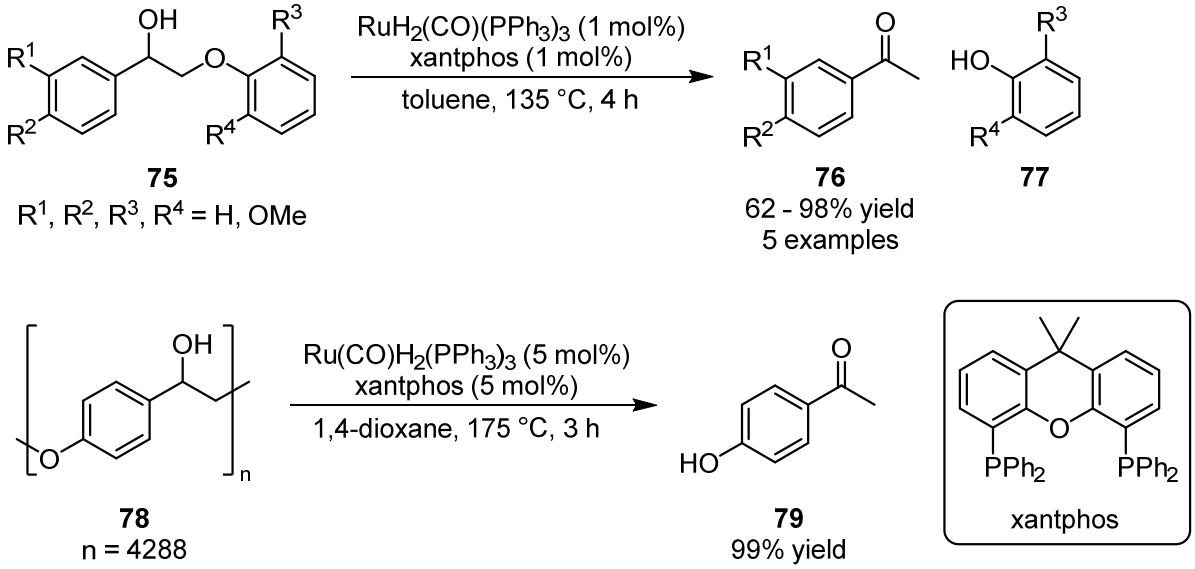

Scheme 1.24 **Redox-neutral cleavage of lignin model compounds and a lignin-like polymer catalyzed by a homogeneous ruthenium xantphos complex as reported by Bergman, Ellman and co-workers.[61]**

For the reaction mechanism, a ruthenium-catalyzed dehydrogenation of the benzylic alcohol moiety in **75** is proposed to form ketone **80**, followed by an ether C–O bond activation by the metal catalyst, which allows for the hydrogenative cleavage of **82**. Variation of the substrate structure showed that the free alcohol group and the aryl ketone intermediate play key roles in the successful transformation. For more complex and therefore more realistic model substrates like **84**, however, the work of Wu *et al.*[62] on the same catalytic transformation while using a preformed metal complex showed that the presence of another free hydroxyl group in γ-position leads to deactivation of the ruthenium catalyst by bidentate coordination of the substrate, showing in low product yields (Scheme 1.25).

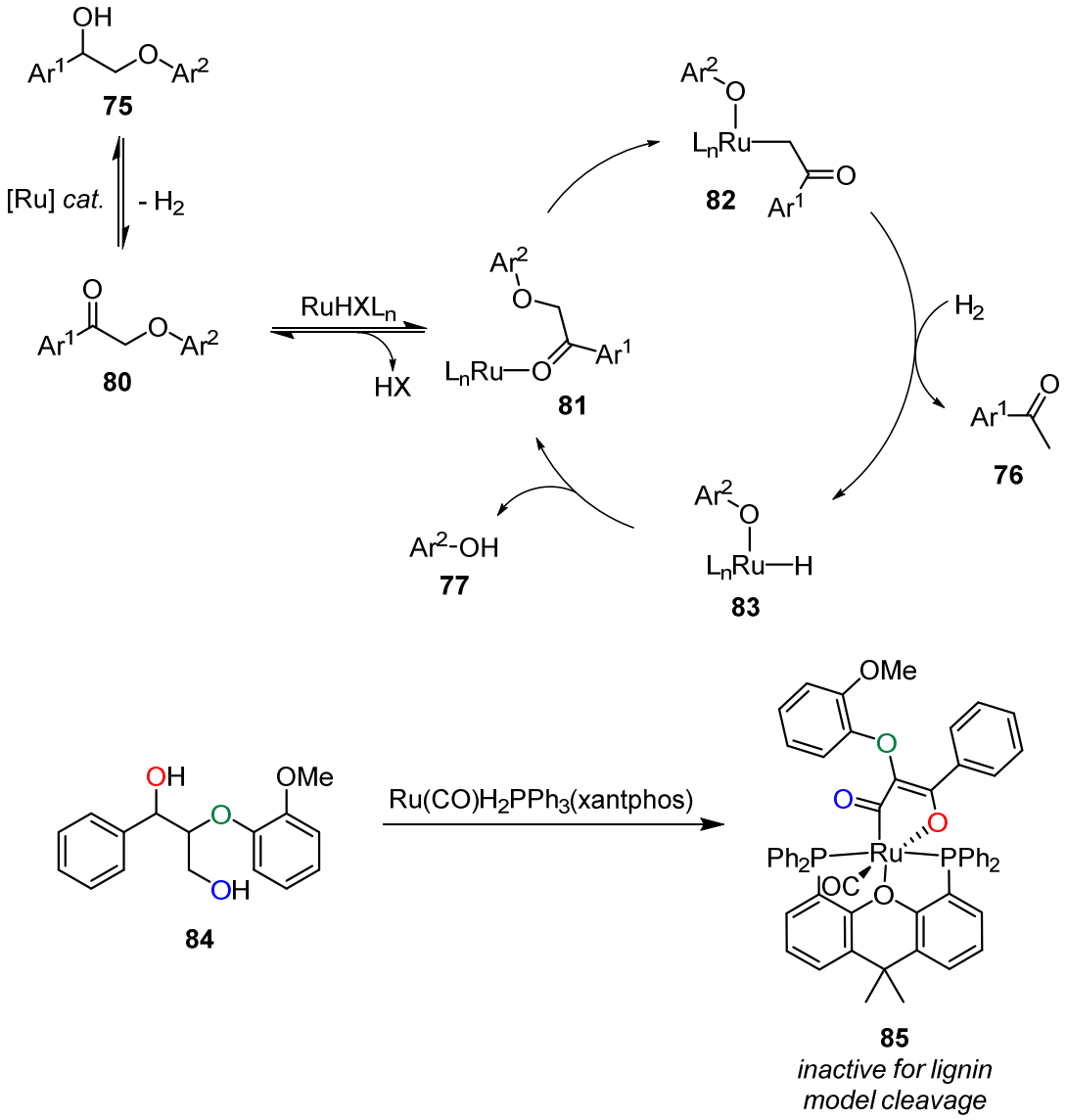

Scheme 1.25 **Proposed mechanism for the redox neutral ruthenium-catalyzed cleavage of lignin model compounds reported by Bergman, Ellman and co-workers (adapted from the original publication).[72] Catalyst deactivation by coordination of more complex substrates shown by Wu *et al.*[73]**

The group of Hartwig[65] developed a method for the cleavage of several lignin model compounds as well as organosolv lignin applying heterogeneous palladium on activated charcoal as catalyst (Scheme 1.26). Successful attempts in the cleavage of a simple lignin model **86** led to the formation of nearly quantitative amounts of acetophenone (**37**) and phenol (**88**) and traces of the oxidized substrate **89**. For more complex model compounds **87** or **54** no catalyst deactivation as found for homogeneous ruthenium complexes occurred. Partial decarbonylation of primary alcohol moieties was observed under slightly harsher reaction conditions; more complex product mixtures were obtained. Further tests showed that the hydrogen used for reduction truly originates from the substrate, moreover the transfer of H_2 from one species onto another lignin model was found possible.

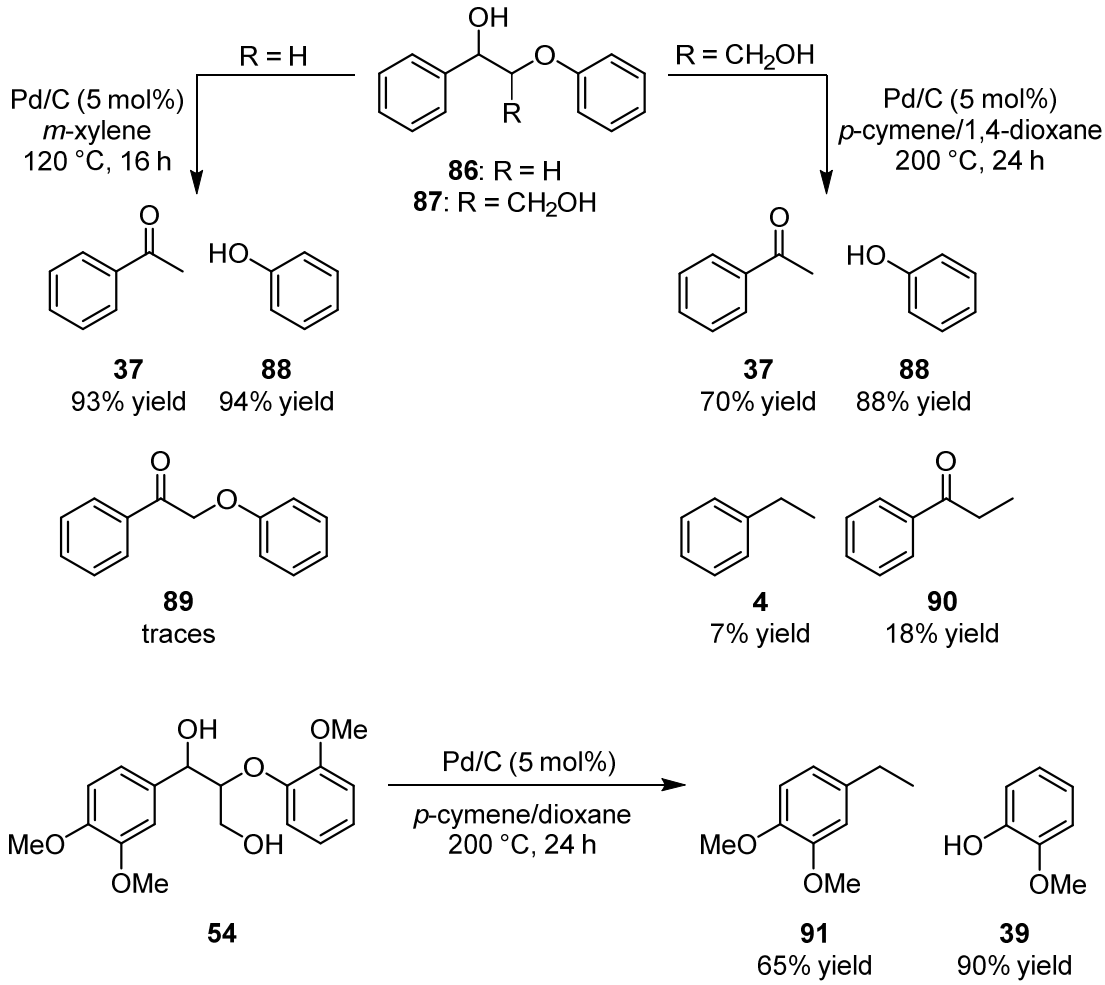

Scheme 1.26 **Cleavage of lignin models under redox neutral condition reported by the group of Hartwig.[65]**

After the successful degradation of synthetic lignin, the cleavage of authentic organosolv lignin failed in the first attempt. It was found that initial treatment with a low amount of Pd/C (1 mol%) under ambient pressure of hydrogen was necessary before the actual cleavage was possible with higher catalyst loading. It was speculated by the authors that aliphatic C–C double bonds, which are present in lignin from natural sources, first need to be saturated to make the ether hydrogenolysis possible. After pretreatment of the lignin samples with hydrogen or by performing the cleavage under a hydrogen atmosphere, a significant decrease in the average molar weight of the obtained fragments compared to the starting material was determined *via* gel permeation chromatography. However, next to the oily oligomeric fraction, a mixture of six monomeric aromatic products **92**–**94** was found after the reaction in collected yields of 9–15% dependent on the source of lignin and the extraction method (Scheme 1.27).

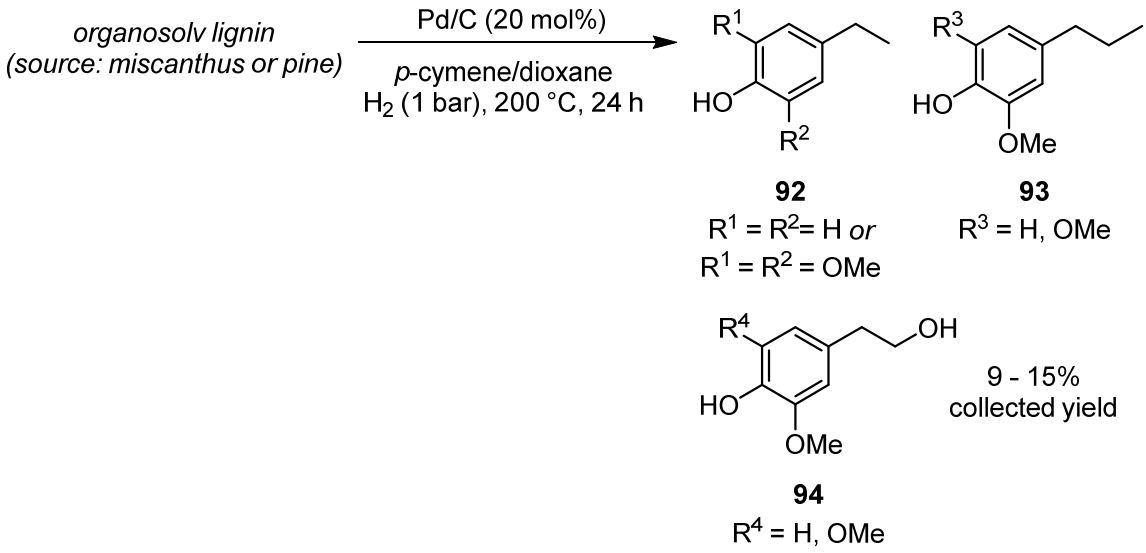

Scheme 1.27 **Redox neutral organosolv lignin degradation reported by Hartwig and co-workers. Prior treatment with a hydrogen atmosphere was necessary for successful cleavage.[65]**

Another method for the redox neutral cleavage of lignin models based on Pd/C was developed by the group of Samec,[66] in which instead of a prior substrate activation, as it was the case for Hartwig's lignin degradation protocol, an activation of the catalyst surface was found necessary. They discovered that the addition of catalytic amounts of a hydride donor was beneficial for the reaction, presumably to remove chemisorbed oxygen from the palladium surface. While hydrogen gas did have this desired effect, sodium borohydride was found superior because of its easier handling also on small scale. Under the optimized reaction conditions, the cleavage of ten lignin model compounds **95** and a lignin-like polymer **78** was achieved under relatively mild conditions in excellent yields (Scheme 1.28).

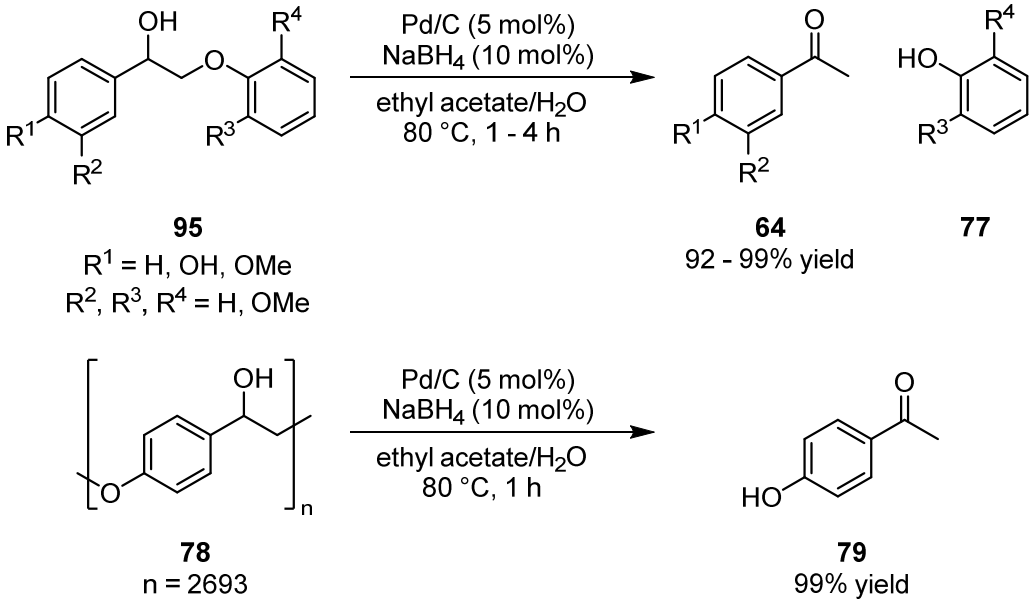

Scheme 1.28 **Redox neutral cleavage of lignin model compounds and a lignin model polymer developed by Samec and co-workers. Addition of catalytic amounts of reductant ensured the activation of the catalyst surface.[66]**

Further studies on limitations concerning the substrate structure showed that the corresponding aryl ketone is an important intermediate generated through dehydrogenation of the benzylic alcohol. Additionally a reaction mechanism was proposed (Scheme 1.29) based on adsorption of the substrate on the catalyst surface (A) *via* an enol intermediate (B). For the hydride transfer preceding the ether cleavage a Horiuti-Polanyi pathway[80] is assumed (C or E). This was based on the finding that both α- and β-hydrogens on the substrate participate in the reaction. Subsequent ether cleavage leads either to an adsorbed enol (D) or carbene (F) species which are released from the catalyst surface through desorption or carbene rearrangement, respectively, alongside the phenolic cleavage product.

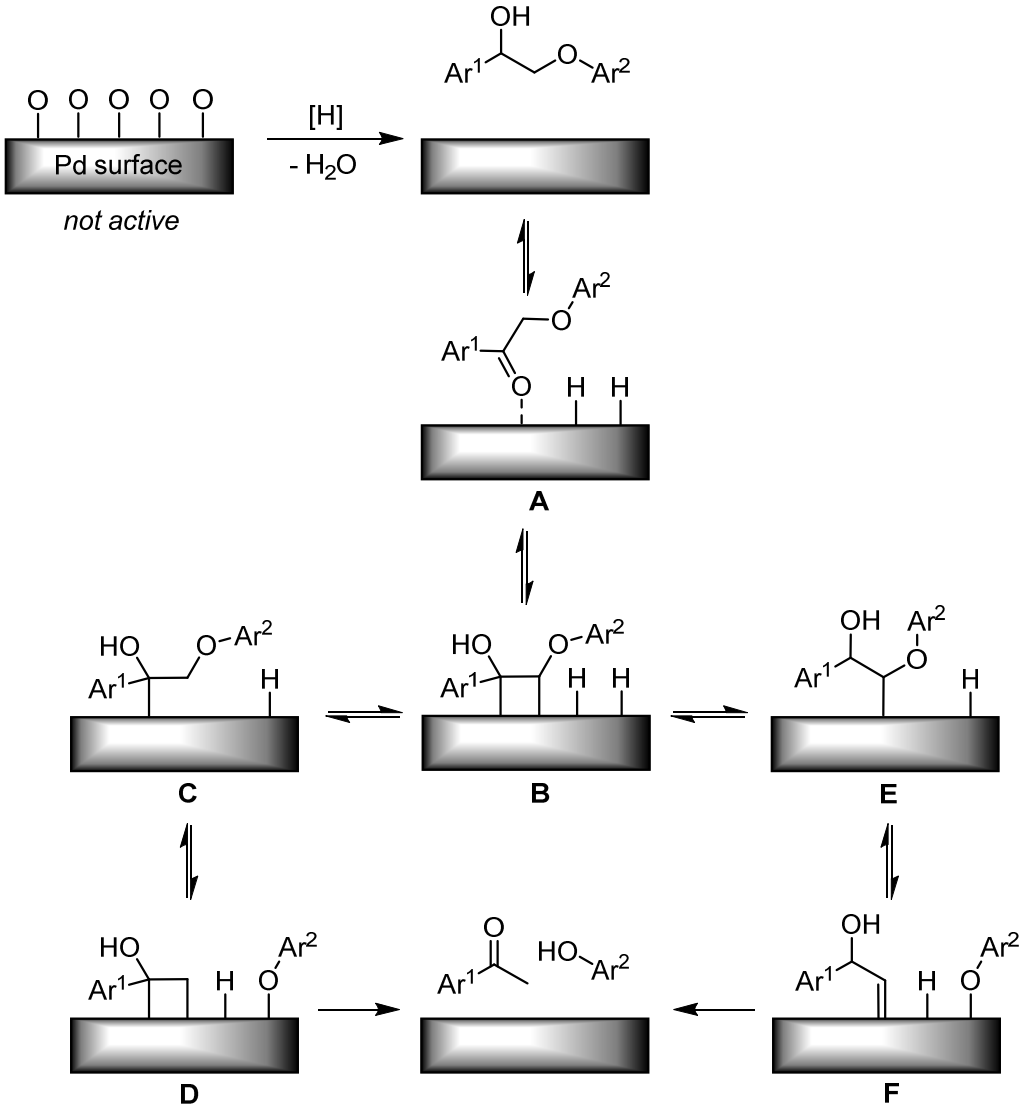

Scheme 1.29 **Proposed reaction mechanism for the redox neutral cleavage of lignin models on a palladium surface (adapted from the original publication).[66]**

When exploring homogeneous vanadium catalysts for the oxidation of lignin models, the group of Toste[76] found that the application of tridentate Schiff base ligands in vanadium-*oxo* complexes leads to a different reactivity: A redox-neutral cleavage of the lignin model **96** was observed, while the obtained product **98** was unprecedented in other works in that field (Scheme 1.30). Investigations of the role of the reaction atmosphere showed that under anaerobic conditions, a slow deactivation of the catalyst into a dimeric species occurred, while this was prevented by the presence of oxygen probably due to an oxidative reformation of the active catalyst. In both cases, no influence on the reaction outcome was observed. Variation on the substrate structure showed the importance of the benzylic hydroxyl group for successful transformation as well as of the presence of an aryloxy group.

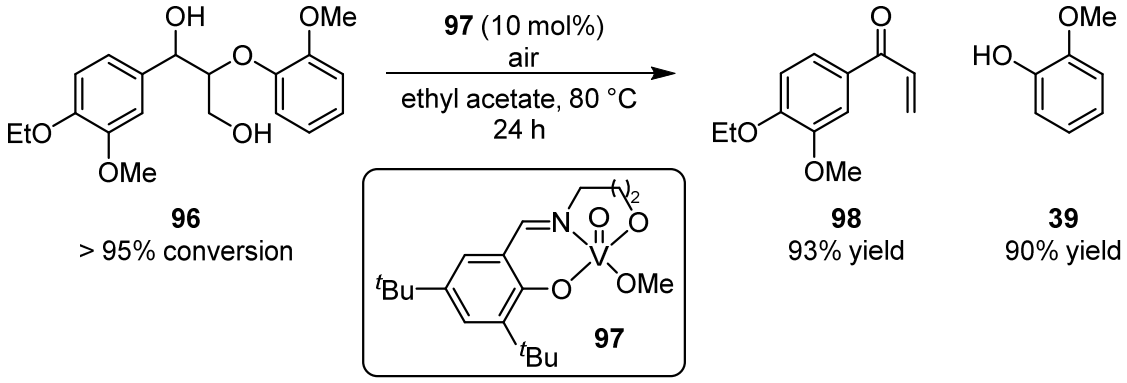

Scheme 1.30 **Redox-neutral cleavage of lignin model compounds reported by Toste and co-workers using a vanadium-*oxo* complex as catalyst.[76]**

Based on their findings, the authors propose a reaction mechanism involving a vanadium(V)/vanadium(IV) catalytic cycle. Unlike the previous methods discussed in this section, the oxidation of the benzylic alcohol moiety does not occur *through* dehydrogenation, but abstraction of a hydrogen atom. As the first mechanistic step the coordination of the alcohol substrate **96** occurs *via* ligand exchange on the vanadium(V) catalyst **97** to generate complex **99** (Scheme 1.31), followed by benzylic hydrogen atom abstraction to form a metal-bound ketyl radical species **100**. Rearrangement of the radical **100** leads to a homolytic C–O bond cleavage and elimination of an aryloxy radical, resulting in species **101**, in which an enolate is coordinated on the metal center. Release of the enone product **98** generates vanadium(IV) complex **102** or **103** which is reoxidized by the previously formed aryloxy radical to the active vanadium(V) species **97**. The dimeric lignin model substrate **96** could be converted into the respective cleavage products in very good yields. Also a trimeric model was transformed (not shown), giving the desired fragments in still good yields, showing the applicability of the catalyst system for more complex substrates.

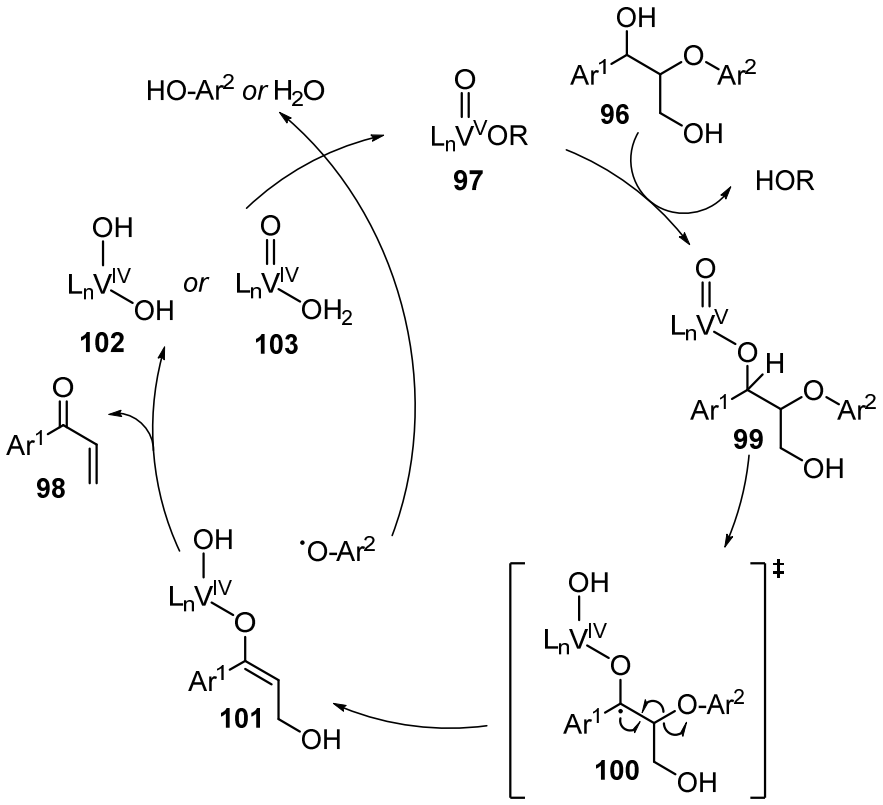

Scheme 1.31 **Proposed reaction mechanism for the redox neutral vanadium-catalyzed cleavage of lignin models (adapted from the original publication).[76]**

Another catalyst used for the cleavage of lignin models which does not rely on the dehydrogenation of the alcohol moiety is *in situ* generated methyldioxorhenium as shown by Cokoja, Kühn and co-workers.[77] The conversion of model substrate **104** was achieved at excellent conversion and yield of the cleavage products **105** and **39** under moderate temperature and catalyst loading (Scheme 1.32). The obtained products differ from other works as the carbonyl function is not found in benzylic position as usual in this class of transformations but in homobenzylic position. Notably, the catalyst could be reused in five consecutive runs without loss of activity, which is remarkable for homogeneous species. Unfortunately, the transformation of a more complex lignin model **54** bearing a γ-hydroxyl group led to very low amounts of the desired aldehyde **106**, next to the phenolic cleavage product **39** in good yield. Several side products were detected, which are thought to arise from reactions decomposing the aldehyde product. Nevertheless, the reaction pathways remain elusive.

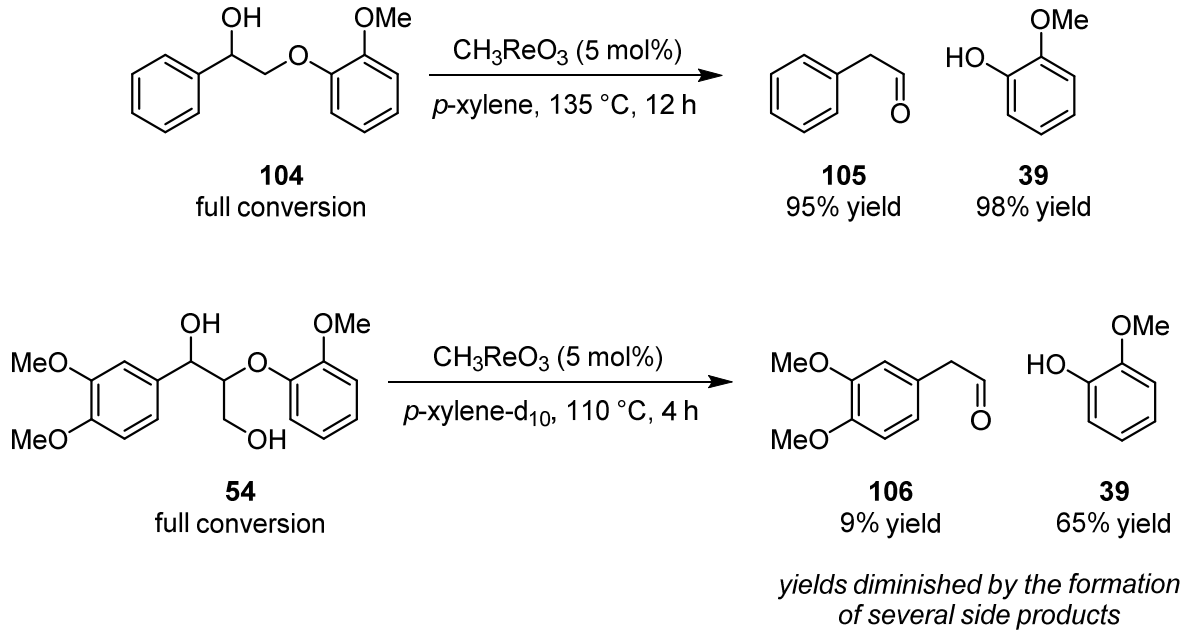

Scheme 1.32 **Redox neutral cleavage of simple and more complex lignin models catalyzed by methyltrioxorhenium developed by Cokoja, Kühn and co-workers.[77]**

To gain a better understanding of the reaction mechanism for the cleavage of the β-O-4 model **104**, the substrate was labeled with isotopes on the benzylic hydroxyl oxygen as well as on the α-hydrogen, also the catalyst itself was marked on the oxygen atoms, applying a ^{17}O enriched species. The experiments showed that an oxygen scrambling between substrate and catalyst occurs and no benzylic hydrogen abstraction was observed. Supplementary DFT calculations led to a proposed reaction mechanism (Scheme 1.33). At first, the introduced catalyst precursor methyltrioxorhenium is reduced by the substrate to methyldioxorhenium, the active catalytic species. A substrate molecule adds to the catalyst, generating a rhenium alkoxide species **108**. Elimination leads to an enol ether **109** and rhenium(V) bis(hydroxo) species **110**. Formal addition of an oxygen and a hydrogen atom from **110** to the double bond of **109** *via* **111** causes the cleavage of the alkyl aryl ether and in the same step forms the aldehyde product. Proton transfer to the generated phenolate regenerates the active catalyst.

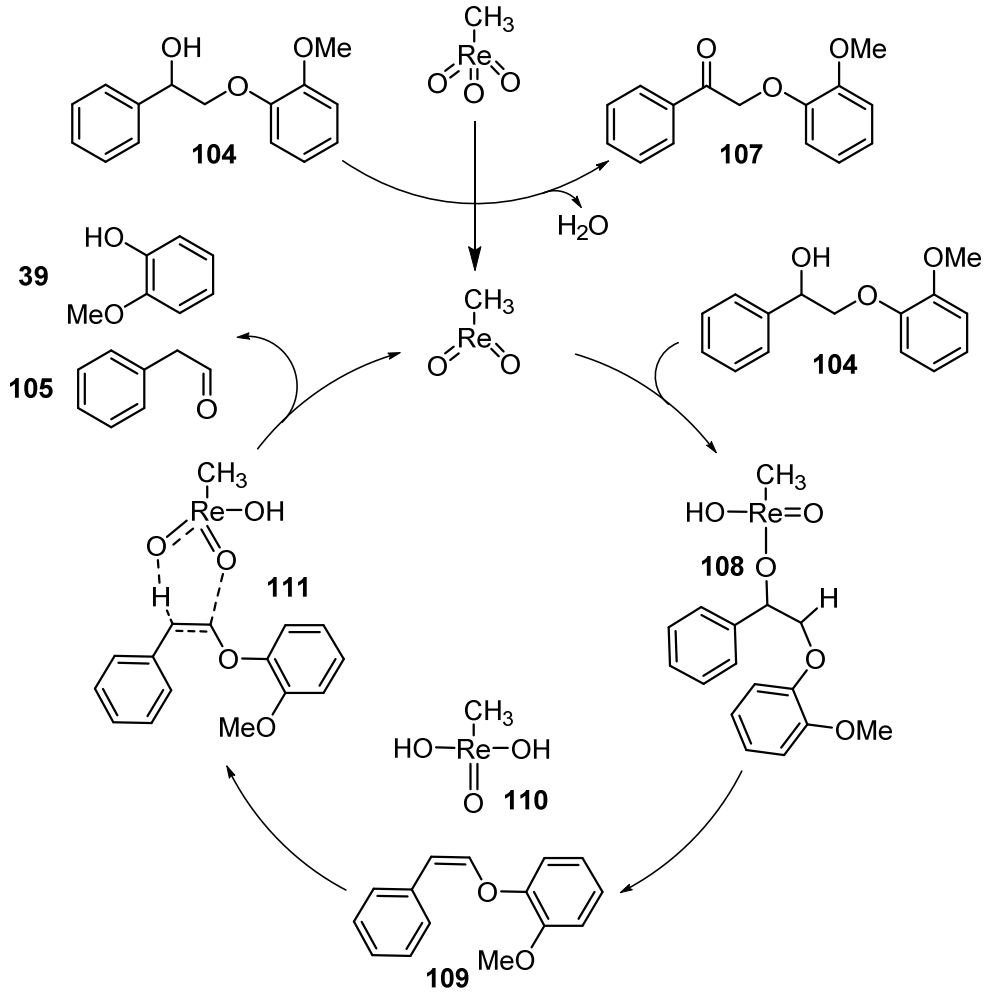

Scheme 1.33 **Proposed reaction mechanism for the methyldioxorhenium-catalyzed cleavage of lignin model compounds.[77]**

In this section, the role of lignin as renewable resource and potential alternative feedstock for the production of aromatic chemicals was discussed. Different approaches for the fractionation of lignocellulose were presented, which allow for the isolation of lignin in different states of structural modification. To convert the isolated lignin polymer into value-added chemicals, a great range of catalytic methods has been in development of which selected examples applying oxidative, reductive or redox neutral conditions were briefly treated. In this thesis, some efforts which were put into the catalytic cleavage of lignin model compounds and analogous substrates are discussed. The developed system and further investigations thereof are presented in section 4.2.

1.5 References

[1] Y. Y. Tye, K. T. Lee, N. Wan, A. Wan, C. P. Leh, *Renew. Sust. Energ. Rev.* **2016**, *60*, 155-172.

[2] P. N. R. Vennestrøm, C. M. Osmundsen, C. H. Christensen, E. Taarning, *Angew. Chem. Int. Ed.* **2011**, *50*, 10502-10509.

[3] C. O. Tuck, E. Pérez, I. T. Horváth, R. A. Sheldon, M. Poliakoff, *Science* **2012**, *337*, 695-699.

[4] P. Y. Dapsens, C. Mondelli, J. Pérez-Ramírez, *ACS Catal.* **2012**, *2*, 1487-1499.

[5] R. Luque, L. Herrero-Davila, J. M. Campelo, J. H. Clark, J. M. Hidalgo, D. Luna, J. M. Marinas, A. A. Romero, *Energy Environ. Sci.* **2008**, *1*, 542-564.

[6] G. W. Huber, S. Iborra, A. Corma, *Chem. Rev.* **2006**, *106*, 4044-4098.

[7] C. S. K. Lin, L. A. Pfaltzgraff, L. Herrero-Davila, E. B. Mubofu, S. Abderrahim, J. H. Clark, A. A. Koutinas, N. Kopsahelis, K. Stamatelatou, F. Dickson, S. Thankappan, Z. Mohamed, R. Brocklesby, R. Luque, *Energy Environ. Sci.* **2013**, *6*, 426-464.

[8] M. Raspolli, A. Galletti, C. Antonetti, in *Biorefinery: From Biomass to Chemicals and Fuels*, De Gruyter, Berlin, Boston, **2012**, pp. 101-122.

[9] F. G. Calvo-Flores, J. A. Dobado, *ChemSusChem* **2010**, *3*, 1227-1235.

[10] J. Zakzeski, P. C. A. Bruijnincx, A. L. Jongerius, B. M. Weckhuysen, *Chem. Rev.* **2010**, *110*, 3552-3599.

[11] P. J. Deuss, K. Barta, *Coord. Chem. Rev.* **2016**, *306*, 510-532.

[12] S. K. Hanson, R. T. Baker, *Acc. Chem. Res.* **2015**, *48*, 2037-2048.

[13] P. J. Deuss, K. Barta, J. G. de Vries, *Catal. Sci. Technol.* **2014**, *4*, 1174-1196.

[14] H. Kobayashi, H. Ohta, A. Fukuoka, *Catal. Sci. Technol.* **2012**, *2*, 869-883.

[15] C. Li, X. Zhao, A. Wang, G. W. Huber, T. Zhang, *Chem. Rev.* **2015**, *115*, 11559-11624.

[16] R. Ma, Y. Xu, X. Zhang, *ChemSusChem* **2015**, *8*, 24-51.

[17] R. Behling, S. Valange, G. Chatel, *Green Chem.* **2016**, *18*, 1839-1854.

[18] G. Chatel, R. D. Rogers, *ACS Sustain. Chem. Eng.* **2014**, *2*, 322-339.

[19] S.-H. Li, S. Liu, J. C. Colmenares, Y.-J. Xu, *Green Chem.* **2016**, *18*, 594-607.

[20] S. Kang, X. Li, J. Fan, J. Chang, *Renew. Sust. Energ. Rev.* **2013**, *27*, 546-558.

[21] W.-J. Liu, H. Jiang, H.-Q. Yu, *Green Chem.* **2015**, *17*, 4888-4907.

[22] E. I. Kozliak, A. Kubátová, A. A. Artemyeva, E. Nagel, C. Zhang, R. B. Rajappagowda, A. L. Smirnova, *ACS Sustain. Chem. Eng.* **2016**, *4*, 5106-5122.

[23] O. Y. Abdelaziz, D. P. Brink, J. Prothmann, K. Ravi, M. Sun, J. García-Hidalgo, M. Sandahl, C. P. Hulteberg, C. Turner, G. Lidén, M. F. Gorwa-Grauslund, *Biotechnol. Adv.* **2016**, *34*, 1318-1346.

[24] Z. Sun, B. Fridrich, A. de Santi, S. Elangovan, K. Barta, *Chem. Rev.* **2018**, *118*, 614-678.

[25] A. G. Vishtal, A. Kraslawski, *BioRes* **2011**, *6*, 3547-3568.

[26] F. S. Chakar, A. J. Ragauskas, *Ind. Crop. Prod.* **2004**, *20*, 131-141.

[27] M. Bunzel, A. Schüßler, G. Tchetseubu Saha, *J. Agr. Food Chem.* **2011**, *59*, 12506-12513.

[28] J. Lora in *Monomers, Polymers and Composites from Renewable Resources* (Eds.: M. N. Belgacem, A. Gandini), Elsevier, Amsterdam, **2008**, pp. 225-241.

[29] J. S. Kim, Y. Y. Lee, T. H. Kim, *Bioresour. Technol.* **2016**, *199*, 42-48.

[30] Q. Song, F. Wang, J. Xu, *Chem. Commun.* **2012**, *48*, 7019-7021.

[31] A. Fujimoto, Y. Matsumoto, H.-M. Chang, G. Meshitsuka, *J. Wood Sci.* **2005**, *51*, 89-91.
[32] S. Wu, D. Argyropoulos, *J. Pulp Pap. Sci.* **2003**, *29*, 235-240.
[33] A. Guerra, I. Filpponen, L. A. Lucia, D. S. Argyropoulos, *J. Agr. Food Chem.* **2006**, *54*, 9696-9705.
[34] A. Brandt, M. J. Ray, T. Q. To, D. J. Leak, R. J. Murphy, T. Welton, *Green Chem.* **2011**, *13*, 2489-2499.
[35] P. Verdía, A. Brandt, J. P. Hallett, M. J. Ray, T. Welton, *Green Chem.* **2014**, *16*, 1617-1627.
[36] A. M. Socha, R. Parthasarathi, J. Shi, S. Pattathil, D. Whyte, M. Bergeron, A. George, K. Tran, V. Stavila, S. Venkatachalam, M. G. Hahn, B. A. Simmons, S. Singh, *Proc. Natl. Acad. Sci.* **2014**, *111*, E3587-E3595.
[37] F. Ferdosian, C. Xu, *Conversion of Lignin into Bio-Based Chemicals and Materials*, Springer Nature, **2017**.
[38] G. H. Tomlinson, H. Hibbert, *J. Am. Chem. Soc.* **1936**, *58*, 348-353.
[39] V. E. Tarabanko, Y. V. Hendogina, D. V. Petuhov, E. P. Pervishina, *React. Kinet. Catal. Lett.* **2000**, *69*, 361-368.
[40] V. E. Tarabanko, D. V. Petukhov, G. E. Selyutin, *Kinet. Catal.* **2004**, *45*, 569-577.
[41] K. Pan, M. Tian, Z.-H. Jiang, B. Kjartanson, A. Chen, *Electrochim. Acta* **2012**, *60*, 147-153.
[42] H. Deng, L. Lin, Y. Sun, C. Pang, J. Zhuang, P. Ouyang, Z. Li, S. Liu, *Catal. Lett.* **2008**, *126*, 106.
[43] S. K. Hanson, R. Wu, L. A. P. Silks, *Angew. Chem. Int. Ed.* **2012**, *51*, 3410-3413.
[44] B. Sedai, C. Díaz-Urrutia, R. T. Baker, R. Wu, L. A. P. Silks, S. K. Hanson, *ACS Catal.* **2011**, *1*, 794-804.
[45] L. Hdidou, K. Khallouk, A. Solhy, B. Manoun, A. Oukarroum, A. Barakat, *Catal. Sci. Technol.* **2018**, *8*, 5445-5453.
[46] X. Liu, H. Zhang, C. Wu, Z. Liu, Y. Chen, B. Yu, Z. Liu, *New J. Chem.* **2018**, *42*, 1223-1227.
[47] Y. Cao, N. Wang, X. He, H.-R. Li, L.-N. He, *ACS Sustain. Chem. Eng.* **2018**, *6*, 15032-15039.
[48] H. Deng, L. Lin, Y. Sun, C. Pang, J. Zhuang, P. Ouyang, J. Li, S. Liu, *Energy Fuels* **2009**, *23*, 19-24.
[49] C. Zhu, W. Ding, T. Shen, C. Tang, C. Sun, S. Xu, Y. Chen, J. Wu, H. Ying, *ChemSusChem* **2015**, *8*, 1768-1778.
[50] W. Deng, H. Zhang, X. Wu, R. Li, Q. Zhang, Y. Wang, *Green Chem.* **2015**, *17*, 5009-5018.
[51] S. Kim, S. C. Chmely, M. R. Nimlos, Y. J. Bomble, T. D. Foust, R. S. Paton, G. T. Beckham, *J. Phys. Chem. Lett.* **2011**, *2*, 2846-2852.
[52] N. Luo, M. Wang, H. Li, J. Zhang, H. Liu, F. Wang, *ACS Catal.* **2016**, *6*, 7716-7721.
[53] C. S. Lancefield, O. S. Ojo, F. Tran, N. J. Westwood, *Angew. Chem. Int. Ed.* **2015**, *54*, 258-262.
[54] L. M. Cooke, J. L. McCarthy, H. Hibbert, *J. Am. Chem. Soc.* **1941**, *63*, 3056-3061.
[55] H. P. Godard, J. L. McCarthy, H. Hibbert, *J. Am. Chem. Soc.* **1941**, *63*, 3061-3066.
[56] E. E. Harris, J. D'Ianni, H. Adkins, *J. Am. Chem. Soc.* **1938**, *60*, 1467-1470.
[57] C. Chauvier, T. Cantat, *ACS Catal.* **2017**, *7*, 2107-2115.
[58] M. Zaheer, R. Kempe, *ACS Catal.* **2015**, *5*, 1675-1684.
[59] A. G. Sergeev, J. F. Hartwig, *Science* **2011**, *332*, 439-443.

[60] Q. Song, F. Wang, J. Cai, Y. Wang, J. Zhang, W. Yu, J. Xu, *Energy Environ. Sci.* **2013**, *6*, 994-1007.
[61] J. M. Nichols, L. M. Bishop, R. G. Bergman, J. A. Ellman, *J. Am. Chem. Soc.* **2010**, *132*, 12554-12555.
[62] A. Wu, B. O. Patrick, E. Chung, B. R. James, *Dalton Trans.* **2012**, *41*, 11093-11106.
[63] T. vom Stein, T. Weigand, C. Merkens, J. Klankermayer, W. Leitner, *ChemCatChem* **2013**, *5*, 439-441.
[64] Y. Ren, M. Yan, J. Wang, Z. C. Zhang, K. Yao, *Angew. Chem. Int. Ed.* **2013**, *52*, 12674-12678.
[65] F. Gao, J. D. Webb, H. Sorek, D. E. Wemmer, J. F. Hartwig, *ACS Catal.* **2016**, 7385-7392.
[66] M. V. Galkin, C. Dahlstrand, J. S. M. Samec, *ChemSusChem* **2015**, *8*, 2187-2192.
[67] M. V. Galkin, S. Sawadjoon, V. Rohde, M. Dawange, J. S. M. Samec, *ChemCatChem* **2014**, *6*, 179-184.
[68] E. Feghali, T. Cantat, *Chem. Commun.* **2014**, *50*, 862-865.
[69] A. G. Sergeev, J. D. Webb, J. F. Hartwig, *J. Am. Chem. Soc.* **2012**, *134*, 20226-20229.
[70] E. Feghali, G. Carrot, P. Thuéry, C. Genre, T. Cantat, *Energy Environ. Sci.* **2015**, *8*, 2734-2743.
[71] Y. Shao, Q. Xia, L. Dong, X. Liu, X. Han, S. F. Parker, Y. Cheng, L. L. Daemen, A. J. Ramirez-Cuesta, S. Yang, Y. Wang, *Nat. Commun.* **2017**, *8*, 16104.
[72] J. M. Nichols, L. M. Bishop, R. G. Bergman, J. A. Ellman, *J. Am. Chem. Soc.* **2010**, *132*, 12554-12555.
[73] A. Wu, B. O. Patrick, E. Chung, B. R. James, *Dalton Trans.* **2012**, *41*, 11093-11106.
[74] A. Wu, J. M. Lauzon, B. R. James, *Catal. Lett.* **2015**, *145*, 511-518.
[75] X. Zhou, J. Mitra, T. B. Rauchfuss, *ChemSusChem* **2014**, *7*, 1623-1626.
[76] S. Son, F. D. Toste, *Angew. Chem. Int. Ed.* **2010**, *49*, 3791-3794.
[77] R. G. Harms, I. I. E. Markovits, M. Drees, W. A. Herrmann, M. Cokoja, F. E. Kühn, *ChemSusChem* **2014**, *7*, 429-434.
[78] Y. Jiang, Z. Li, X. Tang, Y. Sun, X. Zeng, S. Liu, L. Lin, *Energy Fuels* **2015**, *29*, 1662-1668.
[79] N. Luo, M. Wang, H. Li, J. Zhang, T. Hou, H. Chen, X. Zhang, J. Lu, F. Wang, *ACS Catal.* **2017**, *7*, 4571-4580.
[80] I. Horiuti, M. Polanyi, *Trans. Faraday Soc.* **1934**, *30*, 1164-1172.

1.6 Determination of active catalyst species in transition metal-mediated reactions

1.6.1 Classification of different catalyst types

When investigating a chemical reaction catalyzed by a transition metal-based species, a clear image of the operating catalyst is of utmost importance for an understanding of the reaction mechanism as well as to solve problems during the optimization or with potentially occurring substrate incompatibilities. Historically, in 1902 Ostwald distinguished between several classes of catalysts. Next to enzymatic actions, a differentiation was made between homogeneous and heterogeneous catalysts, i.e. catalysts that are present in the same or a different phase as the reactants they interact with, respectively.[1]

However, from today's point of view, no such clear distinction is possible anymore, as works on metal clusters, nanoparticles or colloids are bridging the gap between those two basic concepts of metal catalysis by uniting properties of homogeneous and heterogeneous catalysts (Figure 1.3).[2,3]

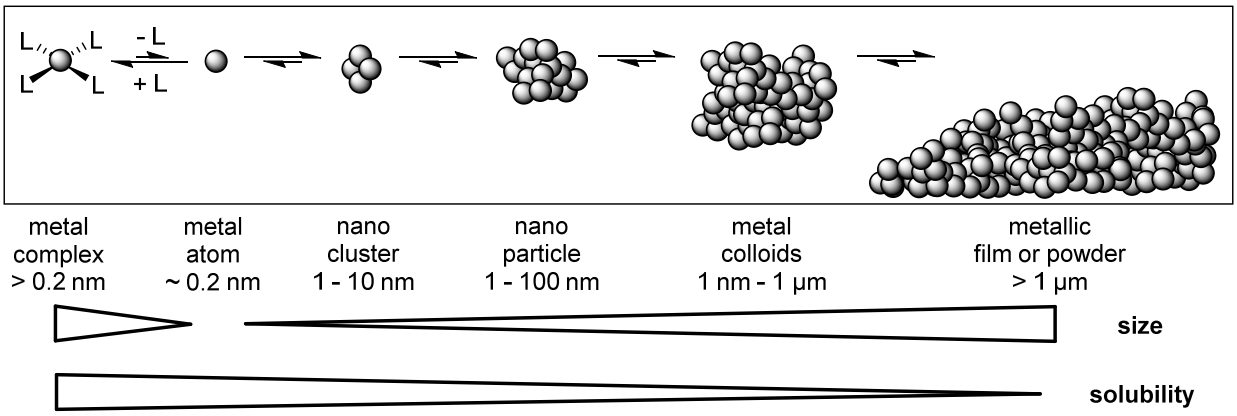

Figure 1.3 **Correlation of size and solubility of different metal catalysts (L: ligand; adapted from the original publication).[4]**

To clarify the ambiguous use of the terms *homogeneous* and *heterogeneous*, Schwartz proposed a new classification for catalysts, not depending on solubility, but rather on the number and character of the active sites included.[5] Based on this concept, Crabtree introduced the concept of *homotopicity* and *heterotopicity*. A homotopic catalyst exhibits only one kind of active site, e.g. a mononuclear metal complex, while a heterotopic catalyst offers several different active sites, like a metal nanoparticle in which the contained atoms show varying activity depending on their position on the particle surface.[6] Nonetheless, this thesis will remain with the general nomenclature of homogeneous and heterogeneous catalysis as this concept is used by a major part of the groups working in the field of catalyst characterization and the known experimental tests in the literature distinguish between those

two types. Dissolved monometallic complexes will be referred to as homogeneous catalysts, while bulk metal, colloids or nanoparticles are considered heterogeneous.

Introducing a defined metal salt or complex into a catalytic reaction, one cannot assume that the applied species is the active catalyst, especially under reducing conditions.[7] Furthermore, under addition of other coordinating compounds, the *in situ* formation of other species is possible whose structure and activity rely on the stoichiometry of the added precursors. Besides the generation of a soluble complex, a dissolved metal precursor can also lead to the formation of non-coordinated metal atoms, which then form larger aggregates dispersed in the solvent, like nanoparticles or colloids, or even insoluble bulk metal present as mirrors or films. While the latter is easy to detect by the naked eye, smaller heterogeneous species like nanoparticles may let a reaction solution appear homogeneous, leading to the false assumption of an operating homogeneous catalyst. Therefore, it is important to apply suitable methods to distinguish between homogeneous, soluble catalyst species and dispersed heterogeneous metal particles.[6,7] In systems exhibiting so-called *cocktails catalysis*, i.e. the simultaneous presence of several different homogeneous and heterogeneous catalyst species, this differentiation can be particularly difficult.[8,9]

1.6.2 Distinction between homogeneous and heterogeneous catalysis

A great number of experiments has been used to distinguish between homogeneous and heterogeneous catalysts. Generally, there is no single test which can give a definite result. It is always necessary to perform several complementary investigations to arrive at a solid conclusion, as it was shown by several previous studies on catalyst characterization.[10-16] Therein, possible incompatibilities of certain tests with some kinds of catalysts have to be considered to prevent false results.

Amongst these tests, a differentiation has to be made between *in operando* and *post operandum* methods. While the first kind gains information about the catalysts while it is active in the reaction, the latter relies on isolation and subsequent investigation of the catalyst material, this may lead to problems which will be adressed later in this section. In the following, the most important *in operando* and *post operandum* techniques for catalyst characterization will be discussed.

Kinetic studies and reaction progress analyses

Catalysis is generally considered a wholly kinetic phenomenon.[17] Thus, kinetic investigations should deliver the most relevant results concerning the nature of the active catalyst. Three *in operando* observables, which allow for conclusions about the active catalyst species being homogeneous or heterogeneous, are the shape of the kinetic profile,

the reproducibility of the reaction progress *versus* time and the comparison of the course of the catalyst precursor decomposition with that of the product formation.[7]

For monitoring a catalyzed reaction, the product yield or the consumption of substrate at defined reaction times are typically plotted against time, yielding a kinetic curve which can either show a linear or sigmoidal shape (Figure 1.4).[7,18] A sigmoidal kinetic curve hints at an active heterogeneous catalyst, as an induction period is observed, during which no substrate conversion occurs. This is due to metal particle formation from a soluble precursor and aggregation thereof. The duration of this lag phase strongly depends on the growth rate of the catalyst particles. In case of a fast aggregation, e.g. in the formation of small nanoparticles, the kinetic plot may resemble the homogeneous case where no induction period is observed.[19] For this reason, it can be stated that the presence of an induction period is a strong evidence for an operating heterogeneous catalyst. Although, if no lag phase is observed, this can be caused by an active homogeneous catalyst, but also by the very fast formation of small dispersed metal particles.[7,18]

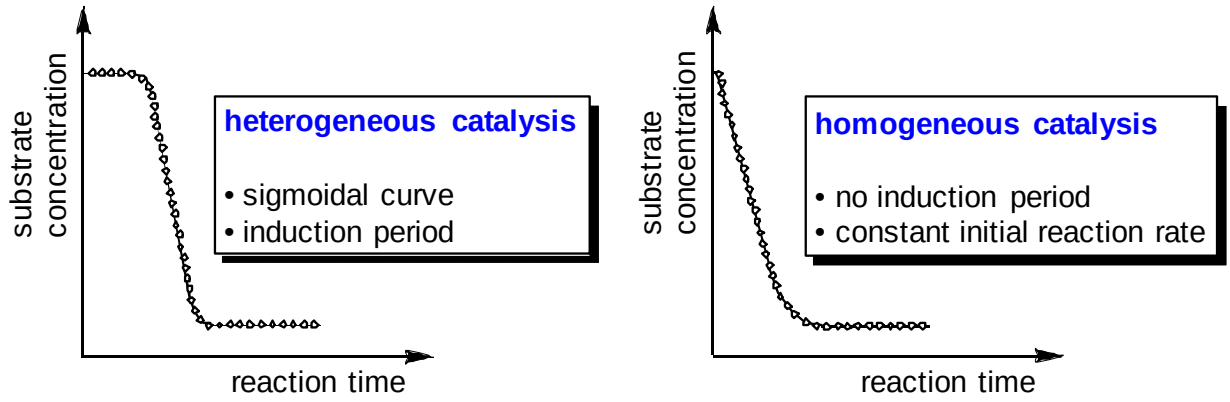

Figure 1.4 **Typical shapes of kinetic curves for a heterogeneously or homogeneously catalyzed reaction (schematic representation).**

The reproducibility of the reaction kinetics is often thought to be a good indicator for the active catalyst species, as homogeneous catalysts show well reproducible kinetics, while heterogeneous ones do not. However, this cannot be taken as evidence for both cases as there are works known on heterogeneous nanoclusters which gave very well reproducible kinetics.[12] So non-reproducible kinetics propose an active heterogeneous catalyst, for the opposite case further investigations are necessary to distinguish between a nanoparticulate and a truly homogeneous catalyst.

If it is possible to monitor the decomposition of the metal precursor into metal particles, the kinetics of this transformation can also be a useful tool for catalyst characterization.[12,19-21] Through comparing the kinetics of the precursor decomposition with that of the product formation, conclusions regarding the active catalyst can be drawn: If both processes show similar shapes of the kinetic curves including identical induction periods, the presence of an active heterogeneous catalysts can be assumed. In this case, measuring of

the reaction rate right after complete catalyst precursor decomposition should give a maximum value as agglomeration or other kinds of catalyst deactivation are not or only slightly active.[7]

Selective catalyst poisoning experiments

A method related to the interpretation of the kinetics of a catalyzed reaction is the poisoning of the catalyst to render it inactive. This *in operando* technique offers the advantage to manipulate the catalyst in its already active state by the simple addition of an inhibiting agent. Therein, qualitative or quantitative poisons can be used.

Qualitative poisoning yields information on the active catalyst *via* selective inhibition of either a homogeneous or heterogeneous species. Quantitative poisons cause deactivation of the catalyst independent of its character. The extent of inhibition depends only on the amount of added poison (Scheme 1.34).[7]

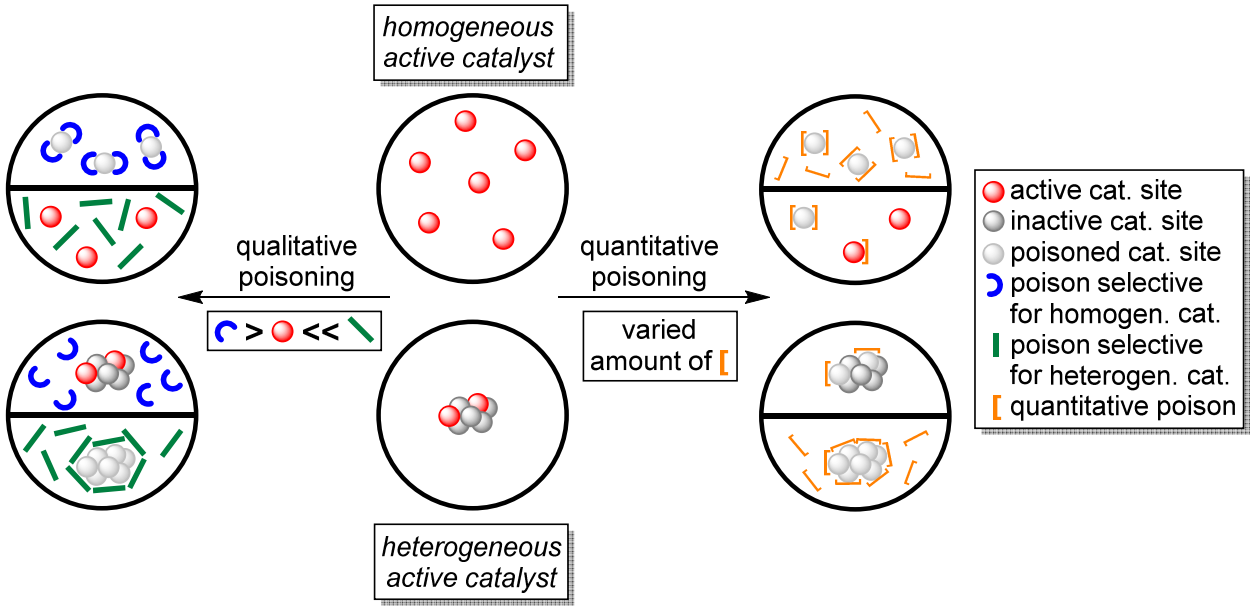

Scheme 1.34 **Inhibition of metal catalysts by different types of catalyst poisons (adapted from the original publication).[4]**

For transition metal catalysts, the most popular qualitative poisoning test, which was already described in the early 20th century,[22] consists in the addition of mercury to the reaction medium.[10-13,15,16,23-26] If suppression of the catalytic reaction is observed, this is considered evidence for an operationally heterogeneous catalyst. Homogeneous metal catalysts are usually shielded by coordinating ligands, thereby deactivation is prevented. The inhibition results from the adsorption of mercury to the metal surface or the formation of amalgams[23] (Scheme 1.35). Yet, this limits the applicability of the test. While group 10 metals, which are known to form amalgams, are effectively poisoned,[12] metals from group 8 or 9 like iridium, rhodium or ruthenium are mostly unaffected.[23] Another drawback is the low

solubility of mercury in organic solvents. To ensure sufficient contact of the poison with the metal catalyst, a high excess needs to be added under vigorous stirring.[12,13] Furthermore, mercury can cause unwanted side reactions[23] and was also shown to react with mononuclear metal complexes.[15,23,27-31] The latter contradicts to the expected exclusive effect of the test on heterogeneous catalysts.

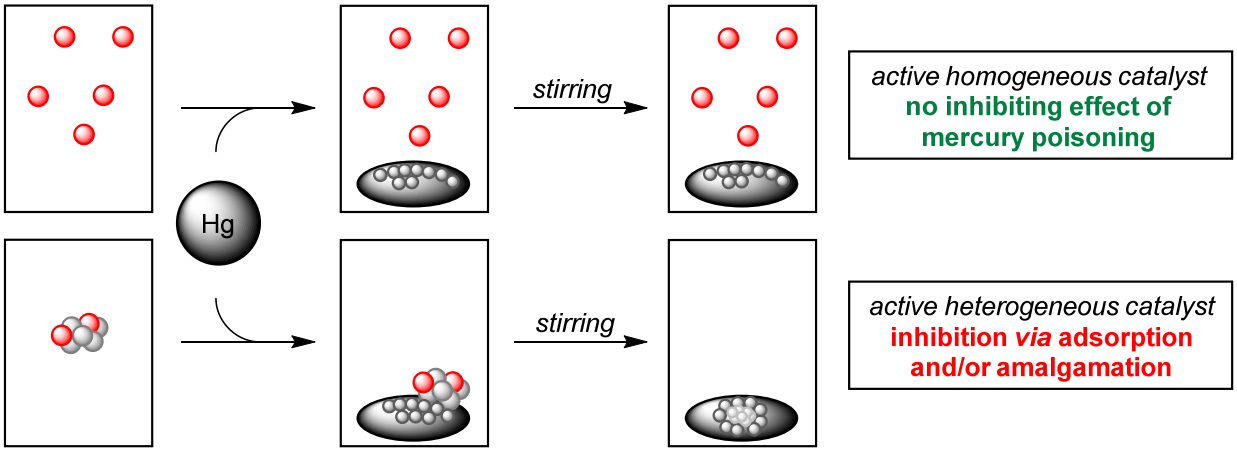

Scheme 1.35 **Effects of the addition of mercury to different types of catalysts (adapted from the original publication).[4]**

Although the test is easy to perform, some working groups applied the method in an incorrect manner, e.g. by just stirring mercury with the precatalyst and subsequent filtering of the solution to start the catalytic reaction without any poison present.[25] To gain useful information, mercury has to be present while the active catalyst is formed. To ensure that, exemplary literature procedures propose the presence of the poison for the full reaction time or the addition only after the reaction has already proceeded to a significant extent.[12,13,16] To evade misinterpretation of experimental results, control experiments should be performed. In case of a positive mercury test, it should be checked if the applied precatalyst reacts with mercury as well. If this is the case, the result of the poisoning test becomes ambiguous. If the addition of mercury has no effect on the reaction and a homogeneous species is presumed to be catalytically active, the influence of the poison on an authentic heterogeneous catalyst should be investigated to give a different result. These control experiments can then deliver solid proof for the characterization of the active catalyst.[16]

A complementary qualitative poisoning test for the selective inhibition of homogeneous catalysts was developed by Crabtree and co-workers.[10] Dibenzo[*a,e*]cyclooctatetraene (dct) was found to deactivate platinum group metal catalysts. The selectivity of the poisoning is assumed to be caused by the rigid tub-like structure of dct, which allows strong coordination through the contained diene moiety and its strong π-acceptor ability (Scheme 1.36). In addition, the sterically demanding structure hinders the adsorption to metal surfaces, which

results in a low effect on heterogeneous catalysts.[6,7,10] Dct was applied as a selective catalyst poison to investigate the homogeneous or heterogeneous character of a number of catalyst systems.[32-43] Furthermore, soluble metal complexes of dct were synthesized and characterized, e.g. for chromium,[44,45] molybdenum,[45] ruthenium,[46] cobalt,[32] rhodium,[47-49] iridium,[48-50] palladium,[51] platinum[51] and copper[52] (Scheme 1.36).

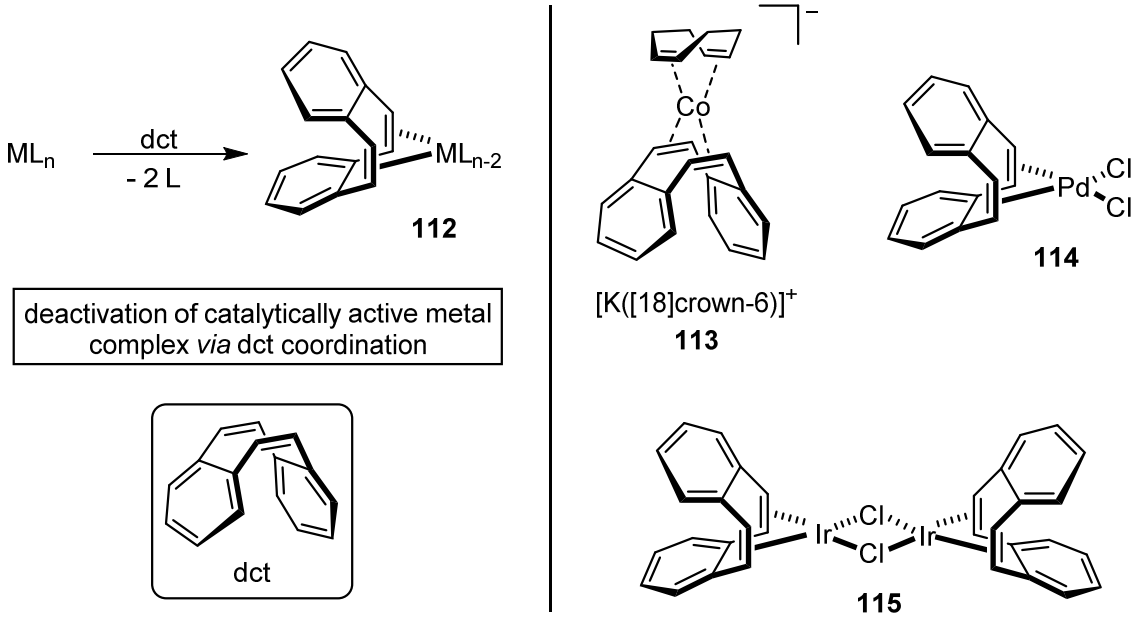

Scheme 1.36 General deactivation pathway for homogeneous metal catalysts *via* dct coordination, selected examples for characterized dct-transition metal complexes.[10,32,49,51]

Non-selective, quantitative catalyst poisoning experiments

In contrast to qualitative catalyst poisons, which yield information about the active catalyst through a specific reactivity or binding affinity, quantitative poisons, like carbon disulfide, phosphines, phosphites or thiophene, allow the investigation of an active catalyst species based on the applied stoichiometry. These ligands bind non-selectively to metal centers and surfaces, blocking the active sites.[12,15,16,53,54] Herein, it is made use of the fact that for a homogeneous, mononuclear catalyst, in theory every introduced metal atom poses a catalytically active site. In case of a heterogeneous system only a part of the total amount of metal, which is placed on the surface of a bulk metal precipitate or a metal particle as active sites, takes part in the catalysis. The residual metal atoms in the bulk have no contact to the reaction medium, and therefore do not contribute to the catalytic activity.[12,19] The varying inhibiting effect of different amounts of poison added to the catalytic reaction can be observed *via* a reaction progress analysis (Figure 1.5).

For homogeneous as for heterogeneous systems, poison amounts far below 1.0 equivalent relative to the metal catalyst result in a partial inhibition and thus a retardation of the reaction. However, with increasing amounts of catalyst poison, the two systems will show different behavior. While a heterogeneous catalyst is completely inhibited by less than 1.0 equivalent

of poison, an excess of poison far above 1.0 equivalent is needed to stop a homogeneously catalyzed reaction. This can be rationalized by the described difference in the available active metal atoms. Yet, this method is limited to reactions operating under relatively low temperatures (below 50 °C), since at higher temperatures the introduced poisons start to dissociate from a heterogeneous metal surface, thus the catalytic activity is restored.[16,55,56]

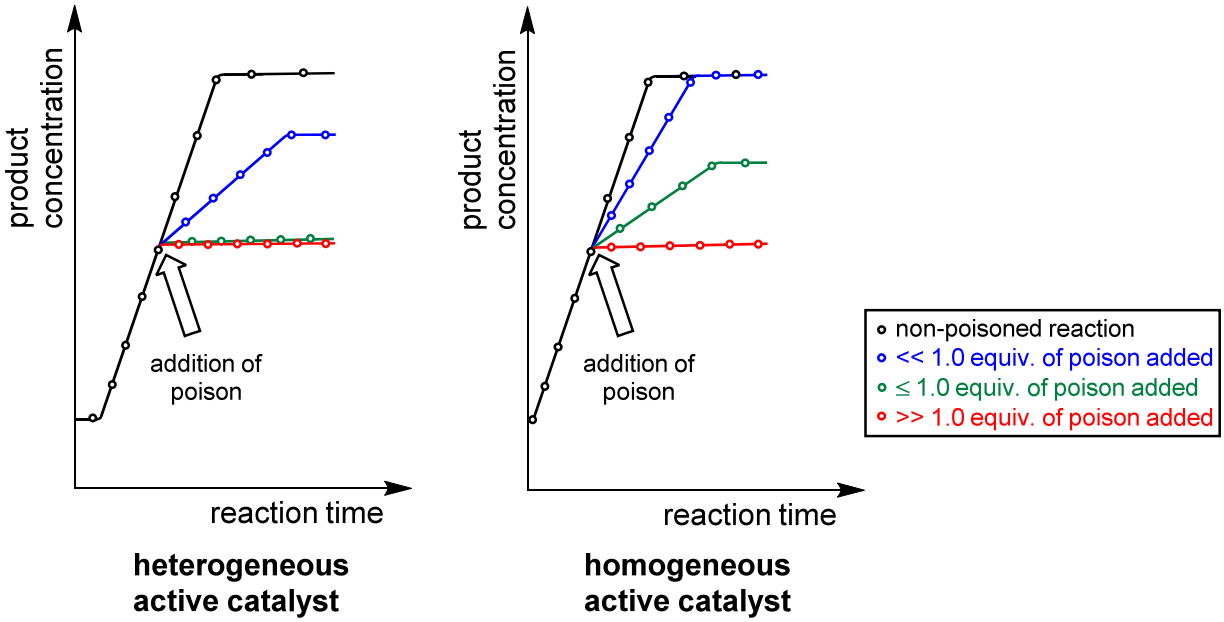

Figure 1.5 **Visualization of quantitative poisoning of homogeneous and heterogeneous catalyst systems in reaction progress plots (schematic representation).**

Collman's three-phase-test

Another *in operando* technique constitutes in the three-phase-test. This method includes a cross-linked polymer to which either a substrate suitable for the investigated catalyst or a catalyst poison are covalently bound. When the polymer beads are introduced into the reaction medium in presence of the catalyst, only soluble catalyst species are able to enter the pores of the polymer to reach either the substrate or the poison.[57] Therefore, a different reaction outcome can be observed for homogeneous or heterogeneous catalysts. Notwithstanding, some control experiments are necessary to verify the obtained results, e.g. if a polymer-bound substrate is actually converted by an authentic soluble catalyst species. Furthermore, a false positive result proposing a homogeneous catalyst can be obtained if small metal nanoparticles are formed, which are able to enter the polymer to convert the substrate.[58] This should be ruled out by using priorly prepared, defined nanoparticles in the test.

Maitlis' hot filtration test

If the formation of solid metal precipitate is suspected, a hot filtration test may be suitable to detect a heterogeneous catalyst.[59] It comprises the use of some filter aid, e.g. powdered celite,[10] cellulose[59] or graphite,[60] which is added to the reaction mixture. Afterwards, filtration over a glass frit is performed to separate the adsorbed catalyst material from the reaction medium. The two obtained fractions, filtrate and filter aid with presumably adhering metal particles, are both examined for catalytic activity. In case the filtrate converts freshly added substrate, the presence of an active homogeneous catalyst is assumed. If substrate conversion is observed on the filter aid, the active heterogeneous catalyst was held back in the filtration step.[6,7]

Despite that the method is easy to perform and no special equipment is necessary in most cases, it suffers some drawbacks. For nanoparticulate catalysts, the pore size of the filter aid may not be sufficiently small, leading to the heterogeneous catalyst passing through the filter.[59] In addition, maintaining *in operando* conditions during the filtration step may not be possible. During or after the manipulation, the formation of heterogeneous catalyst species in the homogeneous fraction can occur, leading to a false positive result.[61] Therefore it should be kept in mind that this method may yield rather *post operandum* information.

Transmission electron microscopy

To determine the presence of nanoparticles in a reaction mixture, transmission electron microscopy (TEM) poses a sensitive *post operandum* technique.[11,12] Even very low particle concentrations down to 10^{-12} M can be detected.[7] However, TEM gives no information on the catalytic activity of the found particles.[7] Another drawback is the sample preparation, which consists in deposition of a drop of the reaction mixture on a grid, followed by evaporation of the solvent. This procedure was shown to promote the formation of metal nanoparticles from a dissolved homogeneous species.[28] It has to be mentioned that the applied electron beam may also induce particle formation.[62] Besides, another limitation of this method is the size of the investigated particles, as nanoparticles with an average size below 1 nm are not detected.[63] Despite the mentioned drawbacks, TEM is an excellent method for the characterization of catalysts when applied together with other analysis techniques.

In this section, the most viable *in operando* and *post operandum* methods for catalyst characterization and the distinction between homogeneous and heterogeneous catalysts were discussed. Due to the nature of catalysis as a kinetic phenomenon, *in operando* investigations like reaction progress analyses or selective catalyst poisoning hold most useful information about the studied catalyst system. Other methods rely on differences in the solubility of homogeneous and heterogeneous species or on microscopic detection of formed metal particles. One project covered in this thesis also includes the characterization of the active catalyst as either homogeneous or heterogeneous, some of the mentioned methods were used therefore. The obtained results are discussed in section 3.3.

1.7 References

[1] W. Ostwald, *Nature* **1902**, *65*, 522-526.
[2] D. Astruc, F. Lu, J. R. Aranzaes, *Angew. Chem. Int. Ed.* **2005**, *44*, 7852-7872.
[3] A. Roucoux, J. Schulz, H. Patin, *Chem. Rev.* **2002**, *102*, 3757-3778.
[4] D. Gärtner, Dissertation, Universität Regensburg **2016**.
[5] J. Schwartz, *Acc. Chem. Res.* **1985**, *18*, 302-308.
[6] R. H. Crabtree, *Chem. Rev.* **2012**, *112*, 1536-1554.
[7] J. A. Widegren, R. G. Finke, *J. Mol. Catal. A: Chem.* **2003**, *198*, 317-341.
[8] V. P. Ananikov, I. P. Beletskaya, *Organometallics* **2012**, *31*, 1595-1604.
[9] D. B. Eremin, V. P. Ananikov, *Coord. Chem. Rev.* **2017**, *346*, 2-19.
[10] D. R. Anton, R. H. Crabtree, *Organometallics* **1983**, *2*, 855-859.
[11] L. N. Lewis, N. Lewis, *J. Am. Chem. Soc.* **1986**, *108*, 7228-7231.
[12] Y. Lin, R. G. Finke, *Inorg. Chem.* **1994**, *33*, 4891-4910.
[13] K. S. Weddle, J. D. Aiken, R. G. Finke, *J. Am. Chem. Soc.* **1998**, *120*, 5653-5666.
[14] R. H. Crabtree, M. F. Mellea, J. M. Mihelcic, J. M. Quirk, *J. Am. Chem. Soc.* **1982**, *104*, 107-113.
[15] R. van Asselt, C. J. Elsevier, *J. Mol. Catal.* **1991**, *65*, L13-L19.
[16] J. A. Widegren, M. A. Bennett, R. G. Finke, *J. Am. Chem. Soc.* **2003**, *125*, 10301-10310.
[17] J. Halpern, *Inorg. Chim. Acta* **1981**, *50*, 11-19.
[18] C. M. Hagen, J. A. Widegren, P. M. Maitlis, R. G. Finke, *J. Am. Chem. Soc.* **2005**, *127*, 4423-4432.
[19] M. A. Watzky, R. G. Finke, *J. Am. Chem. Soc.* **1997**, *119*, 10382-10400.
[20] J. A. Widegren, J. D. Aiken, S. Özkar, R. G. Finke, *Chem. Mater.* **2001**, *13*, 312-324.
[21] J. A. Widegren, R. G. Finke, *Inorg. Chem.* **2002**, *41*, 1558-1572.
[22] C. Paal, W. Hartmann, *Ber. Dtsch. Chem. Ges.* **1918**, *51*, 711-737.
[23] G. M. Whitesides, M. Hackett, R. L. Brainard, J. P. P. M. Lavalleye, A. F. Sowinski, A. N. Izumi, S. S. Moore, D. W. Brown, E. M. Staudt, *Organometallics* **1985**, *4*, 1819-1830.
[24] P. Foley, R. DiCosimo, G. M. Whitesides, *J. Am. Chem. Soc.* **1980**, *102*, 6713-6725.
[25] G. Süss-Fink, M. Faure, T. R. Ward, *Angew. Chem. Int. Ed.* **2002**, *41*, 99-101.
[26] L. N. Lewis, *J. Am. Chem. Soc.* **1986**, *108*, 743-749.
[27] R. A. Jones, F. M. Real, G. Wilkinson, A. M. R. Galas, M. B. Hursthouse, *J. Chem. Soc., Dalton Trans.* **1981**, 126-131.

[28] J. Stein, L. N. Lewis, Y. Gao, R. A. Scott, *J. Am. Chem. Soc.* **1999**, *121*, 3693-3703.
[29] P. J. Dyson, *Dalton Trans.* **2003**, 2964-2974.
[30] N. T. S. Phan, M. Van Der Sluys, C. W. Jones, *Adv. Synth. Catal.* **2006**, *348*, 609-679.
[31] O. N. Gorunova, I. M. Novitskiy, Y. K. Grishin, I. P. Gloriozov, V. A. Roznyatovsky, V. N. Khrustalev, K. A. Kochetkov, V. V. Dunina, *Organometallics* **2018**, *37*, 2842-2858.
[32] P. Büschelberger, D. Gärtner, E. Reyes-Rodriguez, F. Kreyenschmidt, K. Koszinowski, A. Jacobi von Wangelin, R. Wolf, *Chem. Eur. J.* **2017**, *23*, 3139-3151.
[33] U. Chakraborty, E. Reyes-Rodriguez, S. Demeshko, F. Meyer, A. Jacobi von Wangelin, *Angew. Chem. Int. Ed.* **2018**, *57*, 4970-4975.
[34] U. Chakraborty, S. Demeshko, F. Meyer, C. Rebreyend, B. de Bruin, M. Atanasov, F. Neese, B. Mühldorf, R. Wolf, *Angew. Chem. Int. Ed.* **2017**, *56*, 7995-7999.
[35] T. N. Gieshoff, U. Chakraborty, M. Villa, A. Jacobi von Wangelin, *Angew. Chem. Int. Ed.* **2017**, *56*, 3585-3589.
[36] V. Sable, K. Maindan, A. R. Kapdi, P. S. Shejwalkar, K. Hara, *ACS Omega* **2017**, *2*, 204-217.
[37] D. Gärtner, A. L. Stein, S. Grupe, J. Arp, A. Jacobi von Wangelin, *Angew. Chem. Int. Ed.* **2015**, *54*, 10545-10549.
[38] T. N. Gieshoff, M. Villa, A. Welther, M. Plois, U. Chakraborty, R. Wolf, A. Jacobi von Wangelin, *Green Chem.* **2015**, *17*, 1408-1413.
[39] D. Gärtner, A. Welther, B. R. Rad, R. Wolf, A. Jacobi von Wangelin, *Angew. Chem. Int. Ed.* **2014**, *53*, 3722-3726.
[40] C. S. Consorti, F. R. Flores, J. Dupont, *J. Am. Chem. Soc.* **2005**, *127*, 12054-12065.
[41] P. Steffanut, J. A. Osborn, A. DeCian, J. Fisher, *Chem. Eur. J.* **1998**, *4*, 2008-2017.
[42] S. G. Harsy, *Tetrahedron* **1990**, *46*, 7403-7412.
[43] X. L. Luo, R. H. Crabtree, *J. Am. Chem. Soc.* **1989**, *111*, 2527-2535.
[44] N. Bandara, C. N. Ratnaweera, S. R. Gwaltney, W. P. Henry, *J. Organomet. Chem.* **2013**, *745-746*, 86-92.
[45] J. Müller, P. Göser, M. Elian, *Angew. Chem. Int. Ed.* **1969**, *8*, 374-375.
[46] Y. Hiroi, N. Komine, S. Komiya, M. Hirano, *Organometallics* **2014**, *33*, 6604-6613.
[47] P. Zhang, H. Wang, X. Shi, X. Yan, X. Wu, S. Zhang, B. Yao, X. Feng, J. Zhi, X. Li, B. Tong, J. Shi, L. Wang, Y. Dong, *J. Polym. Sci., Part A: Polym. Chem.* **2017**, *55*, 716-725.
[48] W. I. Dzik, L. Fuente Arruga, M. A. Siegler, A. L. Spek, J. N. H. Reek, B. de Bruin, *Organometallics* **2011**, *30*, 1902-1913.
[49] A. Singh, P. R. Sharp, *Inorg. Chim. Acta* **2008**, *361*, 3159-3164.
[50] S. Spiess, C. Welter, G. Franck, J. Taquet, G. Helmchen, *Angew. Chem. Int. Ed.* **2008**, *47*, 7652-7655.
[51] A. Singh, P. R. Sharp, *Organometallics* **2006**, *25*, 678-683.
[52] T. C. W. Mak, H. N. C. Wong, K. Hung Sze, L. Book, *J. Organomet. Chem.* **1983**, *255*, 123-134.
[53] B. J. Hornstein, J. D. Aiken, R. G. Finke, *Inorg. Chem.* **2002**, *41*, 1625-1638.
[54] M. N. Vargaftik, V. P. Zagorodnikov, I. P. Stolarov, I. I. Moiseev, D. I. Kochubey, V. A. Likholobov, A. L. Chuvilin, K. I. Zamaraev, *J. Mol. Catal.* **1989**, *53*, 315-348.
[55] L. Gonzalez-Tejuca, K. Aika, S. Namba, J. Turkevich, *J. Phys. Chem.* **1977**, *81*, 1399-1406.
[56] R. Frety, P. N. Da Silva, M. Guenin, *Catal. Lett.* **1989**, *3*, 9-16.
[57] J. P. Collman, K. M. Kosydar, M. Bressan, W. Lamanna, T. Garrett, *J. Am. Chem. Soc.* **1984**, *106*, 2569-2579.

[58] M. Hori, D. J. Gravert, P. Wentworth, K. D. Janda, *Bioorg. Med. Chem. Lett.* **1998**, *8*, 2363-2368.
[59] J. Hamlin, K. Hirai, A. Millan, P. Maitlis, *J. Mol. Catal.* **1980**, *7*, 543-544.
[60] P. D. Landre, D. Richard, M. Draye, P. Gallezot, M. Lemaire, *J. Catal.* **1994**, *147*, 214-222.
[61] R. M. Laine, *J. Mol. Catal.* **1982**, *14*, 137-169.
[62] E. Bayram, J. C. Linehan, J. L. Fulton, J. A. S. Roberts, N. K. Szymczak, T. D. Smurthwaite, S. Özkar, M. Balasubramanian, R. G. Finke, *J. Am. Chem. Soc.* **2011**, *133*, 18889-18902.
[63] P. Riello, P. Canton, A. Benedetti, *Langmuir* **1998**, *14*, 6617-6619.

2 Aims of this work

As discussed in the first chapter of this thesis, the use of metal-based catalysts for the reductive defunctionalization of oxygen-containing substrates, e.g. alcohols, ethers or carbonyl compounds, is of significant relevance for synthetic transformations on laboratory scale as well as for the valorization of renewable resources in industrial setups. However, already existing methods suffer from drawbacks like high catalyst loadings, the use of hazardous or waste-generating reducing agents and low chemoselectivity or a narrow substrate scope due to the heterogeneous nature of the active catalyst.

In this work, a homogeneous palladium-based catalyst system is applied for the selective defunctionalization of various derivatives of benzylic alcohols. The development of user-friendly protocols was envisioned, including the use of low catalyst loadings and an environmentally benign reductant without the need for specialized equipment (Scheme 2.1).

Initially, a protocol for the selective deoxygenation of benzylic alcohols was devised to afford a scope of the corresponding alkylarenes *via* reductive scission of the strong C–O bond under transfer hydrogenolysis conditions. The developed catalyst system was consecutively investigated regarding the nature of the active catalyst species (chapter 3). Previous literature works on similar systems did only report heterogeneous variants for this transformation. Hence, establishing a homogeneously catalyzed system appeared intriguing.

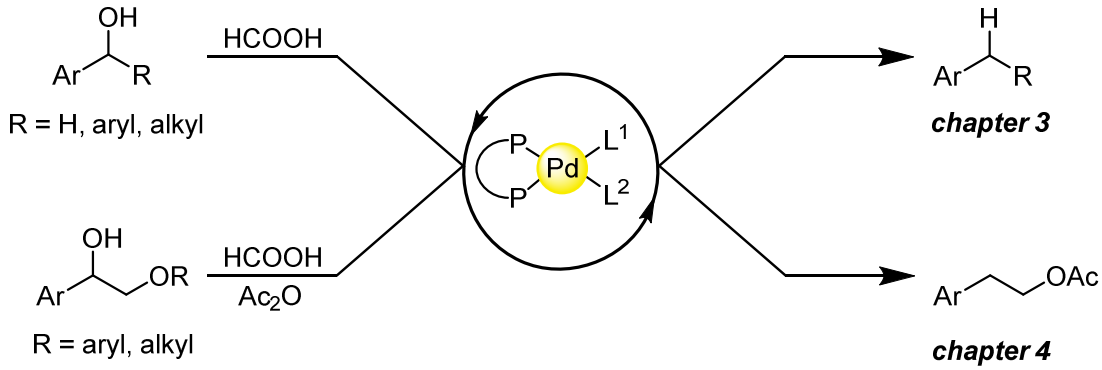

Scheme 2.1 **Selective defunctionalization of benzylic alcohols and benzylic β-alkoxy alcohols through a homogeneous palladium catalyst.**

Furthermore, the catalytic system, which was proven successful in the first project of this thesis, then should be adapted to transform more complex alcohols containing an additional ether functionality (Scheme 2.1). These substrates were chosen for their model character concerning the structural motifs found in lignin, an alternative carbon source from natural feedstock. After a modification of the system led to promising results, initial mechanistic investigations were conducted (chapter 4).

3 Pd-catalyzed transfer hydrogenolysis of benzylic alcohols

Parts of the results discussed in this chapter were published in a peer-reviewed scientific journal: B. Ciszek, I. Fleischer, *Chem. Eur. J.* **2018**, *24*, 12259–12263.

3.1 General motivation

As depicted earlier in this thesis, a range of methodologies for the transfer hydrogenolysis of benzylic alcohols exists. Nonetheless, most of the modern procedures rely on heterogeneous catalysts. Compared to homogeneous systems, these suffer from drawbacks like higher catalyst loadings or lower chemoselectivity. Moreover, a heterogeneous catalyst system offers only limited possibilities for the adaption towards more challenging substrates, leading to a relatively narrow scope of obtainable products. Also, mechanistic investigations are impeded by a lack of options for catalyst modification (see section 1.2).

Reviewing works from the literature on palladium-based catalysts for the transfer hydrogenolysis of benzylic alcohols, it became apparent that previously reported methods that apply soluble palladium precursors in the transformation also use reducing agents which generate considerable amounts of waste[1-3] or make specialized pressure equipment necessary.[4] Reductants which are better to handle or easier to separate from the product after the reaction require heterogeneous palladium catalysts on solid support.[5-8] One of the mentioned reducing agents is formic acid, which favorably provides for a convenient reaction workup and product isolation. Samec and co-workers,[7] amongst others,[5,6] demonstrated the utility of this reagent in the transfer hydrogenolysis of various benzylic alcohols. The transformation was mediated by catalytic amounts of palladium on activated charcoal. Although the developed methodologies were appreciated, the group of Fleischer was intrigued by the lack of a homogeneously palladium-catalyzed variant of this transformation. Therefore, the development of such a catalyst system was targeted, including the use of formic acid as reductant.

3.2 The palladium/dtbpx catalyst system

In the industrial production of bulk chemicals from ethylene, e.g. yielding polyketones of high molecular weight, the application of homogeneous palladium-based complexes containing bidentate phosphine ligands is well-known.[9] In contrast to this, the application of the bidentate phosphine α,α'-bis(di-*tert*-butylphosphino)-*ortho*-xylene (dtbpx, **L1**) as ligand together with a palladium(0) precursor in a catalyst for the methoxycarbonylation of

ethylene (**1**) to methyl propionate (**2**) was commercialized as pre-step towards the production of acrylic glass in the *Lucite alpha* process.[10] The used system led to the formation of **2** in high selectivity and yield. Due to the high importance of this carbonylative transformation, the reaction mechanism was thoroughly investigated, including the characterization of the reaction intermediates and the active catalyst species. The results suggest a cationic palladium(II) hydride complex with the bisphosphine **L1** coordinated *cis* to the metal center. The complex **3** is stabilized by a weakly coordinating anion (Scheme 3.1).[11,12]

Results obtained from works in the Fleischer working group demonstrated that a similar catalyst species generated *in situ* from a soluble palladium(0) precursor and the ligand dtbpx (**L1**) in presence of a Brønsted acid co-catalyst facilitated the alkoxycarbonylation of vinyl arenes **4** to the methyl esters of the respective linear and branched arylpropionic acids **5**. The products were obtained in high yields and with very good selectivities towards the valuable branched regioisomer (Scheme 3.1).[13]

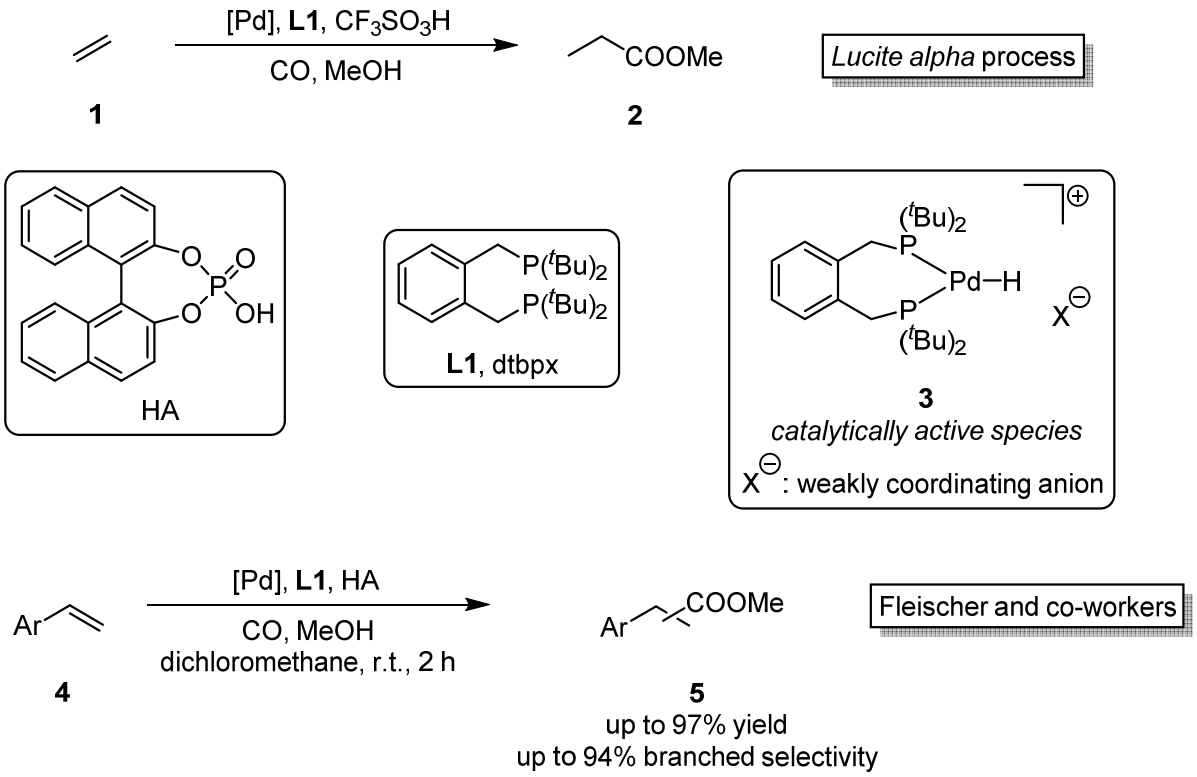

Scheme 3.1 **Application of a homogeneous palladium hydride catalyst in the methoxycarbonylation of alkenes.[10,13]**

For transfer hydrogenolysis reactions of benzylic alcohols on heterogeneous palladium, a metallic palladium species with chemisorbed hydrogen was proposed as active catalyst, representing a heterogeneous palladium hydride.[7] It was speculated if a homogeneous palladium hydride complex, as it is generated in the *Lucite alpha* process and in the alkoxycarbonylation of vinylarenes, could be utilized for the hydrogenolysis of benzylic alcohols.

3.3 Results and discussion

3.3.1 Pd-catalyzed transfer hydrogenolysis using methyl formate as reductant

Initial reaction optimization

For the development of a suitable homogeneous catalyst system for the transfer hydrogenolysis of benzylic alcohols, 1-phenylethanol (**6**) was chosen as model substrate, also for its rudimentary resemblance to the benzylic alcohol motifs contained in the structure of lignin (see section 1.4). For the role of the reducing agent, formic acid and its methyl ester appeared favorable, as these reagents are inexpensive, widely available and bear several advantages concerning transport and handling.[14,15] Furthermore, they are known to act as reductants in presence of a palladium catalyst.[5-7] Moreover, the synthesis of formic acid and methyl formate can be easily conducted from CO_2 and H_2 in absence or presence of methanol, respectively.[15,16]

The choice of the components of the catalyst system was based on previous works in the Fleischer group on the alkoxycarbonylation of alkenes[13] and the conversion of alcohols as substrates in carbonylation reactions.[17] Therein, the previously mentioned ligand **L1** was applied for the *in situ* formation of a palladium phosphine complex, which mediated the carbonylation of alkenes and alcohols under low to moderate CO pressures. Originating from these findings, an initial series of experiments was conducted, applying catalytic amounts of palladium acetylacetonate as a Pd(II) precursor, ligand **L1** and methanesulfonic acid in presence of model substrate **6** and methyl formate as reductant (Table 3.1).

Applying the reaction conditions from the previous carbonylation projects,[13,17] a first run using $Pd(acac)_2$ (1.0 mol%), ligand **L1** (4.0 mol%), methanesulfonic acid (16 mol%) and methyl formate (2.0 equivalents) in 1,2-dichloroethane at 150 °C in a sealed glass pressure tube already led to an encouraging result: The desired product ethylbenzene (**7**) was obtained in 19% yield, amongst traces of **8** and products of higher molecular mass in non-quantified amounts (entry 1). After a reaction time of 18 hours, the formation of a black metallic precipitate on the glass was observed, assumingly the active catalyst underwent decomposition to palladium black.

Exclusion experiments without acid co-catalyst or ligand under otherwise unchanged reaction conditions led to no significant product formation (entries 2, 3). Without methanesulfonic acid, incomplete substrate conversion (95%) was observed, while ester **9** was obtained as a side product. When Pd/C was applied as catalyst under ligand-free conditions, product **7** was obtained in a low yield of 18% (entry 4).

Table 3.1 **Initial optimization experiment for the palladium-catalyzed transfer hydrogenolysis of 1-phenylethanol using methyl formate as reductant.**

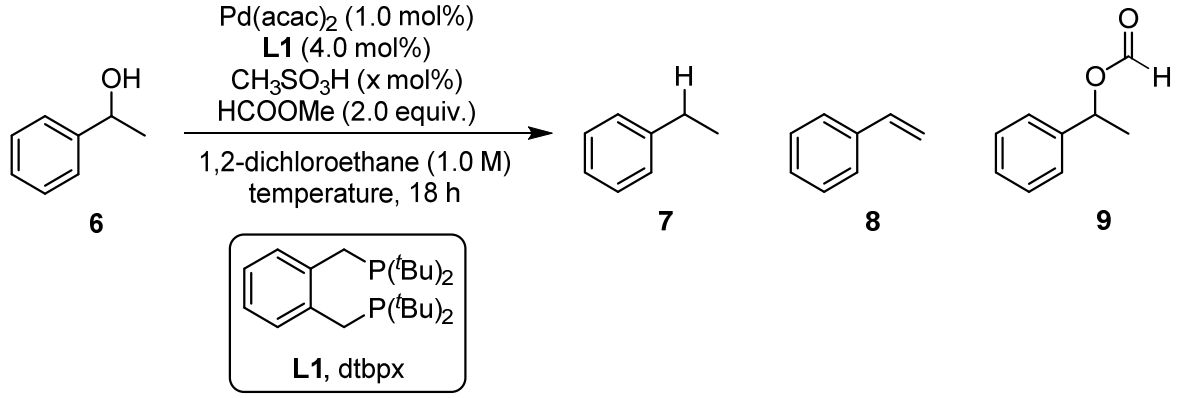

Entry[a]	CH_3SO_3H (x mol%)	temperature [°C]	products (yield [%])[b]
1	16	150	**7** (19), **8** (traces)
2[c]	–	150	**8** (traces), **9** (traces)
3[d]	16	150	–
4[e]	16	150	**7** (18)
5	16	100	**7** (72)
6	10	100	**7** (46), **8** (traces)
7	5.0	100	–
8[f]	16	100	**8** (19)
9[c]	–	100	**9** (8)
10[g]	16	100	**8** (traces)

[a]General reaction conditions: 1-Phenylethanol (1.00 mmol, 120 µL, 1.0 M solution), 1,2-dichloroethane (1 mL), $Pd(acac)_2$ (10 µmol, 3.0 mg, 1.0 mol%), **L1** (40 µmol, 16 mg, 4.0 mol%), CH_3SO_3H (0.16 mmol, 10 µL, 16 mol%), methyl formate (2.00 mmol, 123 µL, 2.00 equivalents), stirred at the respective temperature for 18 h in a sealed glass pressure tube. Unless stated otherwise, full substrate conversion was achieved. [b]Product identification was performed *via* measurement of authentic commercial samples or *via* GC-MS analysis. Yields determined *via* quantitative GC-FID using *n*-pentadecane as internal standard. [c]Exclusion experiment without acid co-catalyst. [d]Exclusion experiment without ligand. [e]5.0 mol% Pd/C (10% *w*/*w*) used as [Pd] source, no ligand added, reaction time: 4 h. [f]Exclusion experiment without [Pd] source. [g]Exclusion experiment without methyl formate.

Lowering of the reaction temperature was beneficial for the desired transformation. Under the given standard conditions at 100 °C, **7** was found in 72% yield (entry 5). A reduced amount of acid co-catalyst of 10 mol% led to a lower product yield of 46%, further lowering of the acid loading to 5.0 mol% prevented the generation of product (entries 6, 7). Without any added palladium source, only styrene formation was observed in 19% yield, accompanied by high-molecular products (entry 8). As expected, an exclusion of the acid co-catalyst at 100 °C did not lead to the desired deoxygenation reaction. As main product, formate **9** was found in 35% yield (entry 9). Without the addition of methyl formate, only traces of styrene could be detected, along with a high amount of a high-molecular side product (entry 10). In

all experiments involving soluble palladium precursors, the formation of black precipitate was observed.

Further optimization of key reaction parameters

To further optimize the reaction, a screening of ligands and acid co-catalysts was conducted. For the ligand screening, mono- and bidentate phosphines were tested in the reaction under standard conditions (Scheme 3.2). For the formation of the desired deoxygenation product **7**, an exclusive ligand effect was observed. Only **L1** promoted the generation of **7**, some of the tested ligands (**L3**, **L4**, **L7, L9**) did not give rise to significant amounts of **7** nor **8**. For the remaining ligands (**L2**, **L5**, **L6, L8**, **L10**) only styrene (**8**) was found in the reaction mixture in moderate yields. In all cases, not further characterized products with higher molecular mass were detected using GC analysis. Plausible reasons for the observed ligand effect will be discussed later in this chapter (section 3.3.3).

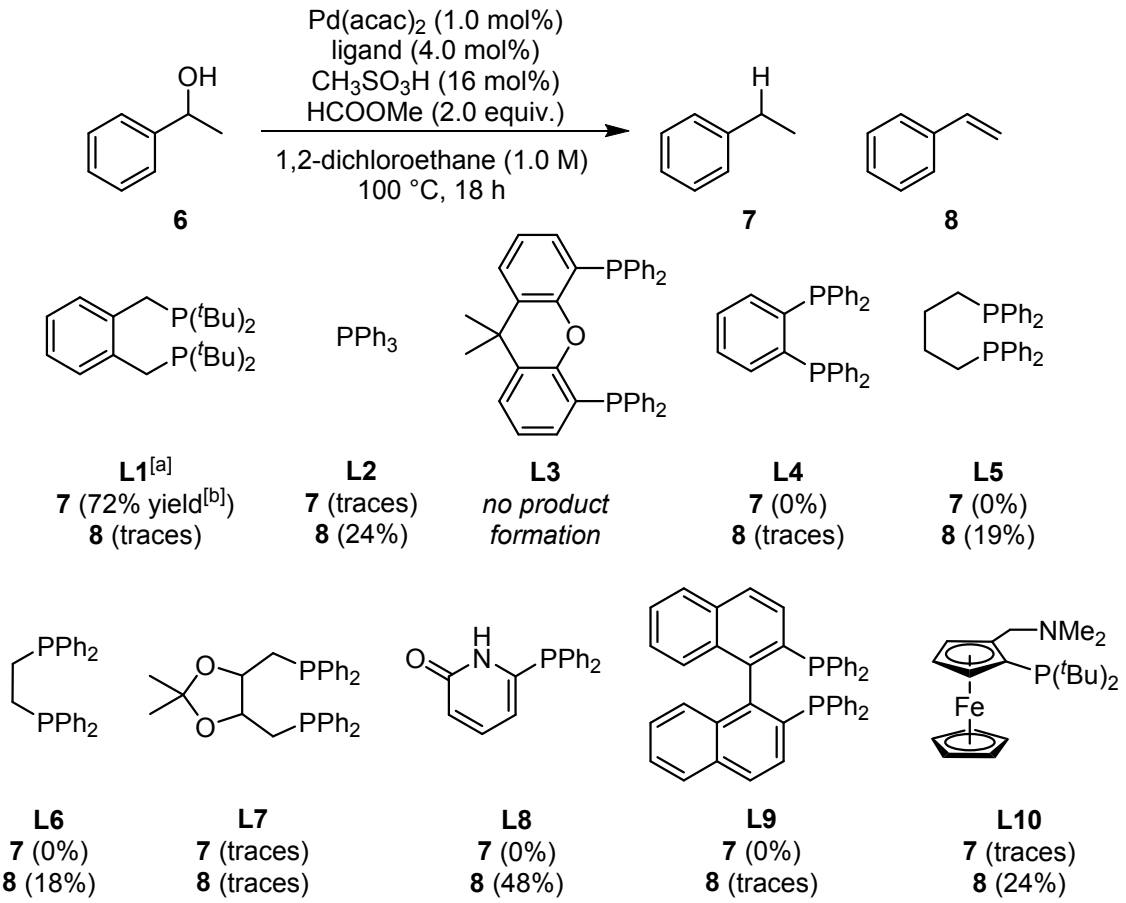

[a]General reaction conditions: 1-Phenylethanol (1.00 mmol, 120 µL, 1.0 M solution), 1,2-dichloroethane (1 mL), $Pd(acac)_2$ (10 µmol, 3.0 mg, 1.0 mol%), ligand (40 µmol, 4.0 mol% for bidentate, 80 µmol, 8.0 mol% for monodentate phosphines), CH_3SO_3H (0.16 mmol, 10 µL, 16 mol%), methyl formate (2.00 mmol, 123 µL, 2.00 equivalents), stirred at 100 °C for 18 h in a sealed glass pressure tube. [b]Product identification was performed *via* measurement of authentic commercial samples or *via* GC-MS analysis. Yields determined *via* quantitative GC-FID using *n*–pentadecane as internal standard.

Scheme 3.2 **Ligand screening for the transfer hydrogenolysis of 1-phenylethanol using methyl formate as reductant.**

Similar results were obtained from the acid co-catalyst screening, which included several organic acids of different pK_a values under else standard reaction conditions (Table 3.2). Besides the already found activity of methanesulfonic acid (72% yield of **7**, entry 1), only *para*-toluenesulfonic acid as co-catalyst yielded the desired product (22%, entry 2). The use of other acids (trifluoroacetic acid, benzoic acid, diphenyl phosphoric acid) gave **9** as only product (entries 3–5). In all reactions, side products of higher molecular mass were found using GC analysis. The observed effect of the tested acid co-catalysts could be rationalized through comparison of the respective acid strengths as well as through the behavior of the corresponding anions in the reaction. A thorough discussion thereof is given in section 3.3.3.

Table 3.2 **Acid co-catalyst screening for the transfer hydrogenolysis of 1-phenylethanol using methyl formate as reductant. pK_a values were obtained from the literature.[18]**

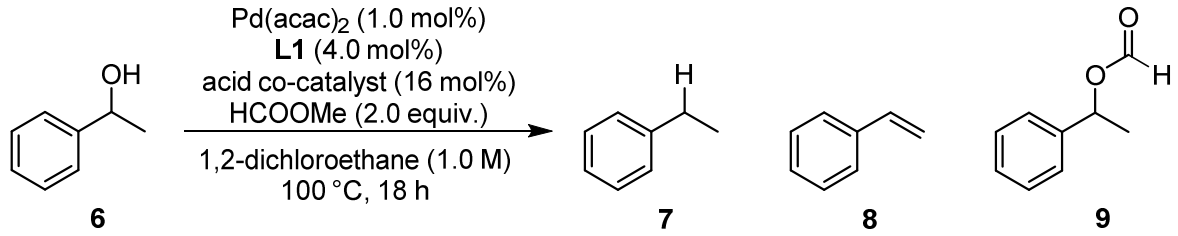

6 **7** **8** **9**

Entry[a]	acid co-catalyst	pK_a (H_2O)	pK_a (DMSO)	products (yield [%])[b]
1	CH_3SO_3H	-1.9	1.6	**7** (72), **8** (traces)
2	*p*-$TolSO_3H$	-2.8	7.1	**7** (22), **8** (14)
3	CF_3COOH	0.23	3.5	**9** (19)
4	PhCOOH	4.2	11.1	**9** (12)
5	$(PhO)_2P(O)OH$	n.a.	3.8	**8** (traces), **9** (12)

[a]General reaction conditions: 1-Phenylethanol (1.00 mmol, 120 µL, 1.0 M solution), 1,2-dichloroethane (1 mL), $Pd(acac)_2$ (10 µmol, 3.0 mg, 1.0 mol%), **L1** (40 µmol, 16 mg, 4.0 mol%), acid co-catalyst (0.16 mmol, 16 mol%), methyl formate (2.00 mmol, 123 µL, 2.00 equivalents), stirred at 100 °C for 18 h in a sealed glass pressure tube. Unless stated otherwise, full substrate conversion was achieved. [b]Product identification was performed *via* measurement of authentic commercial samples or *via* GC-MS analysis. Yields determined *via* quantitative GC-FID using *n*-pentadecane as internal standard.

3.3.2 Pd-catalyzed transfer hydrogenolysis using formic acid as reductant

Initial reaction optimization

After the observation of 1-phenylethyl formate (**9**) in the initial screening experiments, it was speculated that this alternative product was generated as an intermediate in the reaction through an acid-catalyzed transesterification of methyl formate with the alcohol substrate **6**. To investigate this, the application of formic acid as reductant was thought beneficial, as a direct condensation to ester **9** should proceed easier than a transesterification. Furthermore, a reduction with formic acid would give only carbon dioxide and water as by-products. As before, an initial optimization of the reaction system was performed (Table 3.3).

Table 3.3 **Initial optimization experiments for the transfer hydrogenolysis of 1-phenylethanol using formic acid as reductant.**

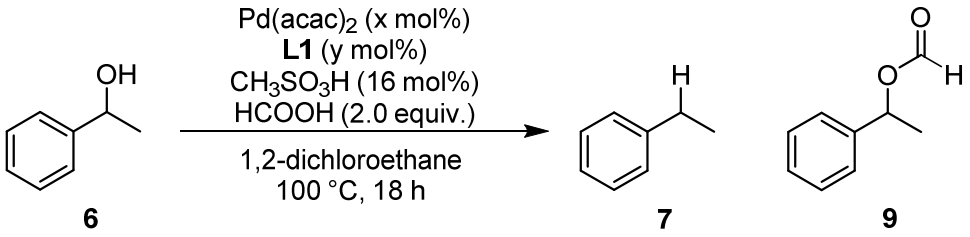

6 **7** **9**

Entry[a]	$Pd(acac)_2$ (x mol%)	**L1** (y mol%)	conc. (**6**) [M]	products (yield [%])[b]
1	1.0	4.0	1.0	**7** (64)
2	1.0	4.0	0.33	**7** (>99)
3	1.0	–	0.33	–
4[c]	1.0	4.0	0.33	**9** (35)
5	–	4.0	0.33	**9** (12)
6	0.5	2.0	0.33	**7** (85)
7[d]	0.5	2.0	0.33	**7** (47)
8[e]	1.0	4.0	0.33	**7** (95)
9[f]	1.0	4.0	0.33	**7** (39), **9** (27)
10[g]	1.0	4.0	0.33	**7** (72), **9** (9)

[a]General reaction conditions: 1-Phenylethanol (1.00 mmol, 120 µL, 1.0 or 0.33 M solution), 1,2-dichloroethane (1 or 3 mL), $Pd(acac)_2$ (10 µmol, 3.0 mg, 1.0 mol%), **L1** (40 µmol, 16 mg, 4.0 mol%), CH_3SO_3H (0.16 mmol, 10 µL, 16 mol%), formic acid (2.0 mmol, 75 µL, 2.0 equivalents), stirred at 100 °C for 18 h in a sealed glass pressure tube. Unless stated otherwise, full substrate conversion was achieved. [b]Product identification was performed *via* measurement of authentic commercial samples or *via* GC-MS analysis. Yields determined *via* quantitative GC-FID using *n*-pentadecane as internal standard. [c]Exclusion experiment without acid co-catalyst. [d]1.0 equivalent of formic acid used. [e]reaction temperature: 80 °C. [f]reaction temperature: 60 °C. [g]reaction temperature: 60 °C, reaction time: 72 h.

Substitution of methyl formate by formic acid under the reaction conditions previously found superior gave the desired product **7** in a very good yield of 64% (entry 1). In contrast to prior experiments, no styrene was detected in the crude reaction mixture, but still the formation of higher-mass products occurred. To prevent this, the volume of the reaction medium was adapted to a concentration of **6** of 0.33 M. This indeed had the desired effect, the suppression of side products led to a quantitative yield of **7** (entry 2). Nonetheless, as in prior experiments, the formation of palladium black was observed.

To clarify the role of the added catalyst components in the reaction, exclusion experiments were conducted. It was found that without added ligand, no product formation took place (entry 3). Without metal precursor or acid co-catalyst, no transfer hydrogenolysis product was generated. Instead, the supposed reaction intermediate **9** was formed in 35% or 12% yield, respectively (entries 4, 5). Lowering of the loading of metal precursor and ligand resulted in only a slightly decreased product yield of 85% (entry 6). Simultaneous reduction

of the added amount of formic acid considerably diminished the yield of **7** (47%, entry 7). At lower temperatures, the reaction still proceeded smoothly, though lower yields of **7** were obtained. While at 80 °C, the reaction delivered still a very good product yield of 95% (entry 8), further decreasing of the temperature to 60 °C resulted in a drop of yield of the deoxygenated product to 39%, besides a yield of 27% of **9** (entry 9). Through prolongation of the reaction time to 72 hours, the product yield under these conditions could be improved to 72% (entry 10).

Further optimization of key reaction parameters

With reaction conditions already resulting in an excellent yield of product **7** in hand, the system should be further optimized, e.g. in terms of catalyst loading, reaction temperature and time. At first, different palladium precursors were tested for their performance in the reaction. The findings are summarized in Table 3.4.

Table 3.4 **Palladium precursor screening in the transfer hydrogenolysis of 1-phenylethanol using formic acid as reductant.**

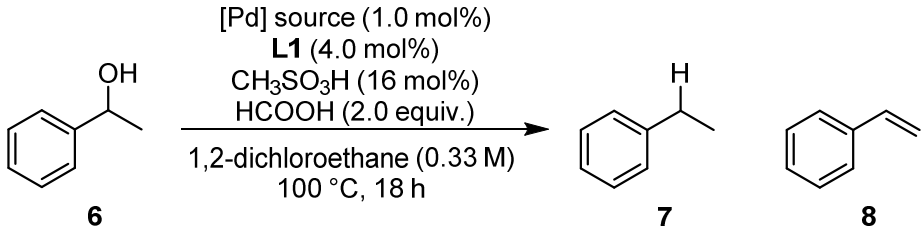

6 **7** **8**

Entry[a]	[Pd] source	products (yield [%])[b]
1	$Pd(acac)_2$	**7** (>99)
2	$Pd(dba)_2$	**7** (92)
3	$Pd(OAc)_2$	**7** (88)
4	$PdCl_2$	**7** (75)
5	Pd/C	**7** (7), **8** (22)
6[c]	Pd/C	–
7	–	**7** (6), **8** (traces)

[a]General reaction conditions: 1-Phenylethanol (1.00 mmol, 120 µL, 0.33 M solution), 1,2-dichloroethane (3 mL), [Pd] source (10 µmol, 1.0 mol%), **L1** (40 µmol, 16 mg, 4.0 mol%), CH_3SO_3H (0.16 mmol, 10 µL, 16 mol%), formic acid (2.0 mmol, 75 µL, 2.0 equivalents), stirred at 100 °C for 18 h in a sealed glass pressure tube. Unless stated otherwise, full substrate conversion was achieved. [b]Product identification was performed *via* measurement of authentic commercial samples or *via* GC-MS analysis. Yields determined *via* quantitative GC-FID using *n*-pentadecane as internal standard. [c]Exclusion experiment without added ligand **L1**.

As evident from previous experiments, the use of $Pd(acac)_2$ as catalyst precursor led to a quantitative yield of **7** (entry 1). With $Pd(dba)_2$ a soluble Pd(0) source was tested in the catalysis, the desired product was obtained in an excellent yield of 92% (entry 2). Other Pd(II) salts, $Pd(OAc)_2$ and $PdCl_2$, were applied showing lower, but still good to very good

product yields of 88% and 75% (entries 3, 4). Pd/C as heterogeneous palladium source did not deliver significant amounts of **7** in presence of **L1**, styrene was found after the reaction besides non-identified products with higher molecular mass (entry 5). Without added ligand, the use of the heterogeneous palladium precursor yielded only higher-mass products (entry 6). Without any metal source, no significant amounts of low-molecular products were obtained (entry 7).

After $Pd(acac)_2$ was found superior as palladium source in the reaction, a screening of various phosphine-based ligands was performed. The chosen ligands were mono- and bidentate, differing in the length and rigidity of the carbon backbone, as well as in the electronic properties of the coordinating phosphorus atoms and their respective bite angles (Scheme 3.3).

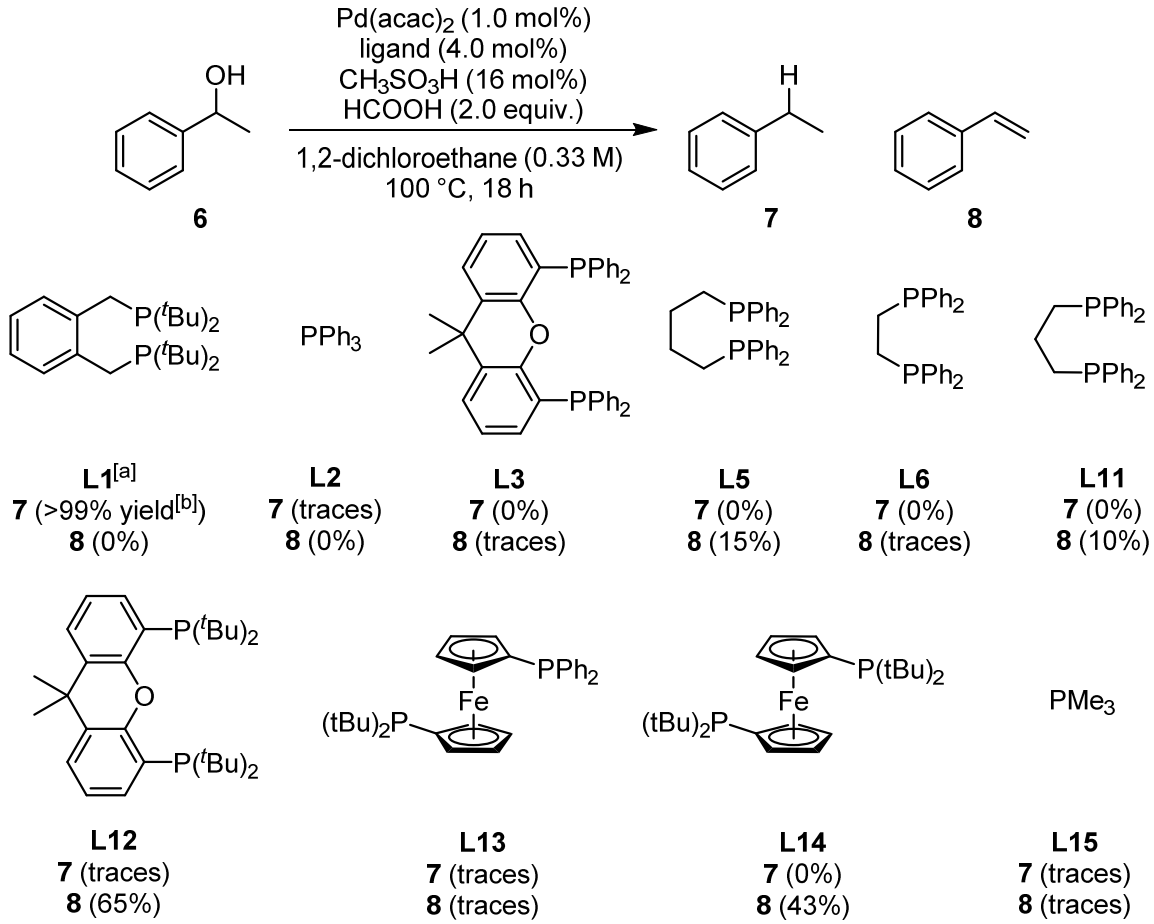

[a]General reaction conditions: 1-Phenylethanol (1.00 mmol, 120 µL, 0.33 M solution), 1,2-dichloroethane (3 mL), $Pd(acac)_2$ (10 µmol, 3.0 mg, 1.0 mol%), ligand (40 µmol, 4.0 mol% for bidentate, 80 µmol, 8.0 mol% for monodentate phosphines), CH_3SO_3H (0.16 mmol, 10 µL, 16 mol%), formic acid (2.0 mmol, 75 µL, 2.0 equivalents), stirred at 100 °C for 18 h in a sealed glass pressure tube. [b]Product identification was performed *via* measurement of authentic commercial samples or *via* GC-MS analysis. Yields determined *via* quantitative GC-FID using *n*–pentadecane as internal standard.

Scheme 3.3 Ligand screening for the palladium-catalyzed transfer hydrogenolysis of 1-phenylethanol using formic acid as reductant.

Similar to the results obtained from the reaction system based on methyl formate as reductant (section 3.3.1), only the use of ligand **L1** led to the formation of significant amounts

of the desired transfer hydrogenolysis product **7** (quantitative yield). For the other tested ligands, **7** was generated only in trace amounts or not at all. Bidentate phosphines with a flexible backbone and relatively electron-poor phosphine groups (**L5**, **L6**, **L11**) or a more rigid backbone but electron-richer phosphine groups (**L12**, **L14**) afforded moderate to high amounts of styrene (**8**, 15–65%). To explain the observed exclusive ligand effect for **L1**, the role of the ligand structure and basicity, especially in interaction with the applied acid co-catalyst, will be discussed in section 3.3.3.

Analogous to the previously investigated transfer hydrogenolysis with methyl formate as reducing agent, an acid co-catalyst screening was also conducted for the reaction with formic acid (Table 3.5).

As before, similar trends in the effect of the added acid co-catalysts were observed. Only methanesulfonic acid and *para*-toluenesulfonic acid led to the desired catalytic activity, furnishing product **7** in quantitative or a very good yield of 76%, respectively (entries 1, 2). For comparably weaker acids, only the suspected reaction intermediate **9** was detected in the reaction mixture (29%–59% yield, entries 3, 4). In the reactions applying two organic phosphoric acids, trace amounts of styrene (entry 5) and ethylbenzene (entry 6) were generated, again ester **9** was obtained as the main product (60%–74% yield).

Table 3.5 **Acid co-catalyst screening for the palladium-catalyzed transfer hydrogenolysis of 1-phenylethanol using methyl formate as reductant. *p*K$_a$ values were obtained from the literature.[18]**

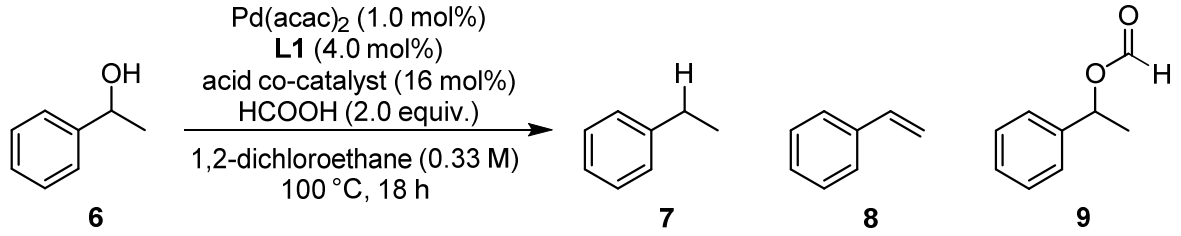

6 **7** **8** **9**

Entry[a]	acid co-catalyst	*p*K$_a$ (H_2O)	*p*K$_a$ (DMSO)	products (yield [%])[b]
1	CH_3SO_3H	-1.9	1.6	**7** (>99)
2	*p*TolSO_3H	-2.8	7.1	**7** (76)
3	CF_3COOH	0.23	3.5	**9** (59)
4	PhCOOH	4.2	11.1	**9** (29)
5	$(PhO)_2P(O)OH$	n.a.	3.8	**8** (traces), **9** (74)
6	BINOL phosphoric acid	n.a.	3.4	**7** (traces), **9** (60)

[a]General reaction conditions: 1-Phenylethanol (1.00 mmol, 120 µL, 0.33 M solution), 1,2-dichloroethane (3 mL), $Pd(acac)_2$ (10 µmol, 3.0 mg, 1.0 mol%), **L1** (40 µmol, 16 mg, 4.0 mol%), acid co-catalyst (0.16 mmol, 16 mol%), formic acid (2.0 mmol, 75 µL, 2.0 equivalents), stirred at 100 °C for 18 h in a sealed glass pressure tube. Unless stated otherwise, full substrate conversion was achieved. [b]Product identification was performed *via* measurement of authentic commercial samples or *via* GC-MS analysis. Yields determined *via* quantitative GC-FID using *n*-pentadecane as internal standard.

Optimization of the loading of catalyst components and the amount of reductant

To conclude the reaction optimization and to obtain an insight into a possible stoichiometry of the active catalyst species, different ratios of the applied catalyst components and varying amounts of reducing agent were used in the reaction (Table 3.6).

Table 3.6 **Optimization of catalyst and reductant loading in the palladium-catalyzed transfer hydrogenolysis using formic acid.**

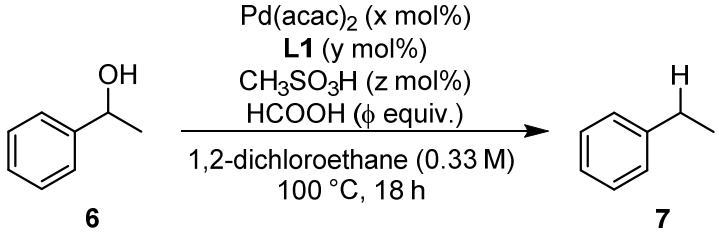

6 **7**

Entry[a]	$Pd(acac)_2$ (x mol%)	**L1** (y mol%)	CH_3SO_3H (z mol%)	HCOOH (ϕ equiv.)	products (yield [%])[b]
1	0.5	4.0	16	2.0	**7** (70)
2	**1.0**	**4.0**	**16**	**2.0**	**7 (>99)**
3	1.5	4.0	16	2.0	**7** (95)
4	2.0	4.0	16	2.0	**7** (90)
5	1.0	2.0	16	2.0	**7** (26)
6	1.0	3.0	16	2.0	**7** (50)
7	**1.0**	**4.0**	**16**	**2.0**	**7 (>99)**
8	1.0	4.0	5.0	2.0	**7** (83)
9	1.0	4.0	10	2.0	**7** (90)
10	**1.0**	**4.0**	**16**	**2.0**	**7 (>99)**
11	1.0	4.0	20	2.0	**7** (75)
12	1.0	4.0	16	1.0	**7** (85)
13	1.0	4.0	16	1.5	**7** (92)
14	**1.0**	**4.0**	**16**	**2.0**	**7 (>99)**
15	1.0	4.0	16	3.0	**7** (98)

[a]General reaction conditions: 1-Phenylethanol (1.00 mmol, 120 µL, 0.33 M solution), 1,2-dichloroethane (3 mL), $Pd(acac)_2$ (respective amount), **L1** (respective amount), methanesulfonic acid (respective amount), formic acid (respective amount), stirred at 100 °C for 18 h in a sealed glass pressure tube. Unless stated otherwise, full substrate conversion was achieved. [b]Product identification was performed *via* measurement of authentic commercial samples or *via* GC-MS analysis. Yields determined *via* quantitative GC-FID using *n*-pentadecane as internal standard.

Variation of the amount of added palladium precursor showed that 1.0 mol% is the optimal amount. For a lower loading of 0.5 mol%, a reduced transfer hydrogenolysis product yield of 70% was obtained (entry 1). In contrast, increasing the palladium amount in the reaction did not significantly change the generated amounts of **7**. For metal loadings of 1.5 and 2.0 mol%, yields over 90% were found (entries 3, 4).

The effect of different amounts of **L1** in the reaction was more evident. For decreased loadings of 2.0 and 3.0 mol%, significantly reduced product yields of 26% and 50% were obtained (entries 5, 6). A similar effect was observed in the variation of the acid co-catalyst loading. It became apparent that lower amounts of methanesulfonic acid (5.0 or 10 mol%) led to a slight decrease of the product yield to 83% or 90%, respectively. For a higher acid co-catalyst loading of 20 mol%, a strong decrease in product yield was found, presumably due to the formation of products with higher molecular mass (entry 11).

Finally, different amounts of reducing agent were applied in the reaction. While lower amounts of formic acid of 1.0 or 1.5 equivalents gave marginally lower amounts of **7**, raising the loading to 3.0 equivalents did not significantly change the reaction outcome (entries 12, 13, 15).

3.3.3 The decisive role of the ligand dtbpx and the acid co-catalyst

In the previous sections, the optimization of the transfer hydrogenolysis of 1-phenylethanol with an *in situ* generated palladium catalyst and formic acid as reducing agent was discussed. During the described series of experiments, a remarkable exclusive effect of both the applied ligand and the added acid co-catalyst became obvious. Only one of the tested ligands, α,α'-bis(di-*tert*-butylphosphino)-*ortho*-xylene (dtbpx, **L1**), formed a metal complex which was catalytically active in the reaction. Furthermore, only the addition of strong sulfonic acids proved successful, here methanesulfonic acid was found superior.

To rationalize the obtained results, literature reports using the ligand dtbpx in presence of acids were reviewed, especially for the formation of catalytically active palladium hydride complexes. First reports on the use of dtbpx for the synthesis of transition metal complexes were given by Shaw and co-workers[19] in the formation of platinum-bisphosphine-*cis*-dihydride complexes and by Crascall *et al.*[20] in the investigation of bisphosphine-η^2-alkene complexes of palladium and platinum.

Later, Clegg, Eastham and co-workers[11,21] performed thorough studies on the ligand after it was found to generate palladium complex **10**, a very efficient catalyst for the industrial methoxycarbonylation of ethene to obtain methyl propanoate. This transformation is known for its application as part of the *Lucite alpha* process. They compared the performance of several derivatives of dtbpx, bearing different substituents on the phosphorus atoms, in the methoxycarbonylation of ethene (Table 3.7).

Table 3.7 **Catalytic activity and selectivity of [Pd(bisphosphine)(η^2-dba)] complexes in the methoxycarbonylation of ethene (TOF: turnover frequency).**[21]

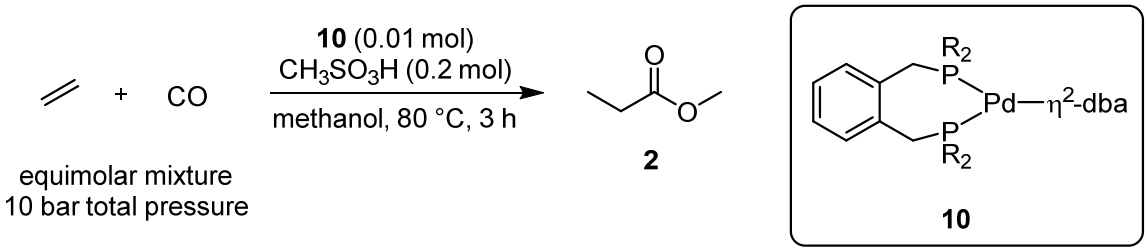

Entry[a]	R	TOF [h^{-1}][b]	product selectivity [%]
1	^{t}Bu	12000	99.9
2	^{i}Pr	200	20
3	Cy	200	25
4	Ph	400	20

[a]General reaction conditions: **10** (0.01 mol), methanesulfonic acid (0.2 mol) in methanol (300 mL) stirred at 80 °C for 3 h in a glass autoclave under ethene/CO mixture (molar ratio 1:1, 10 bar total pressure). [b]Turnover frequency (TOF): molar amount of ethylene consumed per molar amount of **10** per hour.

It became evident that the *tert*-butyl groups on the phosphorus atoms are crucial for the outstanding properties of the resulting palladium complex. Analogues based on di-*iso*-propyl-, di-cyclohexyl- or di-phenylphosphines on the same *ortho*-xylene backbone under identical reaction conditions exhibited by far lower activities and selectivities for the desired methoxycarbonylation product. As decisive properties, the high steric bulk and the high electron density on the phosphine groups of dtbpx were recognized. Further investigations on the reaction mechanism[11] and the catalyst activation and structure[22] resulted in a proposed catalytic cycle based on a cationic palladium(II)-dtbpx-hydride complex **12** (Scheme 3.4, R = CH_3). The vacant coordination site is occupied by an alcohol present as solvent, the cationic complex is stabilized by a triflate counterion.

Clegg *et al.*[22] showed that for [Pd(dtbpx)(η^2-dba)] (**10**) as a precursor complex, the addition of an oxidant, e.g. oxygen or benzoquinone, was required for a successful generation of the palladium hydride species in presence of a primary or secondary alcohol and trifluoromethanesulfonic acid (Scheme 3.4). It was found that the cationic [Pd(dtbpx)(η^2-dbaH)]$^+$ species **11** was formed as intermediate. Substitution of the protonated dba ligand by a molecule of alcohol results in complex **13**. The palladium-hydride bond is presumably formed *via* β-hydride elimination on the alcohol ligand under release of the generated carbonyl compound.

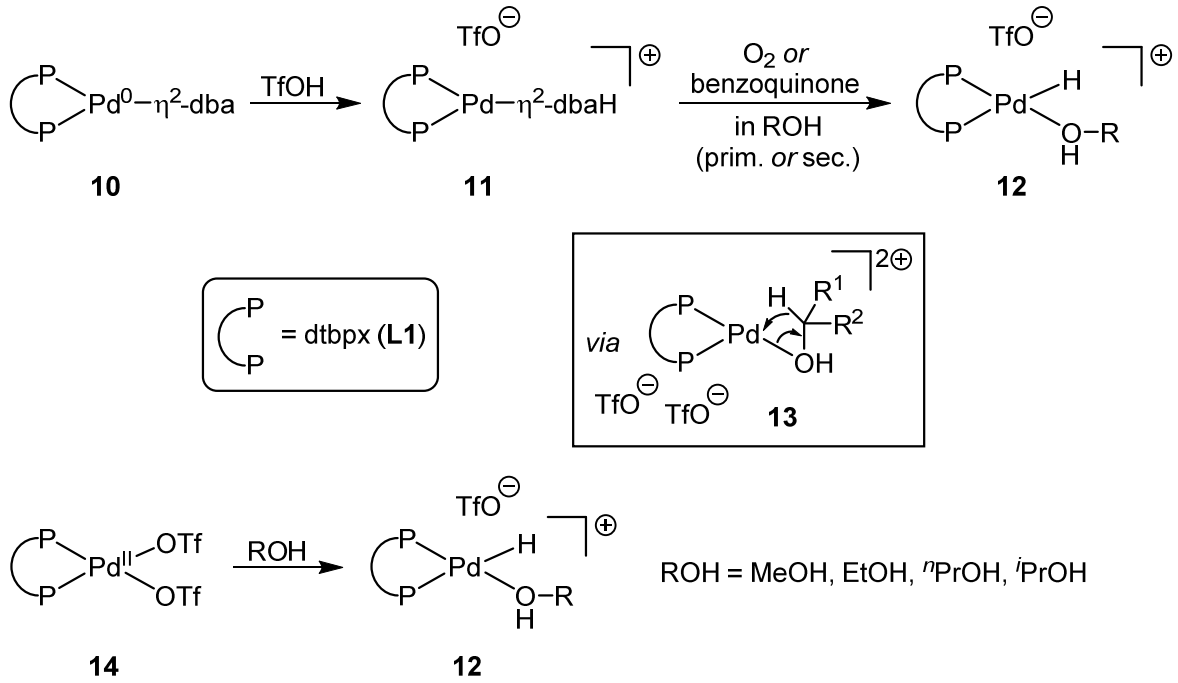

Scheme 3.4 **Generation of palladium-dtbpx-hydride complexes from Pd(0) and Pd(II) precursors (dba: dibenzylideneacetone, TfOH: trifluoromethanesulfonic acid).**[22]

Starting from the palladium(II) precursor [Pd(dtbpx)(η^1-TfO)$_2$] (**14**), it was stated by the authors that dissolving the complex in a primary or secondary alcohol is sufficient for the generation of the palladium hydride complex (Scheme 3.4). Again, ligand exchange on the metal center from triflate to alcohol is assumed to form intermediate **13**, which can undergo β-hydride elimination to the respective palladium hydride complex **12**. The findings of Clegg *et al*.[22] strongly propose that the presence of an alcohol species that is oxidizable through β-hydride elimination and of trifluoromethanesulfonic acid are crucial for the formation of [Pd(dtbpx)H(ROH)] (**12**). In absence of suitable alcohols, a direct formation of the palladium hydride complex is not possible.

Furthermore, the choice of the used acid is crucial for the generation of the palladium hydride (Scheme 3.5). Acids like trifluoromethanesulfonic acid or HBF_4 facilitate the formation of a palladium hydride complex, due to the stabilizing weak coordination of their respective anions. In contrast, acids with strongly coordinating anions, e.g. hydrogen chloride or trifluoroacetic acid, generate complexes of the composition [Pd(dtbpx)Cl_2] or [Pd(dtbpx)(O(O)CCF_3)$_2$], which do not react further to form a Pd–H bond.

A special reactivity is observed when methanesulfonic acid or *para*-toluenesulfonic acid are applied (Scheme 3.5). In these cases, neither the palladium hydride complex nor complexes of the structure [Pd(dtbpx)X_2] (X = MsO^-, TsO^-) are obtained. Instead, η^2-coordination of a single anion X^- is observed, leading to [Pd(dtbpx)(η^2-OMs)][OMs] (**16a**) and [Pd(dtbpx)(η^2-OTs)][OTs] (**16b**), in which both cationic species are stabilized by the respective anion present. For these complexes, the generation of the palladium hydride

complex is presumably hindered by the relatively strong coordination of mesylate and *para*-tosylate compared to triflate. The authors reported that **16a** and **16b** can be transformed to the respective palladium hydride complexes, though harsher conditions need to be applied. Refluxing of **16a** or **16b** in methanol for 1 hour under inert atmosphere leads to a partial formation of the targeted complex **17**.

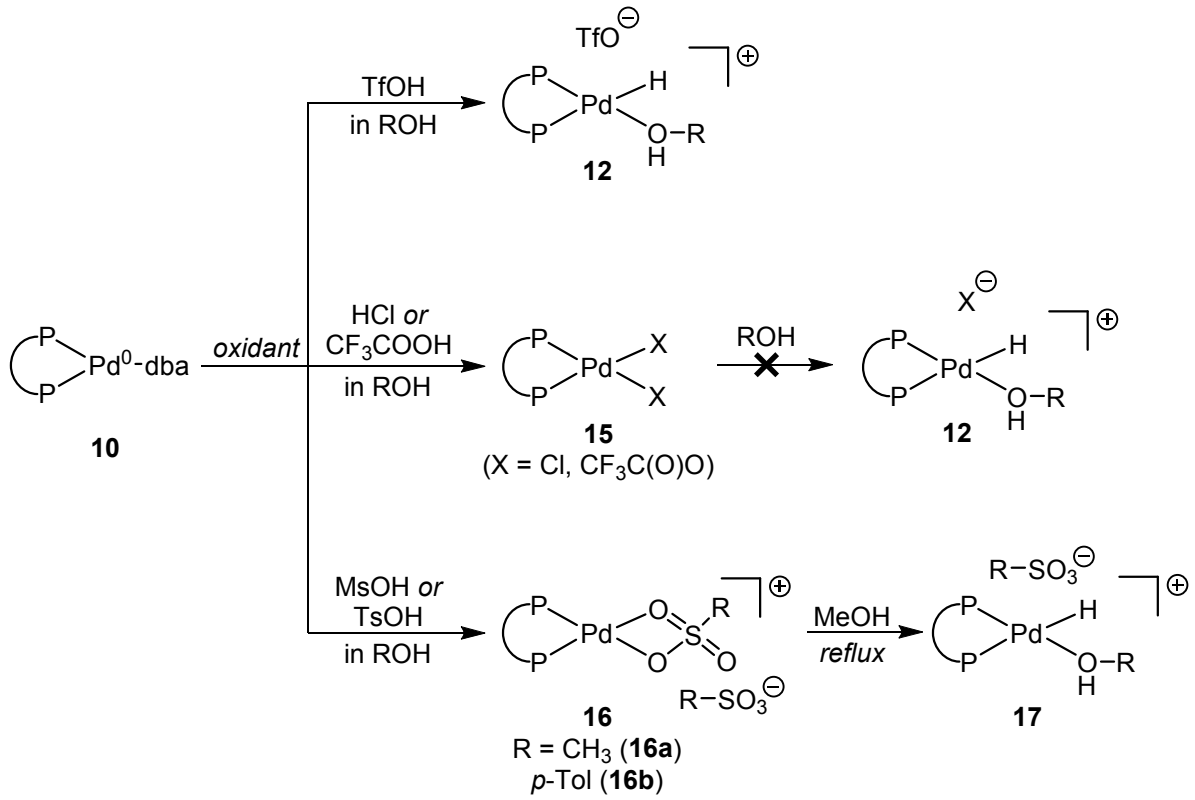

Scheme 3.5 **Different palladium complexes resulting upon treatment of 10 with various acids (TfOH: trifluoromethanesulfonic acid, MsOH: methanesulfonic acid, TsOH: *para*-toluenesulfonic acid).[22]**

In a more recent work by Mecking and co-workers,[23] the use of the preformed complex [Pd(dtbpx)(η^2-OTf)][OTf] (**16c**) in the isomerizing alkoxycarbonylation of unsaturated long-chain fatty acids to the corresponding diesters was shown to outperform an analogous system generated *in situ* from a palladium precursor and excess amounts of phosphine ligand and sulfonic acid (Scheme 3.6). The identity of the preformed catalyst was confirmed by NMR and X-ray measurements. Again, the active catalytic species was presumed to consist of a palladium-(bisphosphine)-hydride complex in which one coordination site is occupied by a not further defined ligand. In agreement to the findings of Eastham *et al.*,[22] the procedure reported by the group of Mecking involves heating of the reaction mixture to 90 °C under a CO atmosphere.

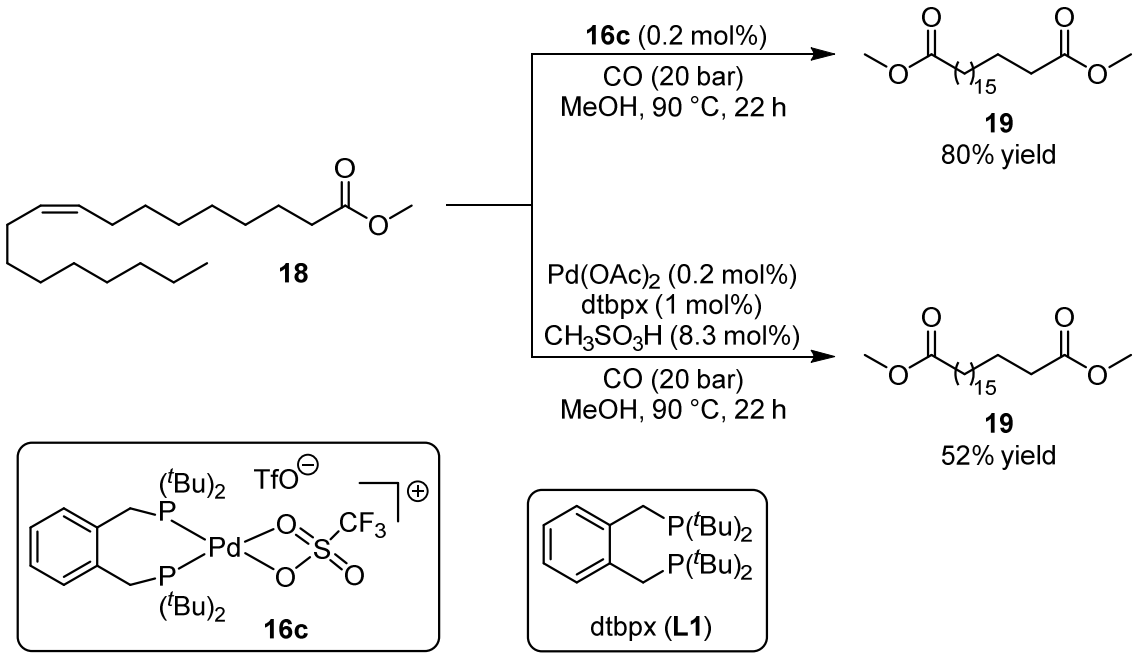

Scheme 3.6 **Isomerizing methoxycarbonylation of methyl oleate mediated by a preformed palladium complex or an *in situ* generated palladium catalyst.[23]**

A different approach towards the generation of homogeneous palladium hydride species comprises the use of formic acid or formate esters. Several works[24-26] demonstrated the decomposition of formates on electron-rich Pd bisphosphine complexes. In general, two distinct pathways appear plausible for this transformation (Scheme 3.7). Oxidative addition of the formyl C–H bond of a formate ester to a Pd(0) center results in a palladium species **21** ligated by a hydride and an alkoxycarbonyl or aryloxycarbonyl ligand. Depending on the structure of the applied formate, the obtained complex **21** remains stable to interact with a substrate (for alkyl formates),[24] or the release of CO gas leads to a palladium aryloxy hydride species **22** (in case of aryl formates).[26] For formic acid, ligand exchange and coordination of a formate anion to a palladium(II) center is possible, resulting in a palladium(II) formato complex **24**. Subsequent β-hydride elimination under emission of CO_2 forms a palladium hydride **25**.[25]

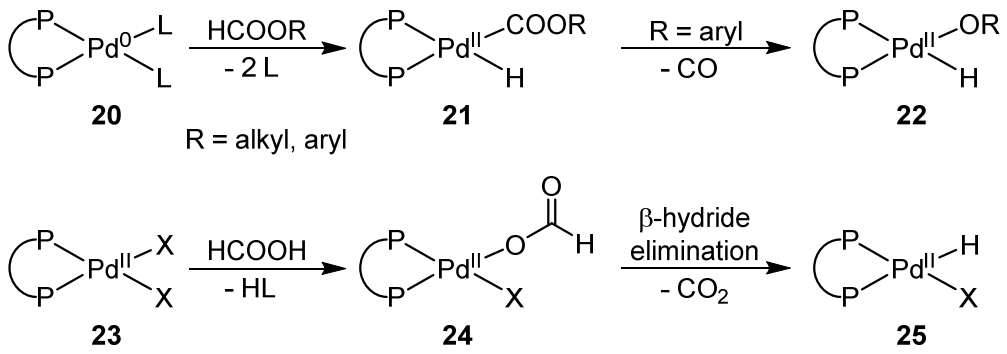

Scheme 3.7 **Generation of palladium bisphosphine hydride complexes *via* formic acid or formate decomposition.[24-26]**

Considering the discussed findings from literature reports on palladium hydride complex formation, some explanations for observations made in the optimization of the palladium-catalyzed transfer hydrogenolysis of 1-phenylethanol (**6**) can be found (Scheme 3.8).

First, the exclusive ligand effect for dtbpx (**L1**) is resolved, due to the steric and electronic properties of the ligand the formation of an electron-rich palladium hydride species is favored. The observed phenomenon that only the use of sulfonic acids as co-catalyst results in the desired catalytic activity indicates the *in situ* formation of a $[Pd(dtbpx)(\eta^2\text{-}OMs)]^+$ species (**16a**) as shown by Clegg *et al.*[22] Therefore, higher temperatures were found necessary for the reaction to proceed. This may be caused by the more challenging generation of a palladium hydride from **16a**.

When palladium precursors different than $Pd(acac)_2$, on which ligand exchange is facilitated by protonation of the coordinated acetylacetonate, are applied in the catalysis, e.g. $PdCl_2$ or $Pd(OAc)_2$, lower yields of the deoxygenated product were obtained. This can be related to the fact that complexes of the composition $[Pd(dtbpx)X_2]$ (with X representing the strongly coordinating ligands Cl^- or AcO^-) were found more difficult to activate towards hydride formation.

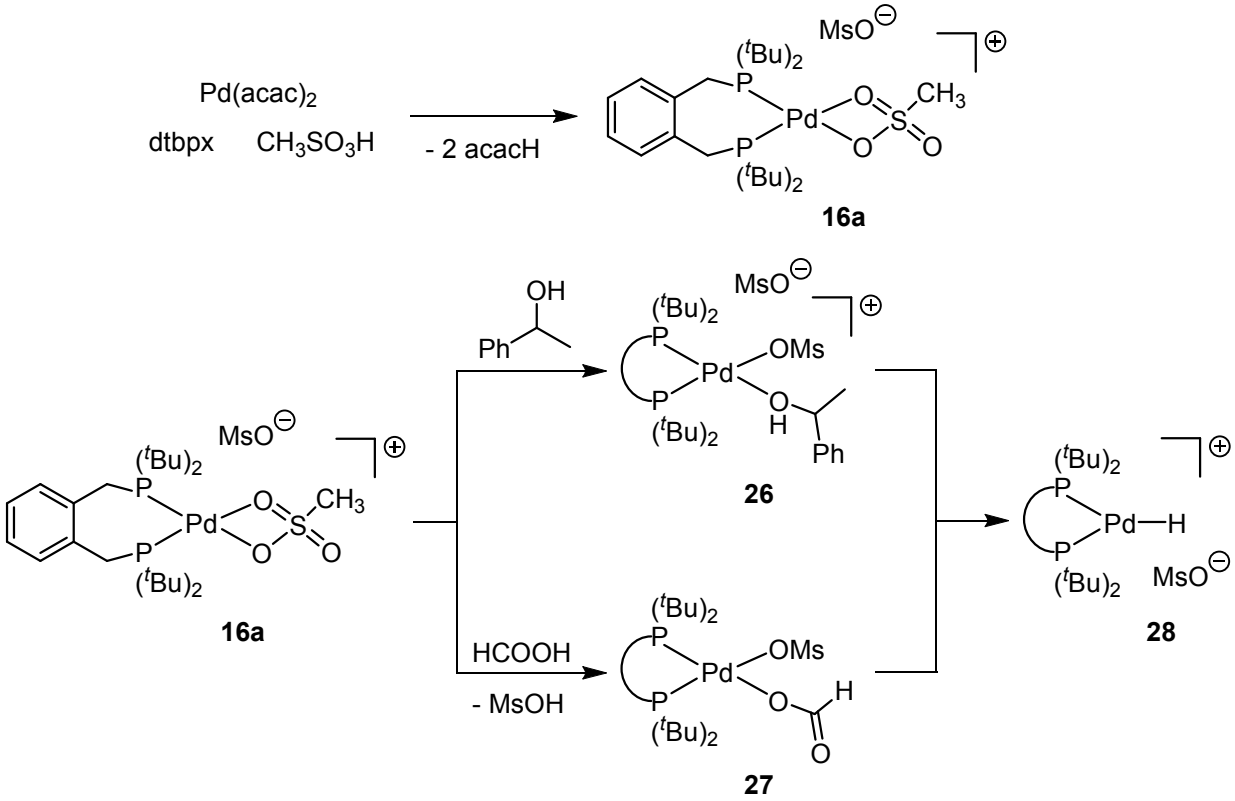

Scheme 3.8 **Formation of possible active palladium hydride catalyst species in the investigated transfer hydrogenolysis of 1-phenylethanol.**

As hydride source, two alternative species present in the catalytic reaction seem plausible. The substrate 1-phenylethanol (**6**) may undergo β-hydride elimination to acetophenone under generation of the active palladium hydride catalyst. The formed ketone may later on be reduced back to alcohol **6** using formic acid as reductant. Nonetheless, the successful transfer hydrogenolysis of alcohols which are not able to undergo β-hydride elimination will be presented later in this chapter. The decomposition of formic acid on electron-rich palladium bisphosphine complexes was discussed earlier in this section. The possible formation of the palladium hydride complex **28** should also be considered *via* this pathway.

3.3.4 The effect of partial *ex situ* ligand oxidation

During the investigation of the substrate scope of the palladium-catalyzed transfer hydrogenolysis, the use of two batches of ligand **L1** from different suppliers resulted in a substantial change in the reaction outcome for several substrates (Scheme 3.9).

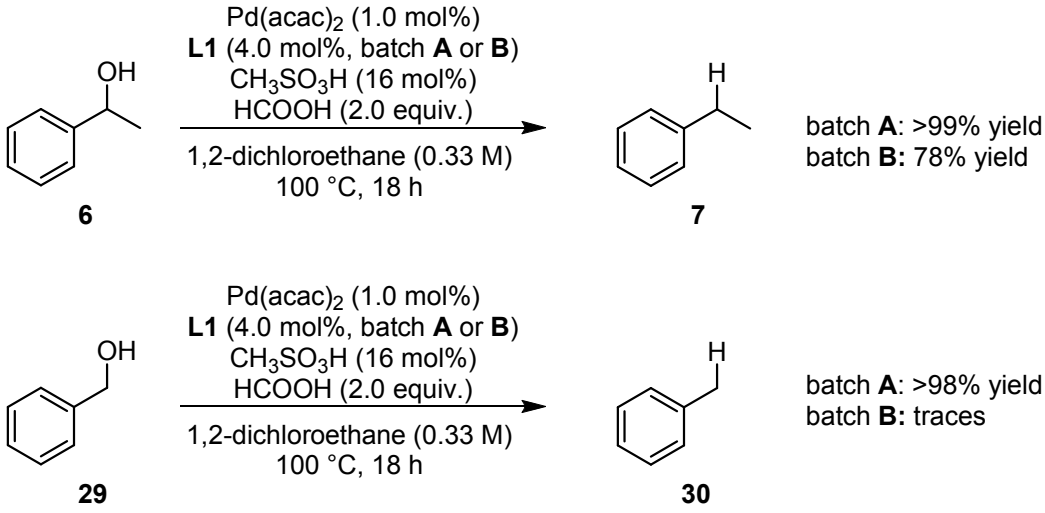

Scheme 3.9 **Observed decrease in product yield in the transfer hydrogenolysis of 1-phenylethanol and benzyl alcohol for different batches of ligand L1.**

To investigate this phenomenon, samples from both batches of **L1** were analyzed *via* ^{31}P-NMR spectroscopy. This showed that the ligand in batch **A**, which led to higher product yields, was delivered already partially oxidized on both phosphorus atoms, while batch **B** contained pure **L1**. For the partially oxidized ligand batch, two ^{31}P signals were obtained, a sharp singlet from **L1** at δ = 24.15 ppm and a broadened singlet from **L1-(O)$_2$** at δ = 62.07 ppm. Integration resulted in a molar ratio of bisphosphine **L1** to bisphosphine dioxide **L1-(O)$_2$** of 3:1 (see section 6.3 for the recorded NMR spectra).

Unfortunately, the effect of bidentate tertiary phosphine oxides in palladium-catalyzed reactions was not thoroughly investigated to date. Only few examples for the use of tertiary phosphine oxides as the only ligand in palladium complexes are reported in the

literature.[27-30] In contrast to this, the use of bisphosphine-monoxides as ligands was demonstrated for a broader scope of transformations like the asymmetric reduction of imines[31] or vinylsulfones,[32] the co-polymerization of functionalized alkenes,[33] the C–C coupling of arenes *via* C–H activation,[34] the deracemization of stereocenters[35] or in asymmetric C–C cross-coupling reactions.[36] Therefore, a series of experiments was conducted to clarify the possible influence of the partial oxidation of the ligand in the developed catalytic reaction. The transfer hydrogenolysis of 1-phenylethanol was performed either with phosphine ligands, which were already tested in the initial ligand screening, now combined with **L1-(O)$_2$** (Table 3.8) or in presence of **L1** while **L1-(O)$_2$** was substituted by other mono- or bidentate tertiary phosphine (di-)oxides (Table 3.9). The total combined amount of phosphine and phosphine oxide equaled 4 mol% in all experiments. Each pairing of phosphine ligand and phosphine oxide was applied together with either Pd(acac)$_2$ or Pd(dba)$_2$ as metal sources. A comparison of the obtained results should exclude possible redox activities between phosphine and palladium precursor.

For the transfer hydrogenolysis experiments applying different phosphine ligands with **L1-(O)$_2$**, results similar to those obtained from the initial reaction optimization were obtained. As before, most of the applied phosphines (**L2**, **L3**, **L5**, **L12**) did not give significant amounts of product **7** for both Pd(acac)$_2$ and Pd(dba)$_2$ as metal source (entries 1–8). Only the addition of **L13**, a ferrocene-based bisphosphine bearing one relatively electron-poor diphenylphosphine group and one electron-rich, bulky di-*tert*-butylphosphine group, to the reaction, led to the formation of **7** in very low yields of 15% (Pd(acac)$_2$, entry 9) and 11% (Pd(dba)$_2$, entry 10). Blank reactions without any phosphine ligand resulted in no significant product formation (entries 11, 12). Thereby, **L1-(O)$_2$** was excluded as catalytically active component. Also, a transformation of the phosphine oxide to the phosphine **L1** under the strongly reducing reaction conditions is not occurring, otherwise catalytic activity would have been evident.

Table 3.8 **Ligand effects in the palladium-catalyzed transfer hydrogenolysis of 1-phenylethanol in presence of L1-(O)$_2$.**

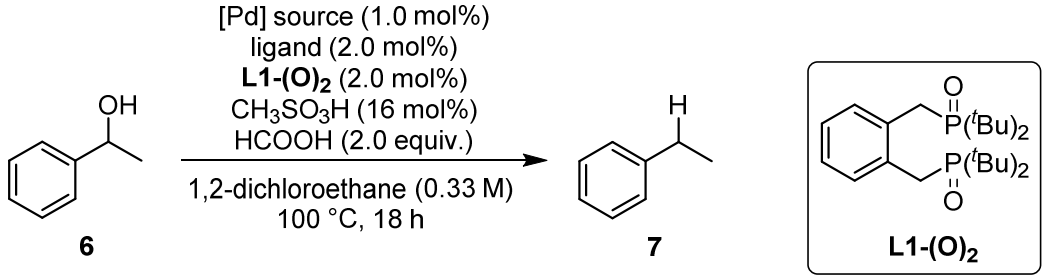

6 **7** **L1-(O)$_2$**

Entry[a]	[Pd] source	ligand	yield (**7**) [%][b]
1	$Pd(acac)_2$	**L2**[c]	traces
2	$Pd(dba)_2$	**L2**[c]	–
3	$Pd(acac)_2$	**L3**	traces
4	$Pd(dba)_2$	**L3**	traces
5	$Pd(acac)_2$	**L5**	traces
6	$Pd(dba)_2$	**L5**	traces
7	$Pd(acac)_2$	**L12**	traces
8	$Pd(dba)_2$	**L12**	traces
9	$Pd(acac)_2$	**L13**	15
10	$Pd(dba)_2$	**L13**	11
11	$Pd(acac)_2$	–[d]	traces
12	$Pd(dba)_2$	–[d]	traces

[a]General reaction conditions: 1-Phenylethanol (1.00 mmol, 120 µL, 0.33 M solution), 1,2-dichloroethane (3 mL), $Pd(acac)_2$ (10 µmol, 3.0 mg, 1.0 mol%) or $Pd(dba)_2$ (10 µmol, 6.0 mg, 1.0 mol%), phosphine ligand (20 µmol, 2.0 mol%), **L1-(O)$_2$** (20 µmol, 8.5 mg, 2.0 mol%), methanesulfonic acid (0.16 mmol, 10 µL, 16 mol%), formic acid (2.0 mmol, 75 µL, 2.0 equivalents), stirred at 100 °C for 18 h in a sealed glass pressure tube. Unless stated otherwise, full substrate conversion was achieved. [b]Product identification was performed *via* measurement of authentic commercial samples or *via* GC-MS analysis. Yields determined *via* quantitative GC-FID using *n*-pentadecane as internal standard. [c]4 mol% of PPh_3 (**L2**) used. [d]4 mol% of **L1-(O)$_2$** used.

Analogously, the effect of several mono- and bidentate tertiary phosphine (di-)oxides on the reaction in presence of the phosphine ligand **L1** was investigated, again either with a Pd(II) or a Pd(0) precursor. Interestingly, all reactions in which $Pd(dba)_2$ was applied reached very good product yields above 90% (entries 2, 4, 6, 8), even a blank reaction without added phosphine oxide (91%, entry 12). For $Pd(acac)_2$ as metal source, differences in the reaction outcome dependant on the introduced phosphine oxide became evident. For monodentate phosphine oxides **L2-(O)** and **L16-(O)** or the bidentate phosphine dioxide **L5-(O)$_2$** with a flexible aliphatic carbon backbone, comparable yields to those obtained from reactions starting from $Pd(dba)_2$ were determined (95–97%, entries 1, 5, 7). **L3-(O)$_2$** was applied as a phosphine oxide with an aromatic, rigid backbone. While the reaction had reached a very good yield when using the Pd(0) source with **L3-(O)$_2$** (93%, entry 4), use of the Pd(II)

precursor resulted in a sharp drop of the product yield to 44% (entry 3). A similar result was obtained for the blank reaction with Pd(II), a product yield of 43% was determined (entry 11).

Table 3.9 **Effects of tertiary phosphine oxides in the transfer hydrogenolysis of 1-phenylethanol in presence of L1.**

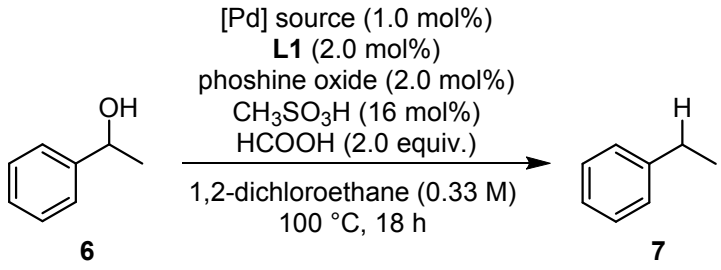

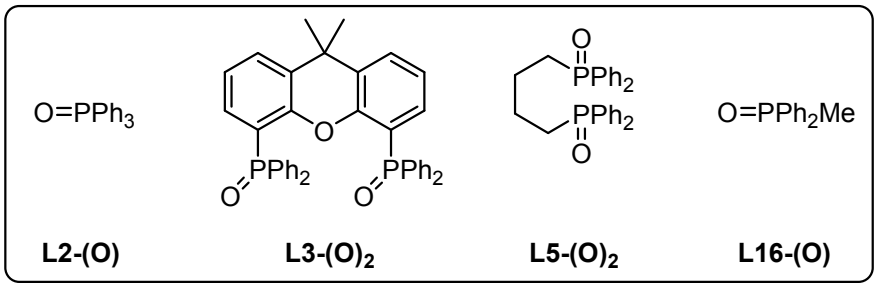

Entry[a]	[Pd] source	phosphine oxide	yield (**7**) [%][b]
1	$Pd(acac)_2$	**L2-(O)**	97
2	$Pd(dba)_2$	**L2-(O)**	92
3	$Pd(acac)_2$	**L3-$(O)_2$**	44
4	$Pd(dba)_2$	**L3-$(O)_2$**	93
5	$Pd(acac)_2$	**L5-$(O)_2$**	95
6	$Pd(dba)_2$	**L5-$(O)_2$**	91
7	$Pd(acac)_2$	**L16-(O)**	96
8	$Pd(dba)_2$	**L16-(O)**	94
11	$Pd(acac)_2$	–	43
12	$Pd(dba)_2$	–	91

[a]General reaction conditions: 1-Phenylethanol (1.00 mmol, 120 µL, 0.33 M solution), 1,2-dichloroethane (3 mL), $Pd(acac)_2$ (10 µmol, 3.0 mg, 1.0 mol%) or $Pd(dba)_2$ (10 µmol, 6.0 mg, 1.0 mol%), **L1** (20 µmol, 7.8 mg, 2.0 mol%), phosphine oxide (20 µmol, 2.0 mol% for bidentate phosphine oxides, 40 µmol, 4.0 mol% for monodentate phosphine oxides), methanesulfonic acid (0.16 mmol, 10 µL, 16 mol%), formic acid (2.0 mmol, 75 µL, 2.0 equivalents), stirred at 100 °C for 18 h in a sealed glass pressure tube. Unless stated otherwise, full substrate conversion was achieved. [b]Product identification was performed *via* measurement of authentic commercial samples or *via* GC-MS analysis. Yields determined *via* quantitative GC-FID using *n*-pentadecane as internal standard.

The results presented in tables 3.8 and 3.9 clearly show that only **L1** forms an active catalyst species in the palladium-catalyzed transfer hydrogenolysis of **6**, **L1-(O)$_2$** alone does not. It was demonstrated that the addition of tertiary phosphine oxides had no influence on the reaction starting from Pd(dba)$_2$ as catalyst precursor. Here, the dibenzylideneacetone ligand could also exhibit a stabilizing interaction with the catalyst. Yet, when Pd(acac)$_2$ was applied as palladium source, only the addition of monodentate or bidentate tertiary phosphine oxides with a flexible backbone increased the yield of the deoxygenated product to values comparable to the reaction with the Pd(0) precursor. The presence of the rigid bidentate tertiary phosphine dioxide **L3-(O)$_2$** yielded similar product amounts as the reaction without added phosphine oxide. Therefore, it is assumed that only monodentate or flexible bidentate phosphine oxides possess a beneficial effect on the reaction. Although the observed effect is not thoroughly understood, the beneficial influence could be related to a weak stabilizing interaction with the palladium catalyst (Scheme 3.10). Unlike in the works discussed in section 3.3.3, no coordinating solvent is present in the transfer hydrogenolysis reaction system to stabilize a possible palladium hydride complex. Here, suitable phosphine oxides could act as labile ligands like in species **31** or **32**, preventing catalyst decomposition and agglomeration of the metal.[28] The oxygen-bound coordination of phosphine oxides was described for Pd(II) centers, but no examples for Pd(0) are known.[27,28,30]

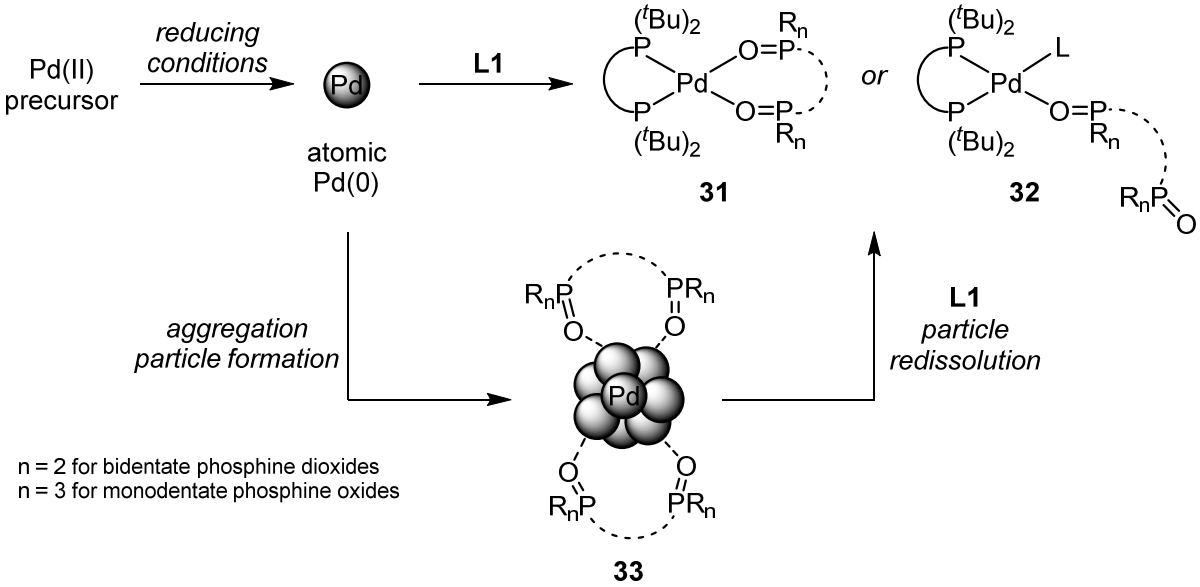

Scheme 3.10 **Proposed stabilizing interactions of tertiary phosphine oxides with palladium centers under transfer hydrogenolysis conditions.**

The phosphine oxides could also exert their stabilizing effect in the reduction of Pd(II) to Pd(0) *in situ*. The generation of atomic Pd(0) is followed by the fast formation of nanoparticles. These particles need to be stabilized in solution to inhibit the agglomeration to bulk metal.[28,37] Phosphine oxides with the right structural properties could weakly coordinate on the particle surface, this stabilizing effect was already shown for nanoparticles generated

from other metal-based precursors.[38-43] In the transfer hydrogenolysis reaction, the stabilized nanoparticles **33** could be redissolved *via* metal leaching induced by the stronger binding ligand **L1** to form a homogeneous palladium species **31** or **32** (Scheme 3.10). The behavior of palladium nanoparticles as metal source and their interaction with **L1** was also investigated during this work and will be discussed in section 3.3.7.

With regard to the effect of tertiary phosphine oxides described in this section, the following experiments were conducted under use of partially oxidized **L1**. The amount of phosphine ligand was adjusted to a loading of 4.0 mol% of **L1**, which was obtained already oxidized from the chemical supplier. Thereby an amount of 1.3 mol% of **L1-(O)$_2$** was introduced to the reaction mixture (molar ratio of **L1** to **L1-(O)$_2$**: 3:1).

3.3.5 Substrate scope and additive screening

Substrate scope

After the optimization of the reaction conditions, the rationalization of the role of the individual catalyst components and the investigation of the effect of the partial oxidation of the applied phosphine ligand **L1**, a thorough substrate screening of the palladium-catalyzed transfer hydrogenolysis was performed. A variety of substituted primary, secondary and tertiary benzylic alcohols, differing in their steric and electronic properties, was subjected to the reaction conditions. In addition, the tolerance of the catalyst system towards introduced functional groups was evaluated. Due to the volatility of a majority of the products, yields were determined *via* quantitative GC-FID. High-boiling products were additionally isolated. The scope of the transformation is presented in Table 3.10.

As found in the optimization experiments, 1-phenylethanol (**6**) was transformed to ethylbenzene (**7**) in quantitative yield. *Ortho*- or *para*-methyl-substituted 1-phenylethanols provided the deoxygenated products **35a** and **35q** in fair to very good yields of 47% and 82% (entries 2, 18). The transformation of the *ortho*- or *para*-methoxy-substituted 1-phenylethanols **34p** and **34b** gave only traces of the desired products, due to an observed acid-induced dehydration and subsequent dimerization of these electron-rich substrates *via* C–C bond formation (entries 3, 17). In contrast, the *meta*-substituted isomer **33s** was deoxygenated in a good yield of 65% (entry 20).

For the *para*-acetoxy-substituted 1-phenylethanol **34m** or substrates **34η**, **34θ**, **34κ** based on aromatic heterocycles, a similar elimination-dimerization pathway is assumed, only products of higher molecular mass were found (entries 14, 34, 35, 36).

1-Phenylethanols bearing a F, Cl or Br substituent in *para*-position were tolerated well in the reaction, no dehalogenation occurred despite the use of palladium as catalyst. The corresponding halogenated ethylbenzenes **35c**, **35d** and **35e** were obtained in good to excellent yields of 62% to 94% (entries 4–6). Contrary to these results, the products **35f** and

35r from the transfer hydrogenolysis of 1-(*para*-iodophenyl)ethanol (**34f**) and 1-(*ortho*-chlorophenyl)ethanol (**34r**) were only generated in trace amounts (entry 7, 19), the intermediary formates were observed exclusively. Electronically deactivating groups in homobenzylic position as found in substrates **34ε** and **34ζ** also stopped the transformation at the respective formates (entries 32, 33).

Attachment of an ester group in *para*-position on the phenyl ring hindered the transfer hydrogenolysis of **34g**. The corresponding substituted ethylbenzene **35g** was obtained in 35% yield, besides a large amount of unreacted formate intermediate (entry 8). Electronically deactivated substrates like **34g**, **34i** or **34k** did not show the desired reactivity, again accumulation of the formate intermediates was observed (entries 9, 10, 12). An amino function in substrate **34j** was found incompatible with the acidic reaction conditions (entry 11).

Biphenyl or naphthyl substituents in the substrates **34l**, **34t** and **34u** resulted in excellent isolated product yields (entries 13, 21, 22). Also 1,2,3,4-tetrahydro-1-naphthol (**34v**), a substrate with a more rigid structure, was transformed into the corresponding hydrocarbon **35v** in quantitative yield (entry 23).

Table 3.10 **Evaluation of the substrate scope for the palladium-catalyzed transfer hydrogenolysis of benzylic alcohols.**

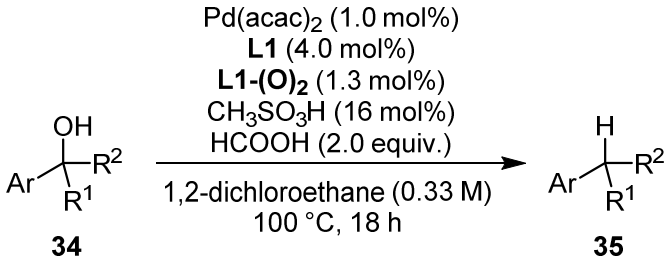

Entry[a]	product	Ar	R^1	R^2	yield [%][b]
1	**7**	Ph	CH_3	H	>99
2	**35a**	4-CH_3-C_6H_4	CH_3	H	47
3	**35b**	4-CH_3O-C_6H_4	CH_3	H	traces[c]
4	**35c**	4-F-C_6H_4	CH_3	H	70
5	**35d**	4-Cl-C_6H_4	CH_3	H	94
6	**35e**	4-Br-C_6H_4	CH_3	H	62
7	**35f**	4-I-C_6H_4	CH_3	H	traces[d]
8	**35g**	4-CO_2CH_3-C_6H_4	CH_3	H	35[d]
9	**35h**	4-CF_3-C_6H_4	CH_3	H	–[d]
10	**35i**	4-NO_2-C_6H_4	CH_3	H	–[d]

Table 3.10 (continued)

Entry[a]	product	Ar	R^1	R^2	yield [%][b]
11	**35j**	4-NH_2-C_6H_4	CH_3	H	–
12	**35k**	4-CN-C_6H_4	CH_3	H	–[d]
13	**35l**	4-Ph-C_6H_4	CH_3	H	>99 (96)
14	**35m**	4-AcO-C_6H_4	CH_3	H	–[c]
15	**35n**	Ph	H	H	98
16	**35o**	4-CH_3-C_6H_4	H	H	93
17	**35p**	2-CH_3O-C_6H_4	CH_3	H	traces[c]
18	**35q**	2-CH_3-C_6H_4	CH_3	H	82
19	**35r**	2-Cl-C_6H_4	CH_3	H	traces
20	**35s**	3-CH_3O-C_6H_4	CH_3	H	65
21	**35t**	1-naphthyl	CH_3	H	(95)
22	**35u**	2-naphthyl	CH_3	H	(94)
23	**35v**	Ph	–$(CH_2)_3$–	H	>99
24	**35w**	Ph	$CH_2C(O)CH_3$	H	59
25	**35x**	Ph	Ph	H	87
26	**35y**	Ph	CH_3	CH_3	75
27	**35z**	Ph	Ph	CH_3	66
28	**35α**	Ph	Ph	Ph	(>99)
29	**35β**	Ph	–CH=CH_2	H	–
30	**35γ**	Ph	–C≡CH	H	–
31	**35δ**	Ph	^{t}Bu	H	traces
32	**35ε**	Ph	CO_2CH_3	H	–[d]
33	**35ζ**	Ph	CF_3	H	–[d]
34	**35η**	2-pyridyl	CH_3	H	–[c]
35	**35θ**	3-pyridyl	CH_3	H	–[c]
36	**35κ**	2-furanyl	CH_3	H	–[c]

[a] General reaction conditions: Alcohol (1.00 mmol, 0.33 M solution), 1,2-dichloroethane (3 mL), $Pd(acac)_2$ (10 µmol, 3.0 mg, 1.0 mol%), **L1** (40 µmol, 16 mg, 4.0 mol%), **L1-(O)$_2$** (1.3 mol%, brought into the reaction as partially oxidized **L1**), methanesulfonic acid (0.16 mmol, 10 µL, 16 mol%), formic acid (2.0 mmol, 75 µL, 2.0 equivalents), stirred at 100 °C for 18 h in a sealed glass pressure tube. Unless stated otherwise, full substrate conversion was achieved. [b]Product identification was performed *via* measurement of authentic commercial samples or *via* GC-MS analysis. Yields determined *via* quantitative GC-FID using *n*-pentadecane as internal standard, isolated yields are given in brackets. [c]The transfer hydrogenolysis was prevented by an acid-induced dehydrative oligomerization. [d]The respective 1-arylethyl formate was found as main product.

For the simple aldol product **34w**, a yield for the deoxygenated aromatic ketone **35w** of 59% was obtained, clearly demonstrating the selectivity of the transfer hydrogenolysis for benzylic alcohols over non-benzylic carbonyls (entry 24). The introduction of C–C multiple bonds as in substrates **34β** and **34γ** inhibited the formation of the hydrogenolysis products, presumably due to a competing addition of the palladium hydride to these substrates (entries 29, 30). For substrate **34δ** containing a *tert*-butyl group in α-position to the benzylic alcohol, no transfer hydrogenolysis occurred (entry 31). Instead, the product of a dehydrative elimination followed by a methyl shift towards the benzylic position was observed.

Primary benzylic alcohols **34n** and **34o** were also successfully transformed into the corresponding toluenes **35n** and **35o** in excellent yields of 98% and 93%, excluding a possible elimination–hydrogenation pathway through styrene derivatives (entries 15, 16). Diphenylmethanol (**34x**), which is also unable to undergo dehydration to an alkene, was converted to the deoxygenated product **35x** in a very good yield of 87% (entry 25). Tertiary benzylic alcohols **34y**, **34z** and **34α** underwent transfer hydrogenolysis in good to quantitative yields, product **35α** could also be isolated (entries 26–28).

Additive screening

Complementary to the discussed substrate screening, the tolerance of the catalyst system towards different functional groups as well as the compatibility of these functional groups with the applied reaction conditions was additionally tested in a brief "robustness screening", as proposed by Glorius and co-workers.[44] As basic principle, additives with a simple structure, for the palladium-catalyzed transfer hydrogenolysis substituted benzenes were chosen, were added to the reaction in equimolar amounts relative to the substrate. The reaction is performed according to the usual procedure and the generated or residual amounts of product or additive, respectively, are determined afterwards, using quantitative GC-FID. The obtained results allow conclusions on chemical compatibilities, especially when compared to the yields detected in the conventional substrate screening. For the palladium-catalyzed transfer hydrogenolysis, a number of additives was chosen, bearing substituents which led to a decreased yield of the corresponding deoxygenation products when introduced on the substrate itself (Table 3.11).

For electron-rich 1-(methoxyphenyl)ethanols, no product formation was observed in the substrate screening. Instead, obviously a dehydrative dimerization occurred, leading to C–C coupled dimers. Therefore, anisole (**36**) was tested as additive in the robustness screening to confirm the electronic activation of these substrate as reason for the side reaction, rather than the reactivity of the methoxy group itself. Indeed, after the reaction both the deoxygenation product **7** and additive **36** were detected on GC in 69% and 62%, respectively (entry 1). Although the transfer hydrogenolysis was hindered by the presence of an additive

bearing a methoxy function, the reaction still proceeded smoothly. Indeed, the additive anisole was consumed in the reaction, presumably due to an acid-induced side reaction involving the electron-rich arene. Nonetheless, a major part of the starting amount was recovered on GC.

Nitrile substitution on the arylethanol substrate resulted in a complete breakdown of the desired reactivity in the substrate screening. For the addition of benzonitrile (**37**) to the reaction, a similar reaction outcome was observed. Ethylbenzene (**7**) was formed in a low yield of 27%, the residual amount of additive **37** was determined as 68% (entry 2). Interestingly, non-converted 1-phenylethyl formate was found, indicating that the nitrile functionality holds an inhibiting effect towards the palladium catalyst, presumably through coordination to the metal and blocking of the active site.

For the reaction in presence of phenylacetylene (**38**), neither the transfer hydrogenolysis product nor the additive were detected (entry 3). Instead, styrene was generated next to a compound of higher *m*/*z* ratio. GC-MS analysis indicated that this side product arose from the acid-catalyzed dimerization of styrene. This result demonstrates the higher reactivity of the applied alkyne **38** towards the reduction catalyst, leading to semi-reduction to styrene. The generated alkene then presumably undergoes dimerization under the acidic reaction conditions due to a lack of further reductant present.

An ester group contained in the substrate for the transfer hydrogenolysis could impede the reaction either through electronic deactivation or as an alternative reaction center, accepting a hydride from the palladium catalyst. The addition of methyl benzoate (**39**) to the reaction showed that the latter is not the case. The transfer hydrogenolysis proceeded nearly undisturbed, producing ethylbenzene in an excellent 98% yield. In addition, the additive was still found in 84% of the initial amount after the catalysis, thus showing the selectivity of the reaction for benzylic alcohols over aromatic esters (entry 4).

Phenyl-2-propanone (**40**) was chosen as an exemplary homobenzylic ketone, the result should be compared to the transformation of the aldol product **34w** in the substrate screening, which showed good selectivity towards the sole deoxygenation of the benzylic alcohol group. Herein, no influence on the transfer hydrogenolysis of substrate **6** became evident as ethylbenzene was detected in a quantitative yield (entry 5). Yet, the ketone additive was also consumed under the reaction conditions, possibly due to the strongly acidic reaction conditions. A moderate residual amount of **40** of 45% was recovered.

The addition of nitrobenzene (**41**) to the reaction was suspected to have a similar effect on the catalyst as was shown for benzonitrile (**37**) due to a similar possible coordination to the metal center. As expected, the transfer hydrogenolysis was nearly completely suppressed, yielding ethylbenzene in a poor amount of 13%, along with styrene and a great amount of unreacted intermediary formate **9**. For the additive **41**, only 55% of the initial

amount were recovered, but no reduction products like aromatic amines were detected *via* GC analysis.

Table 3.11 **Effects of added substituted benzenes on the palladium-catalyzed transfer hydrogenolysis of 1-phenylethanol.**

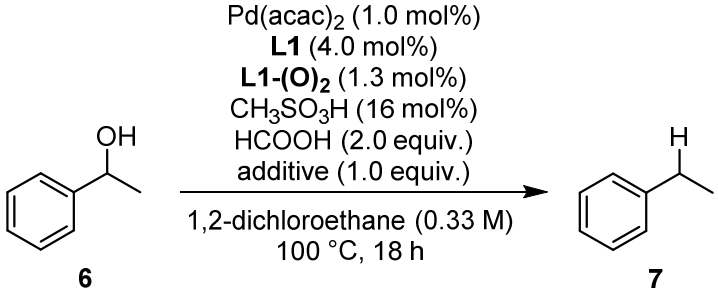

Entry[a]	additive	recovered additive [%]	yield (**7**) [%][b]
1	anisole (**36**)	62	69
2	benzonitrile (**37**)	68	27[c]
3	phenylacetylene (**38**)	–	–
4	methyl benzoate (**39**)	84	98
5	phenyl-2-propanone (**40**)	45	>99
6	nitrobenzene (**41**)	55	13[c]
7	aniline (**42**)	–	–[c]
8	chlorobenzene (**43**)	75	>99
9	bromobenzene (**44**)	86	53

[a]General reaction conditions: 1-Phenylethanol (1.00 mmol, 120 µL, 0.33 M solution), 1,2-dichloroethane (3 mL), $Pd(acac)_2$ (10 µmol, 3.0 mg, 1.0 mol%), **L1** (40 µmol, 16 mg, 4.0 mol%), **L1-(O)$_2$** (1.3 mol%, brought into the reaction as partially oxidized **L1**), methanesulfonic acid (0.16 mmol, 10 µL, 16 mol%), formic acid (2.0 mmol, 75 µL, 2.0 equivalents), additive (1.0 mmol, 1.0 equivalents), stirred at 100 °C for 18 h in a sealed glass pressure tube. Unless stated otherwise, full substrate conversion was achieved. [b]Product identification was performed *via* measurement of authentic commercial samples or *via* GC-MS analysis. Yields determined *via* quantitative GC-FID using *n*-pentadecane as internal standard. [c]1-Phenylethyl formate (**9**) was found as main product.

The incompatibility of amines with the strongly acidic reaction conditions was demonstrated by the performance of aniline (**42**). Immediately after the addition, the formation of a non-soluble salt was observed in the reaction vessel. As a result, only the reaction intermediate 1-phenylethyl formate was detected after the reaction, the desired product and the amine additive were both absent (entry 7).

Halogenated arenes were also tested as additives. Therein, chlorobenzene (**43**) had no influence on the conversion of the alcohol substrate **6**. A quantitative conversion to ethylbenzene was observed, the chloride was recovered in 75% of the starting amount (entry 8). The addition of bromobenzene (**44**) had a graver impact on the deoxygenation reaction. The hydrogenolysis product **7** was formed in a moderate yield of 53%, while the additive was still present in 86% compared to the beginning of the reaction. The consumption

of the aryl halides is rationalized by a possible insertion of a formed Pd(0) species into the C–halogen bond, followed by a reductive dehalogenation.

In conclusion, the brief robustness screening showed the potential of this alternative screening method to evaluate catalyst selectivity or the tolerance of different functional groups towards the reaction conditions. Further, deductions regarding possible catalyst inhibition pathways through certain substituents introduced to the substrate are possible from the obtained results.

3.3.6 Reaction progress analysis and catalyst poisoning experiments

Reaction progress analysis

To further characterize the active catalyst species and to gain an insight into the course of the reaction, the reaction progress was monitored over time. Besides the detection of reaction intermediates and the determination of the optimal reaction time, the shape of the obtained kinetic curve was expected to give important hints towards the homogeneous or heterogeneous nature of the active catalyst. Therefore, the reactor design was slightly changed. The closed screw-caps used to seal the glass pressure tubes were exchanged for caps which allow access to the tightening septum. Furthermore, a stainless steel valve was installed, piercing the septum to allow for the withdrawal of samples from the reaction mixture (Figure 3.1). This setup made the analysis of the reaction mixture at defined times possible without opening the vessel. Through the build-up of internal pressure in the glass tube, opening the valve was sufficient to collect samples on a 100 µL scale. The obtained samples could, after suitable workup and dilution, be analyzed quantitatively *via* GC-FID.

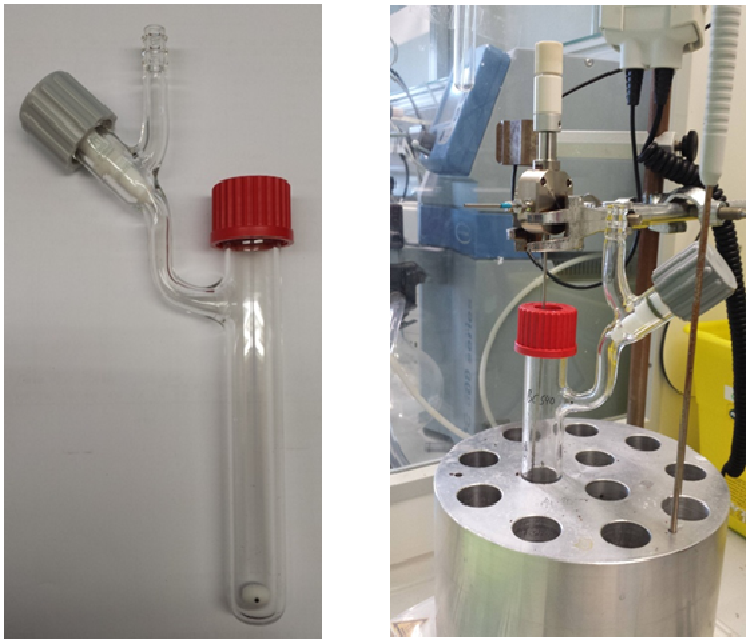

Figure 3.1 **The used glass pressure tubes equipped with a magnetic stirring bar and a closed screw cap (left), altered reactor design with accessible septum and installed stainless steel valve for sampling (right).**

First, the transfer hydrogenolysis of 1-phenylethanol (**6**) was monitored under optimized reaction conditions. The reaction was performed in a 3 mmol scale and the samples for quantitative GC analysis were withdrawn at defined reaction times. Plotting of the detected product yield *versus* the reaction time resulted in a reaction profile (Scheme 3.11).

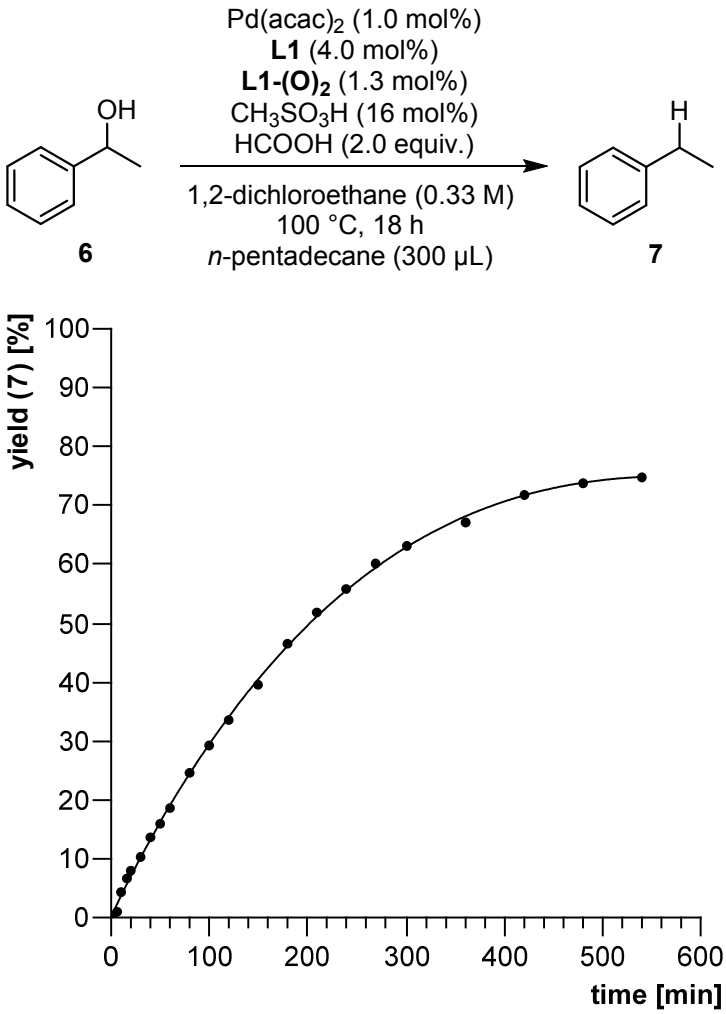

Scheme 3.11 **Reaction profile for the transfer hydrogenolysis of 1-phenylethanol under optimized conditions (the curve was obtained *via* non-linear regression of the measured data points).**

As depicted in section 1.6.2, the shape of the obtained curve allows for a first assumption concerning the homogeneous or heterogeneous character of the catalyst species. In a heterogeneous case an induction period, during which no product formation occurs, is observed. This is related to the formation of non-soluble metallic species from soluble precursors. The lack of an induction period may indicate the presence of an active homogeneous catalyst as well as of fast formed metal nanoparticles.[45-47] For the transfer hydrogenolysis of 1-phenylethanol, no induction period was evident. During the first 5 minutes of the reaction, the fast formation of the intermediate 1-phenylethyl formate (**9**) from the alcohol substrate could be observed on GC after which the conversion to ethylbenzene (**7**) set in. No other side products were detected.

The initial reaction profile shows a clear linear shape. This proposes either an active homogeneous or nanoparticulate catalyst.[45,46] After longer reaction times, the rate of the reaction decreases. This may be due to a lower concentration of available substrate or ageing and therefore deactivation of the catalyst.

More conclusive information about the active catalyst species should be obtained from poisoning experiments applying either qualitative or quantitative poisons. In section 1.6.2 a comprehensive overview of these methods was already given. First, qualitative poisons were used in the transfer hydrogenolysis to resolve the nature of the active catalyst.

Qualitative poisoning experiments

A possible formation of heterogeneous metal particles as catalytically active species should be excluded through a mercury poisoning test. As discussed before in this thesis, elemental mercury is a well-known poison for heterogeneous noble metal catalysts. It adsorbs to metal surfaces or forms amalgams, which leads to the blocking of the active sites and the suppression of the catalysis.[48] In theory, homogeneous metal species are not affected by mercury. Yet, there are examples described in the literature of mercury causing unwanted side reactions or inactivating homogeneous, monometallic catalysts.[48-54]

In this work, 300 equivalents of mercury (relative to palladium) were added to the reaction *via* syringe through the accessible septum (Scheme 3.12). The addition was performed after a reaction time of 80 min to ensure the prior formation of the active catalyst, evident through an already generated yield for ethylbenzene (**7**) of 30%. Vigorous stirring ensured the contact of the whole reaction mixture with the low-soluble mercury.

Before the addition of Hg, the kinetic curve showed an approximately linear shape. Directly after the application of the catalyst poison, product formation ceased, the catalyst was deactivated. This finding in theory is a strong indication for a heterogeneous metal species, e.g. nanoparticles, present in the reaction. Nonetheless, it has to be kept in mind that the mercury test was shown to give false results in certain cases. Jones and co-workers[53] proposed an alternative interpretation of a positive mercury test on palladium-based systems: The suppression of the catalytic reaction should not only be seen as evidence for an operating heterogeneous Pd(0) catalyst, but also mononuclear palladium(0) species or intermediary palladium(0)-containing species could be deactivated by mercury.

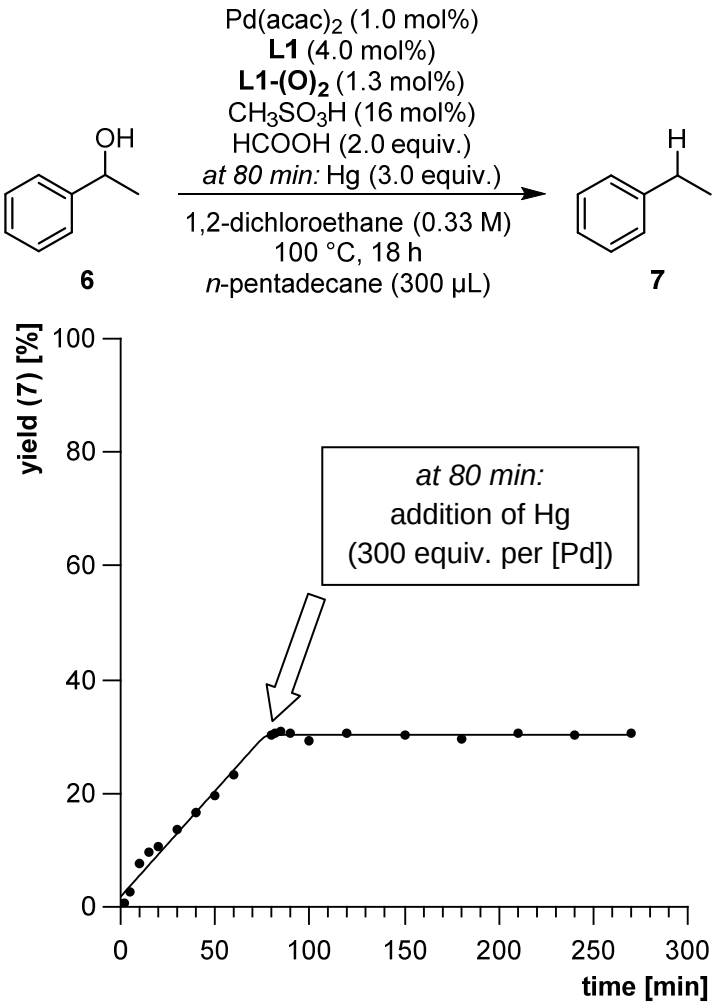

Scheme 3.12 **Reaction profile for the transfer hydrogenolysis of 1-phenylethanol with mercury added as catalyst poison at 80 min (the curve was obtained *via* non-linear regression of the measured data points).**

Finke[46] proposed an obligatory control experiment to rule out false positive results of a performed mercury test. Addition of the poison before the activation of the catalyst should show a possible inhibition of the precursor species. If the reaction is suppressed in this scenario, the information obtained from the mercury test may not be taken into account for a statement about the homogeneous or heterogeneous character of the active catalyst.

Following Finke's proposition, the mercury poisoning test was repeated for the transfer hydrogenolysis of 1-phenylethanol. Contrary to the first run, mercury was already added at the beginning of the reaction without the active catalyst being present (Scheme 3.13). As a result, the formation of only minor traces of product **7** was detected on GC during the first 15 minutes of the reaction. From that point on, the reaction was halted, proposing that the added mercury did deactivate a precursory stage of the active catalyst. As the interaction of Hg with ligand-bound Pd(II) species is found impossible in the literature,[53,55-57] this finding is taken as evidence of an *in situ* reduction of the Pd(II) precursor to atomic Pd(0), which can form aggregates. These can be redissolved by the present phosphine ligand under the given

reaction conditions. Alternatively, direct ligation of Pd(0) and further activation steps towards the active palladium transfer hydrogenolysis catalyst appear possible.

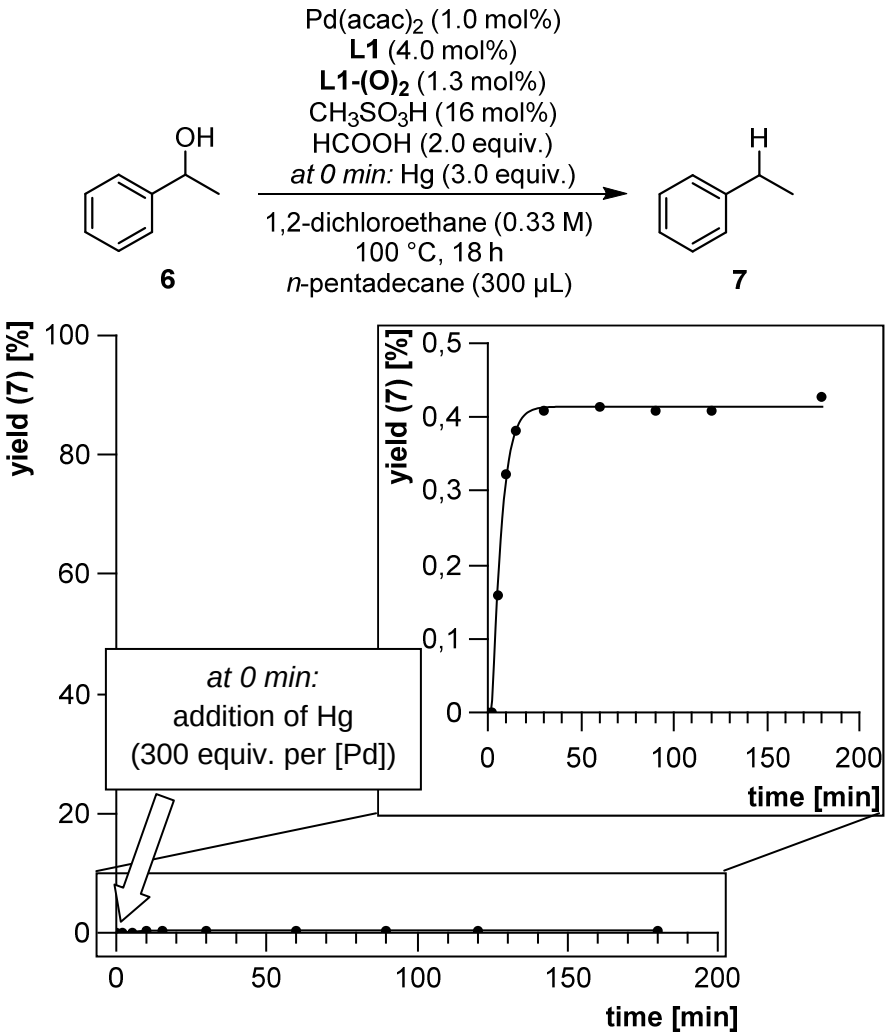

Scheme 3.13 **Reaction profile for the transfer hydrogenolysis of 1-phenylethanol with mercury added as catalyst poison at 0 min (the curve was obtained *via* non-linear regression of the measured data points).**

Complementary to the mercury test, the addition of dibenzo[*a,e*]cyclooctatetraene (dct) as described by Crabtree[58] was performed to gain additional results to classify the operating catalyst in the transfer hydrogenolysis as homogeneous or heterogeneous species. Dct is a rigid, sterically demanding diene for which coordination to homogeneous metal complexes was shown, thereby inhibiting their catalytic activity. Heterogeneous catalysts are not affected by this poison, as its tub-like structure makes the adsorption to a metal surface difficult (see section 1.6.2).

As before in the mercury poisoning test, dct was added as a solution in 1,2-dichloroethane only after the activation of the catalyst was apparent, i.e. after a reaction time of 80 minutes and the formation of a significant amount of product **7**. A slight excess of 2.0 equivalents of dct (relative to palladium) was applied, but no effect on the performance of the catalyst was evident from the reaction profile. Surprisingly, the GC traces for the samples

withdrawn from the reaction showed not only the presence of dct in the mixture, but also of dihydro-dct (*m*/*z* was found increased by two units compared to dct). Therefore, the hydrogenation of one coordinating double bond of the diene is thought to cause a deactivation of the poison rather than of the catalyst. A second run was performed under use of a higher excess of 10 equivalents of dct per [Pd] to ensure the deactivation of the catalyst even in case of partial hydrogenation of the poison (Scheme 3.14). In fact, compared to the non-poisoned reaction, a significant decrease of the reaction rate was observed after the addition of dct, but the catalysis was not stopped completely. Interestingly, under the higher excess of dct, no hydrogenation of the diene was observed on GC, indicating the necessity of such an elevated amount of poison to effectively inhibit the catalyst.

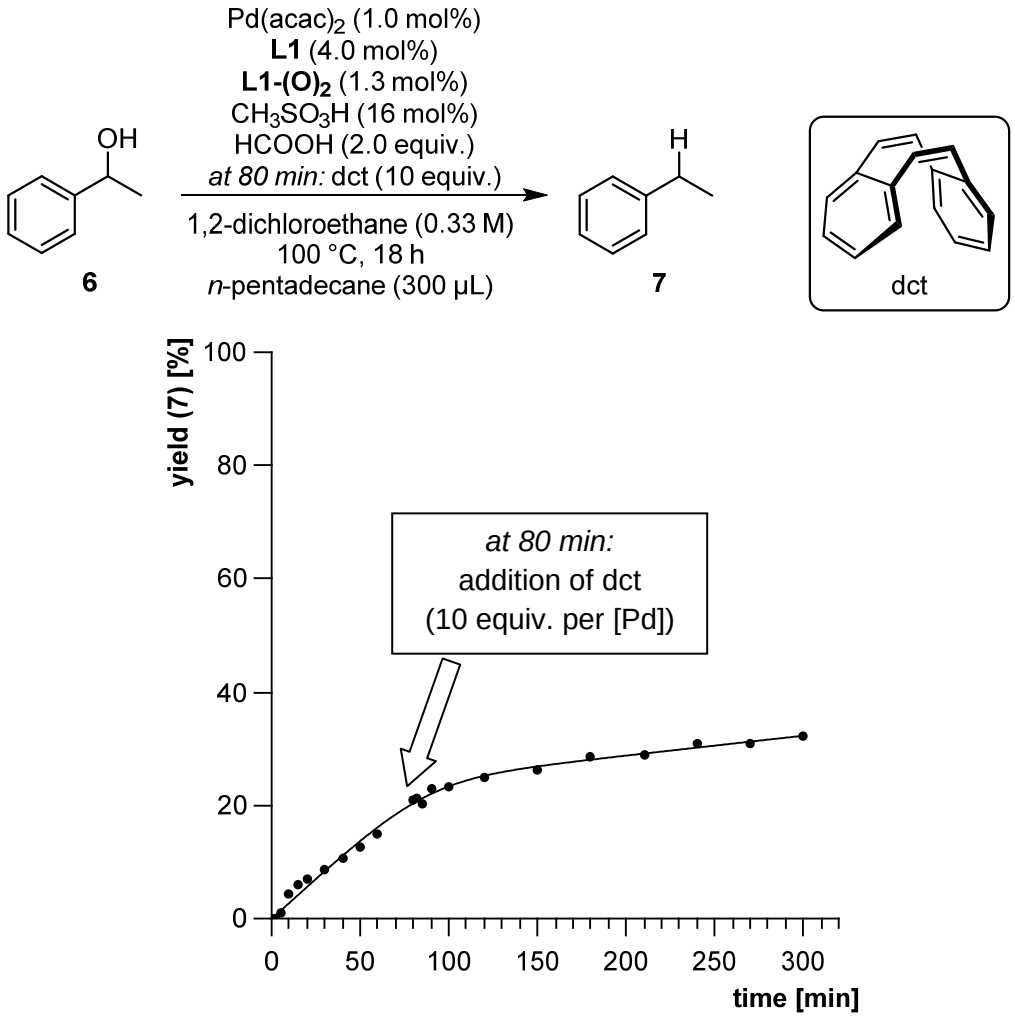

Scheme 3.14 **Reaction profile for the transfer hydrogenolysis of 1-phenylethanol with dct added as catalyst poison at 80 min (the curve was obtained *via* non-linear regression of the measured data points).**

The investigation of the transfer hydrogenolysis by using qualitative catalyst poisons yielded results that hint at an active homogeneous catalyst. Both the addition of mercury and dct to the reaction led to a halt or a slow-down of the catalytic activity. A control experiment showed that mercury already inhibits the formation of the active catalyst by reacting with a

catalyst precursor. The reaction profiles of the non-poisoned reaction and those of the described poisoning tests are compared in Scheme 3.15.

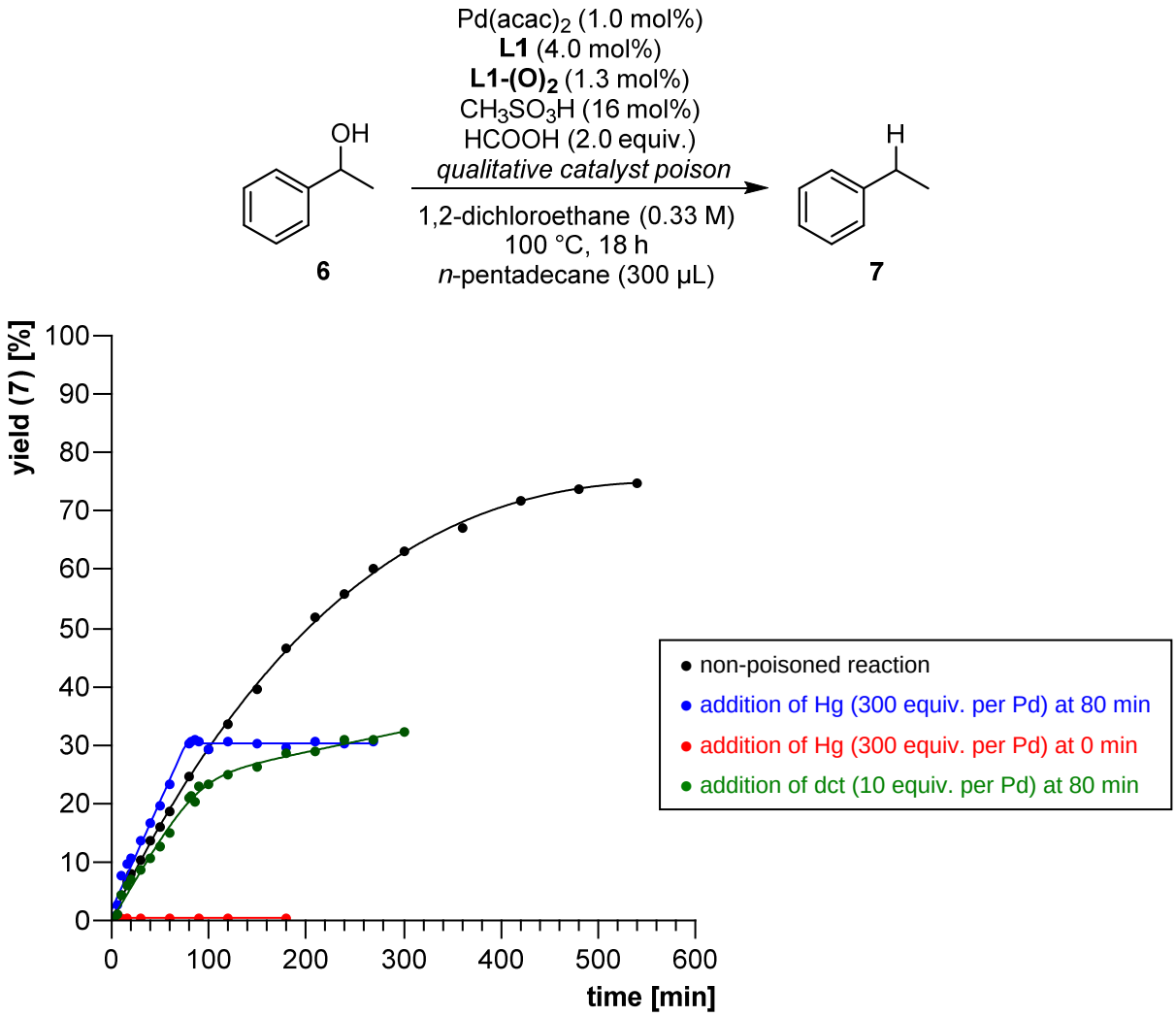

Scheme 3.15 **Reaction profiles for the transfer hydrogenolysis of 1-phenylethanol with added qualitative catalyst poisons (the curves were obtained *via* non-linear regression of the measured data points).**

Quantitative poisoning experiments

The deceleration of the transfer hydrogenolysis through the addition of dct strongly proposes the presence of a homogeneous catalyst species. To gather further experimental proof for this assumption, the use of 1-heptanethiol as a quantitative poison was considered. Quantitative poisons bind non-selectively to homogeneous and heterogeneous catalysts and the applied stoichiometry determines the extent of the catalyst inhibition. Amounts of less than 1.0 equivalent are sufficient to completely deactivate a heterogeneous catalyst, for homogeneous systems far more than 1.0 equivalent of poison relative to the catalyst is necessary (see section 1.6.2).

For the inhibition of the active palladium catalyst in the transfer hydrogenolysis, 1-heptanethiol amounts of 1.0 equivalent and 2.0 equivalents relative to the metal loading were applied (Scheme 3.16). In both cases, an approach analogous to the qualitative poisoning experiments was pursued, in which the formation of the active catalyst was ensured by the observation of significant amounts of product generated in the reaction. As before, the addition of the poison occurred after 80 minutes *via* syringe to the closed reaction vessel.

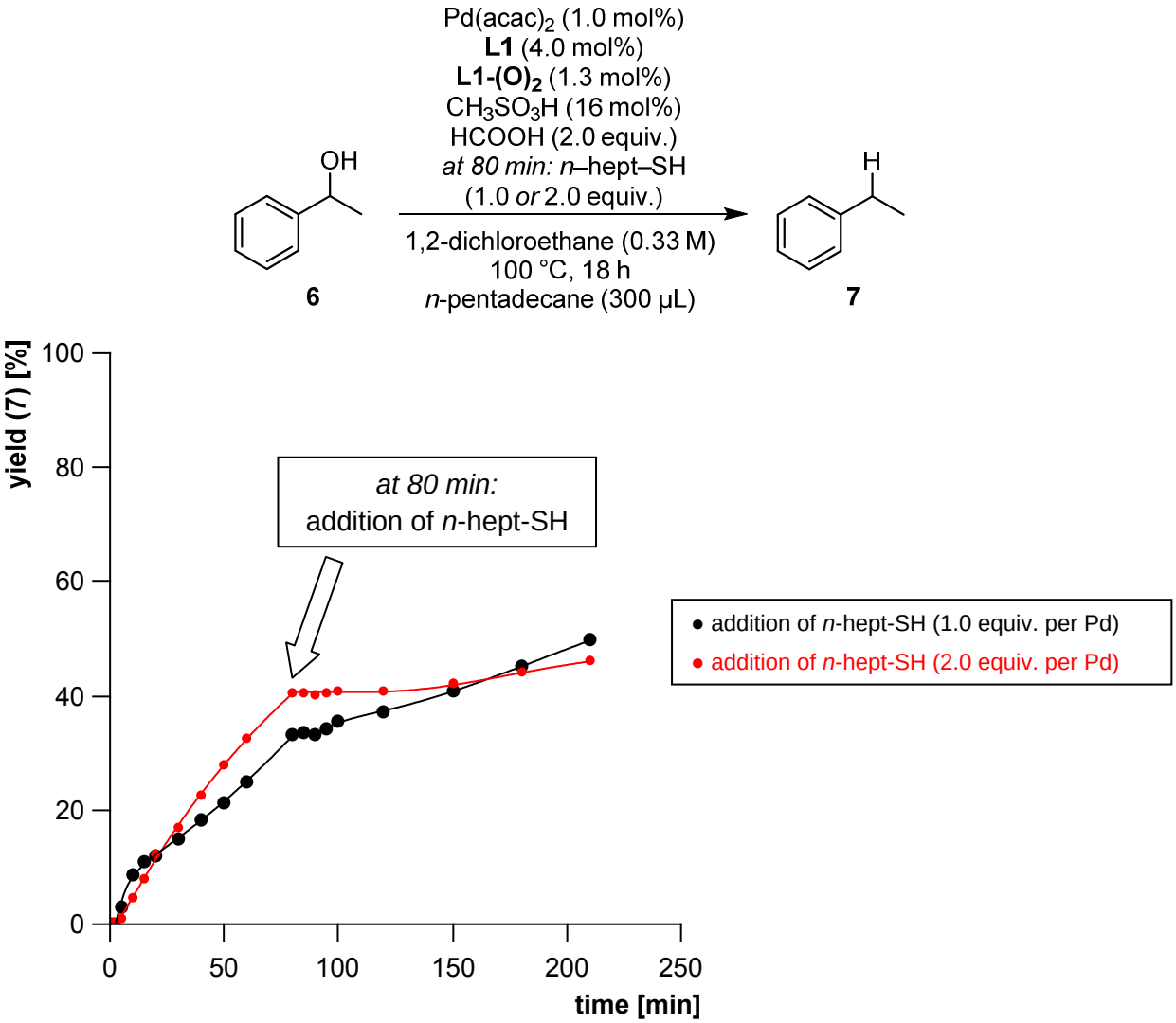

Scheme 3.16 **Reaction profiles for the transfer hydrogenolysis of 1-phenylethanol with heptanethiol (1.0 or 2.0 equivalents relative to [Pd]) added as quantitative catalyst poison (the curves were obtained *via* non-linear regression of the measured data points).**

In both cases, a halt of the catalytic reaction was observed directly after the addition of thiol. Yet, the regeneration of catalytic activity was observed in both experiments, possibly due to the high reaction temperature which may cause thermal desorption of the poison from the catalyst.[46] In the reaction poisoned with 1.0 equivalent of 1-heptanethiol, the complete inhibition of the catalyst lasted for 10 minutes. After a reaction time of 90 minutes, the formation of product continued, though at a lower rate as before under poison-free

conditions. Interestingly, after the addition of 2.0 equivalents of thiol to the reaction the catalyst remained inactive for at least 40 minutes, only after 150 min of total reaction time newly formed product was detected. Also, the rates of the re-established catalytic reactions were substantially lower than before the poisoning.

Comparing both poisoning experiments, the relative decrease of the reaction rate was significantly higher after the addition of 2.0 equivalents of poison. Assuming a similar thermal poison desorption equilibrium in both runs, this observation implies that poison amounts of more than 2.0 equivalents are needed for a permanent deactivation of the catalyst. As discussed in section 1.6.2, this necessity for an overstoichiometric amount of inhibiting agent can be interpreted as an indication for an active homogeneous catalyst.

In conclusion, the discussed findings from the catalyst poisoning experiments indicate an operating homogeneous catalyst. Notwithstanding, the obtained results are no definite proof but rather hints towards the characterization of the active catalyst species. As depicted in section 1.6.2, additional tests, which could be applied in the investigation of the given catalyst system, exist. Phosphines or phosphites can also be utilized as quantitative catalyst poisons, while a three-phase-test or a hot filtration test may yield further qualitative information on the nature of the active catalyst. Transmission electron microscopy as a *post operandum* technique could be applied to demonstrate the presence or absence of metal particles or the change of preformed nanoparticles in the reaction, indicating a potential leaching behavior of the applied ligand.

3.3.7 Mechanistic investigations

Based on the results gained from the reaction optimization, the substrate screening and the catalyst poisoning experiments, additional investigations on the reaction mechanism of the transfer hydrogenolysis of benzylic alcohols were performed.

Confirmation of the reaction intermediate

First, the identity of the found 1-arylethyl formates as intermediates in the transformation should be confirmed (Table 3.12). 1-Phenylethyl formate (**9**) was subjected to the optimized reaction conditions in absence of free formic acid, delivering the desired product ethylbenzene (**7**) in a good yield of 65% (entry 1). In presence of 1.0 equivalent of formic acid, the reaction proceeded to an excellent yield of **7** of 92% (entry 2).

Further, it was speculated that formic acid not only causes an activation of the alcohol substrate *via* esterification, but that a subsequent direct reduction from intermediate **9** occurs. To test this, the reaction of the acetate analogue **45** under standard reaction conditions was followed over time *via* sampling and GC analysis. It became evident that the

acetate did not react immediately to form the deoxygenated product **7**, in fact first a transesterification to the formate intermediate **9** took place. Only after a significant amount of **9** had been generated, the formation of ethylbenzene was observed. After 18 hours, a very good product yield of 88% was obtained (entry 3). Therefore, formate **9** was confirmed as the reaction intermediate. In the transfer hydrogenolysis formic acid acts not only as reducing agent, but also activates the alcohol substrate in a pre-step.

Table 3.12 **Transformation of the suspected reaction intermediate and the respective acetate analogue in the transfer hydrogenolysis.**

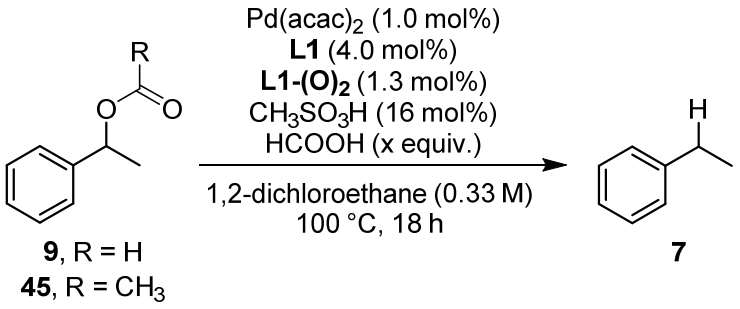

9, R = H
45, R = CH_3

7

Entry[a]	R	formic acid (x equiv.)	yield (**7**) [%][b]
1	H	–	65
2	H	1.0	92
3	CH_3	2.0	88[c]

[a]General reaction conditions: 1-Phenylethyl formate or acetate (1.00 mmol, 0.33 M solution), 1,2-dichloroethane (3 mL), $Pd(acac)_2$ (10 µmol, 3.0 mg, 1.0 mol%), **L1** (40 µmol, 16 mg, 4.0 mol%), **L1-(O)$_2$** (1.3 mol%, brought into the reaction as partially oxidized **L1**), methanesulfonic acid (0.16 mmol, 10 µL, 16 mol%), formic acid (respective amount), stirred at 100 °C for 18 h in a sealed glass pressure tube. Unless stated otherwise, full substrate conversion was achieved. [b]Product identification was performed *via* measurement of authentic commercial samples or *via* GC-MS analysis. Yields determined *via* quantitative GC-FID using *n*-pentadecane as internal standard. [c]Transesterification to 1-phenylethyl formate (**9**) occurred before the deoxygenation step.

Catalyst activity towards non-benzylic or non-alcoholic substrates

Although a screening of benzylic alcohol substrates was already performed for the transfer hydrogenolysis, the activity of the catalyst system towards structurally different substrates was still to be evaluated. A number of reducible compounds was chosen, e.g. aliphatic alcohols, benzylic ketones or vinyl arenes, and subjected to the standard reaction conditions (Table 3.13).

Acetophenone (**46**), a benzylic ketone, was deoxygenated to ethylbenzene in a low yield of 21% (entry 1). No other products were detected by GC and only unreacted starting material was found. This finding shows the selectivity of the transfer hydrogenolysis catalyst towards benzylic alcohols over benzylic carbonyls.

The aliphatic alcohol 2-nonanol (**47**) was tested as substrate in the reaction. No transfer hydrogenolysis product was observed, only the two elimination products 1-nonene (**48**) and 2-nonene (**49**) were found *via* GC-MS analysis (entry 2).

Table 3.13 **Tested non-benzylic or non-alcoholic substrates in the palladium-catalyzed transfer hydrogenolysis.**

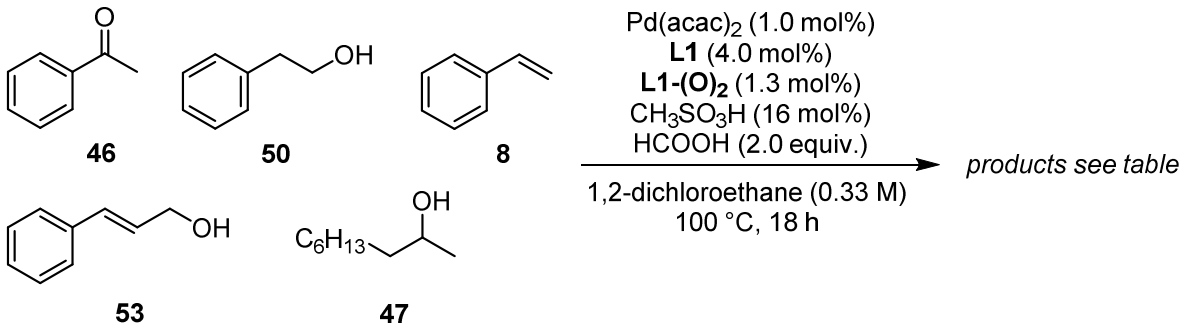

Entry[a]	substrate	products (yield [%])	
1	acetophenone (**46**)	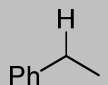 **7**	(21)
2	2-nonanol (**47**)	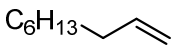 **48** 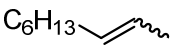 **49**	(not determined)
3	2-phenylethanol (**50**)	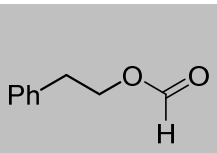 **51** 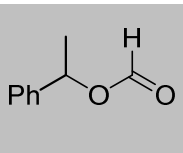 **9**	(not determined)
4	cinnamyl alcohol (**52**)	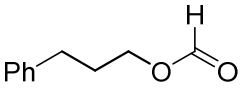 **53** 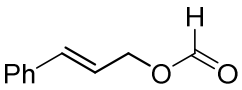 **54**	(not determined)
5	styrene (**8**)	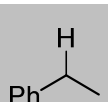 **7**	(94)[c]

[a]General reaction conditions: Substrate (1.00 mmol, 0.33 M solution), 1,2-dichloroethane (3 mL), $Pd(acac)_2$ (10 µmol, 3.0 mg, 1.0 mol%), **L1** (40 µmol, 16 mg, 4.0 mol%), **L1-(O)$_2$** (1.3 mol%, brought into the reaction as partially oxidized **L1**), methanesulfonic acid (0.16 mmol, 10 µL, 16 mol%), formic acid (2.0 mmol, 75 µL, 2.0 equivalents), stirred at 100 °C for 18 h in a sealed glass pressure tube. Unless stated otherwise, full substrate conversion was achieved. [b]Product identification was performed *via* measurement of authentic commercial samples or *via* GC-MS analysis. Yields determined *via* quantitative GC-FID using *n*-pentadecane as internal standard. [c]Formation of 1-phenylethyl formate (**9**) was observed on GC before the deoxygenation step.

Introduction of a phenyl group into the substrate as in 2-phenylethanol (**50**), which is an aromatic, non-benzylic alcohol, did not lead to any deoxygenated product. As expected, 2-phenylethyl formate (**51**) was generated. Notably, also 1-phenylethyl formate (**9**) was detected as minor product, this species is thought to arise from the isomerization of **51** *via* elimination of formic acid and subsequent re-addition in opposite regioselectivity (entry 3). A participation of the catalyst in this isomerization process cannot be excluded, therefore the transfer hydrogenolysis could be prevented in this case. The failed transfer hydrogenolysis of an aliphatic and an aromatic, non-benzylic alcohol demonstrated that only benzylic alcohols are effectively transformed to the respective hydrocarbons by the catalyst.

A similar result was found for the transformation of cinnamyl alcohol (**52**). Again, no transfer hydrogenolysis of the alcohol moiety occured. Yet, the main product obtained was hydrocinnamyl formate (**53**), which was presumably generated *via* hydrogenation of the benzylic C–C double bond in cinnamyl formate (**54**). The latter was found as minor side product after the reaction (entry 4).

Interestingly, styrene (**8**) underwent clean reduction under the transfer hydrogenolysis conditions, ethylbenzene (**7**) was obtained in an excellent yield of 94% (entry 5). To gain an insight into the reaction pathway, samples were withdrawn from the reaction mixture at defined reaction times. GC analysis showed that not a direct hydrogenation of the benzylic C–C double bond occurred, instead the generation of 1-phenylethyl formate (**9**) was observed, which was further transformed *via* the usual transfer hydrogenolysis pathway (Scheme 3.17). The obtained reaction profile shows a constant decrease of the styrene concentration, the beginning formation of ethylbenzene (**7**) was detected only 10 minutes after starting the reaction. The same was observed for the intermediate 1-phenylethyl formate (**9**), both the generation of **9** and **7** occurred at comparable rates. After 60 minutes the initial increase of the amount of **9** ceased, the concentration of the intermediate arrived at a constant value, which only slightly decreased after a reaction time of 240 minutes. This behavior indicates that a dynamic equilibrium is established, in which styrene is consumed in the formation of the intermediary formate, at the same time the reduction of the formate intermediate **9** to ethylbenzene occurs. The formation of **9** from styrene is assumed to proceed *via* the addition of formic acid to the double bond, either under acid or palladium catalysis (Scheme 3.18). For the generation of ethylbenzene a linear kinetic curve was observed, again pointing towards an active homogeneous catalyst for the reduction step.

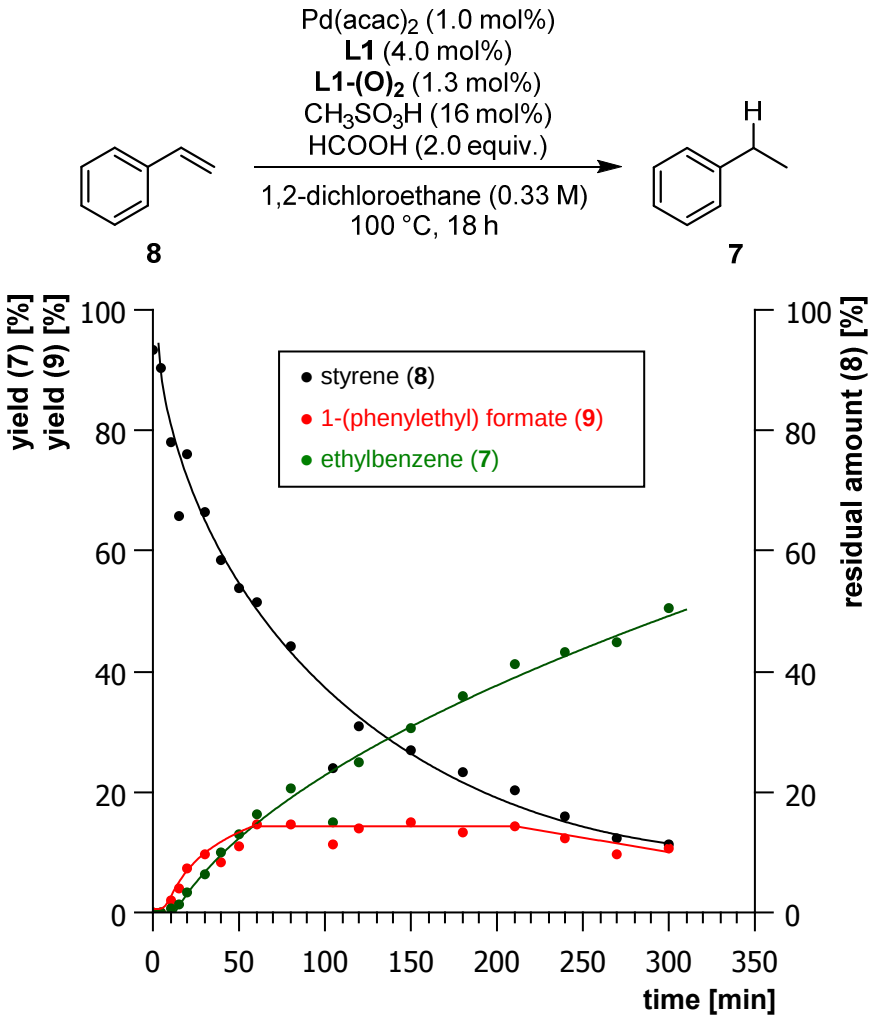

Scheme 3.17 **Reaction profile for the reduction of styrene under transfer hydrogenolysis conditions (the curves were obtained *via* non-linear regression of the measured data points).**

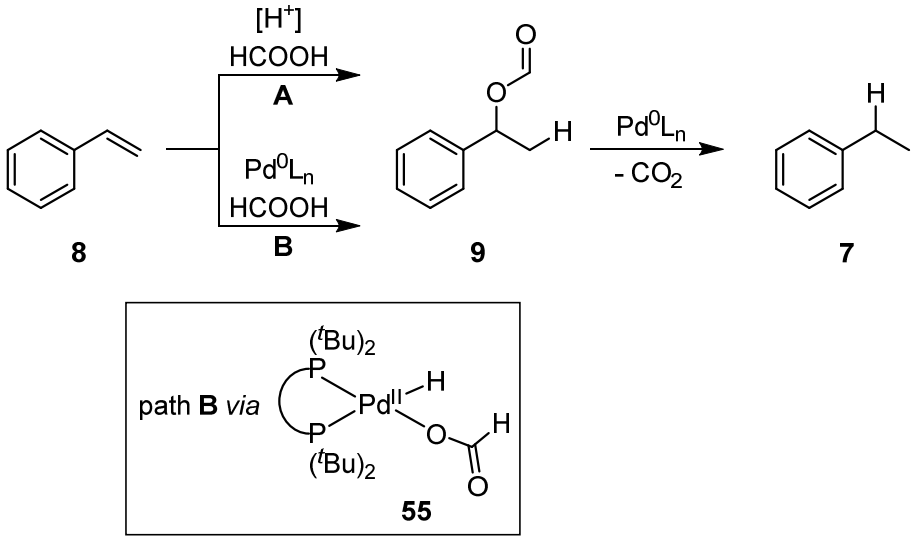

Scheme 3.18 **Proposed reaction pathways for the reduction of styrene under transfer hydrogenolysis conditions.**

Exclusion of palladium nanoparticles as active catalyst species

As discussed in section 3.3.6, experimental results from the catalyst poisoning experiments strongly propose an operating homogeneous catalyst species. Furthermore, in section 3.3.4, the beneficial effect of certain tertiary phosphine oxides on the transfer hydrogenolysis reaction was presented. This phenomenon could be rationalized by a stabilizing interaction of the phosphine oxides with Pd(0), either in atomic form or in larger aggregates. A key aspect of this proposition was the eventual breakdown of the dispersed and stabilized palladium nanoparticles by the present phosphine ligand dtbpx (**L1**) to generate the active homogeneous catalyst species as it was demonstrated in similar works on a palladium/dtbpx catalyst system.[59] To support this theory, commercially available palladium nanoparticles (Pd EnCat 40: 0.4 mmol Pd/g loading) were applied in the transfer hydrogenolysis of 1-phenylethanol. In the reactions, the added amounts of **L1** and **L1-(O)$_2$** as of methanesulfonic acid were varied (Table 3.14). Indeed, an influence on the yield of the deoxygenation product was observed.

Table 3.14 **Performance of Pd nanoparticles as catalyst precursor in presence of varied amounts of ligands L1, L1-(O)$_2$ and methanesulfonic acid.**

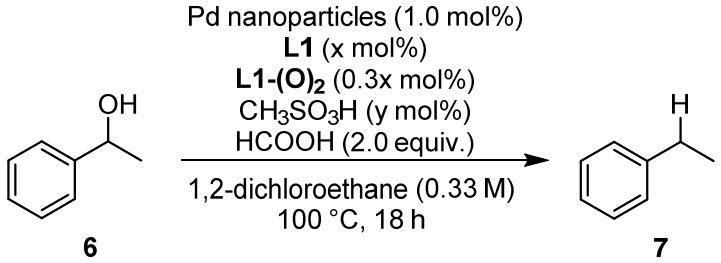

Entry[a]	**L1** (x mol%)	CH_3SO_3H (y mol%)	yield (**7**) [%][b]
1	0	16	traces
2	4.0	16	35
3	8.0	16	61
4	8.0	32	66

[a]General reaction conditions: 1-Phenylethanol (1.00 mmol, 120 µL, 0.33 M solution), 1,2-dichloroethane (3 mL), Pd nanoparticles (10 µmol, 1.0 mol%), **L1** (respective amount), **L1-(O)$_2$** (respective amount, brought into the reaction as partially oxidized **L1**), methanesulfonic acid (respective amount), formic acid (2.0 mmol, 75 µL, 2.0 equivalents), stirred at 100 °C for 18 h in a sealed glass pressure tube. Unless stated otherwise, full substrate conversion was achieved. [b]Product identification was performed *via* measurement of authentic commercial samples or *via* GC-MS analysis. Yields determined *via* quantitative GC-FID using *n*-pentadecane as internal standard.

Under standard reaction conditions, a moderate yield of 35% of product **7** was obtained (entry 2). Assuming that the active catalyst comprises a homogeneous species, this indicates that palladium nanoparticles can serve as metal source in the reaction, from which **L1** is able to leach palladium atoms into solution in form of a metal complex.

In absence of **L1** and **L1-(O)$_2$** under else non-changed reaction conditions, only traces of ethylbenzene (**7**) were detected (entry 1). This result resembles the finding from the reaction

optimization, in which the introduction of heterogeneous Pd/C as metal source also did not yield significant amounts of transfer hydrogenolysis product. This negative result supports the theory of ligand-induced palladium leaching from solid particles.

Raising the ligand loading of **L1** and **L1-(O)$_2$** in the reaction to 8.0 mol% and 2.6 mol%, respectively, caused an increase in product yield to 61% (entry 3). This observation, together with the failed transfer hydrogenolysis under ligand-free conditions and a lower yield from a decreased ligand amount, is taken as strong evidence for the central role of ligand **L1** in the decomposition of the nanoparticles into monoatomic palladium(0) species.

To exclude a possible influence of the acid co-catalyst on the dissolution of the metal particles, a control experiment with 8 mol% of **L1** and 32 mol% of CH_3SO_3H was performed (entry 4). The obtained yield for product **7** of 66% did not change significantly compared to the previous experiment with the identical ligand loading but a lower amount of acid. Therefore, an influence of the acid amount on the nanoparticle decomposition was excluded.

Deuterium labelling experiments

The role of formic acid in the activation of the alcohol substrate was already demonstrated in this section. Further experiments were performed to show that the hydride introduced into the 1-arylethyl formate intermediate in the reduction step originates from formic acid. In addition, it should be investigated if only the hydridic or the hydridic and acidic H atoms are transferred in the transfer hydrogenolysis. Therefore, different deuterated formic acid species **58**–**60** were applied in the transfer hydrogenolysis of 1-(2-naphthyl)ethanol (**56**) (Scheme 3.19). The product **57** generated from the chosen substrate exhibits a higher boiling point, this enables a more facile isolation of the isotope-labelled compounds from the crude reaction mixture *via* distillation.

^{1}H- and ^{2}H-NMR analysis of the isolated transfer hydrogenolysis products showed that in all three experiments deuterated 2-ethylnaphthalenes **57-d** were generated (for the respective NMR spectra see chapter 6.8). Unexpectedly, the incorporated deuterium atoms were distributed on both carbon atoms of the ethyl moiety. Only low amounts of deuterium were detected in the products, probably due to proton-deuteron exchange processes taking place in the reaction medium under the given high proton concentrations. Possible pathways for the deuterium scrambling and the loss of labelled atoms *via* H/D exchange will be discussed later in this section.

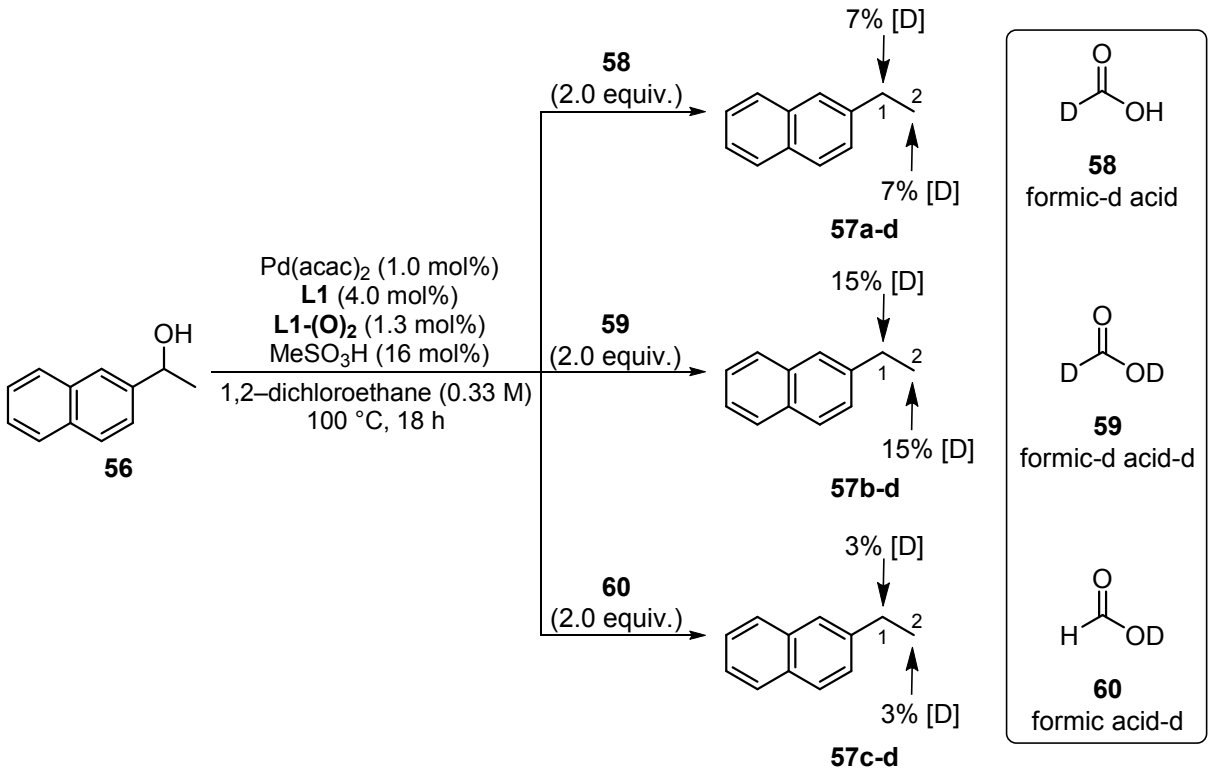

Scheme 3.19 **Isotope labelling experiments in the transfer hydrogenolysis of 1-(2-naphthyl)ethanol applying deuterated formic acid species (deuterium content determined *via* NMR analysis).**

Despite the low incorporation of deuterium into the products, differences in the relative extent of labelling were found. The product **57a-d** generated *via* treatment of the alcohol substrate with formic-d acid (**58**) exhibited a deuterium content of 7% on both alkyl carbons. The use of formic-d acid-d (**59**) resulted in an increased deuterium content of 15% on both positions of the ethyl chain of product **57b-d**, probably due to the additional deuterons present in the reaction medium. The acidic deuteron in formic acid-d (**60**) is not incorporated into the formate intermediate as it is released in the ester condensation. Surprisingly, still a deuterium incorporation of 3% on both positions in the ethyl chain of product **57c-d** was determined.

To obtain a further insight into the presumed deuterium scrambling caused by the palladium catalyst, 1-phenylpropanol (**61**) was subjected to the transfer hydrogenolysis under the use of formic-d acid-d (**59**) (Scheme 3.20).

As before, isolation and subsequent ^{1}H- and ^{2}H-NMR analysis showed that the introduced deuterium atoms were incorporated on all three positions of the propyl chain in product **62-d**. A higher deuterium content than in the previous labelling experiments was observed for each of the alkyl carbon atoms. The methylene groups in **62-d** each exhibited 23% of deuterium, while the terminal methyl group showed an even higher D content of 32%. The fact that all three positions in the alkyl chain were labelled favors a chain-walking mechanism of the palladium bisphosphine complex, this concept was already described in

similar works.[13,60,61] The formal addition of dihydrogen or a mixed H–D species to an intermediary formed alkene moiety is excluded due to the obtained results.

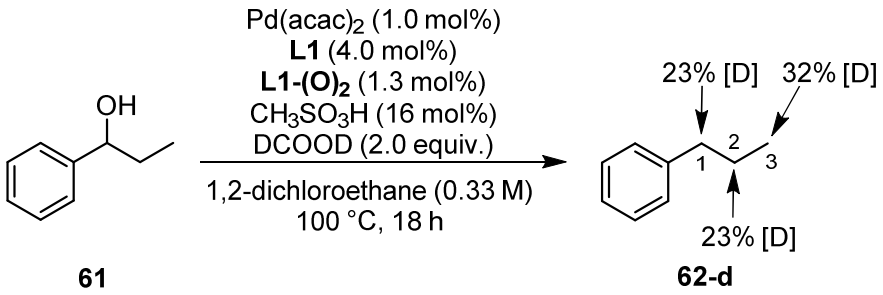

Scheme 3.20 **Isotope labelling experiments in the transfer hydrogenolysis of 1-phenylpropanol applying formic-d acid-d (deuterium content determined *via* NMR analysis).**

To account for the observed scrambling of the deuterium atoms on the alkyl chains, the proposed chain walking mechanism of the palladium catalyst is rationalized as depicted in Scheme 3.21. After the formation of palladium(0) species **20** an oxidative addition of the 1-arylethyl formate intermediate **63-d** over the benzylic C–O bond takes place. The formed palladium formato complex **64-d** is stabilized by a pseudo-allylic interaction of palladium with the π-system of the adjacent arene to form **65-d**. In the literature, dissociation of one phosphine center was reported to open the possibility for the migration of the palladium center on the alkyl chain.[61] This occurs *via* several β-hydride elimination and alkene insertion steps, resulting in the respective palladium alkyl complexes **66-d** and **67-d**, which are stabilized by an agostic interaction with a β-hydrogen.[60,62] Alternatively, the dissociation of the formate ligand would as well open a coordination site and enable the chain walking pathway, yet re-coordination of the formate anion on the migrating palladium center to end the chain walking appears difficult due to the steric bulk of **L1** shielding the metal center. In the pathway involving the dissociation of one phosphine group, subsequent decomposition of the formate ligand under release of CO_2 generates the palladium alkyl deuteride complexes **69-d** and **70-d**, from which the products **71-d** are released *via* reductive elimination of the palladium center.

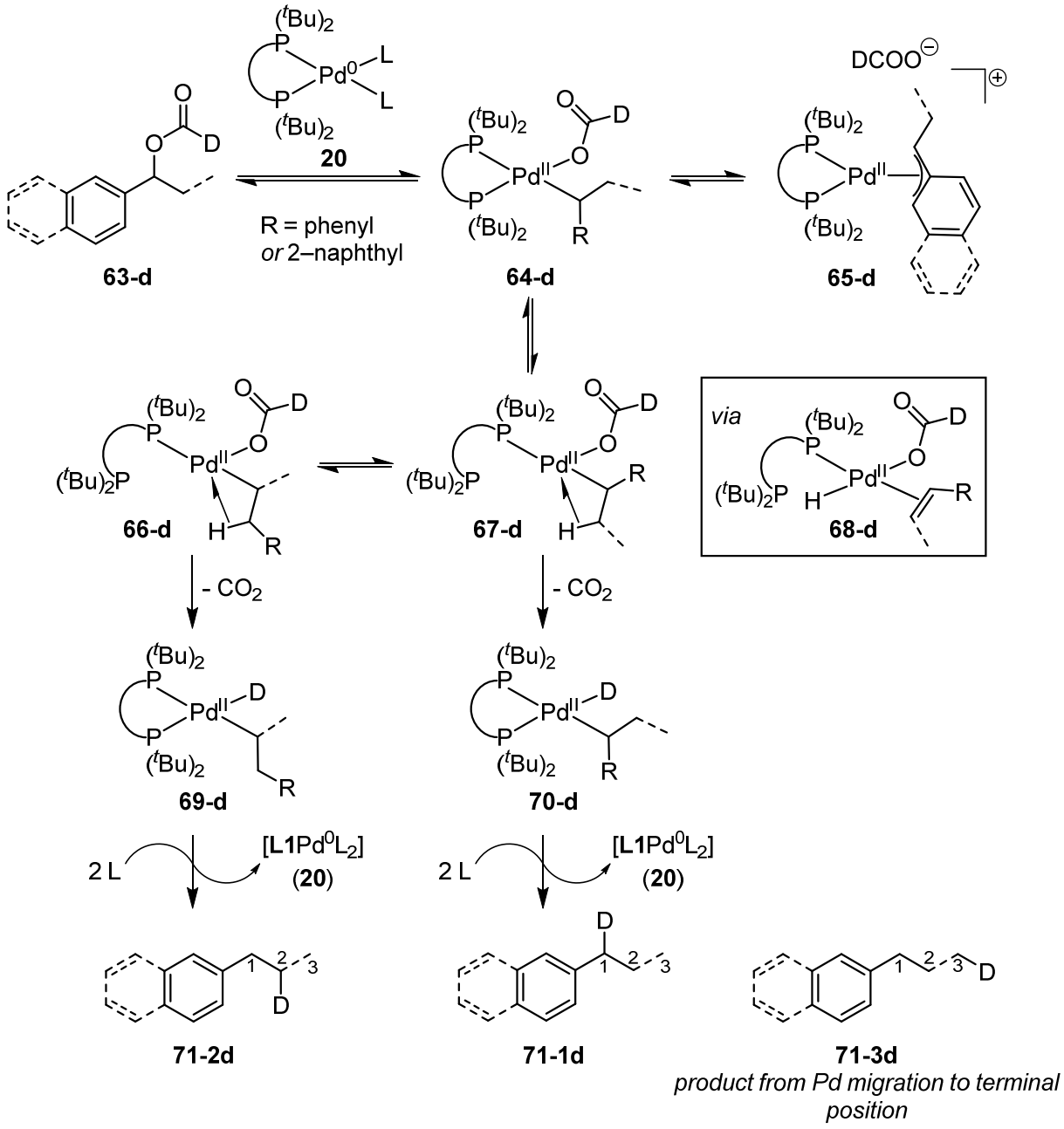

Scheme 3.21 **Proposed reaction pathway for the observed deuterium scrambling in the transfer hydrogenolysis of 1-phenylpropanol or 1-(2-naphthyl)ethanol with deuterated formic acid species.**

From the discussed experimental results, the distribution of deuterium atoms on the formed alkyl chains can be explained. Nonetheless, a major part of the introduced deuterium was not incorporated into the products, as it was evident from the integration of the respective ^{1}H- and ^{2}H-NMR spectra. The loss of deuterium *via* an exchange process with the large excess of protons available in the reaction medium seemed possible. Furthermore, the use of formic acid-d (**60**) in the transfer hydrogenolysis of **56** led to a minor deuteration of the products although the introduced formate anion was not labelled.

To investigate this phenomenon, a transfer hydrogenolysis experiment containing the two substrates **56-d$_3$** (>97% deuterated on the methyl group) and **6** with non-deuterated formic acid was conducted (Scheme 3.22). Besides the loss of deuterium atoms from **56-d$_3$**, a potential intermolecular transfer of deuterium to **6** should be evaluated. Indeed, NMR analysis of the product **57d-d** obtained from **56-d$_3$** showed deuterium scrambling on the ethyl chain and a major loss of deuterium atoms from the molecule. In addition, partial deuteration of the ethylbenzene product **7-d** was observed on both positions in the ethyl chain. This confirms the anticipated intermolecular deuterium transfer from **56-d$_3$** to **6** during the transfer hydrogenolysis.

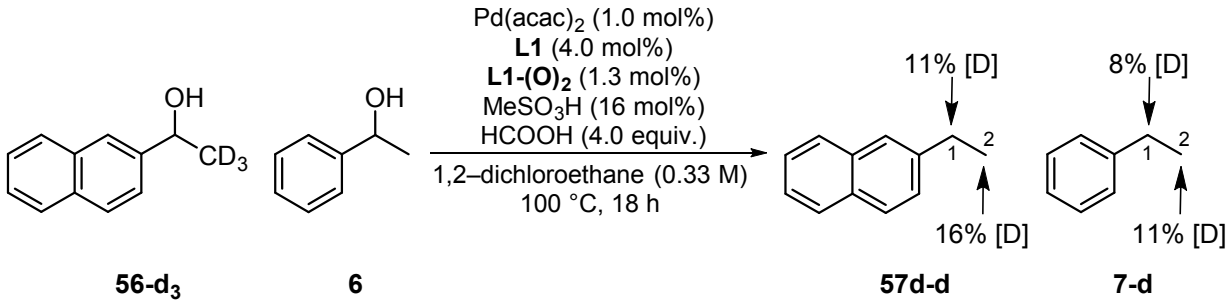

Scheme 3.22 Competition experiment containing a deuterated and a non-deuterated alcohol substrate to investigate deuterium loss and intermolecular deuterium transfer.

These results indicate that a D/H exchange takes place on an intermediary palladium species involved in the catalytic cycle (Scheme 3.23). Presumably, the palladium hydride complex **73**, which performs the migration on the alkyl chain, also allows for a D-H exchange. After the β-hydride elimination step, the palladium center is ligated by only one of the two phosphines in **L1**, a formate, an alkene and a hydride ligand. The non-coordinated phosphine moiety may serve as a basic site, which takes the deuteride or hydride ligand off the metal center as a proton/deuteron, palladium(II) is reduced to palladium(0). The protonated phosphine then undergoes D^+/H^+ exchange (or *vice versa*) with a proton or deuteron from the reaction medium. Thereafter, regeneration of the palladium(II) hydride or deuteride from the phosphonium species and the palladium(0) center occurs, this proton transfer step from phosphonium to palladium was already shown to be productive in similar works on palladium complexes of **L1**.[30,63] Through this described mechanism, the loss of deuterium from labelled substrates as well as its intermolecular incorporation appears possible.

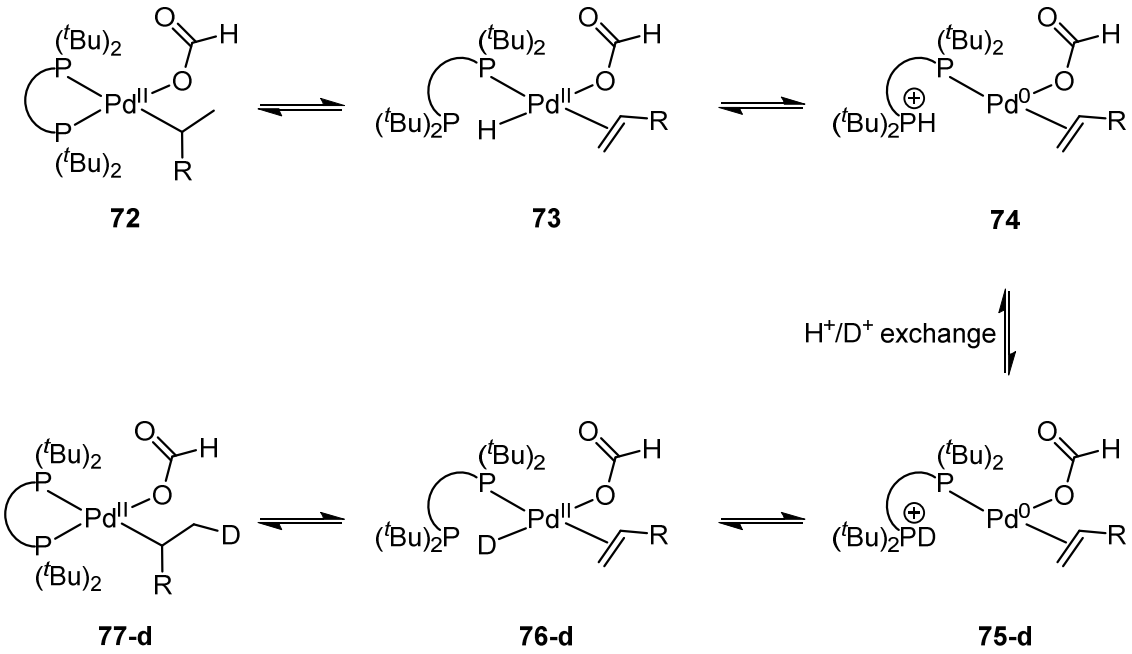

Scheme 3.23 **Proposed mechanism for the D/H exchange observed in the transfer hydrogenolysis reaction.**

Qualitative headspace GC analysis

In successful transfer hydrogenolysis experiments, after the end of the reaction and cooling to room temperature, an internal gas overpressure was observed when opening the sealed glass pressure tube. To investigate the qualitative composition of the gas phase generated in the reactor, headspace GC measurements were performed. Therefore, the optimized model reaction, the transfer hydrogenolysis of 1-phenylethanol, was run in a glass pressure tube with accessible septum. After the reaction, a part of the gas phase over the reaction mixture was withdrawn from the sealed tube through the septum using a gas-tight syringe. The gas was bubbled through an aqueous solution of NaOH to remove acid residues. The purified gas phase was then transferred to a headspace GC vial and injected into a gas chromatograph connected to a thermal conductivity detector. Comparison of the GC trace with measurements of a calibration gas mixture showed that hydrogen and carbon dioxide gas were present in the headspace. Latter is presumed to be generated in the transformation of the 1-arylethyl formate intermediate to the deoxygenated products, while former may be a side product from the decomposition of formic acid on the palladium catalyst species present in the reaction.

Mechanistic proposal

Based on the experiments discussed in this section, a mechanism for the transfer hydrogenolysis of benzylic alcohols is proposed (Scheme 3.24). The reduction of the palladium(II) precursor $Pd(acac)_2$ generates atomic Pd(0), which either aggregates to phosphine oxide-stabilized nanoparticles or directly forms complex **31** containing **L1** and **L1-(O)$_2$** as ligands. The palladium nanoparticles may also serve as a metal reservoir from which **L1** is able to leach metal into solution, again forming complex **31**.

In parallel, the esterification of the benzylic alcohol substrate **6** with formic acid furnishes the 1-arylethyl formate intermediate **9**. For substrates which are able to undergo elimination, the formation of vinylarenes (**8**) cannot be excluded. Yet, alkenes are also transformed into the respective formates under the reaction conditions *via* the addition of formic acid.

After the dissociation of **L1-(O)$_2$** from the metal center, an oxidative addition of intermediate **9** to the palladium(0) complex generates a palladium(II) alkyl formato complex **78**. Decomposition of the formate ligand *via* β-hydride elimination and loss of CO_2 leads to palladium alkyl hydride **79**. Reductive elimination of the metal releases the deoxygenated product and regenerates the active palladium catalyst species.

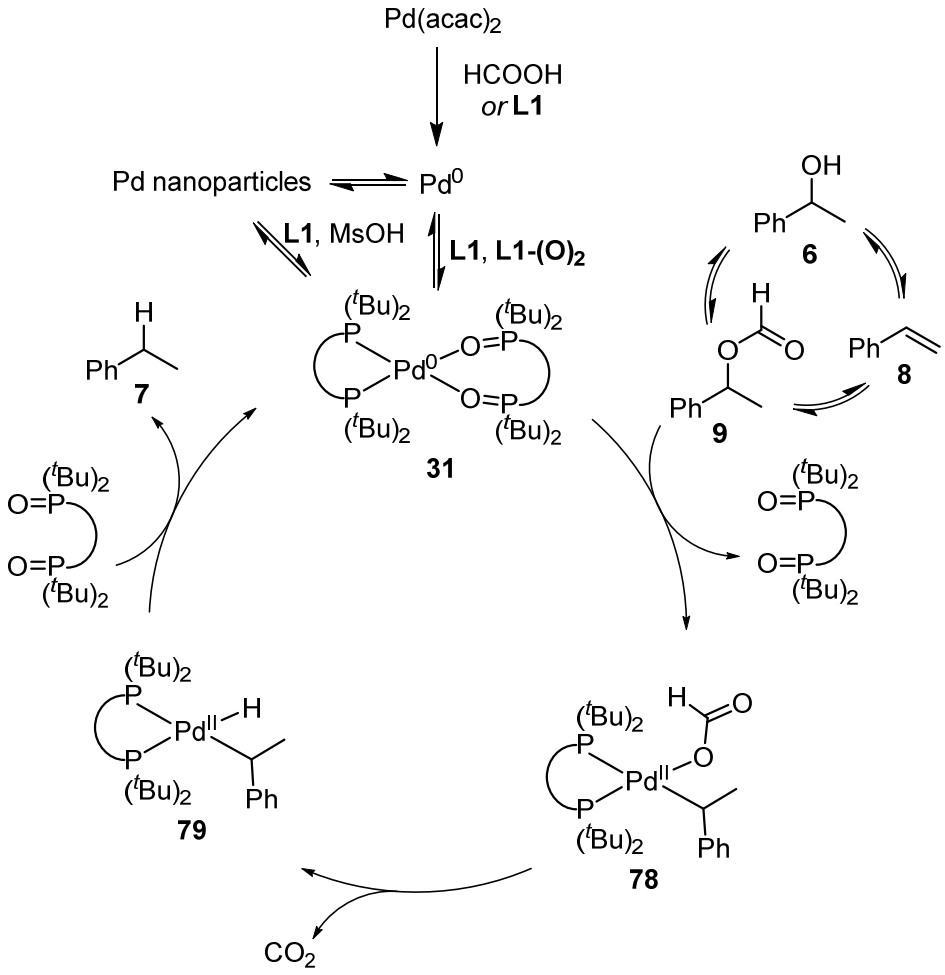

Scheme 3.24 **Proposed reaction mechanism for the palladium-catayzed transfer hydrogenolysis of benzylic alcohols shown for 1-phenylethanol as model substrate.**

3.4 Conclusion and outlook

In this chapter, the development of a new method for the deoxygenation of benzylic alcohols *via* a transfer hydrogenolysis pathway was presented. The transformation is mediated by a palladium-based catalyst system, which was previously applied in the alkoxycarbonylation of alkenes. Formic acid is used as reducing agent, which gives carbon monoxide and water as the only by-products in the reaction, allowing for a simple product purification. A broad substrate scope demonstrated the applicability of the reaction, the targeted deoxygenated hydrocarbons could be obtained in moderate to quantitative yields.

An exclusive ligand effect was observed in the catalysis, which is thought to be caused by the steric and electronic properties of the applied bisphosphine. Furthermore, the presence of tertiary phosphine oxides was found beneficial for the reaction, presumably acting as stabilizers in the formation of the active catalyst. Reaction progress analyses and catalyst poisoning experiments applying different inhibiting agents led to the conclusion that a homogeneous palladium complex is the active catalyst species, while an equilibrium between homogeneous, solubilized metal species and a heterogeneous, nanoparticulate metal reservoir is also thought to operate.

Mechanistic investigations confirmed the identity of an intermediate in the reaction. Furthermore, deuterium labelling experiments and qualitative headspace GC measurements of the atmosphere generated *in situ* allowed for an insight into the reaction mechanism and resulted in a mechanistic proposal.

Future studies on the palladium-catalyzed transfer hydrogenolysis of benzylic alcohols with formic acid should aim at the application of milder reaction conditions, e.g. lower temperatures and catalyst loadings. This may lead to a broader substrate scope for the reaction and open new possible applications. To accomplish this, a systematic investigation of the ligand structure, concerning changes in the bisphosphine backbone as of the substituents bound to the phosphorus atoms appears viable. Through this, a better understanding of the reaction mechanism could be obtained and a further optimization of the individual reaction steps may be possible. The successful use of non-precious metals, like nickel or iron, in the catalysis would contribute to an overall more sustainable transformation.

3.5 References

[1] M. Mirza-Aghayan, R. Boukherroub, M. Rahimifard, *Tetrahedron Lett.* **2009**, *50*, 5930-5932.

[2] H. Wang, L. Li, X.-F. Bai, J.-Y. Shang, K.-F. Yang, L.-W. Xu, *Adv. Synth. Catal.* **2013**, *355*, 341-347.

[3] R. J. Rahaim, R. E. Maleczka, *Org. Lett.* **2011**, *13*, 584-587.

[4] G. La Sorella, L. Sperni, P. Canton, L. Coletti, F. Fabris, G. Strukul, A. Scarso, *J. Org. Chem.* **2018**, *83*, 7438-7446.

[5] J. Feng, C. Yang, D. Zhang, J. Wang, H. Fu, H. Chen, X. Li, *Appl. Catal., A* **2009**, *354*, 38-43.

[6] H. Mao, X. Liao, B. Shi, *Catal. Commun.* **2011**, *12*, 1177-1182.

[7] S. Sawadjoon, A. Lundstedt, J. S. M. Samec, *ACS Catal.* **2013**, *3*, 635-642.

[8] M. G. Musolino, F. Mauriello, C. Busacca, R. Pietropaolo, *Catal. Today* **2015**, *241*, 208-213.

[9] E. Drent, P. H. M. Budzelaar, *Chem. Rev.* **1996**, *96*, 663-682.

[10] G. Cavinato, L. Toniolo, *Molecules* **2014**, *19*, 15116.

[11] G. R. Eastham, B. T. Heaton, J. A. Iggo, R. P. Tooze, R. Whyman, S. Zacchini, *Chem. Commun.* **2000**, 609-610.

[12] W. Clegg, G. R. Eastham, M. R. J. Elsegood, B. T. Heaton, J. A. Iggo, R. P. Tooze, R. Whyman, S. Zacchini, *Organometallics* **2002**, *21*, 1832-1840.

[13] P. H. Gehrtz, V. Hirschbeck, I. Fleischer, *Chem. Commun.* **2015**, *51*, 12574-12577.

[14] D. Mellmann, P. Sponholz, H. Junge, M. Beller, *Chem. Soc. Rev.* **2016**, *45*, 3954-3988.

[15] A. Álvarez, A. Bansode, A. Urakawa, A. V. Bavykina, T. A. Wezendonk, M. Makkee, J. Gascon, F. Kapteijn, *Chem. Rev.* **2017**, *117*, 9804-9838.

[16] S. Moret, P. J. Dyson, G. Laurenczy, *Nat. Commun.* **2014**, *5*, 4017.

[17] B. Ciszek, Master thesis, Universität Regensburg **2015**.

[18] P. Gehrtz, Master thesis, Universität Regensburg **2015**.

[19] C. J. Moulton, B. L. Shaw, *J. Chem. Soc., Chem. Commun.* **1976**, 365-366.

[20] L. E. Crascall, J. L. Spencer, *J. Chem. Soc., Dalton Trans.* **1992**, 3445-3452.

[21] W. Clegg, M. R. J. Elsegood, G. R. Eastham, R. P. Tooze, X. Lan Wang, K. Whiston, *Chem. Commun.* **1999**, 1877-1878.

[22] W. Clegg, G. R. Eastham, M. R. J. Elsegood, B. T. Heaton, J. A. Iggo, R. P. Tooze, R. Whyman, S. Zacchini, *J. Chem. Soc., Dalton Trans.* **2002**, 3300-3308.

[23] F. Stempfle, D. Quinzler, I. Heckler, S. Mecking, *Macromolecules* **2011**, *44*, 4159-4166.

[24] I. Fleischer, R. Jennerjahn, D. Cozzula, R. Jackstell, R. Franke , M. Beller, *ChemSusChem* **2013**, *6*, 417-420.

[25] C. Ortiz-Cervantes, M. Flores-Alamo, J. J. García, *ACS Catal.* **2015**, *5*, 1424-1431.

[26] Y. Katafuchi, T. Fujihara, T. Iwai, J. Terao, Y. Tsuji, *Adv. Synth. Catal.* **2011**, *353*, 475-482.

[27] J. S. L. Yeo, J. J. Vittal, T. S. Andy Hor, *Chem. Commun.* **1999**, 1477-1478.

[28] S. E. Denmark, R. C. Smith, S. A. Tymonko, *Tetrahedron* **2007**, *63*, 5730-5738.

[29] S. Gowrisankar, H. Neumann, D. Gördes, K. Thurow, H. Jiao, M. Beller, *Chem. Eur. J.* **2013**, *19*, 15979-15984.

[30] V. Goldbach, L. Falivene, L. Caporaso, L. Cavallo, S. Mecking, *ACS Catal.* **2016**, *6*, 8229-8238.

[31] A. A. Boezio, J. Pytkowicz, A. Côté, A. B. Charette, *J. Am. Chem. Soc.* **2003**, *125*, 14260-14261.
[32] J.-N. Desrosiers, A. B. Charette, *Angew. Chem. Int. Ed.* **2007**, *46*, 5955-5957.
[33] B. P. Carrow, K. Nozaki, *J. Am. Chem. Soc.* **2012**, *134*, 8802-8805.
[34] Y. Ji, R. E. Plata, C. S. Regens, M. Hay, M. Schmidt, T. Razler, Y. Qiu, P. Geng, Y. Hsiao, T. Rosner, M. D. Eastgate, D. G. Blackmond, *J. Am. Chem. Soc.* **2015**, *137*, 13272-13281.
[35] Y. Ji, H. Li, A. M. Hyde, Q. Chen, K. M. Belyk, K. W. Lexa, J. Yin, E. C. Sherer, R. T. Williamson, A. Brunskill, S. Ren, L.-C. Campeau, I. W. Davies, R. T. Ruck, *Chem. Sci.* **2017**, *8*, 2841-2851.
[36] C. Wu, J. Zhou, *J. Am. Chem. Soc.* **2014**, *136*, 650-652.
[37] J. G. de Vries, *Chem. Rec.* **2016**, *16*, 2787-2800.
[38] S.-W. Kim, S. Kim, J. B. Tracy, A. Jasanoff, M. G. Bawendi, *J. Am. Chem. Soc.* **2005**, *127*, 4556-4557.
[39] S. Sun in *Advanced Magnetic Nanostructures* (Eds.: D. Sellmyer, R. Skomski), Springer US, Boston, MA, **2006**, pp. 239-260.
[40] M. Green, N. Allsop, G. Wakefield, P. J. Dobson, J. L. Hutchison, *J. Mater. Chem.* **2002**, *12*, 2671-2674.
[41] H. Duan, D. Wang, Y. Li, *Chem. Soc. Rev.* **2015**, *44*, 5778-5792.
[42] J. Ma, *Journal of Wuhan University of Technology-Mater. Sci. Ed.* **2011**, *26*, 611-614.
[43] J. Tang, F. Redl, Y. Zhu, T. Siegrist, L. E. Brus, M. L. Steigerwald, *Nano Lett.* **2005**, *5*, 543-548.
[44] K. D. Collins, F. Glorius, *Nat. Chem.* **2013**, *5*, 597.
[45] C. M. Hagen, J. A. Widegren, P. M. Maitlis, R. G. Finke, *J. Am. Chem. Soc.* **2005**, *127*, 4423-4432.
[46] J. A. Widegren, R. G. Finke, *J. Mol. Catal. A: Chem.* **2003**, *198*, 317-341.
[47] M. A. Watzky, R. G. Finke, *J. Am. Chem. Soc.* **1997**, *119*, 10382-10400.
[48] G. M. Whitesides, M. Hackett, R. L. Brainard, J. P. P. M. Lavalleye, A. F. Sowinski, A. N. Izumi, S. S. Moore, D. W. Brown, E. M. Staudt, *Organometallics* **1985**, *4*, 1819-1830.
[49] R. van Asselt, C. J. Elsevier, *J. Mol. Catal.* **1991**, *65*, L13-L19.
[50] R. A. Jones, F. M. Real, G. Wilkinson, A. M. R. Galas, M. B. Hursthouse, *J. Chem. Soc., Dalton Trans.* **1981**, 126-131.
[51] J. Stein, L. N. Lewis, Y. Gao, R. A. Scott, *J. Am. Chem. Soc.* **1999**, *121*, 3693-3703.
[52] P. J. Dyson, *Dalton Trans.* **2003**, 2964-2974.
[53] N. T. S. Phan, M. Van Der Sluys, C. W. Jones, *Adv. Synth. Catal.* **2006**, *348*, 609-679.
[54] O. N. Gorunova, I. M. Novitskiy, Y. K. Grishin, I. P. Gloriozov, V. A. Roznyatovsky, V. N. Khrustalev, K. A. Kochetkov, V. V. Dunina, *Organometallics* **2018**, *37*, 2842-2858.
[55] K. Yu, W. Sommer, M. Weck, C. W. Jones, *J. Catal.* **2004**, *226*, 101-110.
[56] W. J. Sommer, K. Yu, J. S. Sears, Y. Ji, X. Zheng, R. J. Davis, C. D. Sherrill, C. W. Jones, M. Weck, *Organometallics* **2005**, *24*, 4351-4361.
[57] K. Yu, W. Sommer, J. M. Richardson, M. Weck, C. W. Jones, *Adv. Synth. Catal.* **2005**, *347*, 161-171.
[58] D. R. Anton, R. H. Crabtree, *Organometallics* **1983**, *2*, 855-859.
[59] V. Goldbach, M. Krumova, S. Mecking, *ACS Catal.* **2018**, *8*, 5515-5525.
[60] L. Lin, C. Romano, C. Mazet, *J. Am. Chem. Soc.* **2016**, *138*, 10344-10350.
[61] D. Gauthier, A. T. Lindhardt, E. P. K. Olsen, J. Overgaard, T. Skrydstrup, *J. Am. Chem. Soc.* **2010**, *132*, 7998-8009.

[62] P. Roesle, L. Caporaso, M. Schnitte, V. Goldbach, L. Cavallo, S. Mecking, *J. Am. Chem. Soc.* **2014**, *136*, 16871-16881.
[63] S. K. Hess, N. S. Schunck, V. Goldbach, D. Ewe, P. G. Kroth, S. Mecking, *J. Am. Chem. Soc.* **2017**, *139*, 13487-13491.

4 Palladium hydride-induced reductive semipinacol-type rearrangement of benzylic β-aryloxy- and β-alkoxy-alcohols

4.1 General motivation

As discussed in section 1.4.3, the cleavage of lignin models or native lignin to aromatic monomers is one of the key challenges in the chemical valorization of renewable feedstocks. Furthermore, the reduction of the oxygen content in the fragments is necessary to gain platform chemicals like alkylarenes.

After the development of the palladium-catalyzed transfer hydrogenolysis of benzylic alcohols (see chapter 3), the application of the reaction system to more complex substrates, e.g. lignin model compounds, was envisioned (Scheme 4.1). Besides the expected deoxygenation in benzylic position, the performance of ether bonds under the reaction conditions should be evaluated. A reductive C–O ether bond cleavage was thought possible.

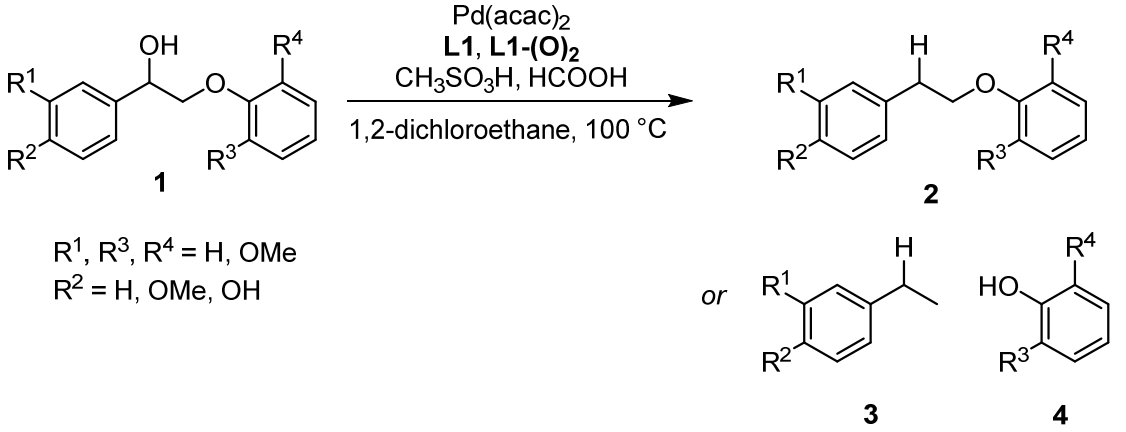

Scheme 4.1 **Envisioned products from the transformation of lignin model compounds under the optimized transfer hydrogenolysis conditions.**

4.2 Results and discussion

4.2.1 Initial reaction optimization

As model substrate for initial reactivity studies, 2-phenoxy-1-phenylethanol (**5**) was chosen, a derivative of 1-phenylethanol. The reaction conditions found effective in the transfer hydrogenolysis were applied, except for the amount of formic acid, which was increased due to the presence of two potentially reducible moieties: the benzylic alcohol group and the alkyl-aryl ether linkage (Table 4.1).

Under the given reaction conditions from the transfer hydrogenolysis (Pd(II) precursor, partially oxidized ligand **L1**, methanesulfonic acid as co-catalyst) with a slightly increased amount of formic acid (4.0 equivalents), formate **6** was found as main product in the reaction mixture, which resulted from esterification of the substrate. In addition, traces of phenol (**7**) were detected *via* GC-MS analysis, besides small amounts of 2-phenylethyl formate (**8**) (entry 1, yields for **8** were not quantified in this series of experiments). While the generation of **7** was thought to occur through a reductive cleavage of the ether C–O bond in the substrate, the reaction pathway towards **8** stayed unclear. Repeating the reaction at an elevated temperature of 120 °C resulted in relatively higher amounts of the products **7** and **8**, but still non-converted substrate **5** and intermediate **6** were present after the reaction (entry 2). Further increasing of the temperature to 150 °C led to a full consumption of both the substrate **5** and formate intermediate **6** and a relatively increased formation of **8** as well as a higher, but still moderate yield of phenol of 46% (entry 3).

Table 4.1 **Initial experiments on the reactivity of 1-phenoxy-2-phenylethanol under transfer hydrogenolysis conditions.**

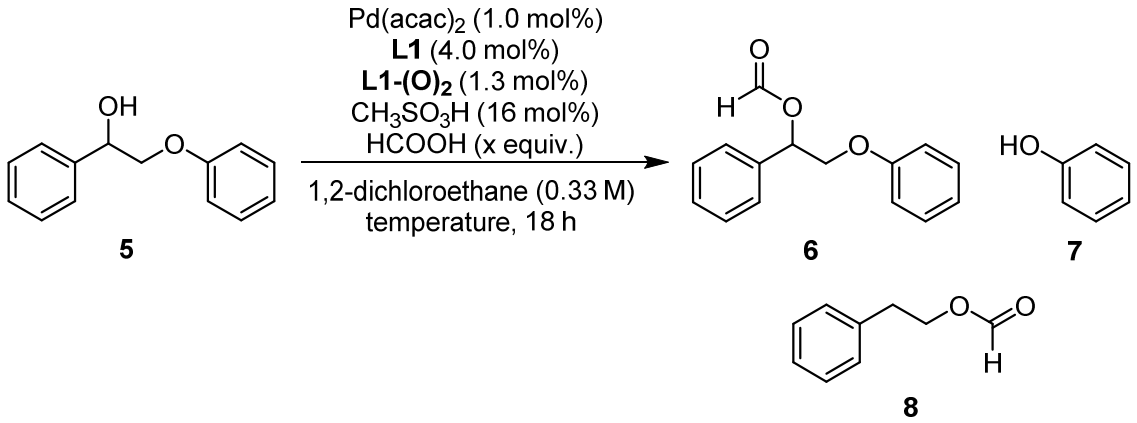

Entry[a]	HCOOH (x equiv.)	temperature [°C]	products (yield [%])[b]
1	4.0	100	**6**,[c] **7** (traces), **8** (traces)
2	4.0	120	**6**,[c] **7** (12), **8**[c]
3	4.0	150	**7** (46), **8**[c]
4	6.0	150	**7** (47), **8**[c]
5	8.0	150	**7** (37), **8**[c]

[a]General reaction conditions: 2-phenoxy-1-phenylethanol (1.00 mmol, 220 mg, 0.33 M solution), 1,2-dichloroethane (3 mL), $Pd(acac)_2$ (10 µmol, 3.0 mg, 1.0 mol%), **L1** (40 µmol, 16 mg, 4.0 mol%), **L1-(O)$_2$** (1.3 mol%, brought into the reaction as partially oxidized **L1**), methanesulfonic acid (0.16 mmol, 10 µL, 16 mol%), formic acid (respective amount), stirred at the respective temperature for 18 h in a sealed glass pressure tube. [b]Product identification was performed *via* measurement of authentic commercial samples or *via* GC-MS analysis. Yields determined *via* quantitative GC-FID using *n*-pentadecane as internal standard. [c]Product yields were not quantified.

Increasing the added amount of the reductant formic acid did not improve the reaction outcome (entries 4, 5). As a possible explanation for the impeded cleavage of substrate **5**, literature reports on the decomposition of aryl formates in presence of catalytic amounts of

palladium were considered.[1,2] This led to the assumption that the generated phenol could undergo esterification with formic acid to phenyl formate (**9**), which then would be decomposed to carbon monoxide and phenol by the palladium catalyst, consuming the reductant in an irreversible side reaction (Scheme 4.2).

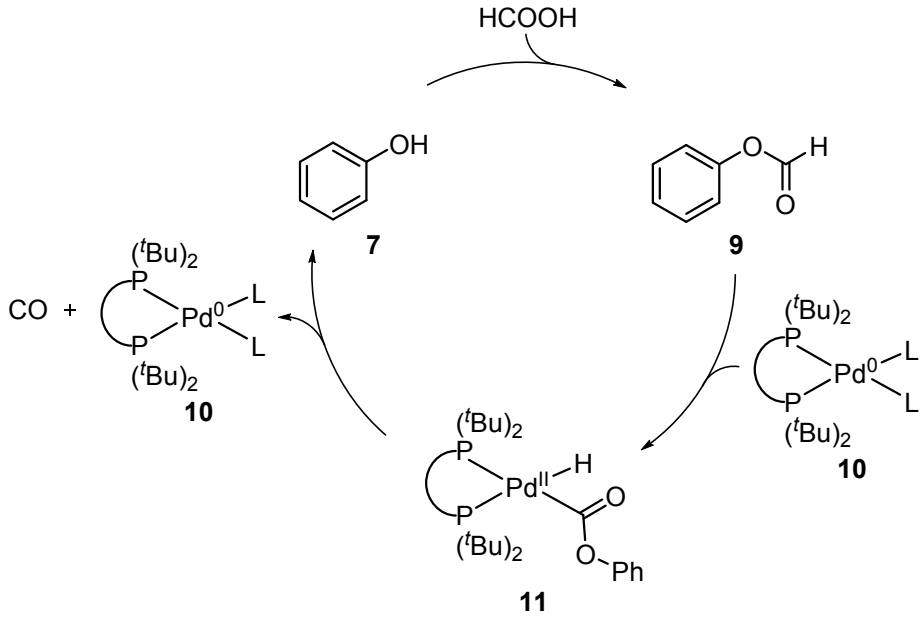

Scheme 4.2 **Assumed mechanism for the decomposition of formic acid *via* phenol esterification and palladium(0) insertion.**

To prevent this, an additive should be used to trap the free phenol. Therefore, acetic anhydride, an inexpensive, readily available bulk chemical was found suitable. A different product scope was observed for these reactions (Table 4.2). 2-Phenylethyl acetate (**13**) was found in the reaction. It constitutes a member of the group of aryl alkyl alcohol simple acid esters, which are widely used as fragrances in cosmetics or household chemical products.[3,4]

The attempted cleavage of substrate **5** at 100 °C in presence of 2.2 equivalents of acetic anhydride only delivered traces of phenol and unreacted acetylated intermediate **12** (entry 1, yields for intermediate **12** were not quantified). Raising the temperature to 150 °C resulted in the generation of phenol in a low yield of 10% as well as fair amounts of the desired cleavage products phenyl acetate (**14**, 38%) and 2-phenylethyl acetate (**13**, 34%, entry 2). Yet, still unreacted acetate **12** was found after the reaction, the mechanism of the formation of **13** from **5** was still unclear and was to be investigated later.

An increased amount of formic acid of 8.0 equivalents with the amount of acetic anhydride kept constant at 2.2 equivalents substantially diminished the yields of the targeted cleavage products (8% **13**, 11% **14**) and led to a stronger formation of phenol (38% yield, entry 3). The higher concentration of formic acid is thought to favor the formation of phenyl formate, which can be decomposed *via* the pathway shown in Scheme 4.2. This consumption of the reducing agent then inhibits an effective cleavage of intermediate **12**.

To prevent the decomposition of formic acid *via* phenyl formate formation, equimolar amounts of formic acid and acetic anhydride were applied in the reaction. The addition of 2.0 equivalents of each formic acid and acetic anhydride gave only low yields of the cleavage products **13** and **14**. Traces of phenol and a high amount of acetate intermediate **12** were found by GC analysis (entry 4).

Table 4.2 **Product distribution for the cleavage of 2-phenoxy-1-phenylethanol under transfer hydrogenolysis conditions in presence of acetic anhydride.**

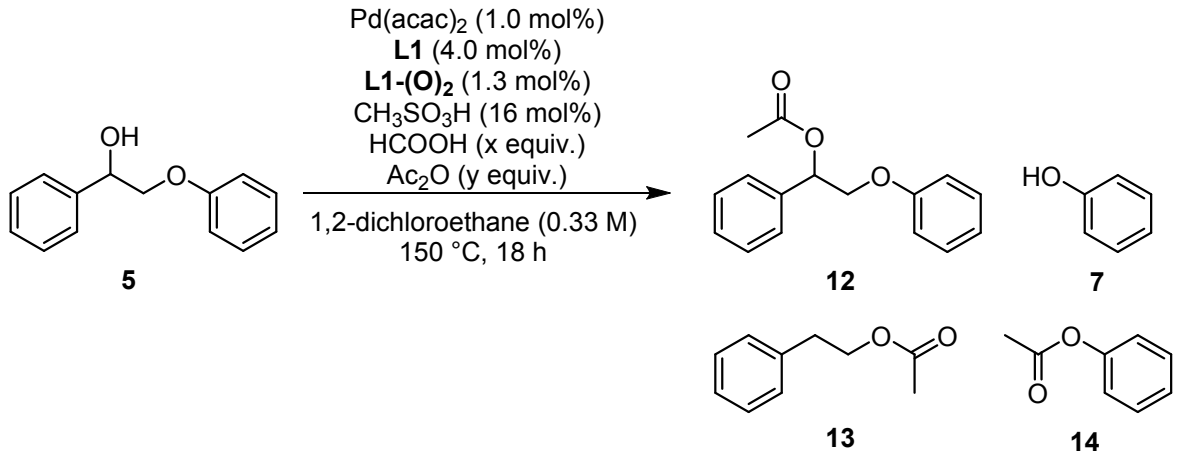

Entry[a]	HCOOH (x equiv.)	Ac_2O (y equiv.)	products (yield [%])[b]
1[c]	4.0	2.2	**7** (traces), **12**[d]
2	4.0	2.2	**7** (10), **12**,[d] **13** (34), **14** (38)
3	8.0	2.2	**7** (38), **12**,[d] **13** (8), **14** (11)
4	2.0	2.0	**7** (traces), **12**,[d] **13** (11), **14** (12)
5	4.0	4.0	**7** (8), **12**,[d] **13** (37), **14** (32)
6	6.0	6.0	**7** (11), **12**,[d] **13** (50), **14** (39)
7	8.0	8.0	**7** (20), **12**,[d] **13** (16), **14** (39)
8	2.0	4.0	**12**,[d] **14** (traces)
9	4.0	8.0	**7** (traces), **12**,[d] **14** (19)
10	4.0	6.0	**7** (traces), **12**,[d] **14** (22)
11	6.0	3.0	**7** (6), **12**,[d] **13** (24), **14** (24)
12	8.0	4.0	**7** (20), **13** (10), **14** (16)
13	8.0	1.0	**7** (40), **13** (traces), **14** (traces)
14	8.0	1.5	**7** (40), **13** (traces), **14** (8)

[a]General reaction conditions: 2-phenoxy-1-phenylethanol (500 µmol, 110 mg, 0.33 M solution), 1,2-dichloroethane (1.5 mL), $Pd(acac)_2$ (5.0 µmol, 1.6 mg, 1.0 mol%), **L1** (20 µmol, 8.1 mg, 4.0 mol%), **L1-(O)$_2$** (1.3 mol%, brought into the reaction as partially oxidized **L1**), methanesulfonic acid (80 µmol, 5.0 µL, 16 mol%), formic acid (respective amount), acetic anhydride (respective amount), stirred at 150 °C for 18 h in a sealed glass pressure tube. Full substrate conversion was achieved in all experiments. [b]Product identification was performed *via* measurement of authentic commercial samples or *via* GC-MS analysis. Yields determined *via* quantitative GC-FID using *n*-pentadecane as internal standard. [c]Reaction temperature: 100 °C. [d]Product yields were not quantified.

Raising the amounts to 4.0 equivalents had a beneficial effect on the reaction outcome. Besides residual intermediate **12** and a very low amount of phenol, fair yields for **13** and **14** of 37% and 32%, respectively, were obtained (entry 5). Even higher quantities of formic acid and acetic anhydride of 6.0 equivalents further improved the product yields of phenyl acetate (39%) and 2-phenylethyl acetate (50%). The detected amount of phenol was low (11%), unreacted **12** was again found in the reaction mixture (entry 6). In presence of 8.0 equivalents of formic acid and acetic anhydride, no increased yields of the cleavage products were observed, instead the generation of free phenol was evident, leading to a significantly diminished yield of 2-phenylethyl acetate of 16% (entry 7).

Furthermore, different ratios of formic acid and acetic anhydride were tested in the cleavage reaction. Starting from 2.0 equivalents of reductant and 4.0 equivalents of anhydride (molar ratio 1:2), only non-converted intermediate **12** and traces of phenol were obtained (entry 8). Doubling the amounts of both reagents led to the generation of **14** in a low yield of 19% besides unreacted intermediate **12** and traces of phenol (entry 9). Changing the applied ratio to 1:1.5 with amounts of formic acid and acetic anhydride of 4.0 equivalents and 6.0 equivalents, respectively, did not significantly change the reaction outcome. Phenyl acetate (**14**) was detected in 22% yield along with intermediate **12** and phenol (entry 10). For all cases in which the amount of acetic anhydride exceeded the amount of formic acid, the desired cleavage product 2-phenylethyl acetate was not observed at all.

Subsequently, the ratio of the two reagents was changed in favor of formic acid. The use of 6.0 equivalents of reductant and 3.0 equivalents of anhydride (molar ratio 2:1) resulted in the formation of **13** and **14**, each in a fair yield of 24%. Unreacted acetate intermediate **12** and low amounts of phenol were also found (entry 11). As observed in prior experiments, increasing of the amounts of formic acid and acetic anhydride to 8.0 equivalents and 4.0 equivalents favored the generation of free phenol (20% yield) and lowered the yields of the desired cleavage products **14** and **13** (entry 12). For very low introduced amounts of acetic anhydride of 1.5 or 1.0 equivalents in presence of 8.0 equivalents of formic acid, moderate yields of 40% for phenol were obtained, while no significant formation of the products **13** and **14** was evident.

4.2.2 Further optimization of key reaction parameters

From the discussed experimental results, it was concluded that equimolar amounts of formic acid and acetic anhydride were most effective in the catalytic cleavage of **5**. A further optimization of other parameters in the reaction was performed to increase the yields of the desired products. An insight into the necessary catalyst components should be gained to draw conclusions concerning the reaction mechanism. In the previous experiments on the performance of substrate **5** under the reaction conditions, the formation of phenol was found

predominant in presence of high amounts of formic acid without simultaneous generation of the respective other cleavage products. Therefore, the influence of the acid concentration in the reaction should be investigated by variation of the introduced amount of methanesulfonic acid (Table 4.3). An activation of the ether C–O bond by the Brønsted acid prior to the bond cleavage was thought possible.

Table 4.3 **Influence of the amount of methanesulfonic acid on the reaction outcome in the cleavage of 2-phenoxy-1-phenylethanol.**

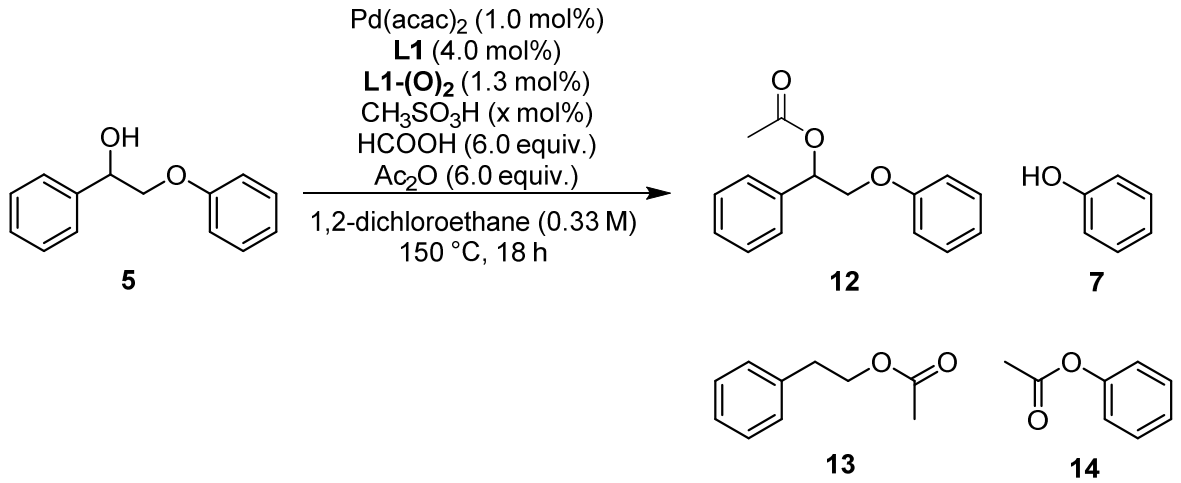

Entry[a]	CH_3SO_3H (x mol%)	products (yield [%])[b]
1	10	**7** (traces), **12**,[c] **13** (5), **14** (7)
2	16	**7** (11), **12**,[c] **13** (50), **14** (39)
3[d]	16	**7** (7), **12**,[c] **13** (traces), **14** (7)
4	20	**7** (12), **13** (14), **14** (51)
5	25	**7** (13), **13** (39), **14** (49)
6	30	**7** (15), **13** (26), **14** (41)

[a]General reaction conditions: 2-phenoxy-1-phenylethanol (500 µmol, 110 mg, 0.33 M solution), 1,2-dichloroethane (1.5 mL), $Pd(acac)_2$ (5.0 µmol, 1.6 mg, 1.0 mol%), **L1** (20 µmol, 8.1 mg, 4.0 mol%), **L1-(O)$_2$** (1.3 mol%, brought into the reaction as partially oxidized **L1**), methanesulfonic acid (respective amount), formic acid (3.0 mmol, 0.12 mL, 6.0 equivalents), acetic anhydride (3.0 mmol, 0.29 mL, 6.0 equivalents), stirred at 150 °C for 18 h in a sealed glass pressure tube. Full substrate conversion was achieved in all experiments. [b]Product identification was performed *via* measurement of authentic commercial samples or *via* GC-MS analysis. Yields determined *via* quantitative GC-FID using *n*-pentadecane as internal standard. [c]Product yields were not quantified. [d]Reaction temperature: 125 °C.

The added amounts of methanesulfonic acid tested ranged from 10 mol% to 30 mol% in presence of equimolar quantities of formic acid and acetic anhydride of 6.0 equivalents. With 10 mol% of methanesulfonic acid added to the reaction mixture, acetate intermediate **12** and non-converted substrate **5** were found as major products after the reaction, the desired cleavage products **14** and **13** were generated in very low amounts along with traces of phenol (entry 1).

As found in previous experiments, introduction of 16 mol% of methanesulfonic acid led to moderate to fair yields for the cleavage products of 39% and 50%, respectively, along with

unreacted intermediate **12** and low amounts of phenol (entry 2). At a lower temperature of 125 °C, the same amount of acid delivered substantially lower product yields for **14** (7%), **13** (7%) and phenol (traces, entry 3). Unreacted acetate intermediate **12** was detected as main product.

Further increasing of the amount of methanesulfonic acid resulted in generally higher product yields. With 20 mol% of acid, a good yield of phenyl acetate of 51% was detected, the yields of 2-phenylethyl acetate (14%) and phenol (12%) remained low (entry 4). The addition of 25 mol% of methanesulfonic acid still generated a comparable yield of **14** of 49%, yet also **13** was detected in 39% yield, besides a still relatively low phenol yield of 13% (entry 5). In contrast, in presence of a higher amount of 30 mol% of acid, the yield of **14** slightly decreased to 41%. For **13** a more significant decline to 26% was evident, while the generated amount of phenol remained nearly unchanged (entry 6).

From these results, the acid concentration is thought to have an influence on the effective cleavage of the ether C–O bond, generating phenol or phenyl acetate at 150 °C. On the other hand, too high amounts of methanesulfonic acid seem to diminish the yield of 2-phenylethyl acetate, presumably a decomposition of the product or non-productive side reactions, e.g. oligomerization, take place.

To investigate the role of the individual components in the reaction, exclusion experiments were performed (Table 4.4). The previously used reaction conditions were applied, except for lowering the respective amounts of formic acid and acetic anhydride to 4.0 equivalents.

Without a palladium precursor, the reaction yielded low to moderate amounts of phenyl acetate (**14**, 29%) and phenol (**7**, 16%), no 2-phenylethyl acetate (**13**) was observed (entry 1). Notably, this result indicates that the palladium catalyst is not implicitly needed for the cleavage of the ether C–O bond in substrate **5**, but that this step is mediated either thermally or acid-catalyzed. A similar result was obtained without addition of the partially oxidized ligand **L1/L1-(O)$_2$**. After the reaction, phenyl acetate was obtained in a fair yield of 45%, phenol was generated in a low yield of 8% (entry 2). Again, no **13** was formed, this hinted at the necessity of the palladium-bisphosphine species for the generation of 2-phenylethyl acetate. Exclusion of the acid co-catalyst resulted in a nearly complete breakdown of the reaction, only traces of phenol and unreacted substrate **5** were detected on GC (entry 3). This finding shows the crucial role of methanesulfonic acid in the cleavage reaction as well as in the substrate activation step *via* acetylation. As expected, in absence of formic acid, only non-cleaved intermediate **12** was found besides traces of phenyl acetate (entry 4). Without acetic anhydride, the substrate was not converted in the reaction and only traces of phenol were formed (entry 5).

Table 4.4 **Exclusion experiments for individual reaction components in the cleavage of 2-phenoxy-1-phenylethanol.**

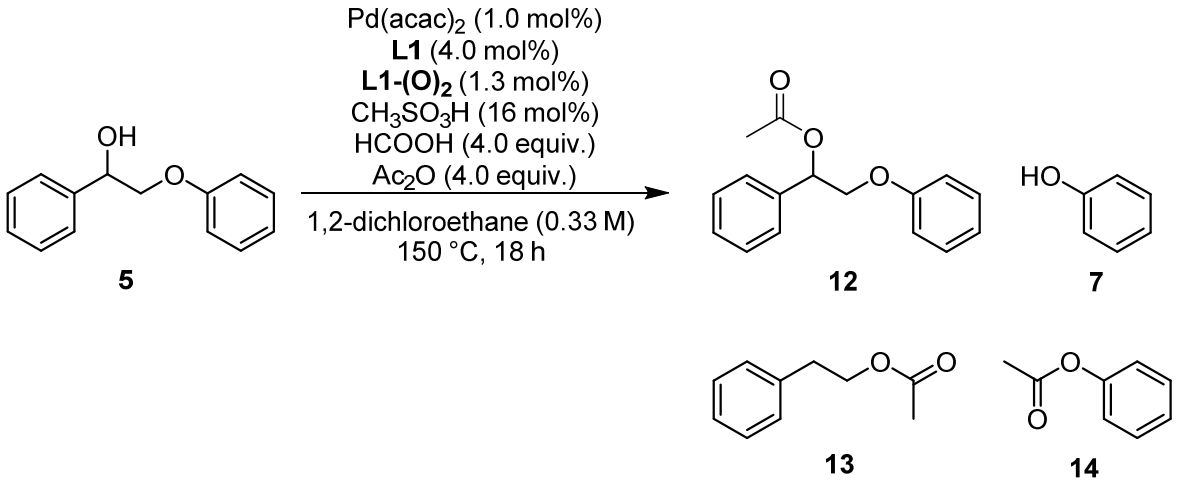

Entry[a]	excluded component	products (yield [%])[b]
1	$Pd(acac)_2$	**7** (16), **14** (29)
2	**L1/L1-(O)$_2$**	**7** (8), **14** (45)
3	CH_3SO_3H	**7** (traces)
4	formic acid	**12**,[c] **14** (traces)
5	acetic anhydride	**7** (traces)

[a]General reaction conditions: 2-phenoxy-1-phenylethanol (500 µmol, 110 mg, 0.33 M solution), 1,2-dichloroethane (1.5 mL), $Pd(acac)_2$ (5.0 µmol, 1.6 mg, 1.0 mol%), **L1** (20 µmol, 8.1 mg, 4.0 mol%), **L1-(O)$_2$** (1.3 mol%, brought into the reaction as partially oxidized **L1**), methanesulfonic acid (80 µmol, 5.0 µL, 16 mol%), formic acid (2.0 mmol, 80 µL, 4.0 equivalents), acetic anhydride (2.0 mmol, 0.19 mL, 4.0 equivalents), stirred at 150 °C for 18 h in a sealed glass pressure tube. [b]Product identification was performed *via* measurement of authentic commercial samples or *via* GC-MS analysis. Yields determined *via* quantitative GC-FID using *n*-pentadecane as internal standard. [c]Product yield was not quantified.

After demonstrating the necessity for all the components applied in the catalysis to obtain the desired cleavage products, a brief investigation concerning the catalyst loading and the substrate concentration was conducted (Table 4.5).

An increased loading of $Pd(acac)_2$ and ligand **L1** of 2.0 mol% and 8.0 mol%, respectively, did not improve the reaction outcome compared to the standard reaction conditions. In contrast, non-converted intermediate **12** was obtained as main product, only very low amounts of the desired cleavage products were formed (entry 1). Simultaneously adapting the amount of methanesulfonic acid resulted in significantly improved product amounts, phenyl acetate was generated in 51% yield, 2-phenylethyl acetate in 41% yield. The amount of undesired phenol remained low (entry 2).

Raising the substrate concentration in the reaction led to substantially higher amounts of the products **13** and **14** compared to the previously applied standard conditions (entry 3 versus entries 4–6). For phenyl acetate, increasing the concentration of the substrate from 0.33 M to 0.5 M caused an improved yield of 49% (32% for 0.33 M), 2-phenylethyl acetate was generated in 50% yield (37% for 0.33 M). The formed amount of phenol remained low

(entry 4). At even higher concentrations of **5** of 0.67 M or 1.0 M, respectively, a decrease of the yield of **14** relative to the 0.5 M reaction became evident, for **13** comparable amounts were obtained for substrate concentrations of 0.5 M and 1.0 M. The generated amounts of phenol increased with the concentration of **5** (entries 5, 6).

Table 4.5 **Influence of catalyst loading and substrate concentration on the cleavage of 2-phenoxy-1-phenylethanol.**

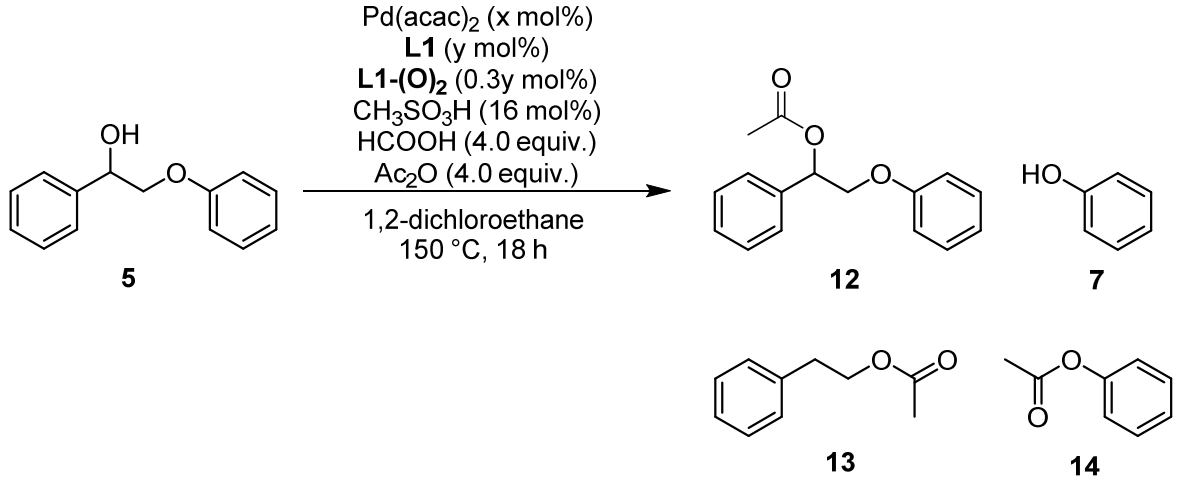

Entry[a]	$Pd(acac)_2$ (x mol%)	**L1** (y mol%)	CH_3SO_3H (z mol%)	conc. (**5**) [M]	products (yield [%])[b]
1	2.0	8.0	16	0.33	**7** (traces), **12**,[c] **13** (7), **14** (6)
2	2.0	8.0	32	0.33	**7** (8), **12**,[c] **13** (41), **14** (51)
3	1.0	4.0	16	0.33	**7** (8), **12**,[d] **13** (37), **14** (32)
4	1.0	4.0	16	0.5	**7** (9), **12**,[c] **13** (50), **14** (49)
5	1.0	4.0	16	0.67	**7** (16), **13** (34), **14** (42)
6	1.0	4.0	16	1.0	**7** (19), **13** (54), **14** (30)

[a]General reaction conditions: 2-phenoxy-1-phenylethanol (500 µmol, 110 mg, respective concentration), 1,2-dichloroethane (respective volume), $Pd(acac)_2$ (respective amount), **L1** (respective amount), **L1-(O)$_2$** (1.3 mol%, brought into the reaction as partially oxidized **L1**), methanesulfonic acid (respective amount), formic acid (2.0 mmol, 80 µL, 4.0 equivalents), acetic anhydride (2.0 mmol, 0.19 mL, 4.0 equivalents), stirred at 150 °C for 18 h in a sealed glass pressure tube. [b]Product identification was performed *via* measurement of authentic commercial samples or *via* GC-MS analysis. Yields determined *via* quantitative GC-FID using *n*-pentadecane as internal standard. [c]Product yield was not quantified.

4.2.3 Further investigations on a structurally altered substrate

In further studies on the palladium-catalyzed cleavage reaction, 2-methoxy-1-phenylethanol (**15**) was chosen as model substrate, not only to demonstrate the applicability of alkoxy moieties as leaving groups, but also to circumvent the possible decomposition of the reductant formic acid *via* the formation of aryl formates, which were shown to be labile in presence of a palladium species.[1,2] Furthermore, the second cleavage product, methyl acetate (**16**), is easier to separate from the product **13** in the purification.

The reaction conditions leading to good yields of the desired cleavage products from 2-phenoxy-1-phenylethanol (**5**) were initially applied and the influence of changes concerning the metal and ligand loadings as well as the amounts of formic acid and acetic anhydride on the reaction outcome were evaluated (Table 4.6). To assess the performance of the catalyst under the respective tested conditions, only the yield of 2-phenylethyl acetate was quantified as the second product, methyl acetate (**16**), was not detectable *via* GC analysis.

Under the reaction conditions which were found superior for the cleavage of 2-phenoxy-1-phenylethanol (**5**), a good yield of 2-phenylacetate of 59% was obtained from the cleavage of 2-methoxy-1-phenylethanol (**15**, entry 1). Lowering the respective amounts of formic acid and acetic anhydride to 1.0, 2.0 or 3.0 equivalents in the reaction with a non-changed loading of the catalyst components resulted in diminished yields of **13** of 21–51% (entries 2–4). For the same amounts of reducing agent and acetyl source, the loadings of palladium precursor and the ligands **L1**/**L1-(O)$_2$** were halved. This led to comparable yields for the corresponding experiments, indicating that a lower loading of the metal catalyst may be sufficient in the reaction (entries 2–4 versus 5–7).

Table 4.6 **Reaction outcome for the cleavage of 2-methoxy-1-phenylethanol under varied amounts of metal catalyst, formic acid and acetic anhydride.**

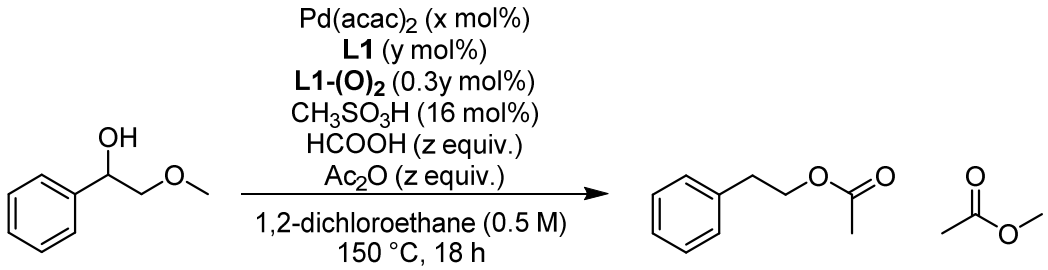

15 **13** **16**

Entry[a]	$Pd(acac)_2$ (x mol%)	**L1** (y mol%)	HCOOH, Ac_2O (z equiv.)	yield (**13**) [%][b]
1	1.0	4.0	4.0	59
2	1.0	4.0	3.0	51
3	1.0	4.0	2.0	38
4	1.0	4.0	1.0	21
5	0.5	2.0	3.0	55
6	0.5	2.0	2.0	47
7	0.5	2.0	1.0	21

[a]General reaction conditions: 2-methoxy-1-phenylethanol (500 µmol, 140 µL, 0.5 M solution), 1,2-dichloroethane (1.0 mL), $Pd(acac)_2$ (respective amount), **L1** (respective amount), **L1-(O)$_2$** (respective amount, brought into the reaction as partially oxidized **L1**), methanesulfonic acid (80 µmol, 5.0 µL, 16 mol%), formic acid (respective amount), acetic anhydride (respective amount), stirred at 150 °C for 18 h in a sealed glass pressure tube. [b]Product identification was performed *via* measurement of authentic commercial samples or *via* GC-MS analysis. Yields determined *via* quantitative GC-FID using *n*-pentadecane as internal standard.

Next, it was speculated that lowering the reaction temperature could prevent the decomposition of the ester product **13** and thereby improve the product yield. Therefore, the cleavage reaction was performed at temperatures of 120–140 °C while applying different loadings of $Pd(acac)_2$ and partially oxidized **L1** as well as of formic acid and acetic anhydride (Table 4.7).

Table 4.7 **Reaction outcome for the cleavage of 2-methoxy-1-phenylethanol under varied amounts of metal catalyst, formic acid and acetic anhydride at different reaction temperatures.**

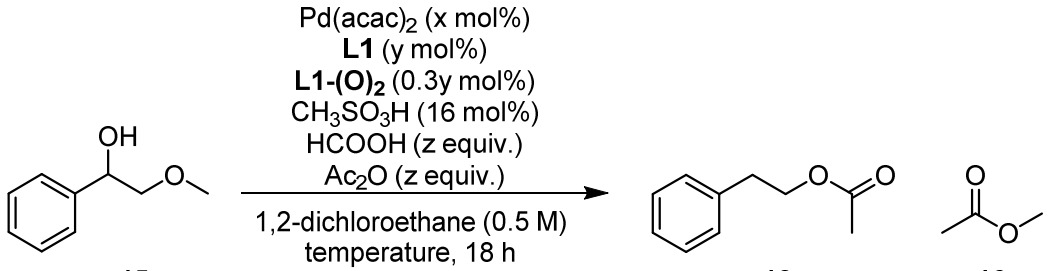

15 **13** **16**

Entry[a]	$Pd(acac)_2$ (x mol%)	**L1** (y mol%)	HCOOH, Ac_2O (z equiv.)	temperature [°C]	yield (**13**) [%][b]
1	1.0	4.0	3.0	130	74
2	1.0	4.0	3.0	120	55
3	1.0	4.0	3.0	140	57
4	1.0[c]	4.0	3.0	130	74
5	0.5	2.0	3.0	130	73
6	0.5	2.0	1.0	130	23
7	0.5	2.0	2.0	130	49
8	0.5	2.0	4.0	130	65
9	0.5[d]	2.0	4.0	130	19
10	0.5	2.0	3.0	120	64
11	0.5	2.0	3.0	140	70
12	0.25	1.0	3.0	130	30
13	0.1	0.4	3.0	130	12
14	0.75	3.0	3.0	130	87

[a]General reaction conditions: 2-methoxy-1-phenylethanol (500 µmol, 140 µL, 0.5 M solution), 1,2-dichloroethane (1.0 mL), $Pd(acac)_2$ (respective amount), **L1** (respective amount), **L1-(O)$_2$** (respective amount, brought into the reaction as partially oxidized **L1**), methanesulfonic acid (80 µmol, 5.0 µL, 16 mol%), formic acid (respective amount), acetic anhydride (respective amount), stirred at the given temperature for 18 h in a sealed glass pressure tube. [b]Product identification was performed *via* measurement of authentic commercial samples or *via* GC-MS analysis. Yields determined *via* quantitative GC-FID using *n*-pentadecane as internal standard. [c]32 mol% of methanesulfonic acid added. [d]8.0 mol% of methanesulfonic acid added.

Lowering the reaction temperature to 130 °C under else non-changed conditions led to a promising result, 2-phenylethyl acetate was obtained in a very good yield of 74% (entry 1). Decreasing the temperature to 120 °C gave **13** in a lower yield of 55% (entry 2), a comparable amount of product was generated in the reaction at 140 °C (entry 3).

A higher amount of methanesulfonic acid of 32 mol% at 130 °C did not change the reaction outcome, the cleavage product was obtained in 74% yield (entry 4).

Findings from previous experiments proposed that a reduced loading of palladium precursor and ligand **L1** of 0.5 mol% and 2.0 mol%, respectively, was sufficient to furnish comparable amounts of product **13**. Indeed, this stoichiometry also led to a very good yield of 2-phenylethyl formate of 73% (entry 5). This result is very similar to the one found for the tested higher amount of palladium and ligand.

For the lower loading of palladium and **L1** (0.5 mol% and 2.0 mol%, respectively), the added amounts of formic acid and acetic anhydride were varied. As expected, 1.0 or 2.0 equivalents of each of the reagents gave lower yields for the targeted product **13** (entries 6, 7). Notwithstanding, a raised amount of 4.0 equivalents did also result in a reduced product amount (entry 8). Additional lowering of the amount of methanesulfonic acid in the reaction to 8.0 mol% caused a sharp drop of the product yield from 65% to 19% (entry 8 versus 9).

Remarkably, changes in the reaction temperature to 120 °C or 140 °C did not have a severe effect on the product yield for the reactions with a lower loading of metal and ligand (entries 10, 11). Comparable amounts of **13** were obtained relative to the reaction performed at 130 °C.

Reducing the amounts of palladium and ligand to even lower amounts of 0.25 mol% and 1.0 mol% (entry 12) or 0.1 mol% and 0.4 mol% (entry 13) at 130 °C led to a substantial loss of turnovers, product **13** was detected in low to moderate yields of 12–30%.

Unexpectedly, the application of 0.75 mol% of $Pd(acac)_2$ and 3.0 mol% of **L1** in the reaction with 3.0 equivalents of each formic acid and acetic anhydride at 130 °C gave 2-phenylethyl formate in a very good yield of 87% (entry 14). These found conditions were further optimized, the findings of these experiments are discussed in the following.

Different palladium precursors were tested in the cleavage reaction (Table 4.8). It was apparent that soluble Pd(II) salts like $PdCl_2$ and $Pd(OAc)_2$, compared to the previously used $Pd(acac)_2$ (87% yield, entry 1), resulted in lower, but still very good yields of **13** of 74% and 71% (entries 2, 3).

Unexpectedly, $Pd(dba)_2$ as homogeneous Pd(0) source performed worse in the reaction, the cleavage product 2-phenylethyl acetate was obtained in a moderate yield of 35% (entry 4). In contrast to this finding, heterogeneous palladium on charcoal as metal source

delivered the product **13** in a higher yield of 46% (entry 5). In this case, palladium leaching into solution by the ligand **L1** is supposed to proceed the active catalyst formation.

The influence of the applied ligand also became evident with palladium nanoparticles as catalyst precursor in the reaction. The presence of **L1** resulted in a low yield of **13** of 13% (entry 6), while in absence of the ligand no product was formed (entry 7).

Table 4.8 Variation of the palladium precursor in the cleavage of 2-methoxy-1-phenylethanol.

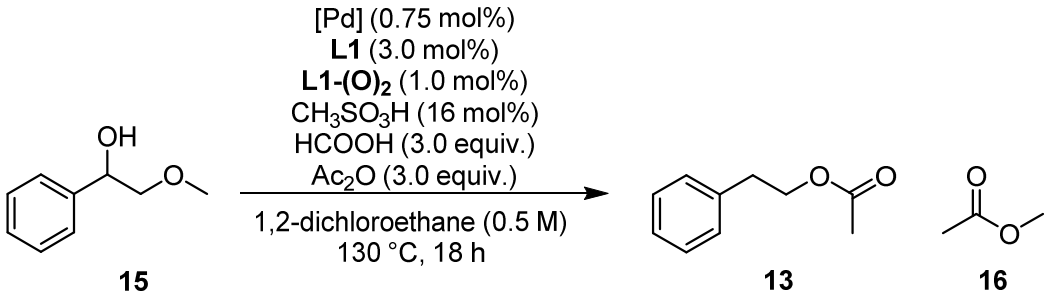

Entry[a]	[Pd] precursor	yield (**13**) [%][b]
1	$Pd(acac)_2$	87
2	$PdCl_2$	74
3	$Pd(OAc)_2$	71
4	$Pd(dba)_2$	35
5	Pd/C	46
6	Pd nanoparticles[c]	13
7	Pd nanoparticles[c,d]	–

[a]General reaction conditions: 2-phenoxy-1-phenylethanol (500 µmol, 110 mg, 0.5 M solution), 1,2-dichloroethane (1.0 mL), [Pd] precursor (0.75 mol%), **L1** (15 µmol, 5.8 mg, 3.0 mol%), **L1-(O)₂** (1.3 mol%, brought into the reaction as partially oxidized **L1**), methanesulfonic acid (80 µmol, 5.0 µL, 16 mol%), formic acid (1.5 mmol, 56 µL, 3.0 equivalents), acetic anhydride (1.5 mmol, 0.14 mL, 3.0 equivalents), stirred at 130 °C for 18 h in a sealed glass pressure tube. [b]Product identification was performed *via* measurement of authentic commercial samples or *via* GC-MS analysis. Yields determined *via* quantitative GC-FID using *n*-pentadecane as internal standard. [c]commercially available nanoparticles used (Pd EnCat 40, palladium loading: 0.4 mmol Pd/g. [d]reaction without added ligands **L1**/**L1-(O)₂**.

Further, the reaction outcome in presence of varied amounts of the acid co-catalyst and under different molar ratios of $Pd(acac)_2$ and the ligands **L1** and **L1-(O)₂** was evaluated. In addition, the influence of different substrate concentrations on the product yield was investigated (Table 4.9).

A reduced amount of methanesulfonic acid of 10 mol% led to a lower yield of product **13** of 58% (entry 2), while raising the acid amount to 20 mol% did not change the reaction outcome compared to the standard reaction conditions (entry 3 versus 1).

Lowering the reaction temperature to 120 °C resulted in a slightly decreased yield of 2-phenylethyl acetate of 75% (entry 4). At a higher temperature of 140 °C, only

approximately half of the amount of **13** generated under standard conditions was obtained, presumably due to enforced decomposition of the formed product (entry 5).

Table 4.9 **Influence of several reaction parameters on the cleavage of 2-methoxy-1-phenylethanol.**

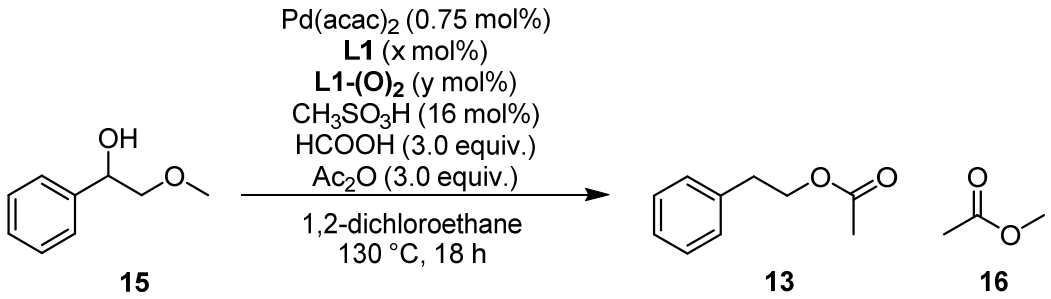

15 **13** **16**

Entry[a]	**L1** (x mol%)	**L1-(O)$_2$** (y mol%)	conc. (**15**) [M]	yield (**13**) [%][b]
1	3.0	1.0	0.5	87
2[c]	3.0	1.0	0.5	58
3[d]	3.0	1.0	0.5	87
4[e]	3.0	1.0	0.5	75
5[f]	3.0	1.0	0.5	42
6	1.5	0.5	0.5	76
7	2.5	0.8	0.5	79
8	4.0	1.3	0.5	76
9	6.0	2.0	0.5	58
10	3.0	–	0.5	62
11	3.0	3.0	0.5	83
12	3.0	4.0	0.5	67
13	3.0	1.0	0.4	69
14	3.0	1.0	0.67	83
15	3.0	1.0	1.0	78

[a]General reaction conditions: 2-phenoxy-1-phenylethanol (500 µmol, 110 mg, 0.5 M solution), 1,2-dichloroethane (respective volume), [Pd] precursor (0.75 mol%), **L1** (respective amount), **L1-(O)$_2$** (respective amount), methanesulfonic acid (80 µmol, 5.0 µL, 16 mol%), formic acid (1.5 mmol, 56 µL, 3.0 equivalents), acetic anhydride (1.5 mmol, 0.14 mL, 3.0 equivalents), stirred at 130 °C for 18 h in a sealed glass pressure tube. [b]Product identification was performed *via* measurement of authentic commercial samples or *via* GC-MS analysis. Yields determined *via* quantitative GC-FID using *n*-pentadecane as internal standard. [c]10 mol% of methanesulfonic acid added. [d]20 mol% of methanesulfonic acid added. [e]reaction temperature: 120 °C [f]reaction temperature: 140 °C.

Varying the amount of the added ligand **L1** in a range from 1.5 to 6.0 mol%, with a constant molar ratio of **L1** and **L1-(O)$_2$** of 3:1, led to diminished yields of **13** of 58–79% (entries 6–9). Exclusion of the phosphine oxide **L1-(O)$_2$** from the reaction resulted in a lower yield of 2-phenylethyl acetate of 62% (entry 10), clearly demonstrating an operating

phosphine oxide effect similar to the one found for the palladium-catalyzed transfer hydrogenolysis described in this thesis (section 3.3.4). Changing the ratio of **L1** and **L1-(O)$_2$** to 1:1 only marginally changed the reaction outcome (entry 11). A higher amount of **L1-(O)$_2$** of 4 mol% hindered the cleavage reaction (entry 12), the phosphine oxide is thought to act as a competing ligand on the palladium center.

Finally, the variation of the substrate concentration to lower or higher amounts relative to the standard conditions did not improve the yield of **13** (entries 13–15).

4.2.4 Investigation of the cleavage product stability

As mentioned earlier in this section, it was assumed that under the reaction conditions, the formed product 2-phenylethyl acetate (**13**) was decomposed or underwent further non-productive side reactions. This was thought to be the reason for the fact that the yield under optimized reaction conditions did not exceed 87%. To investigate this, the cleavage product **13** was subjected to the catalytic reaction analogous to the cleavage of 2-methoxy-1-phenylethanol (Scheme 4.3). Quantitative GC analysis showed that only 88% of the introduced amount of 2-phenylethyl acetate remained in the reaction mixture after 18 hours, no side products were detected (Scheme 4.3). Therefore, the theory of a decomposition of **13** seems valid, the reaction time should be shortened in future optimization studies to encounter this problem.

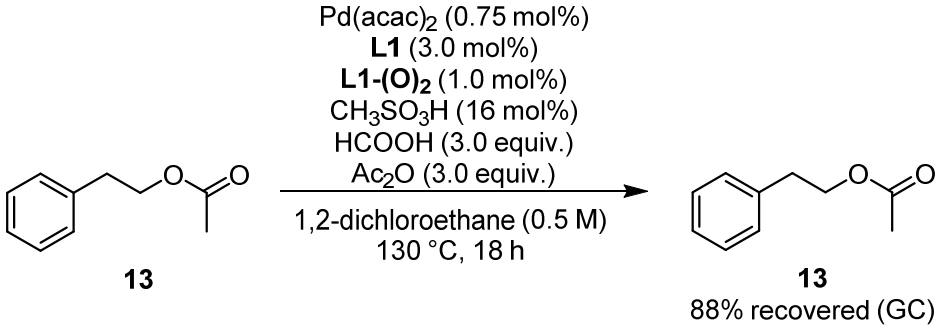

Scheme 4.3 Evaluation of the stability of cleavage product 13 under standard reaction conditions.

4.2.5 Initial substrate screening

The found optimal reaction conditions were successfully applied to two substrates containing different aryl groups. For the tested substrates, the addition of 20 mol% of methanesulfonic acid resulted in higher product yields, although no influence of the increased amount of 20 mol% instead of 16 mol% on the cleavage of 2-methoxy-1-phenylethanol was evident in the optimization. The palladium-catalyzed cleavage of 2-methoxy-1-(1-naphthyl)ethanol (**17**) and 2-methoxy-(4-fluorophenyl)ethanol (**19**) furnished the corresponding products 2-(1-naphthyl)ethyl acetate (**18**) and 2-(4-fluorophenyl)ethyl acetate (**20**) in good to excellent yields. Under the optimized reaction conditions, the initially

used model substrate **5** could be converted to 2-phenylethyl acetate in a yield of 55% (Scheme 4.4).

In the attempted conversion of 1-methoxy-2-propanol (**21**), a substrate bearing an alkyl group instead of an aryl moiety, no product formation was observed (Scheme 4.4). This indicates the necessity of an aryl group adjacent the alcohol moiety for a successful transformation. The reason for this is assumed to be the selectivity of the palladium hydride catalyst towards the benzylic position, as it was already shown for the transfer hydrogenolysis of benzylic alcohols (see section 3.3).

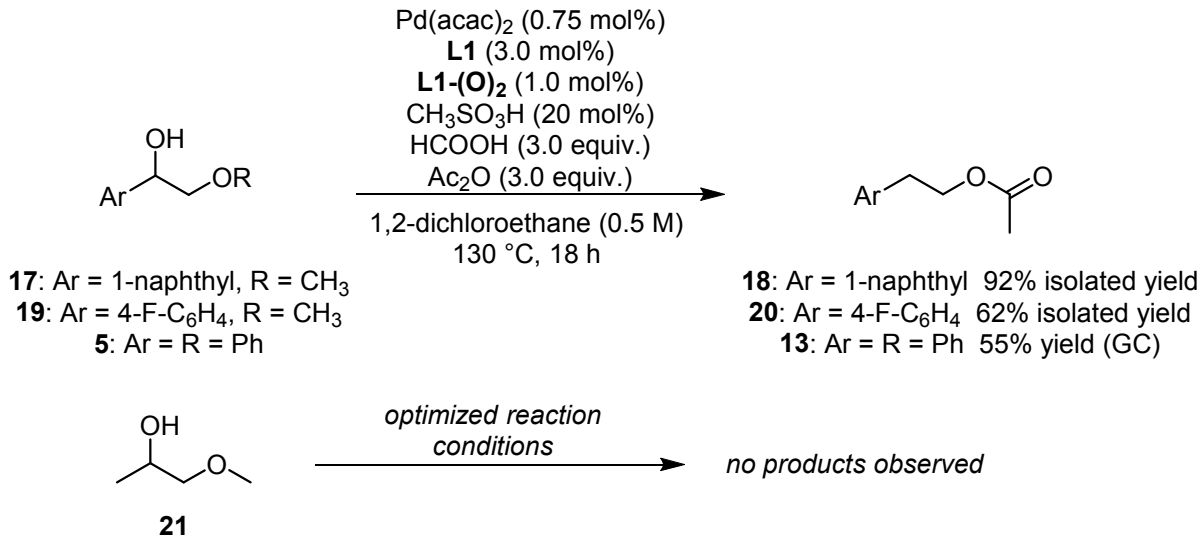

Scheme 4.4 Initially converted substrates in the palladium-catalyzed cleavage reaction.

4.2.6 Mechanistic investigations

Reaction pathway elucidation

As mentioned before in this chapter, the mechanism of the developed palladium-catalyzed cleavage reaction was not fully understood during the reaction optimization. Some findings indicated that the acid co-catalyst plays a crucial role in the cleavage of the alkyl aryl ether bond in 2-phenoxy-1-phenylethanol (**5**). Nonetheless, the pathway for the formation of 2-phenylethyl acetate from substrates **5** and **15** remained unclear. In theory, two distinct reaction sequences appeared plausible (Scheme 4.5).

Transfer hydrogenolysis of the benzylic alcohol moiety in the applied substrates seemed possible, leading to ether **22**. From this compound, product **13** could be generated *via* hydrolytic cleavage of the ether C–O bond, followed by acetylation of the formed free alcohol.

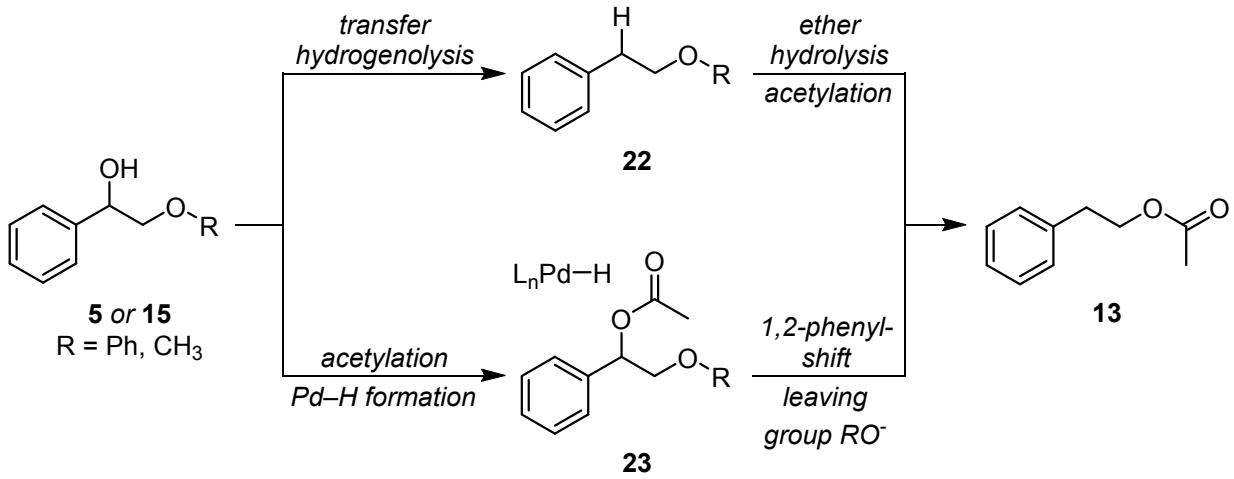

Scheme 4.5 **Possible reaction pathways for the palladium-catalyzed cleavage of β-aryloxy or β-alkoxy benzylic alcohols.**

Another possible pathway is initiated by the acetylation of the substrate generating compound **23**. Simultaneously, a palladium hydride complex (for possible formation mechanisms see section 3.3.3) is formed under the reaction conditions. Hydride transfer from the metal complex to **23** induces a 1,2-shift of the phenyl moiety and a cleavage of the ether C–O bond, resulting in product **13**. This resembles the mechanism of a semipinacol-rearrangement,[5] although no carbonyl function is generated.

To obtain an insight into the operating reaction mechanism, substrate **24**, a derivative of the previously used model substrate **5**, was introduced into the catalytic cleavage reaction under still non-optimized conditions (Scheme 4.6). The introduction of two methyl groups on the methylene group should thereby make the distinction of the carbon atoms in the formed product possible. Through this, the position of the phenyl group after the cleavage can be determined, confirming or excluding a 1,2-shift.

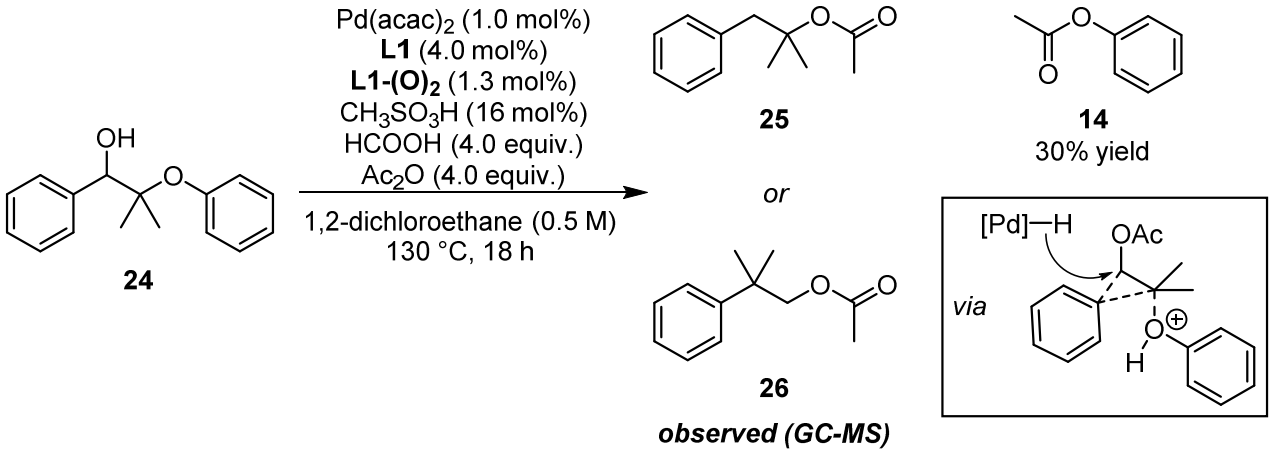

Scheme 4.6 **Modification of the substrate in the cleavage reaction to elucidate the basic reaction mechanism.**

Besides a yield of 30% of phenyl acetate (**14**), of the other two possible products **25** and **26**, only **26** was obtained (the amount of **26** was not quantified). Yet, the product was identified unambigously through comparison of the GC retention times and the mass spectrometry fragmentation patterns with authentic commercial or synthesized samples of both possible compounds. This finding demonstrates that the investigated palladium-catalyzed reaction proceeds through a 1,2-shift of the contained phenyl group under simultaneous cleavage of the C–O ether bond. To deliver further proof for this mechanism, ^{13}C-labelling of the benzylic carbon in 2-methoxy-1-phenylethanol (**15**) was thought expedient, yet the synthesis of the labelled substrate and its application in the catalytic reaction are still ongoing.

A similar mechanism was proposed in a work on the cleavage of structurally resembling substrates reported by Cantat and co-workers,[6] which was already described in the introductional chapter of this thesis (see section 1.4.3). Therein, the metal-free catalyst system was based on catalytic amounts of the Lewis acid $B(C_6F_5)_3$ and Et_3SiH as reducing agent (Scheme 4.7). Substrate activation is thought to occur through silylation of the contained oxygen moieties, while the priorly generated hydroborate $HB(C_6F_5)_3^-$ transfers a hydride to the intermediate **30** after the 1,2-phenyl shift, furnishing silyl ether **27**. An alternative reaction mechanism proceeding *via* the intramolecular formation of a silylated epoxide (not shown in Scheme 4.7) was excluded based on DFT calculations.

For the palladium-catalyzed cleavage reaction presented in this thesis, parallels in regard to the activation of the substrate and the active catalyst structure are apparent. While in the work of Cantat and co-workers the formation of a silyl ether or Lewis acidic activation of the alkyl aryl ether form the reactive intermediate, the palladium based method relies on acetylation of the benzylic alcohol and the presence of a strong Brønsted acid co-catalyst to facilitate the alkyl aryl ether cleavage *via* protonation. Both catalysts have in common that they transfer a hydride to the substrate, although they differ in their nature as metal complex or metal-free borane.

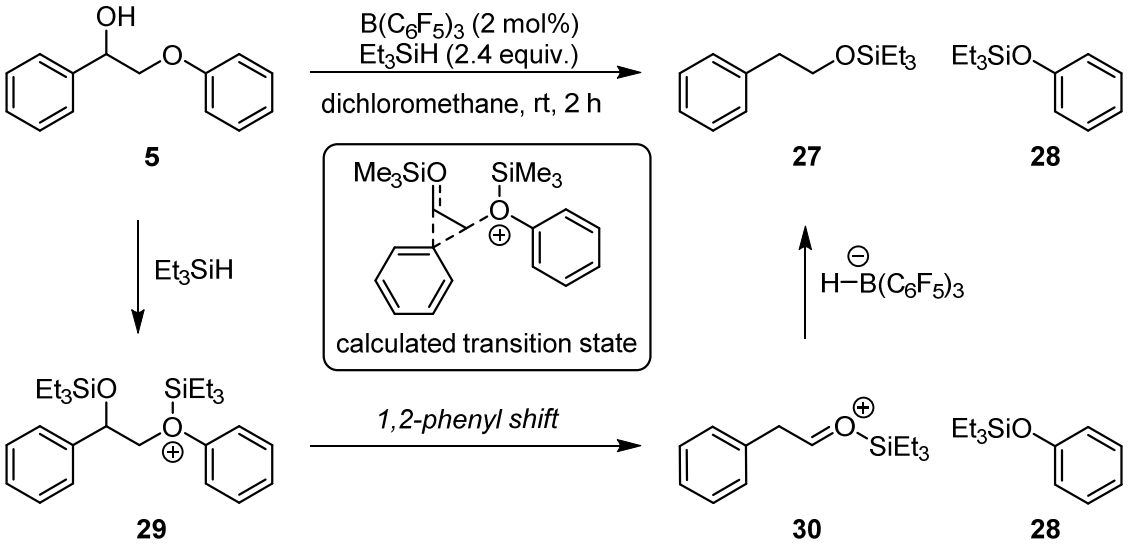

Scheme 4.7 **Cleavage of 2-phenoxy-1-phenylethanol using a borane catalyst and a silane reductant *via* a 1,2-phenyl-shift reported by Cantat and co-workers.[6]**

Qualitative headspace GC analysis

As discussed before for the transfer hydrogenolysis of benzylic alcohols, an internal gas overpressure was also evident in the reactor after the palladium-catalyzed cleavage reaction. To investigate this, headspace GC measurements were performed for the cleavage of 2-methoxy-1-phenylethanol (**15**). The sampling of the gas phase from the closed reaction vessel was carried out as already described in section 3.3.7. GC analysis showed the presence of hydrogen, carbon monoxide and carbon dioxide gas. Especially the generation of CO in the reaction was surprising, as no direct CO source was introduced to the mixture. Yet, reviewing the optimization experiments showed that the application of equimolar amounts of formic acid and acetic anhydride resulted in high yields of the cleavage products.

Therefore, the formation of a mixed acetic formic anhydride is assumed to occur in the reaction. Thermal decomposition of this labile species leads to the formation of carbon monoxide and acetic acid.[7] Moreover, the activation of the mixed anhydride on a palladium(0) complex and subsequent decarbonylation may also generate a palladium hydride complex which can act as a reducing species towards the reaction intermediate (Scheme 4.8). Oxidative addition over the hydridic C–H bond directly generates a palladium(II) hydride **31** with a labile acetoxycarbonyl ligand. Decarbonylation of the latter gives palladium(II) bisphosphine complex **32** which is stabilized by a hydride and an acetate ligand.[8]

Alternatively, parallel processes leading to the formation of a homogeneous palladium hydride from methanesulfonic acid and formic acid, as discussed in section 3.3.3, cannot be excluded and should also be considered.

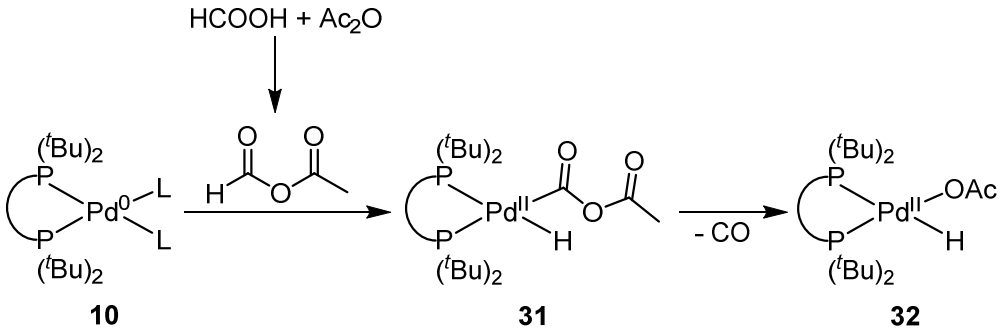

Scheme 4.8 **Proposed pathway for the formation of a palladium(II) hydride complex *via* activation of acetic formic anhydride on a palladium(0) center.[8]**

The detected hydrogen and carbon dioxide may originate from the reduction of various palladium species by formic acid[9] or carbon monoxide and water present in the system.[10]

Mechanistic proposal

With the experimental finding from the reaction optimization and the mechanistic investigations taken into account, a reaction mechanism for the palladium-catalyzed semipinacol-type rearrangement of β-aryloxy and β-alkoxy benzylic alcohols is proposed (Scheme 4.9). Initially, the introduced Pd(II) precursor is reduced by formic acid or by CO generated from the thermal decomposition of acetic formic anhydride and water present under the reaction conditions (non-dried solvent and reagents). Coordination of **L1** generates palladium(0) bisphoshine complex **33** in which the bisphosphine dioxide **L1-(O)$_2$** acts as an additional stabilizing ligand *via* a weak interaction with the metal center. The presence of the bisphosphine dioxide was shown to be beneficial for the reaction, yet too high amounts also hindered the transformation, assumably by occupying the coordination sites on the palladium complex. Addition of acetic formic anhydride to the palladium(0) complex generates palladium(II) hydride complex **32** under release of carbon monoxide.

The alcohol substrate is activated *via* acetylation with acetic anhydride. The formed species **23** is able to accept a hydride from palladium complex **32** and undergoes a 1,2-aryl shift under cleavage of the alkyl aryl or dialkyl ether bond to generate the desired 1-arylethyl acetate product, either in a concerted or stepwise fashion. The free coordination site on the palladium center may be occupied by acetate present in the reaction mixture, generating **34**, a 16 valence electron metal complex. This complex then is reduced by carbon monoxide in presence of water to regenerate palladium(0) complex **33**, again stabilized by **L1-(O)$_2$**. This reduction step seems to play a crucial role in the reaction. It became evident that withdrawing samples from the reactor *via* a stainless steel on/off-valve or *via* syringe, a partial loss of the gas atmosphere occurred. As a result, the reaction stopped at lower yields than in the corresponding undisturbed case. From complex **33**, palladium hydride **32** is generated again by decomposition of acetic formic anhydride, closing the catalytic cycle.

Notwithstanding, the discussed mechanism is preliminary, further investigations are necessary to thoroughly elucidate the reaction pathway, especially concerning the formation of the active catalyst and its regeneration after the reduction step.

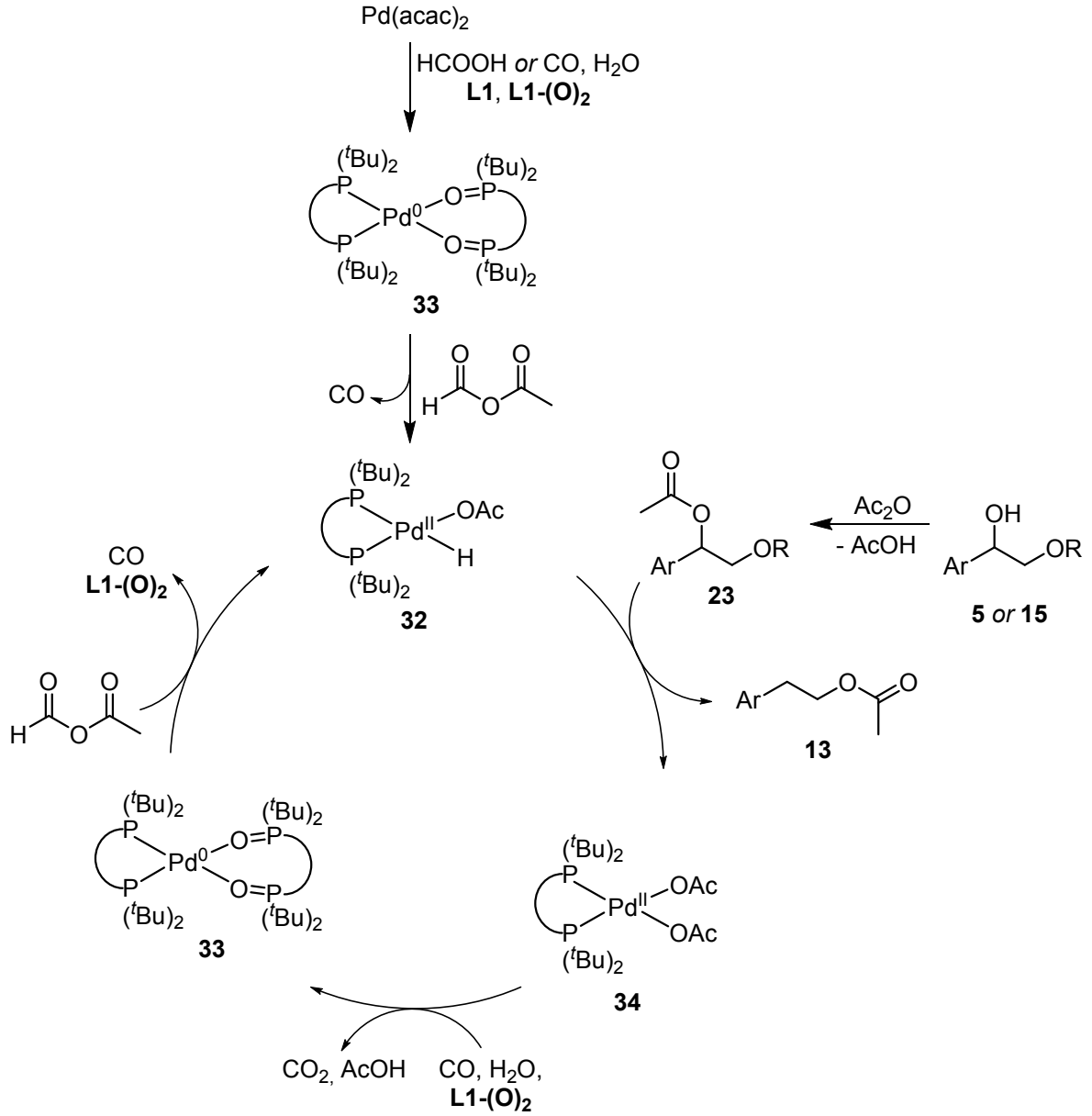

Scheme 4.9 **Proposed reaction mechanism for the palladium-catalyzed semipinacol-type rearrangement of β-aryloxy or β-alkoxy benzylic alcohols.**

4.3 Conclusion and outlook

In this chapter, the developed method for a palladium-catalyzed cleavage of β-aryloxy or β-alkoxy benzylic alcohols was presented. Although the reaction was optimized regarding the loading of the catalyst components as well as the amounts of the reductant and the substrate activation agent, further studies on a possible decomposition of the 2-arylethyl acetate products should be performed. Therein, a shorter reaction time could be found sufficient to furnish the desired products in higher yields than these obtained under the given conditions.

Different anhydrides should be tested in the reaction to evaluate the possibility of generating ester products other than acetates. Therefore, not only carboxylic acid anhydrides, but also others, e.g. sulfonic anhydrides, could possibly be converted to valuable products (Scheme 4.10).

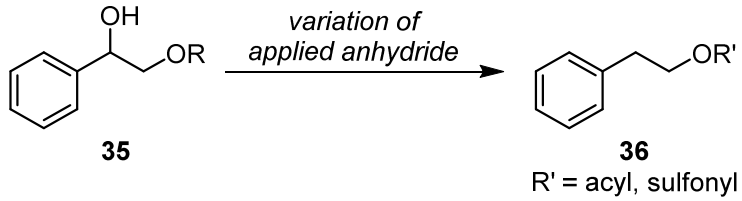

Scheme 4.10 **Possible extension of the substrate scope in the semipinacol-type rearrangement via variation of the introduced anhydride.**

Moreover, the transformation was shown to be applicable to only four substrates so far, containing aryl migrating groups as well as aryloxy and alkoxy leaving groups. Here, a thorough substrate screening should be performed, demonstrating the influence of steric and electronic variations on the migration aryl moiety (Figure 4.1). Additionally, different aryloxy and alkoxy leaving groups should be tested, as well as sulfides or amines. Also, an *in situ* generation of the leaving group should be probed, possibly enabling the rearrangement of aromatic diols (Figure 4.1).

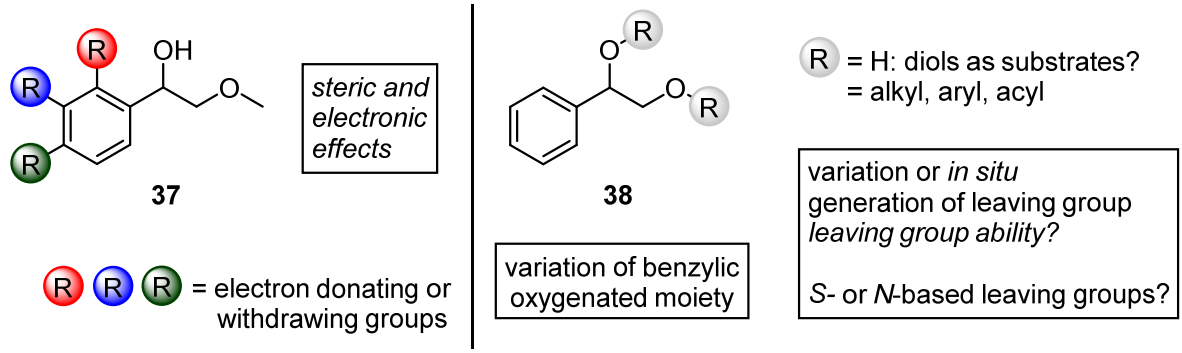

Figure 4.1 **Evaluation of substrates exhibiting different steric and electronic properties, variation of the oxygenated moieties.**

Variation of the carbon skeleton of the substrates may provide further information about the reaction mechanism, e.g. on the migratory aptitude or the selectivity of the migrating group in case of two substituents attached in benzylic position (Figure 4.2).

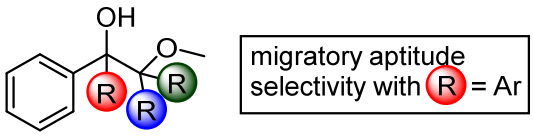

39

Figure 4.2 **Introduction of additional substituents to investigate migration aptitude and selectivity.**

The application of the developed method on cyclic substrates can lead to a rearrangement with or without contraction of the ring, depending on the given substrate structure. Here, the influence of the ring size should be evaluated (Scheme 4.11).

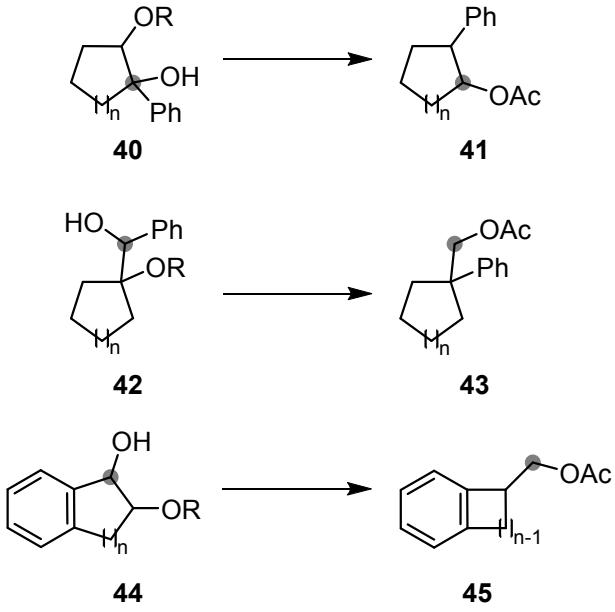

40 **41**

42 **43**

44 **45**

Scheme 4.11 **Possible rearrangement of cyclic substrates including ring contraction.**

The substrates used in this thesis for the semipinacol-type rearrangement contain one or two stereogenic centers. From a mechanistic point of view, the transformation of enantiomerically enriched diastereomers appears interesting, as it may allow a further understanding of the migration step regarding the concerted or non-concerted character of the rearrangement. In case of a concerted mechanism, the enantiomeric ratio in the substrate should be retained, while a pathway consisting of two distinct steps, exclusion of the leaving group and migration, would lead to racemization (Scheme 4.12).

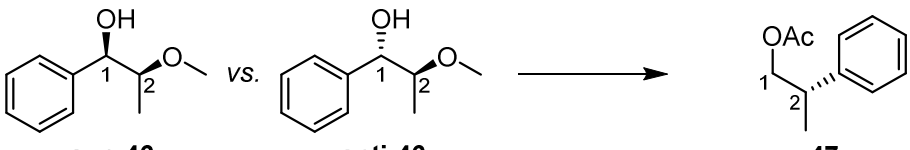

syn-46 **anti-46** **47**

same reactivity for both diastereomers? *retention or racemization?*

Scheme 4.12 **Investigation of the stereoselectivity of the semipinacol-type rearrangement.**

4.4 References

[1] Y. Katafuchi, T. Fujihara, T. Iwai, J. Terao, Y. Tsuji, *Adv. Synth. Catal.* **2011**, *353*, 475-482.

[2] I. Fleischer, R. Jennerjahn, D. Cozzula, R. Jackstell, R. Franke , M. Beller, *ChemSusChem* **2013**, *6*, 417-420.

[3] D. McGinty, D. Vitale, C. S. Letizia, A. M. Api, *Food Chem. Toxicol.* **2012**, *50*, 491-497.

[4] D. Belsito, D. Bickers, M. Bruze, P. Calow, M. L. Dagli, A. D. Fryer, H. Greim, Y. Miyachi, J. H. Saurat, I. G. Sipes, *Food Chem. Toxicol.* **2012**, *50*, S269-S313.

[5] L. Kürti, B. Czakó, *Strategic applications of named reactions in organic synthesis: Background and detailed mechanisms*, Elsevier Academic Press, **2005**.

[6] E. Feghali, T. Cantat, *Chem. Commun.* **2014**, *50*, 862-865.

[7] S. Cacchi, G. Fabrizi, A. Goggiamani, *J. Comb. Chem.* **2004**, *6*, 692-694.

[8] Y. Wang, W. Ren, Y. Shi, *Org. Biomol. Chem.* **2015**, *13*, 8416-8419.

[9] C. Ortiz-Cervantes, M. Flores-Alamo, J. J. García, *ACS Catal.* **2015**, *5*, 1424-1431.

[10] A. F. Holleman, N. Wiberg, *Lehrbuch der Anorganischen Chemie*, Walter de Gruyter, Berlin, **2007**.

5 Summary / Zusammenfassung

The catalytic conversion of oxygen-containing feedstocks to deoxygenated, value-added chemicals states an important transformation in organic chemistry, not only for syntheses on laboratory scale, but also for industrial setups, e.g. in the valorization of renewable resources derived from biomass. In the introductory section of this thesis, the importance of the development of efficient and selective methods for the reductive deoxygenation of various substrates, like alcohols, carbonyl compounds or ethers, is demonstrated by highlighting recent outstanding literature works. Therein, a focus was set on transition metal-catalyzed methodologies for the reductive cleavage of benzylic C–O bonds either *via* hydrogenolysis using H_2 gas or *via* transfer hydrogenolysis applying formal hydrogen sources.

Regarding the valorization of biomass, works from the emerging field of the isolation and depolymerization of lignin and studies on the cleavage of lignin model compounds *via* transition metal-catalyzed oxidative, reductive or redox neutral methods were reviewed.

Moreover, the known methods for the characterization of an operating transition metal catalyst as homogeneous or heterogeneous were discussed. These comprise, amongst other manipulations, the interpretation of reaction profiles and the application of catalyst poisons in the investigated reactions.

The second part of this thesis covers the development of a palladium-catalyzed transfer hydrogenolysis of benzylic alcohols. Formic acid was applied as hydride source to furnish a scope of deoxygenated alkylarenes. The user-friendly transformation could be realized under a metal loading as low as 1.0 mol%, a partially oxidized bisphosphine ligand and an acid co-catalyst were further components of the active catalyst (Scheme 5.1).

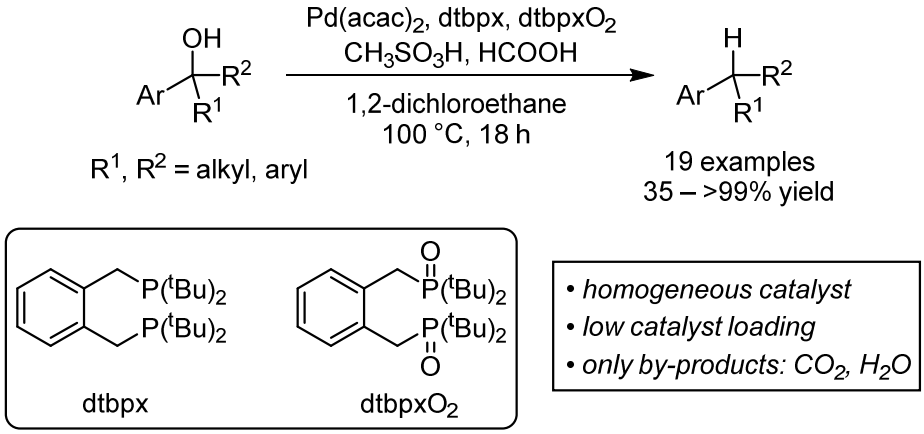

Scheme 5.1 **Palladium-catalyzed transfer hydrogenolysis of benzylic alcohols with formic acid as reducing agent.**

The reducing agent, which was introduced in a low amount of only 2.0 equivalents, generates carbon dioxide and water as only by-products, enabling a simple product purification. In contrast to related previous works, the active catalyst in the presented system was shown to be homogeneous by using some of the methods for catalyst characterization discussed in the introduction. In addition, the pathway of substrate activation was elucidated. Isotope labelling experiments allowed for the proposal of a reaction mechanism.

The adaption of the developed transfer hydrogenolysis protocol for more challenging substrates, as presented in the third part of this thesis, led to the development of a palladium-catalyzed semipinacol-type rearrangement of β-aryloxy or β-alkoxy benzylic alcohols (Scheme 5.2). As products, 2-arylethyl acetates were generated *via* the migration of an aryl moiety in the substrates and the simultaneous cleavage of an ether C–O bond. A palladium hydride complex is assumed to be involved in a necessary reduction step. Compared to the transfer hydrogenolysis, the catalyst loading could be reduced to 0.75 mol% of palladium in presence of the priorly used ligand and acid co-catalyst. For the readily available reductant formic acid and the inexpensive substrate activating agent acetic anhydride, a low amount of 3.0 equivalents each was found sufficient.

Although the optimal reaction conditions were already determined and applied in the transformation of several substrates, further investigations will be performed to broaden the substrate scope and to obtain a deeper understanding of the reaction mechanism as of the palladium species involved in the catalytic cycle.

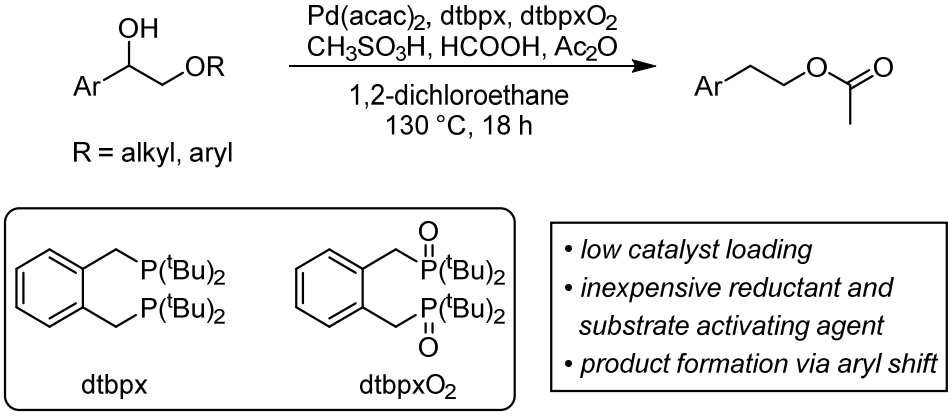

Scheme 5.2 **Palladium-catalyzed semipinacol-type rearrangement of β-aryloxy or β-alkoxy benzylic alcohols to 2-arylethyl acetates.**

Die katalytische Umwandlung sauerstoffhaltiger Ausgangsprodukte zu sauerstofffreien, höherwertigen Chemikalien stellt eine wichtige Transformation in der organischen Chemie dar, nicht nur für Synthesen im Labormaßstab, sondern auch im industriellen Umfeld, z.B. bei der Wertschöpfung von aus Biomasse erzeugten, erneuerbaren Rohstoffen. Im einleitenden Teil dieser Arbeit wird die Bedeutung der Entwicklung effizienter und selektiver Methoden für die reduktive Desoxygenierung diverser Substrate wie Alkohole, Carbonylverbindungen oder Ether aufgezeigt, hierzu werden die neuesten herausragenden Arbeiten aus der Literatur hervorgehoben. Dabei wird der Fokus auf übergangsmetallkatalysierte Methoden zur reduktiven Spaltung benzylischer C–O-Bindungen gelegt, entweder mittels Hydrogenolyse unter Verwendung von H_2-Gas oder durch Transferhydrogenolyse mit formalen Wasserstoffquellen.

Hinsichtlich der Wertschöpfung von Biomasse wurde ein Überblick über Arbeiten aus dem aufkommenden Feld der Isolierung und Depolymerisation von Lignin sowie zu Studien zur Spaltung von Ligninmodellverbindungen durch übergangsmetallkatalysierte oxidative, reduktive oder redoxneutrale Methoden gegeben.

Darüber hinaus wurden die bekannten Methoden für die Charakterisierung aktiver Übergangsmetallkatalysatoren als homogen oder heterogen diskutiert. Diese umfassen, neben anderen Manipulationen, die Interpretation von Reaktionsprofilen sowie die Anwendung von Katalysatorgiften in den untersuchten Reaktionen.

Der zweite Teil dieser Dissertation behandelt die Entwicklung einer Palladium-katalysierten Transferhydrogenolyse benzylischer Alkohole. Ameisensäure wurde als Hydridquelle verwendet, um eine Auswahl an desoxygenierten Alkylarenen herzustellen. Die benutzerfreundliche Transformation konnte mit einer niedrigen Metallbeladung von 1,0 mol% realisiert werden, ein teilweise oxidierter Bisphosphinligand sowie eine Säure als Cokatalysator sind weitere Komponenten des aktiven Katalysators (Schema 5.3).

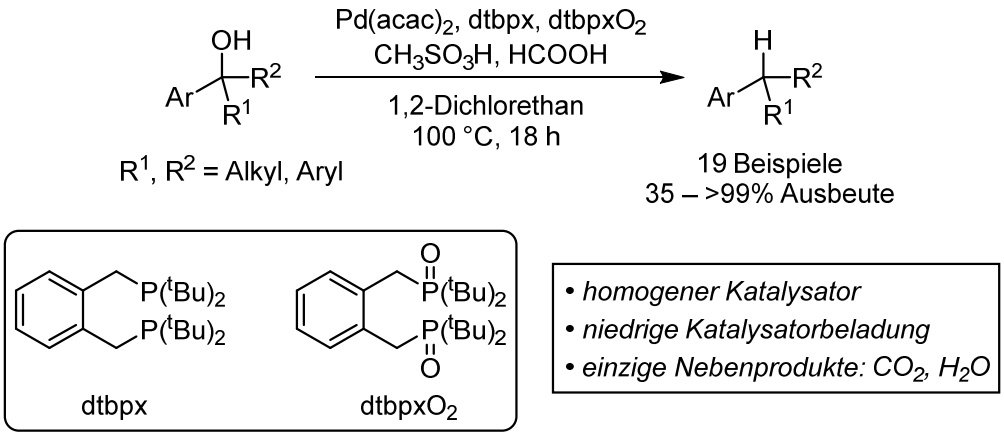

Schema 5.3 **Homogene Palladium-katalysierte Transferhydrogenolyse benzylischer Alkohole mit Ameisensäure als Reduktionsmittel.**

Das Reduktionsmittel, welches lediglich in einer geringen Menge von 2,0 Äquivalenten verwendet wurde, erzeugt Kohlendioxid und Wasser als einzige Nebenprodukte, dies ermöglicht eine einfache Aufreinigung der Reaktionsprodukte.
Durch Anwendung einiger in der Einleitung diskutierter Methoden zur Charakterisierung von Katalysatoren wurde gezeigt, dass der aktive Katalysator in dem präsentierten System homogener Natur ist. Dies steht im Gegensatz zu verwandten vorhergehenden Arbeiten, welche auf heterogenen Palladiumkatalysatoren basieren. Zusätzlich wurde der Reaktionspfad der Substrataktivierung aufgeklärt. Experimente zur Isotopenmarkierung ermöglichten den Vorschlag eines Reaktionsmechanismus.

Die Anpassung des entwickelten Protokolls zur Transferhydrogenolyse an anspruchsvollere Substrate, wie im dritten Teil dieser Arbeit präsentiert, führte zur Entwicklung einer Palladium-katalysierten Semipinacol-artigen Umlagerung von β-Aryloxy- oder β-Alkoxy-benzylischen Alkoholen (Schema 5.4). Als Produkte wurden 2-Arylethylacetate durch die Umlagerung einer Arylgruppe in den Substraten unter gleichzeitiger Spaltung einer Ether-C–O-Bindung erzeugt. Es wird angenommen, dass ein Palladium-Hydrid-Komplex an einem notwendigen Reduktionsschritt beteiligt ist.
Im Vergleich zu der Transferhydrogenolyse konnte die Katalysatorbeladung auf 0,75 mol% an Palladium gesenkt werden, in Gegenwart der zuvor verwendeten Liganden und des Säure-Cokatalysators. Für die gut verfügbare Ameisensäure als Reduktionsmittel sowie Acetanhydrid als günstiges Reagenz zur Aktivierung des Substrats wurden niedrige Mengen von jeweils 3,0 Äquivalenten als ausreichend ermittelt.

Obwohl die optimalen Reaktionsbedingungen bereits bestimmt und in der Umsetzung einiger Substrate angewendet wurden, werden weitere Untersuchungen erfolgen, um die Substratbreite zu erweitern und um ein besseres Verständnis des Reaktionsmechanismus sowie der im Katalysezyklus beteiligten Palladiumspezies zu erhalten.

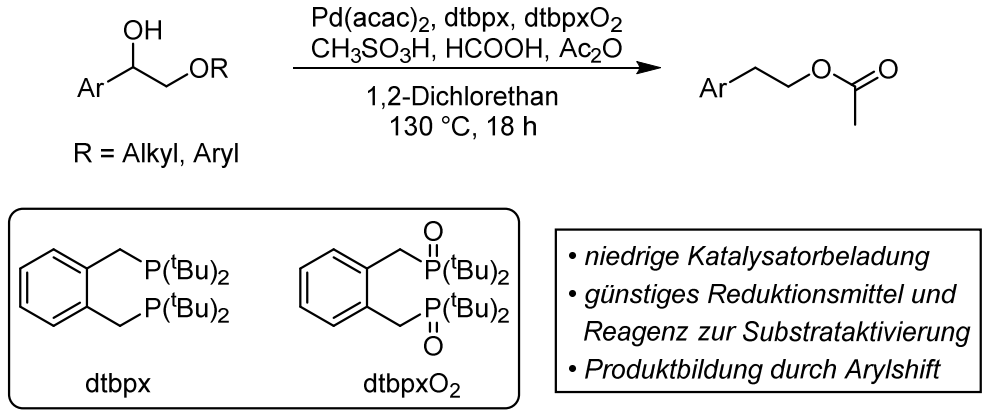

Schema 5.4 **Palladium-katalysierte Semipinacol-artige Umlagerung von β-Aryloxy- oder β-Alkoxy-benzylischen Alkoholen zu 2-Arylethylacetaten.**

6 Experimental part

6.1 General information

The ligand α,α'-bis-(di-*tert*-butylphosphino)-*ortho*-xylene (dtbpx, **L1**) was obtained commercially from ABCR or Strem chemicals, respectively, and stored in the glovebox (Glovebox Systemtechnik GS MEGA 4, H_2O < 0.1 ppm, O_2 < 0.3 ppm). All other reagents were purchased from ABCR, Acros, Alfa Aesar, Fluka, Merck, Sigma Aldrich or TCI and used without further purification unless otherwise noted. Solvents were distilled prior to use.

Reactions sensitive to oxygen or moisture were carried out in glassware which was flame-dried under vacuum prior to use. All catalytic reactions were performed under an inert atmosphere of nitrogen or argon in glass pressure tubes bearing a PTFE stopcock. The tubes were sealed with screw-caps containing a silicone rubber gasket coated with PTFE.

Degassing of solvents was performed by bubbling argon through the respective liquid for at least 30 min or by three cycles of freeze-pump-thaw treatment. If necessary, solvents were dried according to literature procedures.[1]

Column chromatography was carried out using silica gel (60 Å) as stationary phase, either manually using gravity flow conditions in a standard glass column setup under isocratic elution or on an Interchim Puriflash system under gradient elution (flash column chromatography). Gradients were developed depending on the solvent ratios of a binary eluent system found ideal for a R_f ~ 0.25 on TLC (ratio X/Y, Y is the strong solvent, X+Y = 100), Standard program: 0 – 1 CV: isocratic Y/4, 1 – 12 CV: gradient to Y*2, 12 – 15 CV: isocratic Y*2. Flow rates: 23 g SiO_2 50 µm - 15 mL/min, 37 g SiO2 50 µm - 26 mL/min. Ideal solvent ratios are given for every isolated product.

Thin layer chromatography (TLC) was performed with aluminium plates coated with silica gel 60 F254 (layer thickness: 0.2 mm) and analyzed under UV-light (254 nm) or stained with a potassium permanganate solution.

6.2 Analytical techniques

Nuclear magnetic resonance spectroscopy (NMR)

NMR spectra were recorded using Bruker Avance 400 (^{1}H: 400 MHz, ^{13}C:101 MHz, ^{31}P: 162 MHz) or Bruker Avance 300 (^{1}H: 300 MHz, ^{13}C: 75 MHz, ^{31}P: 121 MHz) machines. Measurements were performed in commercially available deuterated solvents without TMS at ambient temperature. For ^{2}H-NMR experiments, non-deuterated solvents were used under addition of one drop of a respective deuterated solvent as reference. ^{13}C-NMR experiments

were performed in proton-decoupled mode. Chemical shifts δ are reported in parts per million [ppm] relative to the solvent signals as internal standard (^{1}H: $CDCl_3$: δ = 7.26 ppm, C_6D_6: δ = 7.16 ppm; ^{13}C: $CDCl_3$: δ = 77.1 ppm, C_6D_6: δ = 128.1 ppm), exception: ^{31}P spectra were measured in decoupled mode and referenced externally to phosphoric acid (δ = 0 ppm). Coupling constants *J* are given in Hertz [Hz]. ^{1}H NMR splitting patterns are designated as follows: s = singlet; bs = broad singlet; d = doublet; t = triplet; q = quartet; m = multiplet.
Already published NMR spectra are not shown in this thesis may be retrieved from the supporting information of the peer-reviewed contribution:
B. Ciszek, I. Fleischer, *Chem. Eur. J.* **2018**, *24*, 12259–12263.

Gas chromatography (GC)

GC-FID analysis was carried out on a HP6890 GC system with injector 7683B and Agilent 7820A system by using dry hydrogen as a carrier gas. Program: 50-280M10: Heating from 50 °C to 280 °C within 10 min after injection. The internal standard method was used for quantitative GC-FID in order to determine yields. For calibration, samples with defined amounts of substrate and standard (*n*-pentadecane) were measured with GC-FID and the obtained data was used to plot the ratio of peak areas A(substrate)/A(standard) against the mass ratio m(substrate)/m(standard). The resulting slope, after linear regression, is equivalent to the response factor R, which can be used to quantify unknown samples by using equation 1. y-Intercepts are unconsidered.

$$\frac{m\,(substrate)}{m\,(standard)} \cdot R = \frac{A\,(substrate)}{A\,(standard)} \qquad (1)$$

GC-MS analysis was performed on an Agilent 7820A GC system with Quadrupole MS Agilent 7820A (EI), an Agilent 190915-433UI column (30 m x 250 µm x 0.25 µm) was used. Carrier gas: dry hydrogen. Program: 50-280M15: Heating from 50 °C to 280 °C within 15 minutes after injection. Constant column flow mode: 1.2 mL/min.

GC samples were prepared by treating the reaction mixture with a respective amount of QuadraSil Mercaptopropyl metal scavenger and addition of *n*-pentadecane as internal standard (in case of quantitative analysis). The reaction mixture was diluted with dichloromethane to approximately half the initial concentration, and filtered over celite and basic aluminium oxide "super I". The diluted filtrate was injected into the gas chromatograph.

High resolution mass spectrometry analyses were were carried out by the mass spectrometry department of the Institute of Organic Chemistry, University of Tübingen.

Qualitative headspace GC measurements of gas samples withdrawn from sealed reactors were performed on a Thermo Fisher Scientific Trace 1310 Auxiliary oven coupled with a 1310 gas chromatograph containing a 5 Å molecular sieve column (0.53 mm diameter, length: 30 m). The measurements were done at the Center for Applied Geoscience of the University of Tübingen with help from Dr. Thomas Wendel.

Melting point measurements

Melting points were determined using a Schorpp MPM-HV3 with automated or visual detection and are uncorrected (heating rate 1 °C/min).

6.3 ^{31}P-NMR analysis of the phosphine ligand L1

After variations in the reactivity of different batches of ligand **L1** were observed, ^{31}P-NMR analysis of the applied batches was performed.

Integration of the ^{31}P-signals at δ = 24.15 and 62.07 ppm resulted in a calculated molar ratio of **L1** to **L1-(O)$_2$** of 75:25 in batch A. For batch B, only the signal at 24.15 ppm was found showing no contamination of the batch with **L1-(O)$_2$**. The ^{31}P-shifts of phosphine and phosphine oxide are in accordance with the literature.[2,3] The determined ratio was used to calculate the necessary mass of partially oxidized **L1** for a total amount of 4 mol% of non-oxidized **L1** in the transfer hydrogenolysis reaction. The thereby introduced amount of **L1-(O)$_2$** equals 1.3 mol%.

Batch A

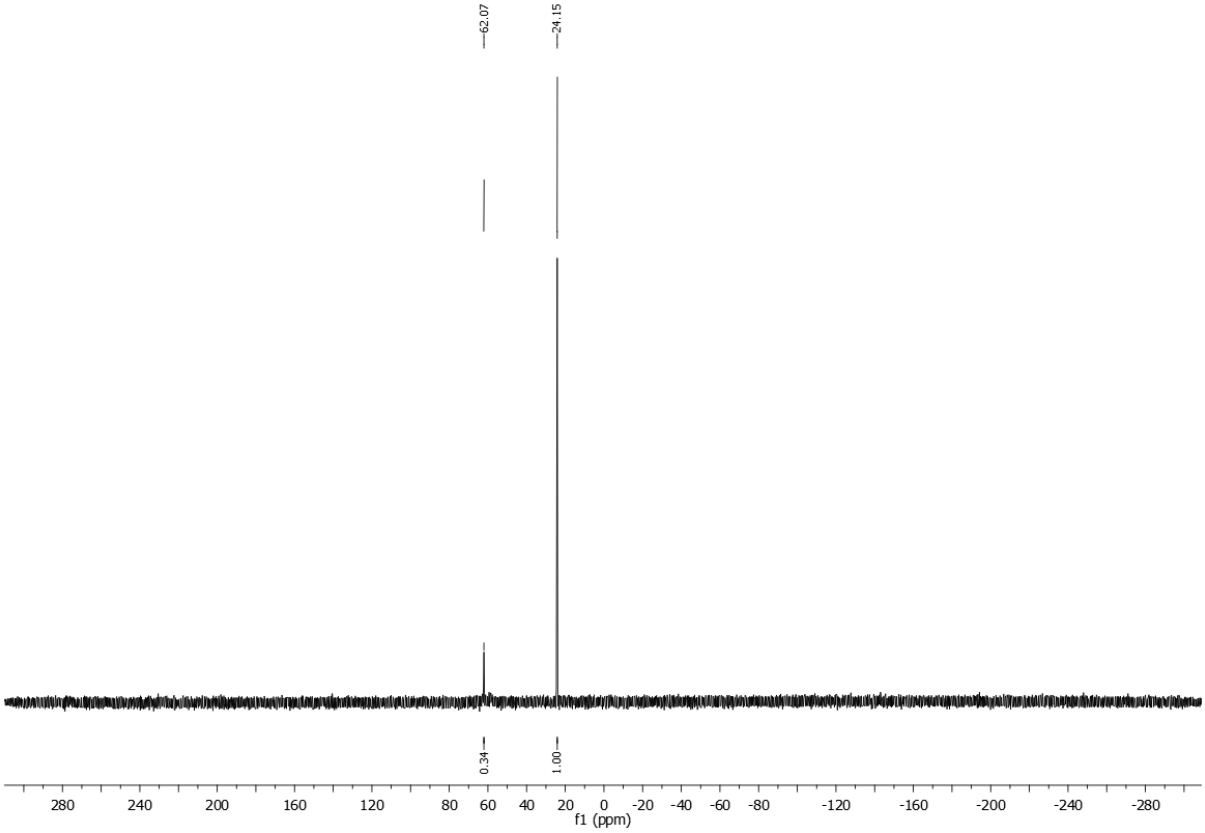

Batch B

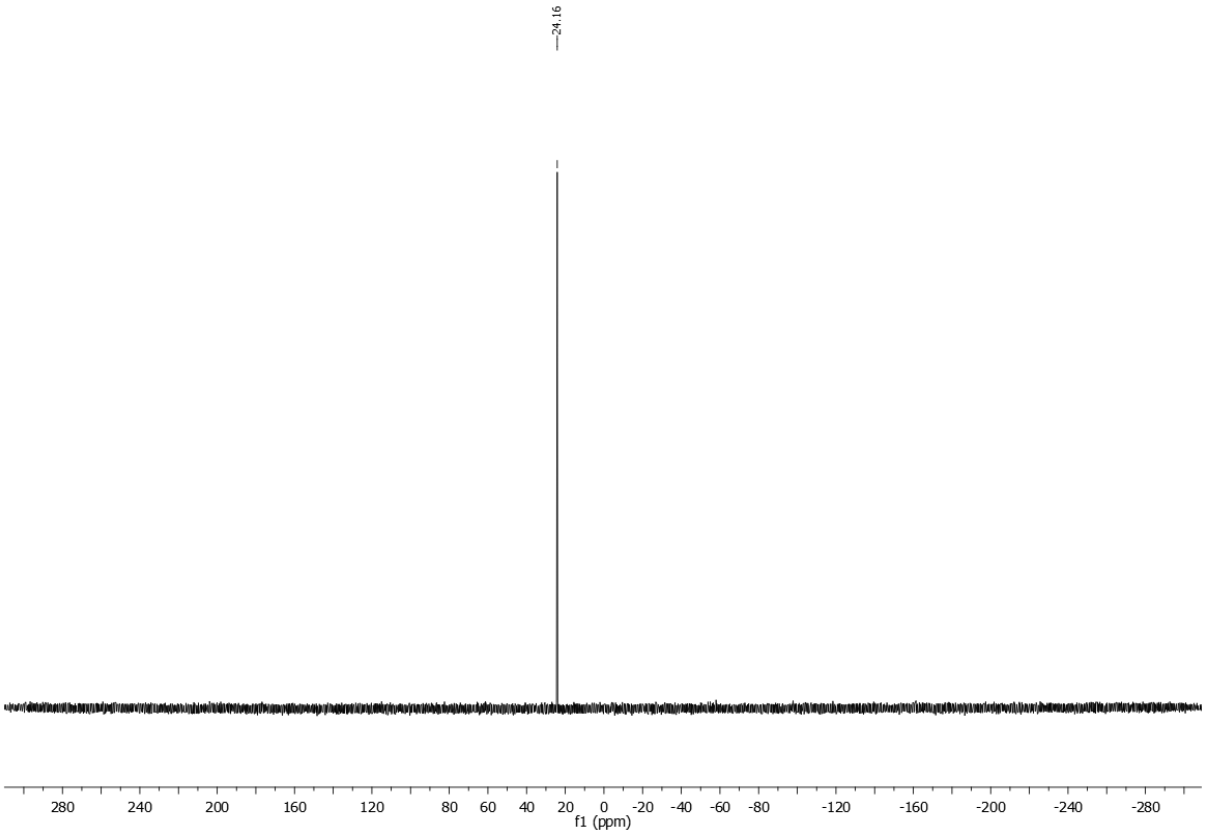

6.4 General experimental procedures for developed palladium-catalyzed reactions

GP A: Palladium-catalyzed transfer hydrogenolysis of 1-phenylethanol using methyl formate as reductant

A flame-dried screw-capped glass pressure tube with stirring bar was brought into the glovebox and loaded with partially oxidized dtbpx (53 µmol, 21 mg, 4.0 mol% dtbpx, dtbpx to dtbpxO_2 molar ratio 3:1). The pressure tube was taken out of the glovebox and Pd(acac)$_2$ (10 µmol, 3.0 mg, 1.0 mol%) was added under a slight counterstream of argon. The tube was sealed with a screw-cap and evacuated for at least 30 min. The tube was re-filled with argon and charged with 1-phenylethanol (1.0 mmol, 0.12 mL, 1.0 equiv.) and degassed 1,2-dichloroethane as solvent (1.0 mL). Under stirring methanesulfonic acid (0.16 mmol, 10 µL, 16 mol%) and methyl formate (2.0 mmol, 0.12 µL, 2.0 equiv.) were added *via* microsyringe. The pressure tube and screw-cap were purged with argon, then the tube was sealed tightly and stirred for 18 h at 100 °C in an aluminium heating block. After the reaction, the tube was left to cool to room temperature, opened, and the reaction was analyzed *via* GC-FID.

GP B: Palladium-catalyzed transfer hydrogenolysis of benzylic alcohols using formic acid as reductant

A flame-dried screw-capped glass pressure tube with stirring bar was brought into the glovebox and loaded with partially oxidized dtbpx (53 µmol, 21 mg, 4.0 mol% dtbpx, dtbpx to dtbpxO_2 molar ratio 3:1). The pressure tube was taken out of the glovebox and Pd(acac)$_2$ (10 µmol, 3.0 mg, 1.0 mol%) was added under a slight counterstream of argon. The tube was sealed with a screw-cap and evacuated for at least 30 min. The tube was re-filled with argon and charged with the alcohol substrate (1.0 mmol, 1.0 equiv.) and degassed 1,2-dichloroethane as solvent (3.0 mL). Under stirring methanesulfonic acid (0.16 mmol, 10 µL, 16 mol%) and formic acid (2.0 mmol, 75 µL, 2.0 equiv.) were added *via* microsyringe. The pressure tube and screw-cap were purged with argon, then the tube was sealed tightly and stirred for 18 h at 100 °C in an aluminium heating block. After the reaction, the tube was left to cool to room temperature, opened, and the reaction was either analyzed *via* GC-FID or the product was isolated.

GP C: Additive screening in the transfer hydrogenolysis of 1-phenylethanol with formic acid as reductant

The reaction was set up according to the general procedure B. Together with the substrate 1-phenylethanol, the respective additive (1.0 equiv.) was added to the reaction mixture.

GP D: Reaction monitoring and catalyst poisoning tests in the palladium-catalyzed transfer hydrogenolysis of 1-phenylethanol with formic acid as reductant

The reaction was set up according to general procedure B in a 3 mmol scale of 1-phenylethanol and *n*-pentadecane (300 µL) as internal standard was added. After all reagents except for formic acid were loaded into the pressure tube, the screw cap was exchanged for a cap with accessible septum, which was equipped with an on/off stainless steel valve. The cap was purged with argon and screwed on, the valve was purged with argon and then the reactor was sealed tightly. After the reaction mixture was heated to 100 °C in the heating block, formic acid was added *via* microsyringe to determine the starting point of the reaction. Samples from the reaction mixture were taken through the valve at defined reaction times and analyzed *via* GC-FID. For the poisoning experiments, elementary mercury or a solution of dct or heptanethiol were added *via* syringe through the septum to the reaction mixture after a reaction time of 80 min.

GP E: Palladium-catalyzed reductive rearrangement of β-aryloxy or β-alkoxy benzylic alcohols

A flame-dried screw-capped glass pressure tube with stirring bar was brought into the glovebox and loaded with partially oxidized dtbpx (15 µmol, 5.8 mg, 3.0 mol% dtbpx, dtbpx to dtbpxO_2 molar ratio 3:1). The pressure tube was taken out of the glovebox and Pd(acac)$_2$ (3.8 µmol, 1.1 mg, 0.75 mol%) was added under a slight counterstream of argon. The tube was sealed with a screw-cap and evacuated for at least 30 min. The tube was re-filled with argon and charged with the β-aryloxy or β-alkoxy alcohol substrate (0.5 mmol, 1.0 equiv.) and degassed 1,2-dichloroethane as solvent (1.0 mL). Under stirring methanesulfonic acid (0.10 mmol, 6.4 µL, 20 mol%), formic acid (1.5 mmol, 56 µL, 3.0 equiv.) and acetic anhydride (1.5 mmol, 0.14 mL, 3.0 equiv.) were added *via* microsyringe. The pressure tube and screw-cap were purged with argon, then the tube was sealed tightly and stirred for 18 h at 130 °C in an aluminium heating block. After the reaction, the tube was left to cool to room temperature, opened, and the reaction was either analyzed *via* GC-FID or the product was isolated.

6.5 Procedures for substrate syntheses

6.5.1 Synthesized substrates for the palladium-catalyzed transfer hydrogenolysis of benzylic alcohols using formic acid as reductant

General procedure for the synthesis of benzylic alcohols via ketone reduction

Following a literature procedure,[4] in a round bottom flask (100 mL) the respective benzylic ketone (10 mmol, 1.0 equiv.) was dissolved in methanol (40 mL) and cooled to 0 °C in an ice bath. $NaBH_4$ (20 mmol, 0.76 g, 2.0 equiv.) was added in one portion and the reaction mixture was allowed to warm to room temperature while stirring. After TLC analysis showed completion, the reaction was quenched with saturated aqueous solution of NH_4Cl (10 mL). *p*H was adjusted to ~ 3 and methanol was removed on the rotary evaporator. The mixture was extracted with dichloromethane (3 × 15 mL), the organic phases were collected, dried over Na_2SO_4 and filtered. After evaporation of the solvent the desired alcohols were obtained in pure form.

1-(4-methylphenyl)ethanol (**34a**)

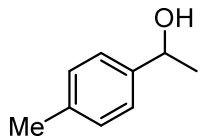

34a

The compound **34a** was obtained from the respective benzylic ketone using the general procedure as a colorless oil in 86% yield.

$C_9H_{12}O$ (136.19 g/mol)

***R*f:** 0.19 (cyclohexane/ethyl acetate 80:20).

m.p.: ambient temperature.

^{1}H-NMR (400 MHz, $CDCl_3$): δ_H/ppm= 7.30 – 7.25 (m, 2H, C<u>H</u>$_{arom}$), 7.19 – 7.14 (m, 2H, C<u>H</u>$_{arom}$), 4.87 (q, *J* = 6.4 Hz, 1H, C<u>H</u>OH), 2.35 (s, 3H, C<u>H</u>$_3$), 1.77 (bs, 1H, O<u>H</u>), 1.49 (d, *J* = 6.5 Hz, 3H, CH(OH)C<u>H</u>$_3$).

^{13}C-NMR (75 MHz, CDCl3): δ_C/ppm= 142.9, 137.2, 129.2, 125.4, 70.3, 25.1, 21.1.

GC-MS (EI): m/z = 136.1 (31, [$M^{+\bullet}$]), 121.1 (100, [$M^{+\bullet}$]-[$CH_3^{\bullet}$]), 103.1 (6, [$M^{+\bullet}$]-[$CH_3^{\bullet}$]-[$OH^{\bullet}$]).

The found analytical data were in accordance with the available literature data.[5]

1-(4-fluorophenyl)ethanol (**34c**)

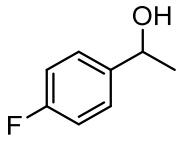

34c

The compound **34c** was obtained from the respective benzylic ketone using the general procedure as a colorless oil in 32% yield.

C_8H_9FO (140.16 g/mol)

***R*$_f$:** 0.20 (cyclohexane/ethyl acetate 80:20).

m.p.: ambient temperature.

^{1}H-NMR (400 MHz, $CDCl_3$): δ_H/ppm= 7.40 – 7.29 (m, 2H, C$\underline{H}_{arom}$), 7.08 – 6.98 (m, 2H, C$\underline{H}_{arom}$), 4.90 (q, *J* = 6.4 Hz, 1H, C$\underline{H}$OH), 1.72 (bs, 1H, O$\underline{H}$), 1.48 (d, *J* = 6.4 Hz, 3H, C$\underline{H}_3$).

^{13}C-NMR (101 MHz, $CDCl_3$): δ_C/ppm = 162.1 (d, *J* = 244.9 Hz) , 141.6 (d, *J* = 3.1 Hz), 127.1 (d, *J* = 8.0 Hz), 115.2 (d, *J* = 21.3 Hz), 69.7, 25.2.

^{19}F-NMR (282 MHz, $CDCl_3$): δ_F/ppm= -115.8.

GC-MS (EI): m/z = 140.1 (6, $[M^{+\bullet}]$), 125.0 (27, $[M^{+\bullet}]$-$[CH_3^{\bullet}]$), 123.1 (13, $[M^{+\bullet}]$-$[OH^{\bullet}]$), 122.0 (100, $[M^{+\bullet}]$-$[F^{\bullet}]$), 95.0 (8, $[M^{+\bullet}]$-$[CH_3CH_2OH^{\bullet}]$.

The found analytical data were in accordance with the available literature data.[6]

1-(4-chlorophenyl)ethanol (**34d**)

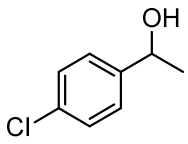

34d

The compound **34d** was obtained from the respective benzylic ketone using the general procedure as a yellowish oil in 85% yield.

C_8H_9ClO (156.61 g/mol)

***R*$_f$:** 0.21 (cyclohexane/ethyl acetate 80:20).

m.p.: ambient temperature.

^{1}H-NMR (400 MHz, $CDCl_3$): δ_H/ppm= 7.35 – 7.27 (m, 4H, C<u>H</u>$_{arom}$), 4.88 (q, *J* = 6.5 Hz, 1H, C<u>H</u>OH), 1.78 (bs, 1H, O<u>H</u>), 1.47 (d, *J* = 6.5 Hz, 3H, C<u>H</u>$_3$).

^{13}C-NMR (75 MHz, $CDCl_3$): δ_C/ppm= 144.3, 133.1, 128.6, 126.8, 69.8, 25.3.

GC-MS (EI): m/z = 156.0 [21, $M^{+\bullet}$], 141.0 (100, $[M^{+\bullet}]$-$[CH_3^{\bullet}]$), 121.1 (15, $[M^{+\bullet}]$-$[Cl^{\bullet}]$), 113.0 (48, $[M^{+\bullet}]$-$[CHOHCH_3^{\bullet}]$), 103.0 (21, $[M^{+\bullet}]$-$[OH^{\bullet}]$-$[Cl^{\bullet}]$).

The found analytical data were in accordance with the available literature data.[7]

1-(4-iodophenyl)ethanol (**34f**)

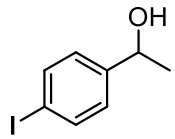

34f

The compound **34f** was obtained from the respective benzylic ketone using the general procedure as a white solid in 91% yield.

C_8H_9IO (246.06 g/mol)

***R*$_f$:** 0.19 (cyclohexane/ethyl acetate 80:20).

m.p.: 49.2 °C

^{1}H-NMR (400 MHz, $CDCl_3$): δ_H/ppm= 7.71 – 7.65 (m, 2H, C$\underline{H}_{arom}$), 7.16 – 7.10 (m, 2H, C$\underline{H}_{arom}$), 4.86 (q, *J* = 6.5 Hz, 1H, C$\underline{H}$OH), 1.58 (bs, 1H, O$\underline{H}$), 1.47 (d, *J* = 6.5 Hz, 3H, C$\underline{H}_3$).

^{13}C-NMR (101 MHz, $CDCl_3$): δ_C/ppm= 145.5, 137.6, 127.4, 92.7, 69.9, 25.3.

GC-MS (EI): m/z = 248.0 (13, $[M^{+\bullet}]$), 229.9 (76, $[M^{+\bullet}]$-$[H_2O]$), 216.9 (15, $[M^{+\bullet}]$-$[OH^{\bullet}]$-$[CH_3^{\bullet}]$), 203.9 (4, $[M^{+\bullet}]$-$[CH_2(OH)CH_3^{\bullet}]$), 121.1 (6, $[M^{+\bullet}]$-$[I^{\bullet}]$), 104.1 (100, $[M^{+\bullet}]$-$[OH^{\bullet}]$-$[I^{\bullet}]$).

The found analytical data were in accordance with the available literature data.[8]

1-(4-nitrophenyl)ethanol (**34i**)

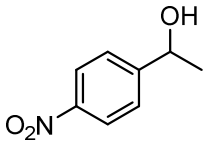

34i

The compound **34i** was obtained from the respective benzylic ketone using the general procedure as a yellow oil in 90% yield.

$C_8H_9NO_3$ (167.16 g/mol)

***R*$_f$:** 0.10 (cyclohexane/ethyl acetate 80:20).

m.p.: ambient temperature.

^{1}H-NMR (400 MHz, $CDCl_3$): δ_H/ppm= 8.30 – 8.01 (m, 2H, C$\underline{H}_{arom}$), 7.63 – 7.39 (m, 2H, C$\underline{H}_{arom}$), 5.02 (q, *J* = 6.5 Hz, 1H, C$\underline{H}$OH), 1.85 (bs, 1H, O$\underline{H}$), 1.52 (d, *J* = 6.5 Hz, 3H, C$\underline{H}_3$).

^{13}C-NMR (101 MHz, $CDCl_3$): δ_C/ppm= 153.1, 126.1, 123.8, 69.5, 25.6.

GC-MS (EI): m/z = 167.0 (2, [$M^{+\bullet}$]), 152.0 (100, [$M^{+\bullet}$]-[$CH_3^{\bullet}$]), 121.1 (60, [$M^{+\bullet}$]-[$NO_2^{\bullet}$]), 107.0 (63, [$M^{+\bullet}$]-[$NO_2^{\bullet}$]-[$CH_3^{\bullet}$]).

The found analytical data were in accordance with the available literature data.[8]

1-(4-cyanaphenyl)ethanol (**34k**)

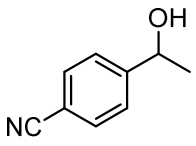

34k

The compound **34k** was obtained from the respective benzylic ketone using the general procedure as a colorless oil in 76% yield.

C_9H_9NO (147.18 g/mol)

***R*$_f$:** 0.08 (cyclohexane/ethyl acetate 80:20).

m.p.: ambient temperature.

^{1}H-NMR (400 MHz, $CDCl_3$): δ_H/ppm= 7.68 – 7.59 (m, 2H, C$\underline{H}_{arom}$), 7.54 – 7.44 (m, 2H, C$\underline{H}_{arom}$), 4.96 (q, *J* = 6.5 Hz, 1H, C$\underline{H}$OH), 1.93 (bs, 1H, O$\underline{H}$), 1.49 (d, *J* = 6.5 Hz, 3H, C$\underline{H}_3$).

^{13}C-NMR (101 MHz, $CDCl_3$): δ_C/ppm= 151.1, 132.4, 126.1, 118.9, 111.1, 69.7, 25.4.

GC-MS (EI): m/z = 147.1 (6, $[M^{+\bullet}]$), 132.1 (80, $[M^{+\bullet}]$-$[CH_3^{\bullet}]$), 104.1 (100, $[M^{+\bullet}]$-$[CN^{\bullet}]$-$[OH^{\bullet}]$).

The found analytical data were in accordance with the available literature data.[9]

1-(4-(methoxycarbonyl)phenyl)ethanol (**34g**)

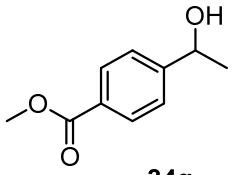

34g

The compound **34g** was obtained from the respective benzylic ketone using the general procedure as a colorless oil in 73% yield.

$C_{10}H_{12}O_3$ (180.20 g/mol)

***R*$_f$:** 0.28 (cyclohexane/ethyl acetate 80:20).

m.p.: ambient temperature.

^{1}H-NMR (400 MHz, $CDCl_3$): δ_H/ppm= 8.04 – 7.98 (m, 2H, C<u>H</u>$_{arom}$), 7.46 – 7.41 (m, 2H, C<u>H</u>$_{arom}$), 4.96 (q, *J* = 6.5 Hz, 1H, C<u>H</u>OH), 3.91 (s, 3H, C(O)OC<u>H</u>$_3$), 1.90 (bs, 1H, O<u>H</u>), 1.50 (d, *J* = 6.5 Hz, 3H, CH(OH)C<u>H</u>$_3$).

^{13}C-NMR (75 MHz, $CDCl_3$): δ_C/ppm= 167.0, 150.9, 129.9, 129.2, 125.3, 70.0, 52.1, 25.3.

GC-MS (EI): m/z = 180.1 (14, [$M^{+\bullet}$]), 165.1 (94, [$M^{+\bullet}$]-[$CH_3^\bullet$]), 149.1 (27, [$M^{+\bullet}$]-[$CH_3O^\bullet$]), 134.1 (15, [$M^{+\bullet}$]-[$CH_3O^\bullet$]-[$CH_3^\bullet$]), 121.1 (31, [$M^{+\bullet}$]-[$CH_3OC(O)^\bullet$]), 105.0 (42, [$M^{+\bullet}$]-[$CH_3OC(O)^\bullet$]-[$OH^\bullet$]).

The found analytical data were in accordance with the available literature data.[10]

1-(4-biphenyl)ethanol (**34l**)

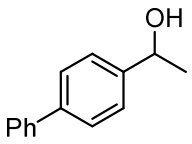

34l

The compound **34l** was obtained from the respective benzylic ketone using the general procedure as a white solid in 88% yield.

$C_{14}H_{14}O$ (198.27 g/mol)

***R*$_f$:** 0.34 (cyclohexane/ethyl acetate 80:20).

m.p.: 96.7 °C.

^{1}H-NMR (400 MHz, $CDCl_3$): δ_H/ppm= 7.63 – 7.55 (m, 4H, C<u>H</u>$_{arom}$), 7.49 – 7.41 (m, 4H, C<u>H</u>$_{arom}$), 7.39 – 7.31 (m, 1H, C<u>H</u>$_{arom}$), 4.97 (q, *J* = 6.5 Hz, 1H, C<u>H</u>OH), 1.70 (bs, 1H, O<u>H</u>), 1.55 (d, *J* = 6.5 Hz, 3H, C<u>H</u>$_3$).

^{13}C-NMR (75 MHz, $CDCl_3$): δ_C/ppm= 144.8, 140.9, 140.5, 128.8, 127.3, 127.1, 125.9, 70.2, 25.2.

GC-MS (EI): m/z = 198.1 (1, [$M^{+\bullet}$]), 181.1 (55, [$M^{+\bullet}$]-[$OH^{\bullet}$]), 166.1 (100, [$M^{+\bullet}$]-[$OH^{\bullet}$]-[$CH_3^{\bullet}$]), 153.1 (17, [$M^{+\bullet}$]-[$CH(OH)CH_3^{\bullet}$]).

The found analytical data were in accordance with the available literature data.[11]

1-(2-methoxyphenyl)ethanol (**34p**)

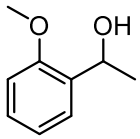

34p

The compound **34p** was obtained from the respective benzylic ketone using the general procedure as a colorless oil in 46% yield.

$C_9H_{12}O_2$ (152.19 g/mol)

***R*$_f$:** 0.21 (cyclohexane/ethyl acetate 80:20).

m.p.: ambient temperature.

^{1}H-NMR (400 MHz, $CDCl_3$): δ_H/ppm= 7.34 (dd, *J* = 7.5, 1.6 Hz, 1H, C$\underline{H}_{arom}$), 7.25 (td, *J* = 7.9, 1.7 Hz, 1H, C$\underline{H}_{arom}$), 6.97 (td, *J* = 7.5, 0.8 Hz, 1H, C$\underline{H}_{arom}$), 6.89 (d, *J* = 8.2 Hz, 1H, C$\underline{H}_{arom}$), 5.10 (q, *J* = 6.5 Hz, 1H, C$\underline{H}$OH), 3.87 (s, 3H, COC$\underline{H}_3$), 1.51 (d, *J* = 6.5 Hz, 3H, CH(OH)C$\underline{H}_3$).

^{13}C-NMR (75 MHz, $CDCl_3$): δ_C/ppm= 156.6, 133.5, 128.3, 126.1, 120.8, 110.5, 66.6, 55.3, 22.9.

GC-MS (EI): m/z = 152.1 (22, [$M^{+\bullet}$]), 137.0 (100, [$M^{+\bullet}$]-[$CH_3^{\bullet}$]), 119.0 (70, [$M^{+\bullet}$]-[$CH_3^{\bullet}$]-[$OH^{\bullet}$]), 107.0 (52, [$M^{+\bullet}$]-[$CH_3^{\bullet}$]-[$CH_3O^{\bullet}$]).

The found analytical data were in accordance with the available literature data.[12]

1-(2-methylphenyl)ethanol (**34o**)

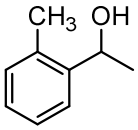

34o

The compound **34o** was obtained from the respective benzylic ketone using the general procedure as a colorless oil in 51% yield.

$C_9H_{12}O_2$ (136.19 g/mol)

***R*$_f$:** 0.27 (cyclohexane/ethyl acetate 80:20).

m.p.: ambient temperature.

^{1}H-NMR (400 MHz, $CDCl_3$): δ_H/ppm= 7.52 (d, *J* = 7.4 Hz, 1H, C$\underline{H}_{arom}$), 7.28 – 7.11 (m, 3H, C$\underline{H}_{arom}$), 5.14 (q, *J* = 6.4 Hz, 1H, C$\underline{H}$OH), 2.35 (s, 3H, $C_{arom}C\underline{H}_3$), 1.69 (bs, 1H, O$\underline{H}$), 1.47 (d, *J* = 6.4 Hz, 3H, CH(OH)C$\underline{H}_3$).

^{13}C-NMR (75 MHz, $CDCl_3$): δ_C/ppm= 143.8, 134.3, 130.4, 127.2, 126.4, 124.5, 66.9, 23.9, 18.9.

GC-MS (EI): m/z = 136.1 (2, [$M^{+\bullet}$]), 119.1 (100, [$M^{+\bullet}$]-[$OH^{\bullet}$]), 104.1 ([$M^{+\bullet}$]-[$OH^{\bullet}$]-[$CH_3^{\bullet}$]).

The found analytical data were in accordance with the available literature data.[12]

1-(3-methoxyphenyl)ethanol (**34s**)

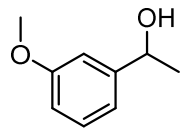

34s

The compound **34s** was obtained from the respective benzylic ketone using the general procedure as a yellowish oil in 91% yield.

$C_9H_{12}O_2$ (152.19 g/mol)

***R*$_f$:** 0.23 (cyclohexane/ethyl acetate 80:20).

m.p.: ambient temperature.

^{1}H-NMR (400 MHz, $CDCl_3$): δ_H/ppm= 7.27 (t, *J* = 8.1 Hz, 1H, C<u>H</u>$_{arom}$), 6.95 (m, 2H, C<u>H</u>$_{arom}$), 6.82 (m, 1H, C<u>H</u>$_{arom}$), 4.88 (q, *J* = 6.4 Hz, 1H, C<u>H</u>OH), 3.82 (s, 3H, COC<u>H</u>$_3$), 1.82 (bs, 1H, O<u>H</u>), 1.49 (d, *J* = 6.5 Hz, 3H, CH(OH)C<u>H</u>$_3$).

^{13}C-NMR (75 MHz, $CDCl_3$): δ_C/ppm= 159.8, 147.6, 129.6, 117.7, 112.9, 110.9, 70.4, 55.3, 25.2.

GC-MS (EI): m/z = 152.1 (7, [$M^{+\bullet}$]), 134.1 (100, [$M^{+\bullet}$]-[H_2O]), 121.1 (38, [$M^{+\bullet}$]-[$CH_3O^{\bullet}$]), 104.1 (22, [$M^{+\bullet}$]-[$OH^{\bullet}$]-[$CH_3O^{\bullet}$]).

The found analytical data were in accordance with the available literature data.[13]

1-(2-naphthyl)ethanol (**34u**)

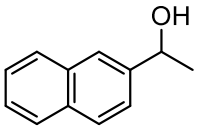

34u

The compound **34u** was obtained from the respective benzylic ketone using the general procedure as a white solid in 88% yield.

$C_{12}H_{12}O$ (172.23 g/mol)

***R*$_f$:** 0.20 (cyclohexane/ethyl acetate 80:20).

m.p.: 74.4 °C

^{1}H-NMR (400 MHz, $CDCl_3$): δ_H/ppm= 7.91 – 7.75 (m, 4H, C$\underline{H}_{arom}$), 7.57 – 7.37 (m, 3H, C$\underline{H}_{arom}$), 5.08 (q, *J* = 6.5 Hz, 1H, C$\underline{H}$OH), 1.73 (bs, 1H, O$\underline{H}$), 1.59 (d, *J* = 6.5 Hz, 3H, C$\underline{H}_3$).

^{13}C-NMR (75 MHz, $CDCl_3$): δ_C/ppm= 143.2, 132.9, 128.4, 127.9, 127.7, 126.2, 125.8, 123.8, 70.6, 25.2.

GC-MS (EI): m/z = 172.1 (2, $[M^{+\bullet}]$), 154.1 (71, $[M^{+\bullet}]$-$[H_2O]$), 140.1 (100, $[M^{+\bullet}]$-$[OH^{\bullet}]$-$[CH_3^{\bullet}]$), 127.1 (17, $[M^{+\bullet}]$-$[CH(OH)CH_3^{\bullet}]$.

The found analytical data were in accordance with the available literature data.[13]

1,2,3,4-tetrahydronaphthalen-1-ol (**34v**)

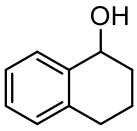

34v

The compound **34v** was obtained from the respective benzylic ketone using the general procedure as a brown oil in 83% yield.

$C_{10}H_{12}O$ (148.21 g/mol)

***R*$_f$:** 0.12 (cyclohexane/ethyl acetate 90:10).

m.p.: ambient temperature.

^{1}H-NMR (400 MHz, $CDCl_3$): δ_H/ppm= 7.48 – 7.39 (m, 1H, C$\underline{H}_{arom}$), 7.24 – 7.17 (m, 2H, C$\underline{H}_{arom}$), 7.15 – 7.07 (m, 1H, C$\underline{H}_{arom}$), 4.79 (m, 1H, C$\underline{H}$OH), 2.90 – 2.66 (m, 2H, C$\underline{H}_2$), 2.08 – 1.87 (m, 3H, C$\underline{H}_2$), 1.79 (m, 1H, C$\underline{H}_2$), 1.65 (bs, 1H, O$\underline{H}$).

^{13}C-NMR (75 MHz, $CDCl_3$): Sδ_C/ppm= 138.8, 137.2, 129.1, 128.7, 127.6, 126.2, 68.2, 32.3, 29.3, 18.8.

GC-MS (EI): m/z = 148.1 (20, $[M^{+\bullet}]$), 130.1 (100, $[M^{+\bullet}]$-$[H_2O]$), 119.1 (55, $[M^{+\bullet}]$-$[CHOH^{\bullet}]$), 105.0 (21, $[M^{+\bullet}]$-$[CH_2CHOH^{\bullet}]$).

The found analytical data were in accordance with the available literature data.[12]

2,2-dimethyl-1-phenylpropan-1-ol (**34δ**)

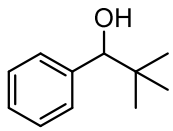

34δ

The compound **34δ** was obtained from the respective benzylic ketone using the general procedure as a colorless oil in 41% yield.

$C_{11}H_{16}O$ (164.25 g/mol)

***R*$_f$:** 0.16 (cyclohexane/ethyl acetate 95:5).

m.p.: ambient temperature.

^{1}H-NMR (400 MHz, $CDCl_3$): δ_H/ppm= 7.34 – 7.26 (m, 5H, C<u>H</u>$_{arom}$), 4.40 (s, 1H, C<u>H</u>OH), 1.80 (bs, 1H, O<u>H</u>), 0.93 (s, 9H, C(C<u>H</u>$_3$)$_3$).

^{13}C-NMR (75 MHz, $CDCl_3$): δ_C/ppm= 142.2, 127.6, 127.6, 127.3, 82.4, 35.6, 25.9.

GC-MS (EI): m/z = 164.1 (3, [$M^{+\bullet}$]), 146.1 (3, [$M^{+\bullet}$]-[H_2O]), 131.1 (9, [$M^{+\bullet}$]-[$OH^{\bullet}$]-[$CH_3^{\bullet}$]), 107.1 (100, [$M^{+\bullet}$]-[$C_4H_9^{\bullet}$]).

The found analytical data were in accordance with the available literature data.[10]

1-(3-pyridyl)ethanol (**34θ**)

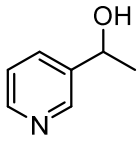

34θ

The compound **34θ** was obtained from the respective ketone using the general procedure as a colorless oil in 88% yield.

C_7H_9NO (123.16 g/mol)

***R*$_f$:** 0.18 (cyclohexane/ethyl acetate 80:20).

m.p.: ambient temperature.

^{1}H-NMR (400 MHz, $CDCl_3$): δ_H/ppm= 8.55 (d, *J* = 1.5 Hz, 1H, C<u>H</u>$_{arom}$), 8.51 – 8.44 (m, 1H, C<u>H</u>$_{arom}$), 7.74 (dt, *J* = 7.9, 1.8 Hz, 1H, C<u>H</u>$_{arom}$), 7.31 – 7.24 (m, 1H, C<u>H</u>$_{arom}$), 4.95 (q, *J* = 6.5 Hz, 1H, C<u>H</u>OH), 2.59 (bs, 1H, O<u>H</u>), 1.52 (d, *J* = 6.5 Hz, 3H, C<u>H</u>$_3$).

^{13}C-NMR (75 MHz, $CDCl_3$): δ_C/ppm= 148.6, 147.3, 141.2, 133.3, 123.6, 68.0, 25.3.

GC-MS (EI): m/z = 123.1 (29, [$M^{+\bullet}$]), 108.0 (100, [$M^{+\bullet}$]-[$CH_3^{\bullet}$]).

The found analytical data were in accordance with the available literature data.[14]

1-(2-pyridyl)ethanol (**34η**)

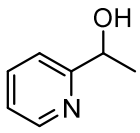

34η

The compound **34η** was obtained from the respective ketone using the general procedure as a colorless oil in 20% yield.

C_7H_9NO (123.16 g/mol)

***R*$_f$:** 0.19 (cyclohexane/ethyl acetate 80:20).

m.p.: ambient temperature.

^{1}H-NMR (400 MHz, $CDCl_3$): δ_H/ppm= 8.54 (d, *J* = 4.8 Hz, 1H, C$\underline{H}_{arom}$), 7.69 (td, *J* = 7.7, 1.7 Hz, 1H, C$\underline{H}_{arom}$), 7.28 (d, *J* = 8.7 Hz, 1H, C$\underline{H}_{arom}$), 7.24 – 7.16 (m, 1H, C$\underline{H}_{arom}$), 4.89 (q, *J* = 6.5 Hz, 1H, C$\underline{H}$OH), 1.51 (d, *J* = 6.5 Hz, 3H, C$\underline{H}_3$).

^{13}C-NMR (75 MHz, $CDCl_3$): δ_C/ppm= 163.0, 148.1, 136.8, 122.3, 119.8, 68.8, 24.3.

GC-MS (EI): m/z =123.1 (9, [$M^{+\bullet}$]), 106.1 (100, [$M^{+\bullet}$]-[$OH^{\bullet}$]).

The found analytical data were in accordance with the available literature data.[14]

1-(2-naphthyl)ethanol-d_3 (**56-d_3**)

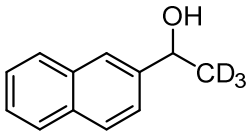

56-d_3

The compound **56-d_3** was obtained from the respective ketone using the general procedure as a white solid in 97% yield.

$C_{12}H_9D_3O$ (175.25 g/mol)

***R*$_f$:** 0.25 (hexane/ethyl acetate 90:10).

m.p.: 71.4 °C.

^{1}H-NMR (400 MHz, $CDCl_3$): δ_H/ppm= 7.88 – 7.78 (m, 4H, C<u>H</u>$_{arom}$), 7.56 – 7.40 (m, 3H, C<u>H</u>$_{arom}$), 5.07 (s, 1H, C<u>H</u>OH), 1.73 (bs, 1H, O<u>H</u>).

^{13}C-NMR (75 MHz, $CDCl_3$): δ_C/ppm= 132.9, 128.4, 127.9, 127.7, 126.2, 125.8, 123.8, 70.4.

GC-MS (EI): m/z = not determined due to high boiling point. 175.1 (4, [$M^{+\bullet}$]), 156.0 (58, [$M^{+\bullet}$]-[HDO]), 140.1 (100, [$M^{+\bullet}$]-[$OH^{\bullet}$]-[$CD_3^{\bullet}$]).

So far, no analytical data was available for this compound in the literature.

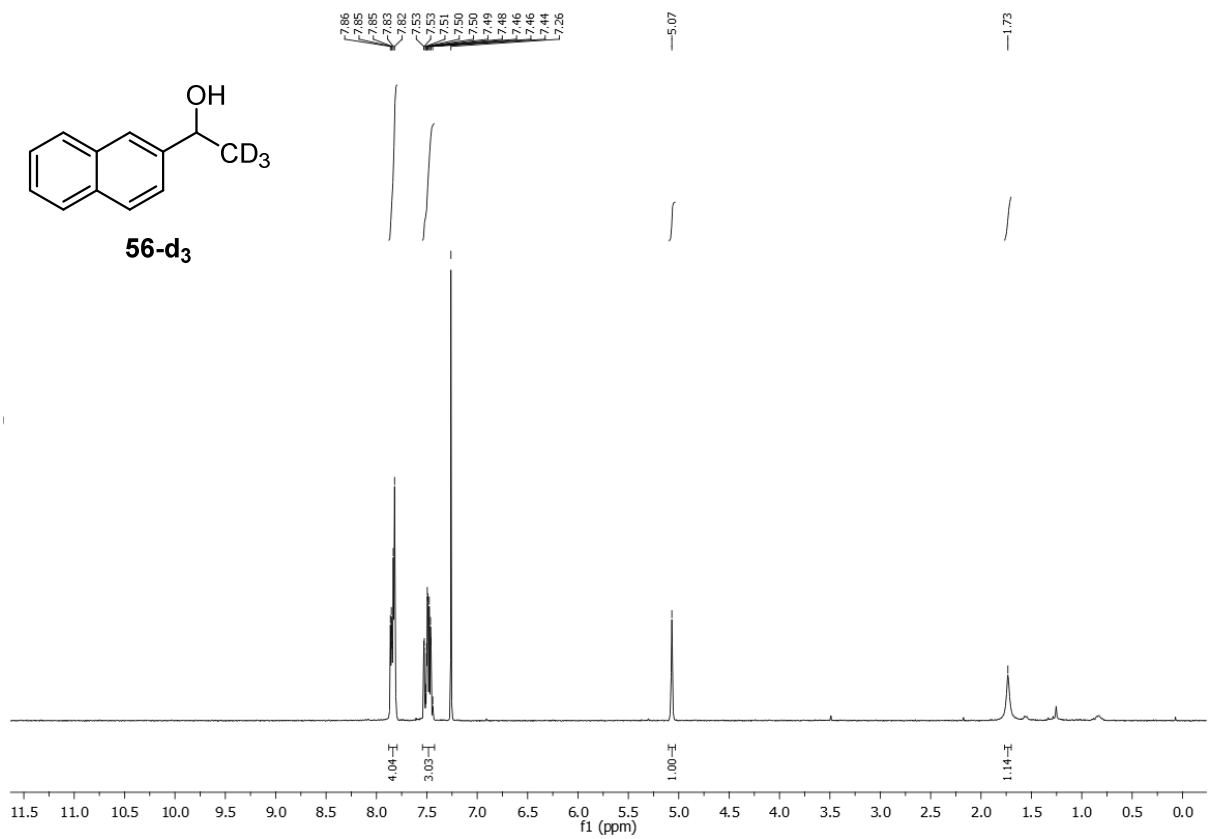
OH
CD3
56-d3
7.86
7.85
7.85
7.83
7.82
7.53
7.53
7.51
7.50
7.50
7.49
7.48
7.46
7.46
7.44
7.26
5.07
1.73
4.04
3.03
1.00
1.14
f1 (ppm)

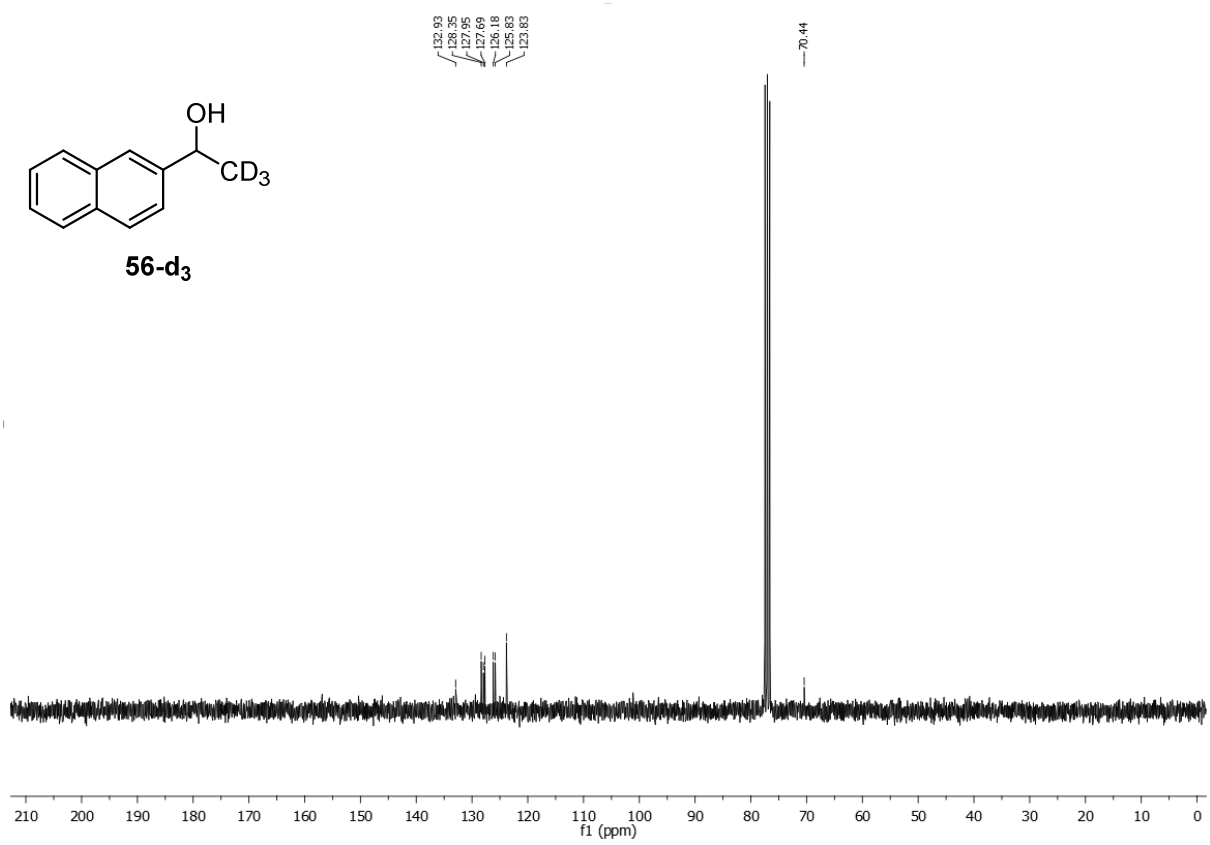
OH
CD3
56-d3
132.93
128.35
127.95
127.69
126.18
125.83
123.83
70.44
f1 (ppm)

Procedure for the synthesis of 4-hydroxy-4-phenyl-butan-2-one (34w)

According to a modified literature procedure,[15] to an ice-cold solution of benzaldehyde (10 mmol, 1.0 mL, 1 equiv.) in acetone (14 mL) and water (14 mL) was added pyrrolidine (10 mmol, 0.82 mL, 1 equiv.). The mixture was stirred at 0 °C for 10 min and extracted with dichloromethane (3 × 15 mL). The organic phase was washed with diluted hydrochloric acid and dried over $MgSO_4$. Evaporation of the solvent yielded the crude product which was purified *via* column chromatography (petroleum ether/ethyl acetate 60:40) to give pure **34w** as a colorless oil (0.77 g, 47% yield).

4-hydroxy-4-phenyl-butan-2-one (**34w**)

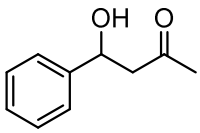

34w

$C_{10}H_{12}O_2$ (164.20 g/mol)

***R*$_f$:** 0.51 (petroleum ether/ethyl acetate 60:40).

m.p.: ambient temperature.

^{1}H-NMR (400 MHz, $CDCl_3$): δ_H/ppm= 7.37 – 7.26 (m, 5H, C$\underline{H}_{arom}$), 5.16 (dd, *J* = 9.0, 3.4 Hz, 1H, C$\underline{H}$OH), 2.86 (qd, *J* = 17.6, 6.2 Hz, 2H, C$\underline{H}_2$), 2.20 (s, 3H, C$\underline{H}_3$).

^{13}C-NMR (75 MHz, $CDCl_3$): δ_C/ppm=209.1, 142.7, 128.6, 127.7, 125.6, 69.9, 52.0, 30.8.

GC-MS (EI): m/z = 164.1 (1, $[M^{+\bullet}]$), 148.1 (4, $[M^{+\bullet}]$-$[O^{\bullet}]$), 132.1 (8, $[M^{+\bullet}]$-$[O^{\bullet}]$-$[OH^{\bullet}]$), 117.1 (14, $[M^{+\bullet}]$-$[O^{\bullet}]$-$[OH^{\bullet}]$-$[CH_3^{\bullet}]$), 105.0 (100, $[M^{+\bullet}]$-$[OH^{\bullet}]$-$[C(O)CH_3^{\bullet}]$).

The found analytical data were in accordance with the available literature data.[15]

6.5.2 Synthesized substrates for the palladium-catalyzed reductive semipinacol-type rearrangement of β-aryloxy or β-alkoxy benzylic alcohols

2-phenoxy-1-phenyl-ethanol (**5**)

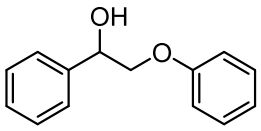

5

The compound **5** was obtained from the respective ketone using the general procedure presented in section 6.5.1 as a white solid in 93% yield.

$C_{14}H_{14}O_2$ (214.26 g/mol)

***R*$_f$:** 0.38 (hexane/ethyl acetate 90:10).

m.p.: 58.2 °C.

^{1}H-NMR (400 MHz, $CDCl_3$): δ_H/ppm= 7.50 – 7.45 (m, 2H, C<u>H</u>$_{arom}$), 7.44 – 7.38 (m, 2H, C<u>H</u>$_{arom}$), 7.38 – 7.27 (m, 3H, C<u>H</u>$_{arom}$), 7.02 – 6.97 (m, 1H, C<u>H</u>$_{arom}$), 6.96 – 6.91 (m, 2H, C<u>H</u>$_{arom}$), 5.14 (dd, *J* = 8.8, 3.1 Hz, 1H, C<u>H</u>OH), 4.13 (dd, *J* = 9.6, 3.2 Hz, 1H, C<u>H</u>$_2$), 4.03 (dd, *J* = 8.9, 0.7 Hz, 1H, C<u>H</u>$_2$), 2.86 (bs, 1H, O<u>H</u>).

^{13}C-NMR (75 MHz, $CDCl_3$): δ_C/ppm= 158.4, 139.7, 129.6, 128.6, 128.2, 126.3, 121.3, 114.7, 73.3, 72.6.

GC-MS (EI): m/z = 214.1 (9, $[M^{+\bullet}]$), 196.1 (55, $[M^{+\bullet}]$-$[H_2O]$), 120.0 (11, $[M^{+\bullet}]$-$[C_6H_5O^{\bullet}]$), 108.1 (100, $[M^{+\bullet}]$-$[C_6H_5OCH_2^{\bullet}]$).

The found analytical data were in accordance with the available literature data.[16]

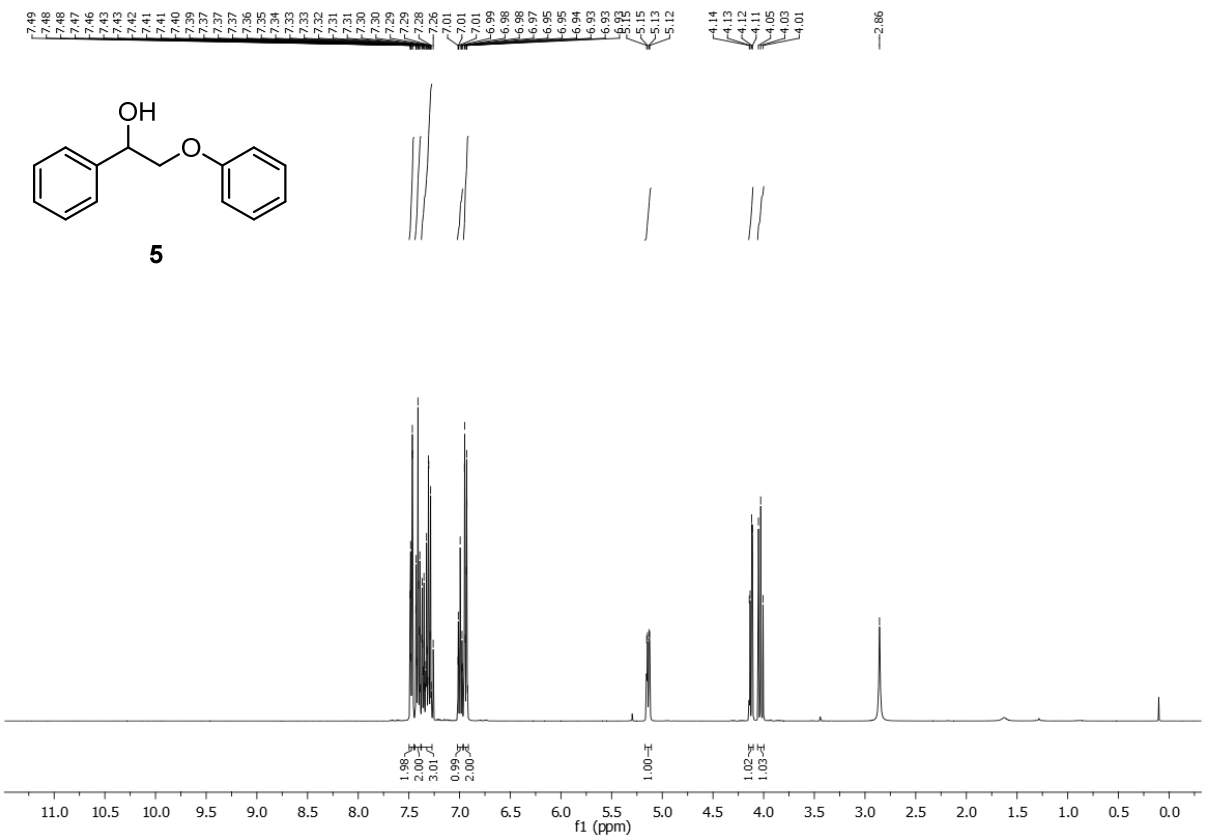
OH
O
5
f1 (ppm)

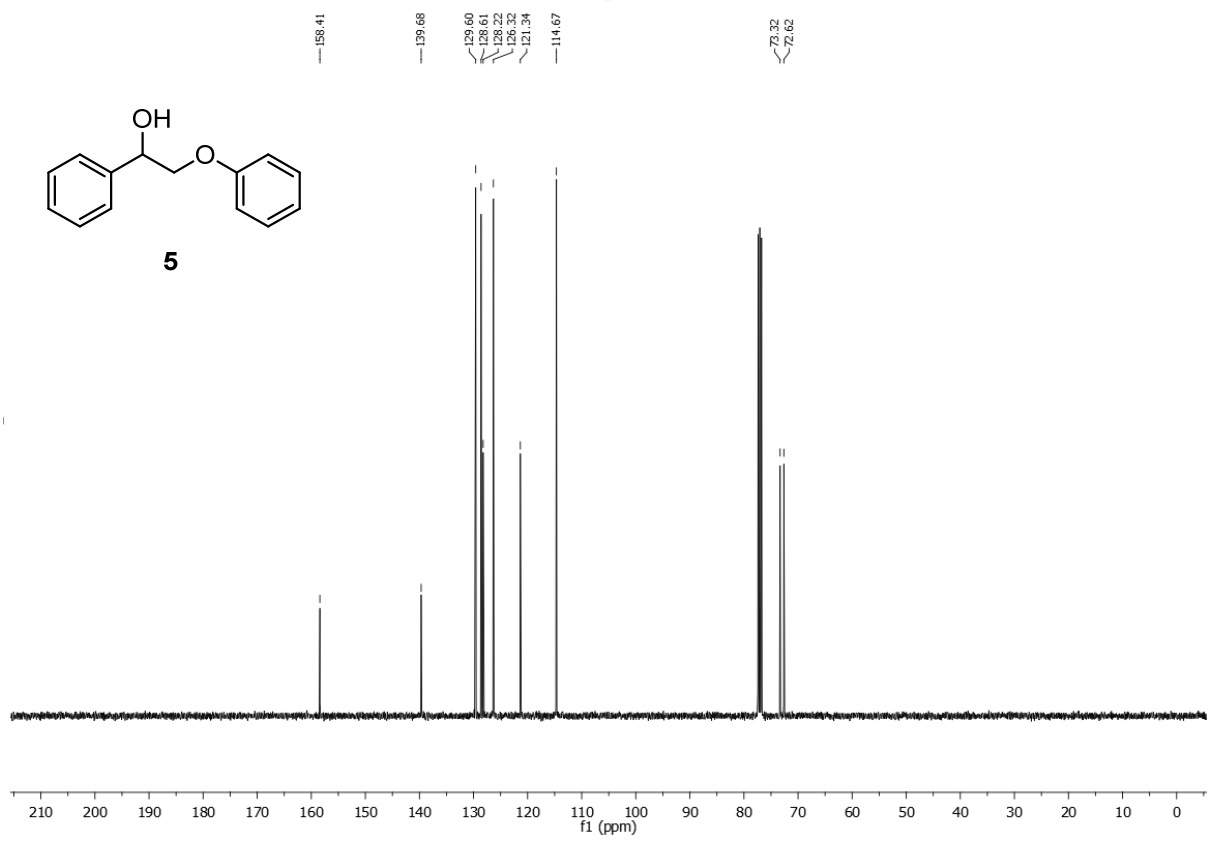
OH
O
5
f1 (ppm)

2-methoxy-1-phenyl-ethanol (**15**)

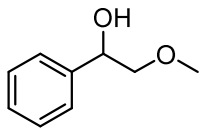

15

The compound **15** was obtained from the respective ketone using the general procedure presented in section 6.5.1 as a colorless oil in 76% yield.

$C_9H_{12}O_2$ (152.19 g/mol)

***R*$_f$:** 0.36 (hexane/ethyl acetate 90:10).

m.p.: ambient temperature.

^{1}H-NMR (400 MHz, $CDCl_3$): δ_H/ppm= 7.41 – 7.33 (m, 4H, C<u>H</u>$_{arom}$), 7.30 (ddd, *J* = 6.7, 3.8, 1.7 Hz, 1H, C<u>H</u>$_{arom}$), 4.90 (dd, *J* = 8.9, 3.2 Hz, 1H, C<u>H</u>OH), 3.55 (dd, *J* = 9.8, 3.2 Hz, 1H, C<u>H</u>$_2$O), 3.48 – 3.40 (m, 4H, C<u>H</u>$_2$O and OC<u>H</u>$_3$), 2.75 (bs, 1H, O<u>H</u>).

^{13}C-NMR (75 MHz, $CDCl_3$): δ_C/ppm= 140.2, 128.4, 127.9, 126.2, 78.2, 72.7, 59.0.

GC-MS (EI): m/z = 152.0 (100, [$M^{+\bullet}$]), 137.0 (2, [$M^{+\bullet}$]-[$CH_3^{\bullet}$]).

The found analytical data were in accordance with the available literature data.[17]

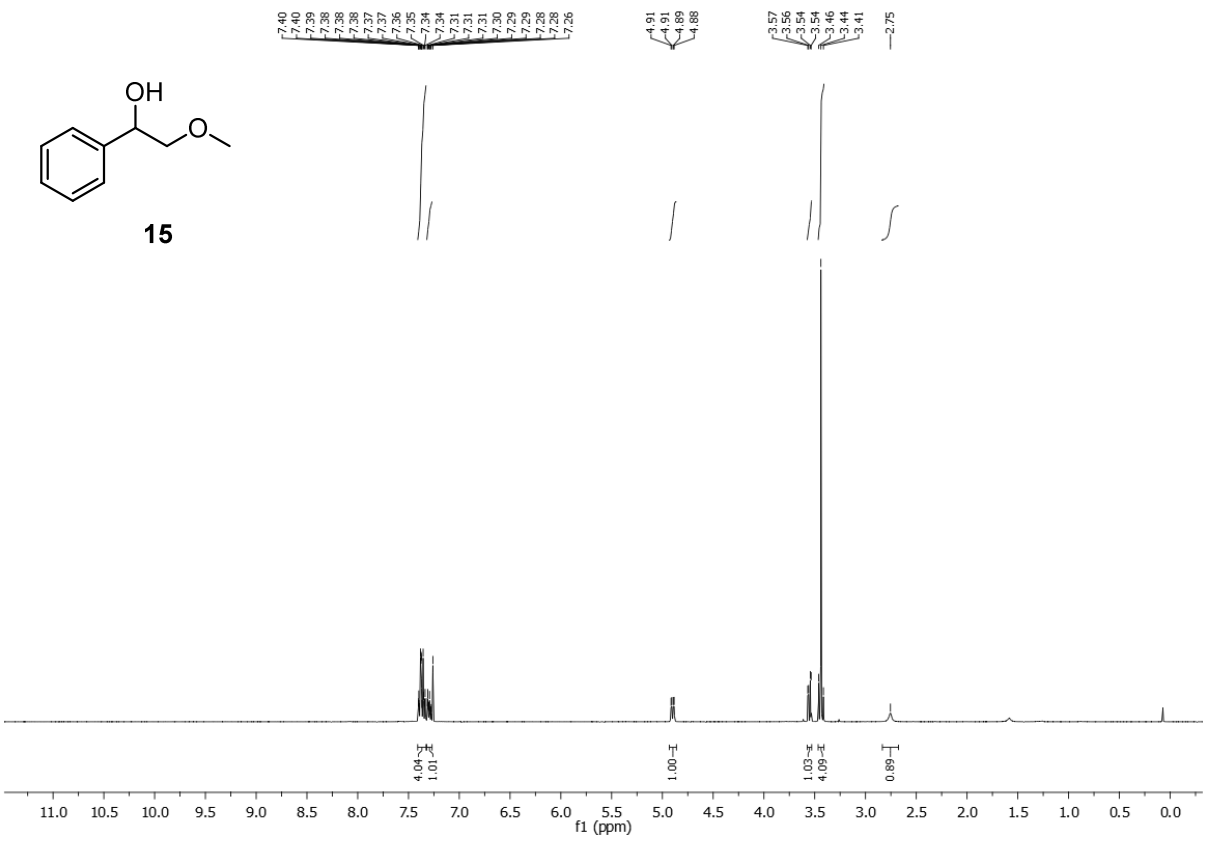
7.40
7.40
7.39
7.38
7.38
7.38
7.37
7.37
7.36
7.35
7.34
7.34
7.31
7.31
7.31
7.30
7.29
7.29
7.28
7.28
7.26
4.91
4.91
4.89
4.88
3.57
3.56
3.54
3.54
3.46
3.44
3.41
2.75
OH
O
15
4.04
1.01
1.00
1.03
4.09
0.89
11.0 10.5 10.0 9.5 9.0 8.5 8.0 7.5 7.0 6.5 6.0 5.5 5.0 4.5 4.0 3.5 3.0 2.5 2.0 1.5 1.0 0.5 0.0
f1 (ppm)

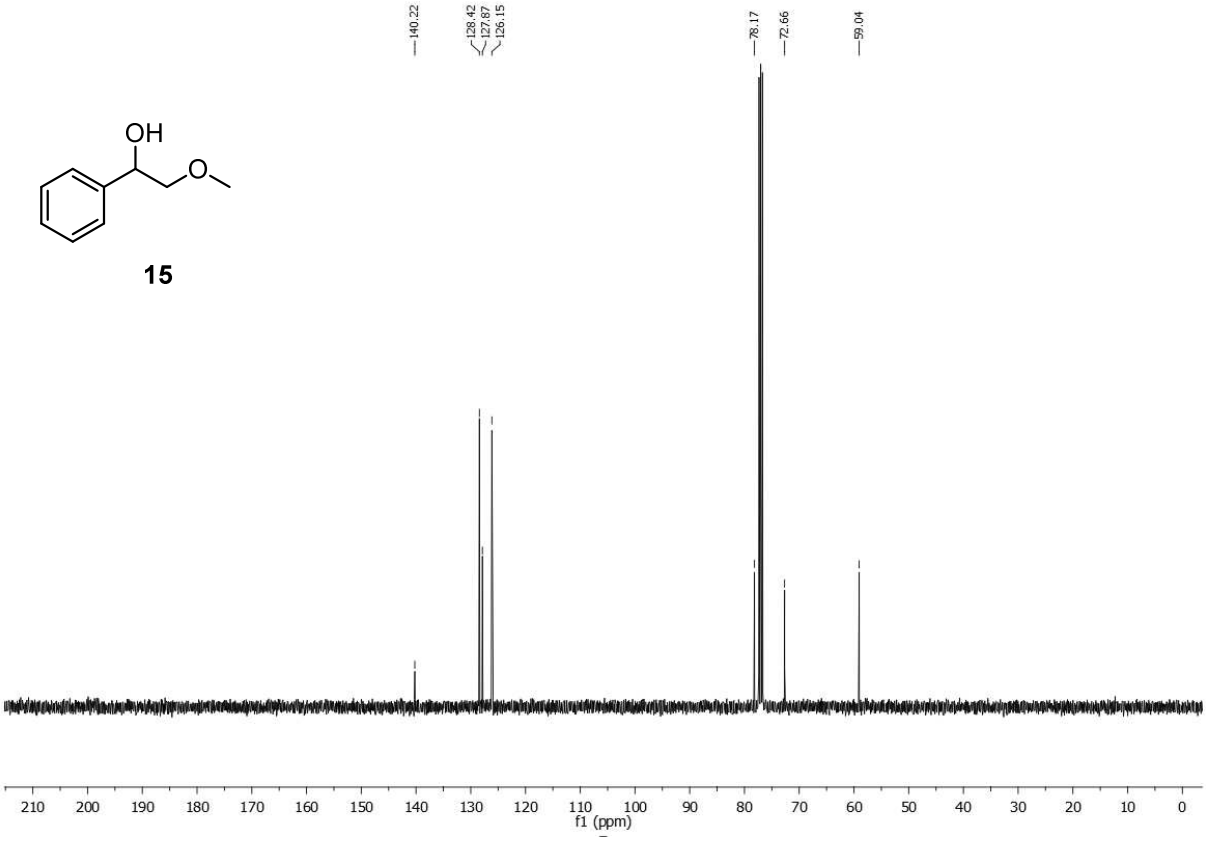
140.22
128.42
127.87
126.15
78.17
72.66
59.04
OH
O
15
210 200 190 180 170 160 150 140 130 120 110 100 90 80 70 60 50 40 30 20 10 0
f1 (ppm)

2-methoxy-1-(4-fluorophenyl)ethanol (**19**)

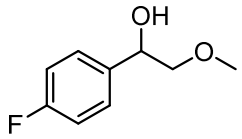

19

The compound **19** was obtained from the respective ketone using the general procedure presented in section 6.5.1 as a dark red oil in quantitative yield.

$C_9H_{11}FO_2$ (170.18 g/mol)

***R*$_f$:** 0.19 (hexane/ethyl acetate 80:20).

m.p.: ambient temperature.

^{1}H-NMR (400 MHz, $CDCl_3$): δ_H/ppm= 7.38 – 7.32 (m, 2H, C$\underline{H}_{arom}$), 7.04 (ddd, *J* = 10.8, 5.9, 2.5 Hz, 2H, C$\underline{H}_{arom}$), 4.87 (dd, *J* = 8.8, 3.2 Hz, 1H, C$\underline{H}$OH), 3.52 (dd, *J* = 9.8, 3.3 Hz, 1H, C$\underline{H}_2$O), 3.43 (s, 3H, OC$\underline{H}_3$), 3.39 (dd, *J* = 9.7, 8.9 Hz, 1H, C$\underline{H}_2$O), 2.79 (bs, 1H, O$\underline{H}$).

^{13}C-NMR (75 MHz, $CDCl_3$): δ_C/ppm= 162.4 (d, *J* = 245.7 Hz), 135.9, 127.8 (d, *J* = 8.1 Hz), 115.3 (d, *J* = 21.4 Hz), 78.1, 72.0, 59.1.

^{19}F-NMR (376 MHz, $CDCl_3$): δ_F/ppm = -114.7.

GC-MS (EI): m/z = 170.0 (5, $[M^{+\bullet}]$), 152.0 (21, $[M^{+\bullet}]$-$[H_2O]$), 125.0 (100, $[M^{+\bullet}]$-$[CH_3OCH_2^{\bullet}]$), 109.0 (55, $[M^{+\bullet}]$-$[CH_3OCH_2^{\bullet}]$-$[OH^{\bullet}]$).

The found analytical data were in accordance with the available literature data.[18]

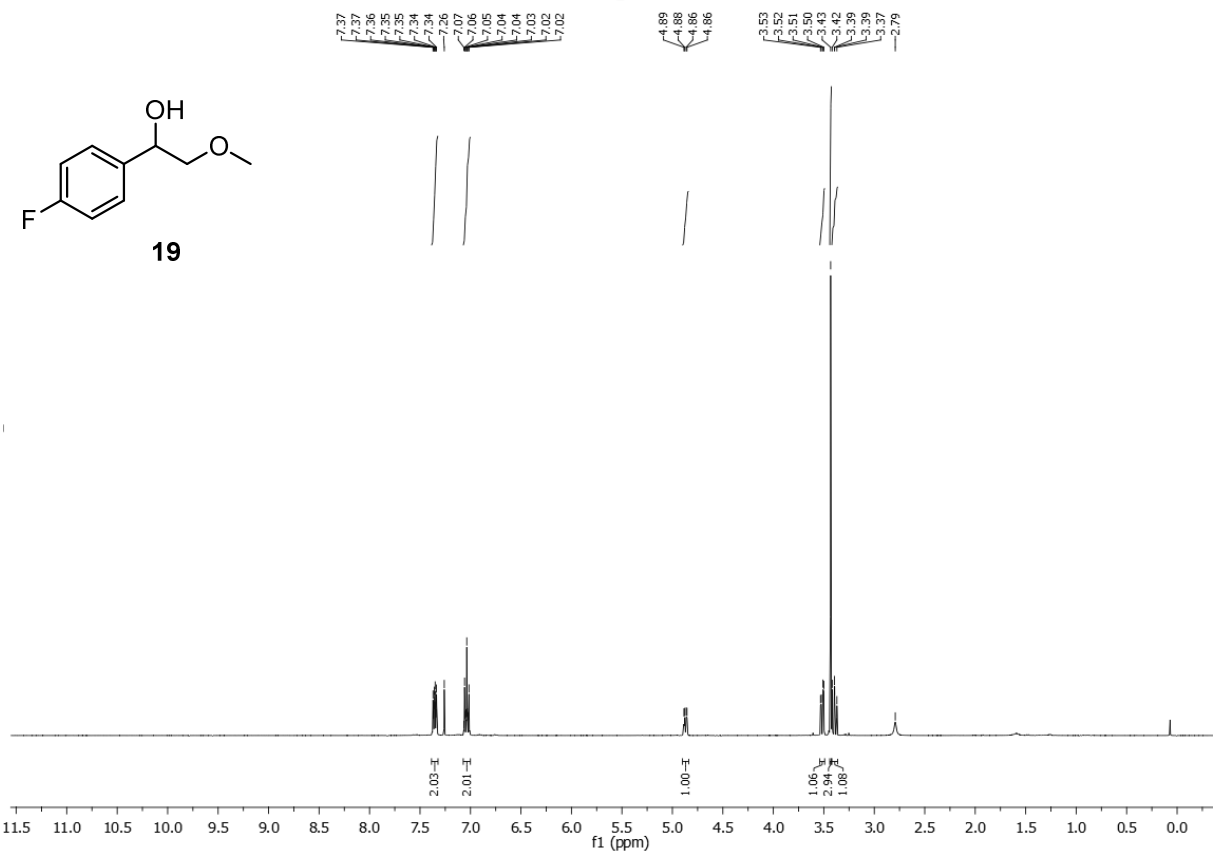
OH
O
F
19
7.37
7.37
7.36
7.35
7.35
7.34
7.34
7.26
7.07
7.06
7.05
7.04
7.04
7.03
7.02
7.02
4.89
4.88
4.86
4.86
3.53
3.52
3.51
3.50
3.43
3.42
3.39
3.39
3.37
2.79
2.03
2.01
1.00
1.06
2.94
1.08
f1 (ppm)

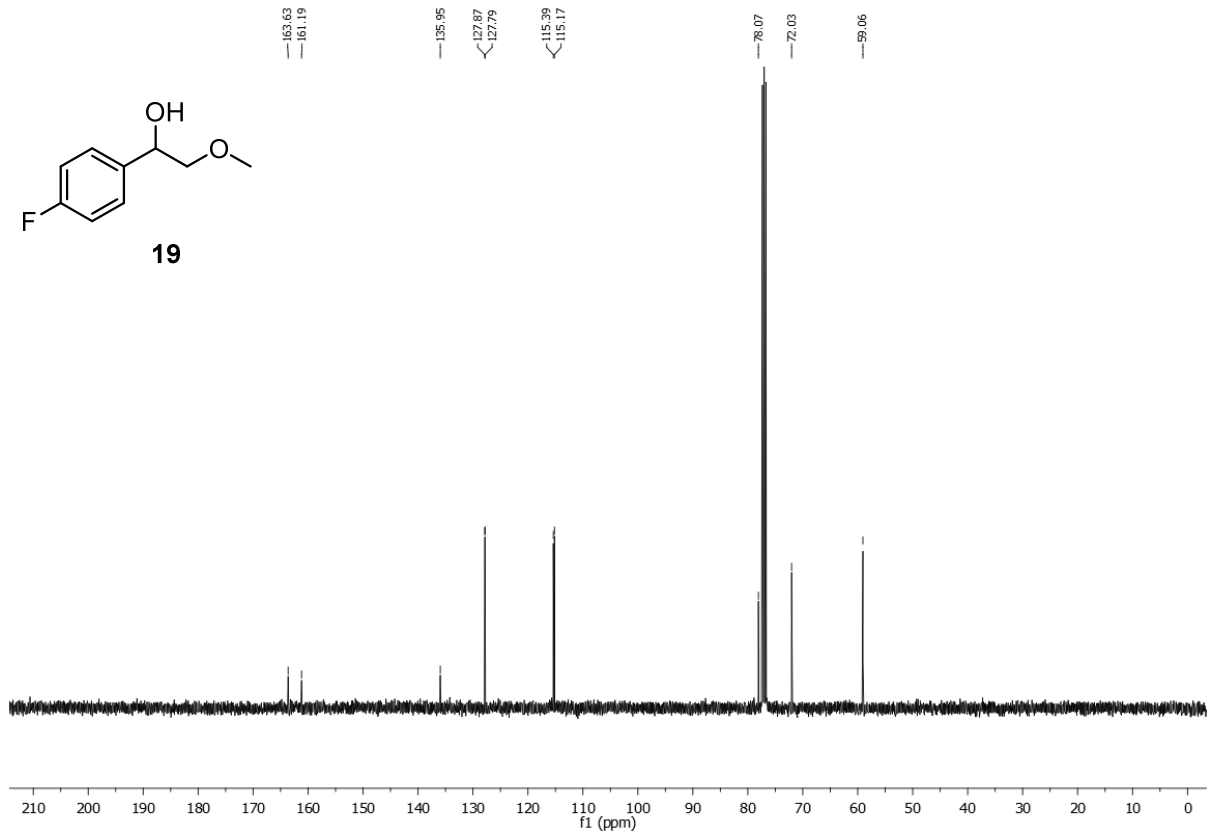
OH
O
F
19
163.63
161.19
135.95
127.87
127.79
115.39
115.17
78.07
72.03
59.06
f1 (ppm)

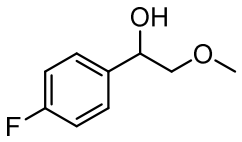
OH
O
F

19

114.69
10
0
-10
-20
-30
-40
-50
-60
-70
-80
-90
-100
-110
-120
-130
-140
-150
-160
-170
-180
-190
-200
-210
f1 (ppm)

2-methyl-2-phenoxy-1-phenylpropanol (**24**)

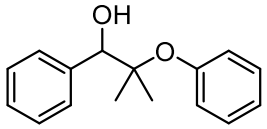

24

The compound **24** was obtained from the respective ketone using the general procedure presented in section 6.5.1 as colorless oil in 95% yield.

$C_{16}H_{18}O_2$ (242.32 g/mol)

***R*$_f$:** 0.13 (hexane/diethyl ether 95:5).

m.p.: ambient temperature.

^{1}H-NMR (400 MHz, $CDCl_3$): δ_H/ppm= 7.45 (dd, *J* = 8.0, 1.2 Hz, 2H, C$\underline{H}_{arom}$), 7.37 – 7.27 (m, 5H, C$\underline{H}_{arom}$), 7.15 – 7.10 (m, 1H, C$\underline{H}_{arom}$), 7.04 – 7.00 (m, 2H, C$\underline{H}_{arom}$), 4.80 (s, 1H, C$\underline{H}$OH), 1.20 (s, 3H, C$\underline{H}_3$), 1.16 (s, 3H, C$\underline{H}_3$).

^{13}C-NMR (75 MHz, $CDCl_3$): δ_C/ppm= 154.4, 139.8, 129.3, 128.1, 128.0, 127.9, 124.6, 124.2, 83.9, 80.5, 23.6, 20.5.

GC-MS (EI): m/z = 242.1 (1, [$M^{+\bullet}$]), 225.1 (3, [$M^{+\bullet}$]-[$OH^{\bullet}$]), 149.1 (11, [$M^{+\bullet}$]-[$C_6H_5O^{\bullet}$]), 135.1 (54, [$M^{+\bullet}$]-[$C_6H_5CH(OH)^{\bullet}$]), 120.1 (100, [$M^{+\bullet}$]-[$C_6H_5CH(OH)^{\bullet}$]-[$CH_3^{\bullet}$].

The found analytical data were in accordance with the available literature data.[19]

Procedure for the synthesis of 2-methoxy-1-(1-naphthyl)ethanol (17)

Following a non-optimized modified literature procedure,[20] magnesium turnings (6.6 mmol, 0.16 g, 1.2 equiv.) were suspended in dry THF (15 mL) under an argon atmosphere. Under stirring, 1-bromonaphthalene (5.5 mmol, 0.77 mL, 1.1 equiv.) was added and the mixture was refluxed until a darkening of the suspension became evident. The mixture was cooled to room temperature, then a solution of methoxyacetonitrile (5.0 mmol, 0.38 mL, 1.0 equiv.) in dry THF (5 mL) was added dropwise to the Grignard reagent, and the mixture was heated to 70 °C for 5 hours. The reaction was quenched by the slow addition of a saturated aqueous solution of NH_4Cl (15 mL). After *p*H was adjusted to ~ 2, the crude product was hydrolyzed in a separation funnel. The aqueous phase was neutralized using a saturated aqueous solution of Na_2CO_3 and extracted with dichloromethane (3 × 20 mL). The organic phases were combined, dried over Na_2SO_4 and filtered. After evaporation of the solvent *in vacuo*, an oily residue was obtained, which was redissolved in methanol (20 mL). The stirred solution was cooled to 0 °C in an ice bath and $NaBH_4$ (10 mmol, 0.38 g, 2.0 equiv.) was added in portions. The reaction was allowed to warm to room temperature and stirred until TLC control showed completion. After quenching with aqueous saturated NH_4Cl solution (15 mL) and adujsting *p*H to ~ 3, methanol was removed on the rotary evaporator. The remaining aqueous phase was extracted with dichloromethane (3 × 20 mL), the organic phases were combined, dried over Na_2SO_4 and filtered. The crude product solution was concentrated and purified by flash column chromatography (hexane/ethyl acetate 80:20) to furnish **17** as a colorless oil (442 mg, 44% yield).

2-methoxy-1-(1-naphthyl)ethanol (**17**)

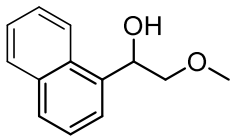

17

The compound **17** was obtained from 1-bromonaphthalene as a colorless oil in 44% yield.

$C_{13}H_{14}O_2$ (202.25 g/mol)

***R*$_f$:** 0.30 (hexane/ethyl acetate 80:20).

m.p.: ambient temperature.

^{1}H-NMR (400 MHz, $CDCl_3$): δ_H/ppm= 8.07 (d, *J* = 8.3 Hz, 1H, C$\underline{H}_{arom}$), 7.91 – 7.85 (m, 1H, C$\underline{H}_{arom}$), 7.78 (dd, *J* = 20.0, 7.7 Hz, 2H, C$\underline{H}_{arom}$), 7.51 (qdd, *J* = 6.8, 5.9, 1.5 Hz, 3H, C$\underline{H}_{arom}$), 5.72 (dt, *J* = 8.9, 2.4 Hz, 1H, C$\underline{H}$OH), 3.78 (dd, *J* = 10.0, 2.8 Hz, 1H, C$\underline{H}_2$O), 3.54 (dd, *J* = 9.9, 9.0 Hz, 1H, C$\underline{H}_2$O), 3.48 (s, 3H, OC$\underline{H}_3$), 2.91 (bs, *J* = 5.4 Hz, 1H, O$\underline{H}$).

^{13}C-NMR (75 MHz, $CDCl_3$): δ_C/ppm= 135.7, 133.7, 130.5, 129.0, 128.3, 126.2, 125.6, 123.6, 122.7, 77.6, 69.7, 59.1.

GC-MS (EI): m/z = 202.1 (9, [$M^{+\bullet}$]), 172.1 (2, [$M^{+\bullet}$]-[$CH_3O^{\bullet}$]), 155.0 (100, [$M^{+\bullet}$]-[$CH_3OCH_2^{\bullet}$]), 141.1 (9, [$M^{+\bullet}$]-[$CH_3OCH_2^{\bullet}$]-[$OH^{\bullet}$]), 127.0 (95, [$M^{+\bullet}$]-[$CH_3OCH_2CH(OH)^{\bullet}$]).

The found analytical data were in accordance with the available literature data.[20]

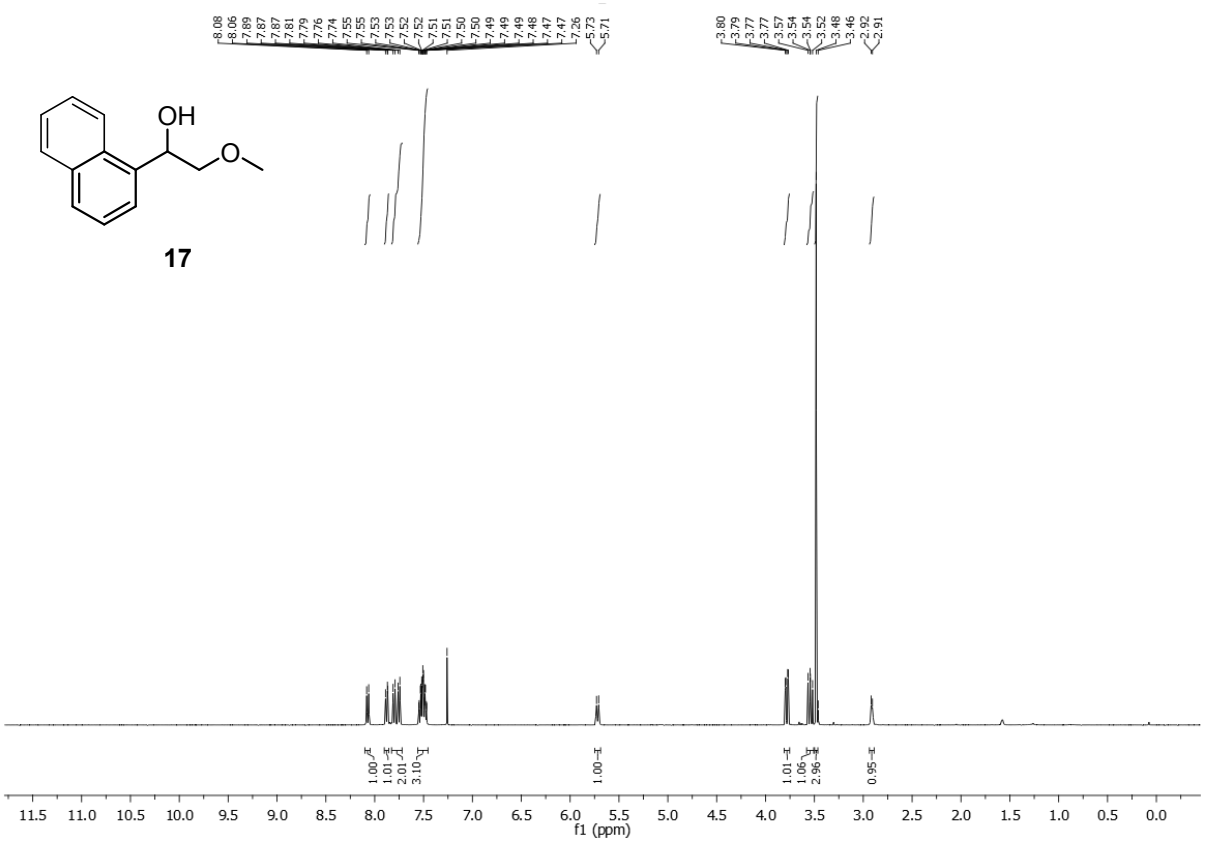
OH
O
17
f1 (ppm)

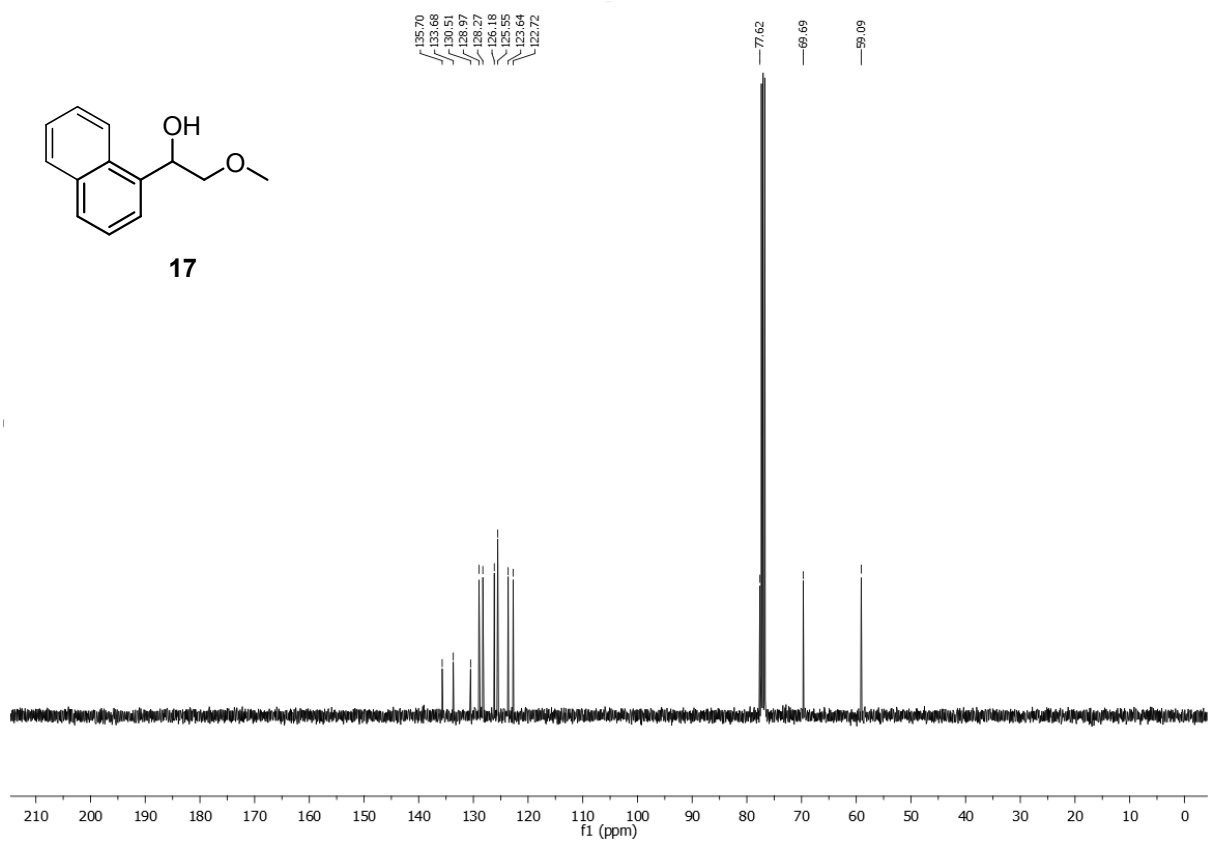
OH
O
17
f1 (ppm)

6.5.3 Synthesized substrate precursors for the palladium-catalyzed reductive semipinacol-type rearrangement of β-aryloxy or β-alkoxy benzylic alcohols

Procedure for the synthesis of 2-phenoxy-1-phenylethanone

According to a literature procedure,[21] a 250 mL round-bottom flask was charged with phenol (28 mmol, 2.6 g, 1.1 equiv.) and K_2CO_3 (38 mmol, 5.2 g, 1.5 equiv.). The solids were suspended in acetone (75 mL) and a solution of 2-bromoacetophenone (25 mmol, 5.0 g, 1.0 equiv.) in acetone (75 mL) was added dropwise under stirring in 30 min. The flask was equipped with a reflux condenser and the reaction mixture was refluxed over night. After cooling the reaction to room temperature, residual solids were filtered off and the filtrate was concentrated *in vacuo*. The obtained crude product was recrystallized from methanol to give 2-phenoxy-1-phenylethanone as a white solid (3.6 g, 77% yield).

2-phenoxy-1-phenylethanone

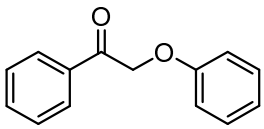

The compound was obtained from 2-bromoacetophenone as a white solid in 77% yield.

$C_{14}H_{12}O_2$ (212.25 g/mol)

***R*$_f$:** 0.20 (hexane/ethyl acetate 95:5).

m.p.: 72.5 °C.

^{1}H-NMR (400 MHz, $CDCl_3$): δ_H/ppm= 8.04 – 7.99 (m, 2H, C$\underline{H}_{arom}$), 7.66 – 7.59 (m, 1H, C$\underline{H}_{arom}$), 7.54 – 7.46 (m, 2H, C$\underline{H}_{arom}$), 7.29 (ddd, *J* = 7.6, 6.0, 2.3 Hz, 2H, C$\underline{H}_{arom}$), 7.02 – 6.93 (m, 3H, C$\underline{H}_{arom}$), 5.28 (s, 2H, C$\underline{H}_2$O).

^{13}C-NMR (75 MHz, $CDCl_3$): δ_C/ppm= 194.6, 158.0, 134.6, 133.9, 129.6, 128.9, 128.2, 121.7, 114.8, 70.8.

GC-MS (EI): m/z = 212.1 (8, [$M^{+\bullet}$]), 119.1 (100, [$M^{+\bullet}$]-[$C_6H_5O^{\bullet}$]), 105.0 (23, [$M^{+\bullet}$]-[$C_6H_5OCH_2^{\bullet}$]).

The found analytical data were in accordance with the available literature data.[21]

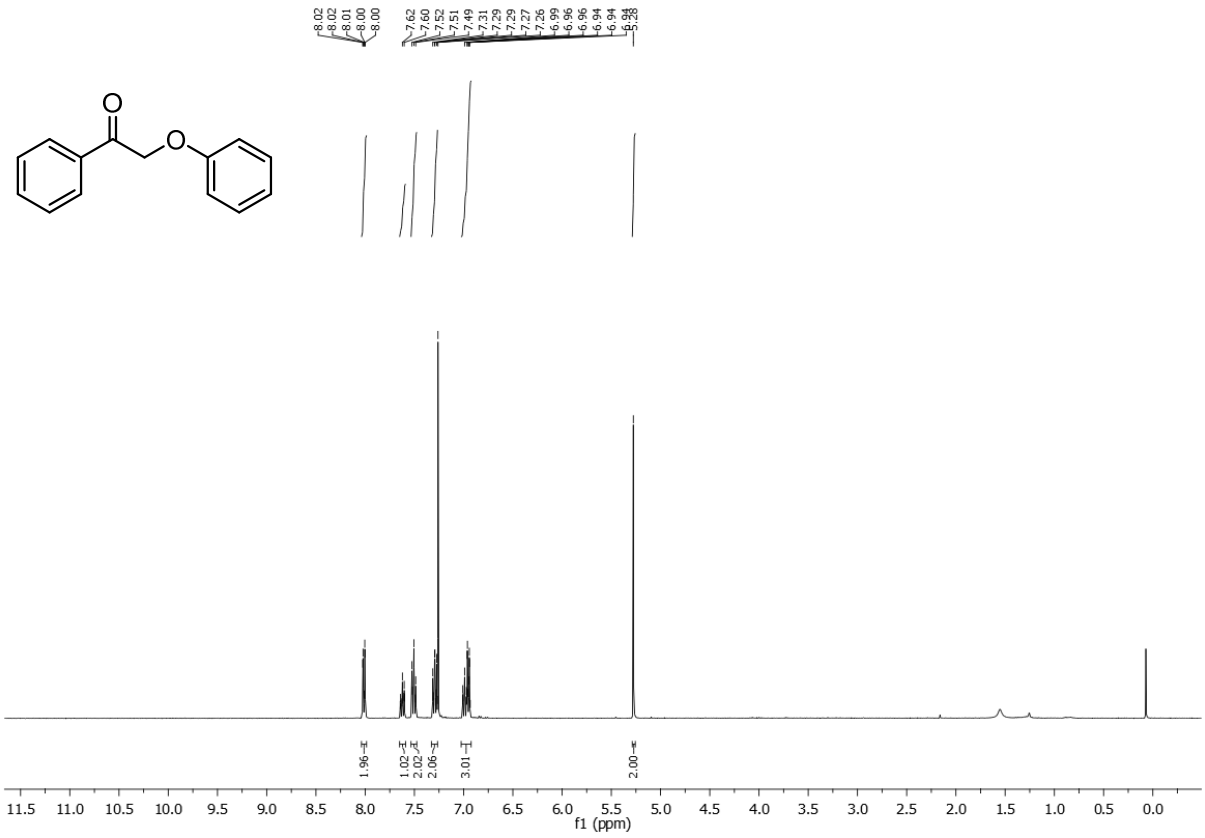
8.02
8.02
8.01
8.00
8.00
7.62
7.60
7.52
7.51
7.49
7.31
7.29
7.29
7.27
7.26
6.99
6.96
6.96
6.94
6.94
5.28
1.96
1.02
2.02
2.06
3.01
2.00
f1 (ppm)

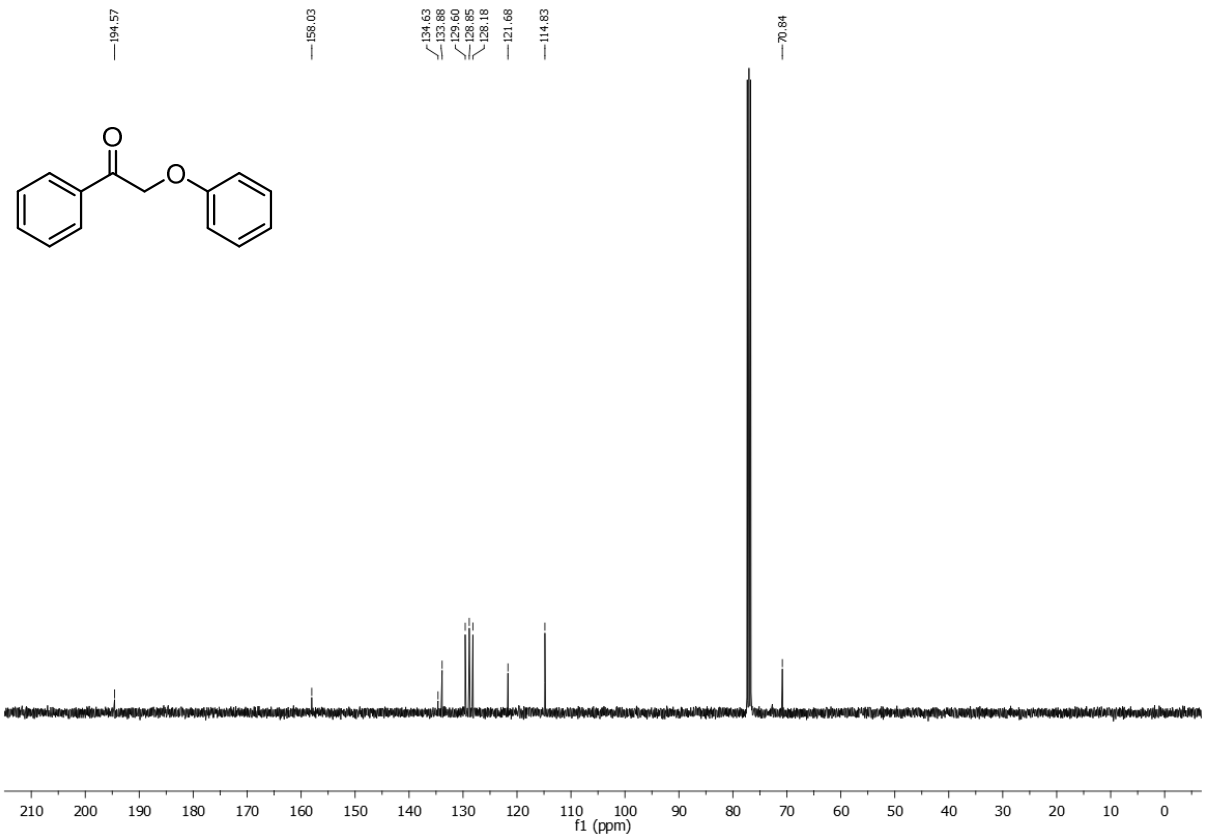
194.57
158.03
134.63
133.88
129.60
128.85
128.18
121.68
114.83
70.84
f1 (ppm)

Procedure for the synthesis of 2-phenoxy-1-phenylpropanone

Following a modified literature procedure,[21] sodium hydride (21 mmol, 0.50 g, 57% in mineral oil, 2.2 equiv.) was suspended in anhydrous THF (25 mL) under an argon atmosphere and cooled to 0 °C in an ice bath. Under stirring, 2-phenoxy-1-phenylethanone (9.4 mmol, 2.0 g, 1.0 equiv.) was added as solution in anhydrous THF (10 mL). After stirring for 15 min, methyl iodide (20 mmol, 1.2 mL, 2.1 equiv.) was added dropwise at 0 °C. The mixture was heated to 40 °C for 1h and cooled to 0 °C. After quenching by the slow addition of water (25 mL), the reaction mixture was extracted with ethyl acetate (3 × 15 mL). The combined organic phases were washed with brine (2 × 15 mL), dried over Na_2SO_4 and filtered. After evaporation of the solvent, the crude product was purified by column chromatography (hexane/diethyl ether 99:1) to afford 2-methyl-2-phenoxy-1-phenylpropanone as colorless oil (590 mg, 52% yield).

2-methyl-2-phenoxy-1-phenylpropanone

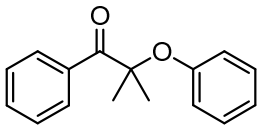

The compound was obtained from 2-phenoxy-1-phenylethanone as colorless oil in 52% yield.

$C_{16}H_{16}O_2$ (240.30 g/mol)

***R*$_f$:** 0.18 (hexane/diethyl ether 99:1).

m.p.: ambient temperature.

^{1}H-NMR (400 MHz, $CDCl_3$): δ_H/ppm= 8.32 (dt, *J* = 8.6, 1.7 Hz, 2H, C$\underline{H}_{arom}$), 7.50 (dt, *J* = 4.0, 1.6 Hz, 1H, C$\underline{H}_{arom}$), 7.39 (ddd, *J* = 8.1, 2.9, 1.3 Hz, 2H, C$\underline{H}_{arom}$), 7.17 – 7.11 (m, 2H, C$\underline{H}_{arom}$), 6.92 – 6.87 (m, 1H, C$\underline{H}_{arom}$), 6.76 (ddd, *J* = 4.6, 3.4, 1.9 Hz, 2H, C$\underline{H}_{arom}$), 1.70 (s, 6H, C$\underline{H}_3$)

^{13}C-NMR (75 MHz, $CDCl_3$): δ_C/ppm= 202.5, 155.4, 134.4, 133.0, 130.1, 129.3, 128.4, 121.9, 118.7, 84.9, 26.0.

GC-MS (EI): m/z = 240.1 (4, $[M^{+\bullet}]$), 225.1 (2, $[M^{+\bullet}]$-$[CH_3^{\bullet}]$), 147.1 (4, $[M^{+\bullet}]$-$[C_6H_5O^{\bullet}]$), 135.1 (100, $[M^{+\bullet}]$-$[C_6H_5C(O)^{\bullet}]$), 105.1 (33, $[M^{+\bullet}]$-$[C_6H_5OC(CH_3)_2^{\bullet}]$), 93.1 (16, $[M^{+\bullet}]$-$[C_6H_5C(O)C(CH_3)_2^{\bullet}]$.

The found analytical data were in accordance with the available literature data.[22]

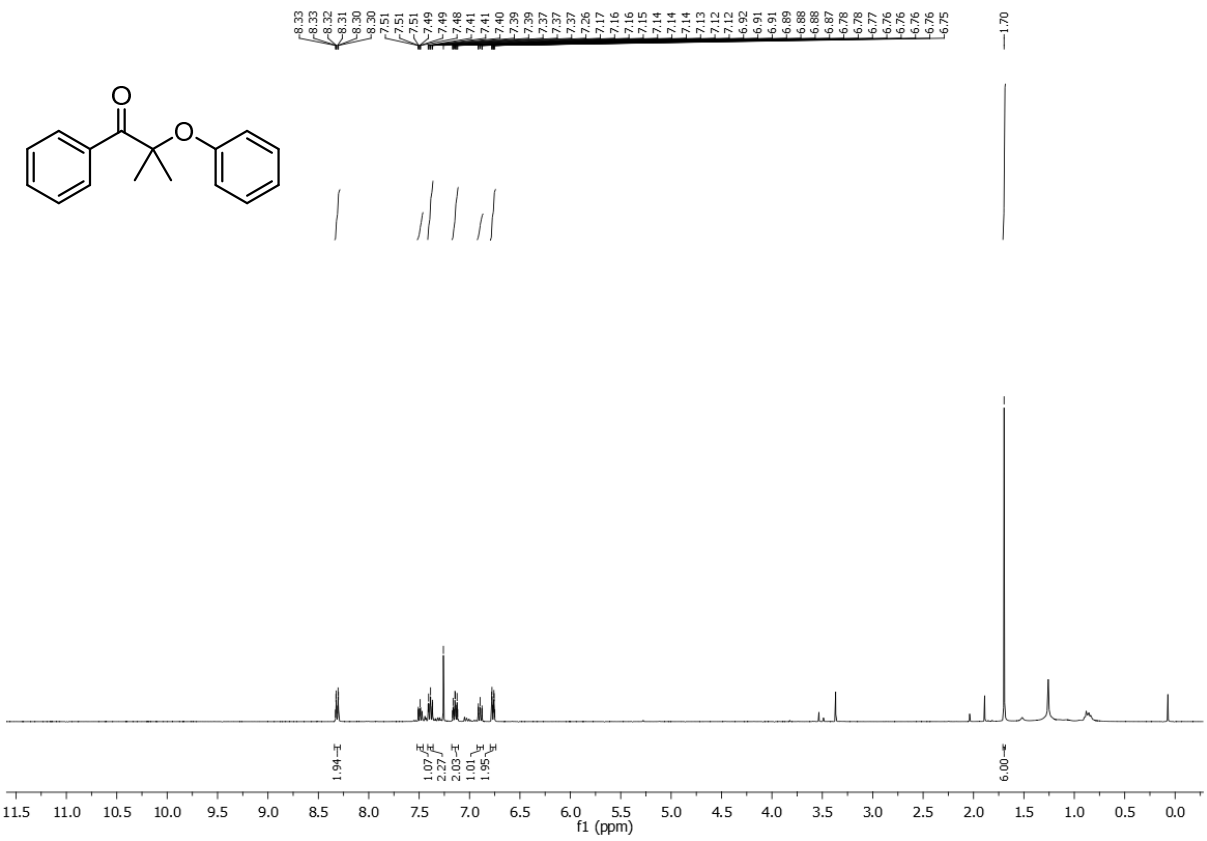
8.33
8.33
8.32
8.31
8.30
8.30
7.51
7.51
7.51
7.49
7.49
7.48
7.41
7.41
7.40
7.39
7.39
7.37
7.37
7.37
7.26
7.17
7.16
7.16
7.15
7.14
7.14
7.14
7.13
7.12
7.12
6.92
6.91
6.91
6.89
6.88
6.88
6.87
6.78
6.78
6.77
6.76
6.76
6.76
6.76
6.75
1.70
O
O
1.94
1.07
2.27
2.03
1.01
1.95
6.00
11.5 11.0 10.5 10.0 9.5 9.0 8.5 8.0 7.5 7.0 6.5 6.0 5.5 5.0 4.5 4.0 3.5 3.0 2.5 2.0 1.5 1.0 0.5 0.0
f1 (ppm)

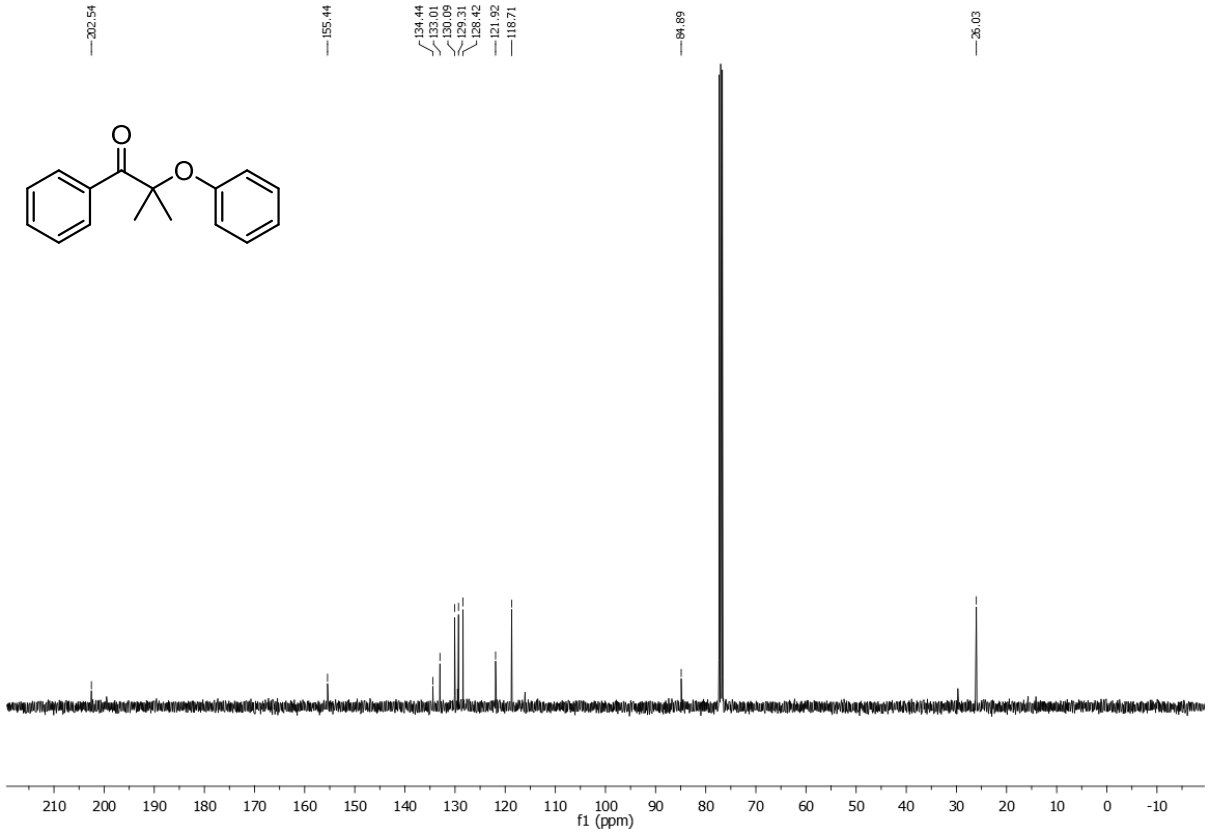
202.54
155.44
134.44
133.01
130.09
129.31
128.42
121.92
118.71
84.89
26.03
O
O
210 200 190 180 170 160 150 140 130 120 110 100 90 80 70 60 50 40 30 20 10 0 -10
f1 (ppm)

Procedure for the synthesis of 1-(4-fluorophenyl)-2-methoxy-ethanone

Following a non-optimized modified literature procedure,[23] a solution of 1-bromo-4-fluorobenzene (15 mmol, 1.5 mL, 1.5 equiv.) in dry diethyl ether (10 mL) under an argon atmosphere was cooled to 0 °C in an ice bath and treated with a solution on *n*-butyllithium (15 mmol, 9.4 mL, 1.6 M in hexane, 1.5 equiv.). The mixture was stirred under cooling for 2 hours, changing color to a deep orange. Then a solution of methoxyacetonitrile (10 mmol, 0.75 mL, 1.0 equiv) in dry diethyl ether (5 mL) was added at 0 °C. The reaction was allowed to warm to room temperature while stirring for 3 hours. After quenching with a saturated aqueous solution of NH_4Cl (10 mL), *p*H was adjusted to ~ 2 and the crude product was hydrolyzed in a separation funnel. The mixture was neutralized with a saturated aqueous solution of Na_2CO_3. The phases were separated and the aqueous solution was extracted with diethyl ether (3 × 15 mL). The combined organic phases were dried over Na_2SO_4 and filtered. The solution of the crude product was concentrated *in vacuo* and purified by flash column chromatography (hexane/ethyl acetate 90:10). The product 1-(4-fluorophenyl)-2-methoxy-ethanone was obtained as orange solid (670 mg, 40% yield).

1-(4-fluorophenyl)-2-methoxy-ethanone

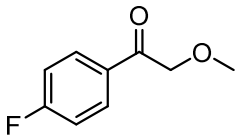

The compound was obtained from 1-bromo-4-fluorobenzene as an orange solid in 40% yield.

$C_9H_9FO_2$ (168.17 g/mol)

***R*$_f$:** 0.19 (hexane/ethyl acetate 90:10).

m.p.: 45.0 °C.

^{1}H-NMR (400 MHz, $CDCl_3$): δ_H/ppm= 8.09 – 7.92 (m, 2H, C$\underline{H}_{arom}$), 7.20 – 7.03 (m, 2H, C$\underline{H}_{arom}$), 4.66 (s, 2H, C$\underline{H}_2$O), 3.50 (s, 3H, OC$\underline{H}_3$).

^{13}C-NMR (75 MHz, $CDCl_3$): δ_C/ppm= 194.8, 166.0 (d, *J* = 255.5 Hz), 131.3 (d, *J* = 3.1 Hz), 130.7 (d, *J* = 9.4 Hz), 115.9 (d, *J* = 21.9 Hz), 75.3, 59.5.

^{19}F-NMR (376 MHz, $CDCl_3$): δ_F/ppm = -104.1.

GC-MS (EI): m/z = 168.0 (1, [$M^{+\bullet}$]), 137.0 (27, [$M^{+\bullet}$]-[$CH_3O^{\bullet}$]), 123.0 (100, [$M^{+\bullet}$]-[$CH_3OCH_2^{\bullet}$]), 95.0 (47, [$M^{+\bullet}$]-[$C(O)CH_2OCH_3^{\bullet}$]).

The found analytical data were in accordance with the available literature data.[24]

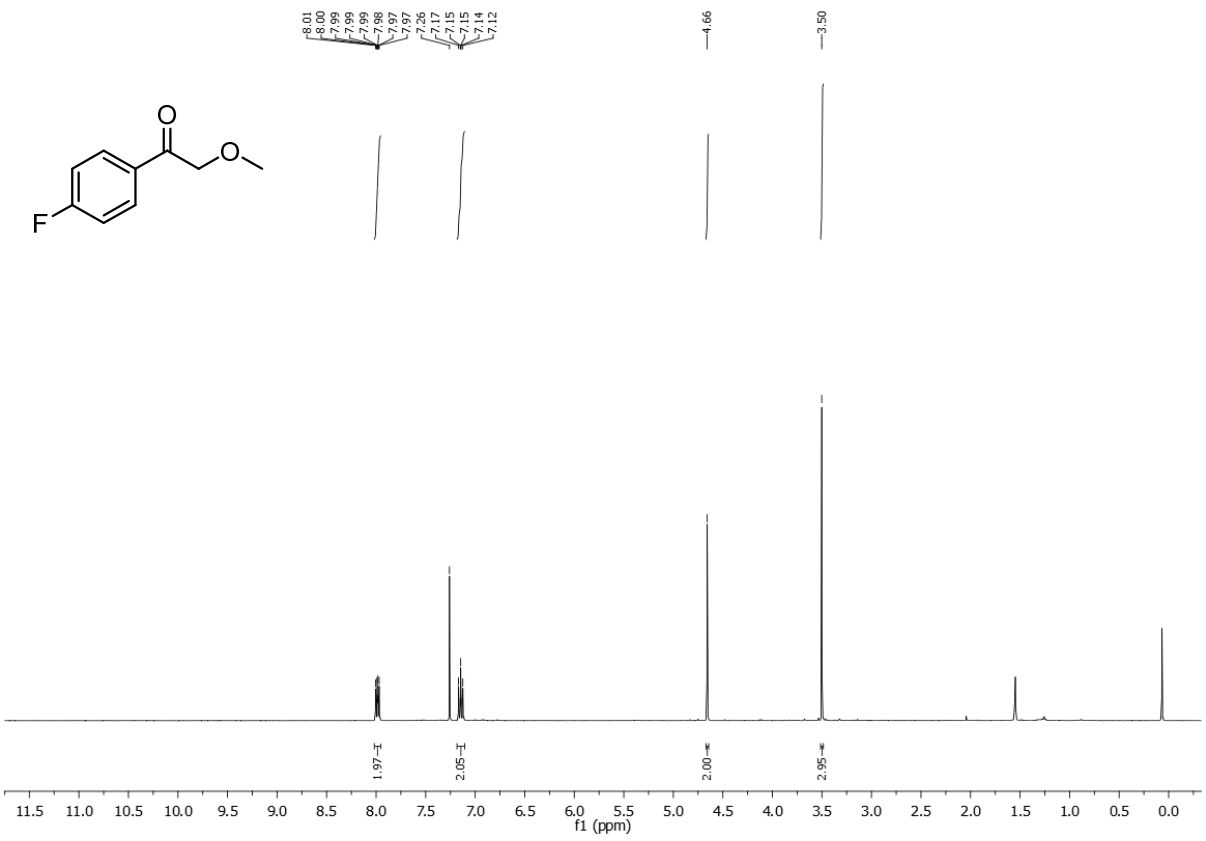
8.01
8.00
7.99
7.99
7.99
7.98
7.97
7.97
7.26
7.17
7.15
7.15
7.14
7.12
4.66
3.50
O
O
F
1.97
2.05
2.00
2.95
11.5 11.0 10.5 10.0 9.5 9.0 8.5 8.0 7.5 7.0 6.5 6.0 5.5 5.0 4.5 4.0 3.5 3.0 2.5 2.0 1.5 1.0 0.5 0.0
f1 (ppm)

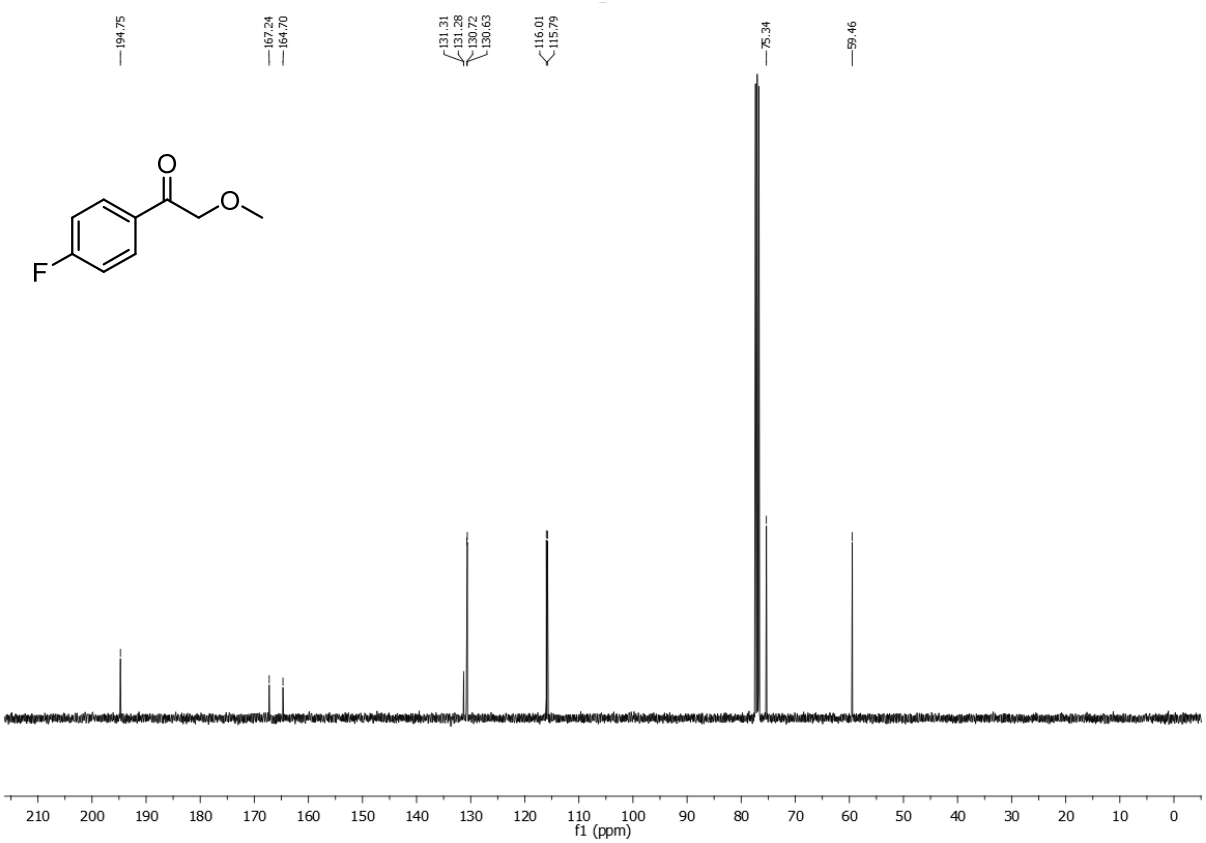
194.75
167.24
164.70
131.31
131.28
130.72
130.63
116.01
115.79
75.34
59.46
O
O
F
210 200 190 180 170 160 150 140 130 120 110 100 90 80 70 60 50 40 30 20 10 0
f1 (ppm)

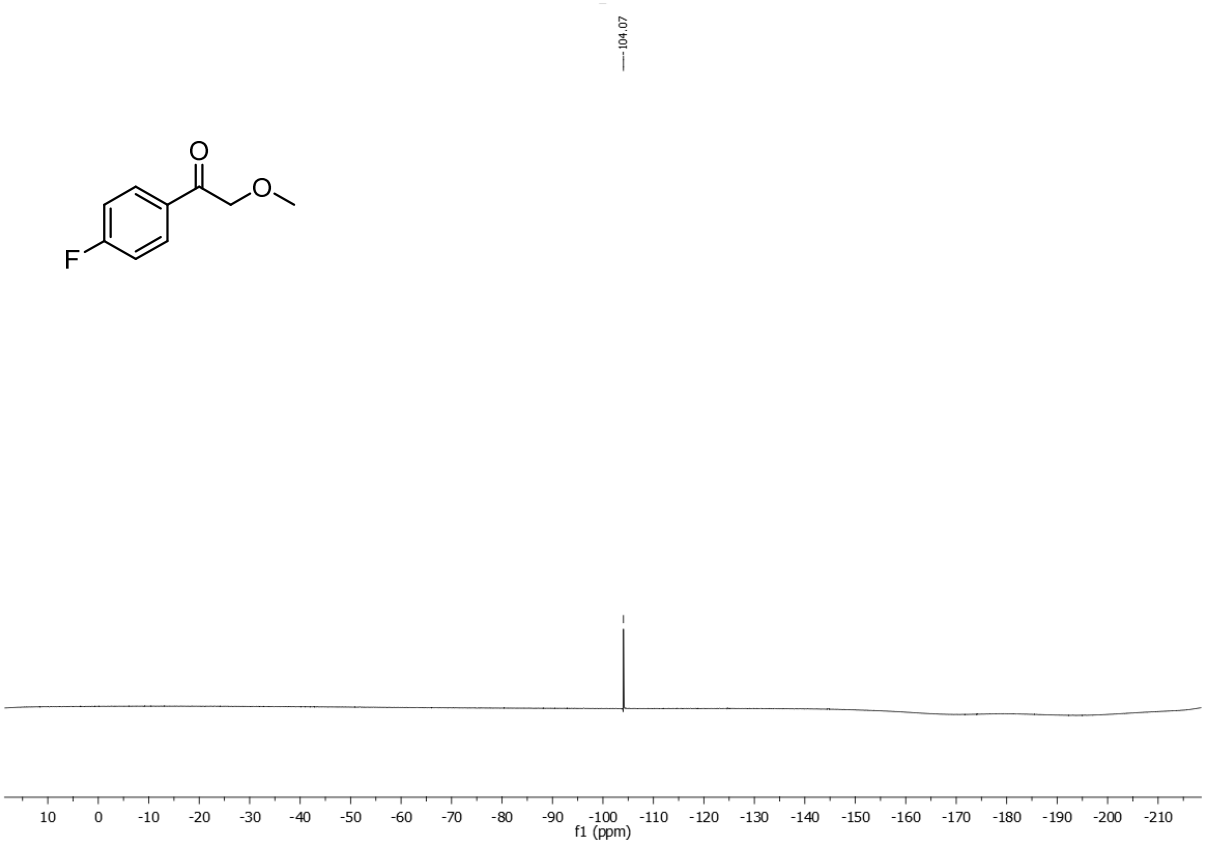
104.07
O
O
F
10
0
-10
-20
-30
-40
-50
-60
-70
-80
-90
-100
-110
-120
-130
-140
-150
-160
-170
-180
-190
-200
-210
f1 (ppm)

6.6 Miscellaneous syntheses

Procedure for the oxidation of dtbpx

According to a literature procedure,[2] a solution of dtbpx (3.8 mmol, 150 mmol) in THF (30 mL) was treated with aqueous H_2O_2 solution (38 mmol, 3.9 mL, 30% *w*/*w*, 10 equiv.). The mixture was stirred over night at room temperature, then the solvents were removed under high vacuum. Further drying yielded the product **L1-(O)$_2$** as a white solid in 78% yield.

α, α'-bis-(di-*tert*-butylphosphino)-o-xylene dioxide (**L1-(O)$_2$**)

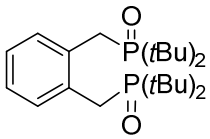

L1-(O)$_2$

$C_{24}H_{44}O_2P_2$ (426.56 g/mol)

***R*$_f$:** not determined.

m.p.: 150.0 °C

^{1}H NMR (300 MHz, C_6D_6):δ_H/ppm = 7.34 – 7.25 (m, 2H), 7.02 – 6.97 (m, 2H), 3.99 (d, *J* = 11.6 Hz, 4H), 1.13 (d, *J* = 12.9 Hz, 36H).

^{31}P NMR (121 MHz, C_6D_6):δ_P/ppm = 61.4 (s).

HRMS (ESI): m/z = [MNa^+] calc. for $C_{24}H_{44}O_2P_2$ 449.27087, found 449.27101.

The found analytical data were in accordance with the available literature data.[2]

Procedure for the synthesis of 1-phenylethyl formate (9)

A round bottom flask (50 mL) was equipped with a stirring bar and charged with 1-phenylethanol (5.0 mmol, 0.60 mL, 1.0 equiv.) and formic acid (10 mmol, 0.38 mL, 2.0 equiv.). The reagents were dissolved in 1,2-dichloroethane (15 mL) and methanesulfonic acid (0.80 mmol, 52 µL, 16 mol%) was added under stirring. The reaction mixture was stirred overnight. After TLC analysis indicated completion of the reaction, the reaction mixture was washed with saturated aqueous solution of $NaHCO_3$ (3 × 10 mL), dried over Na_2SO_4 and filtered. Evaporation of the solvent yielded pure 1-phenylethyl formate as a colorless oil (0.69 g, 92% yield).

1-phenylethyl formate (**9**)

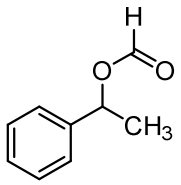

9

$C_9H_{12}O$ (150.18 g/mol)

***R*$_f$:** 0.35 (cyclohexane/ethyl acetate 95:5).

m.p.: ambient temperature.

^{1}H-NMR (400 MHz, $CDCl_3$):δ_H/ppm= 8.09 (s, 1H, HC(O)O), 7.40 – 7.28 (m, 5H, CH_{arom}), 6.02 (q, *J* = 6.6 Hz, 1H), 1.59 (d, *J* = 6.6 Hz, 3H).

^{13}C-NMR (75 MHz, CDCl3): δ_C/ppm= 160.4, 140.9, 128.6, 128.2, 126.2, 72.2, 22.1.

GC-MS (EI): m/z = 150.1 (4, $[M^{+\bullet}]$), 121.1 (2, $[M^{+\bullet}]$-$[CHO^{\bullet}]$), 105.1 (100, $[M^{+\bullet}]$-$[CO_2H^{\bullet}]$).

The found analytical data were in accordance with the available literature data.[25]

Procedure for the synthesis of 2-acetonaphthone-d_3

According to a literature procedure,[26] 2-acetonaphthone (10 mmol, 1.7 g, 1.0 equiv.) was added to a solution of pyrrolidine (1 mmol, 83 µL, 10 mol%) in D_2O (15 mL) and anhydrous 1,4-dioxane (15 mL). The reaction mixture was stirred at room temperature for 24 h and poured on H_2O (100 mL). After extracting the mixture with diethyl ether (3 × 50 mL), the combined organic phases were washed with water (1 × 30 mL) and brine (1 × 30 mL), dried over Na_2SO_4 and filtered. Evaporation of the solvent *in vacuo* afforded 2-acetonaphthone-d_3 as a yellowish solid (1.67 g, 97% yield).

2-acetonaphthone-d_3

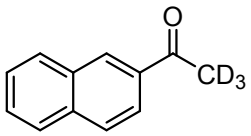

$C_{12}H_7D_3O$ (173.23 g/mol)

***R*$_f$:** not determined.

m.p.: 54.5 °C.

^{1}H-NMR (400 MHz, $CDCl_3$): δ_H/ppm= 8.47 (s, 1H, C<u>H</u>$_{arom}$), 8.07 – 7.95 (m, 2H, C<u>H</u>$_{arom}$), 7.89 (dd, *J* = 8.3, 4.9 Hz, 2H, C<u>H</u>$_{arom}$), 7.65 – 7.52 (m, 2H, C<u>H</u>$_{arom}$).

GC-MS (EI): not determined due to high boiling point.

The found analytical data were in accordance with the available literature data.[26]

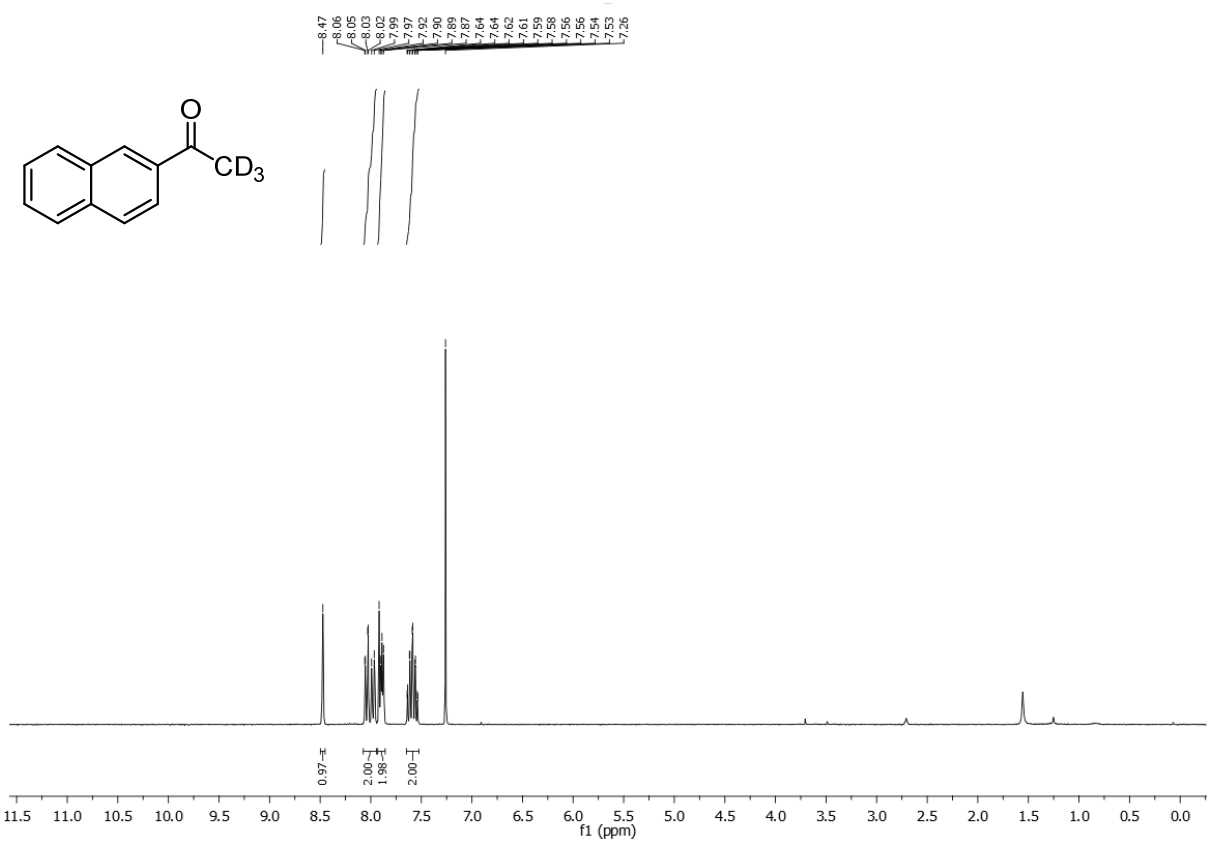
8.47
8.06
8.05
8.03
8.02
7.99
7.97
7.92
7.90
7.89
7.87
7.64
7.64
7.62
7.61
7.59
7.58
7.56
7.56
7.54
7.53
7.26
O
CD3
0.97
2.00
1.98
2.00
11.5 11.0 10.5 10.0 9.5 9.0 8.5 8.0 7.5 7.0 6.5 6.0 5.5 5.0 4.5 4.0 3.5 3.0 2.5 2.0 1.5 1.0 0.5 0.0
f1 (ppm)

Procedure for the synthesis of 2-methyl-2-phenylpropanol

According to a literature procedure,[27] $LiAlH_4$ (6.7 mmol, 0.25 g, 1.1 equiv.) was suspended in anhydrous diethyl ether (27 mL) under an argon atmosphere and cooled to 0 °C in an ice bath. Under stirring, a solution of 2-methyl-2-phenylpropanoic acid (6.1 mmol, 1.0 g, 1.0 equiv.) in anhydrous diethyl ether (15 mL) was added dropwise under cooling. The reaction mixture was stirred at 0 °C for 3 hours. The reaction was quenched by the slow addition of water (30 mL) at 0 °C, leading to the formation of a white precipitate. The mixture was stirred for 15 minutes and filtered. Diethyl ether (25 mL) was added to the filtrate, followed by washing with water (40 mL) and brine (40 mL). The organic phase was dried over Na_2SO_4 and filtered. Evaporation of the solvent *in vacuo* afforded 2-methyl-2-phenylpropanol as a colorless oil (0.51 g, 56% yield).

2-methyl-2-phenylpropanol

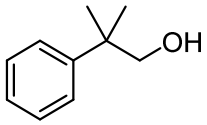

$C_{10}H_{14}O$ (150.22 g/mol)

***R*$_f$:** 0.30 (petroleum ether/diethyl ether 90:10)

m.p.: ambient temperature.

^{1}H-NMR (400 MHz, $CDCl_3$): δ_H/ppm= 7.42 – 7.32 (m, 4H, C$\underline{H}_{arom}$), 7.25 – 7.20 (m, 1H, C$\underline{H}_{arom}$), 3.62 (s, 2H, C$\underline{H}_2$OH), 1.35 (s, 6H, C$\underline{H}_3$), 1.34 (bs, 1H, O$\underline{H}$).

^{13}C-NMR (75 MHz, CDCl3): δ_C/ppm= 146.3, 128.5, 126.3, 126.2, 73.1, 40.1, 25.3.

GC-MS (EI): 150.1 (13, $[M^{+\bullet}]$), 132.1 (10, $[M^{+\bullet}]$-$[OH^{\bullet}]$), 119.1 (100, $[M^{+\bullet}]$-$[CH_2OH^{\bullet}]$), 103.1 (5, $[M^{+\bullet}]$-$[CH_2OH^{\bullet}]$-$[CH_3^{\bullet}]$), 91.1 (58, $[M^{+\bullet}]$-$[CH_2OH^{\bullet}]$-$[CH_3^{\bullet}]$-$[CH_3^{\bullet}]$).

The found analytical data were in accordance with the available literature data.[27]

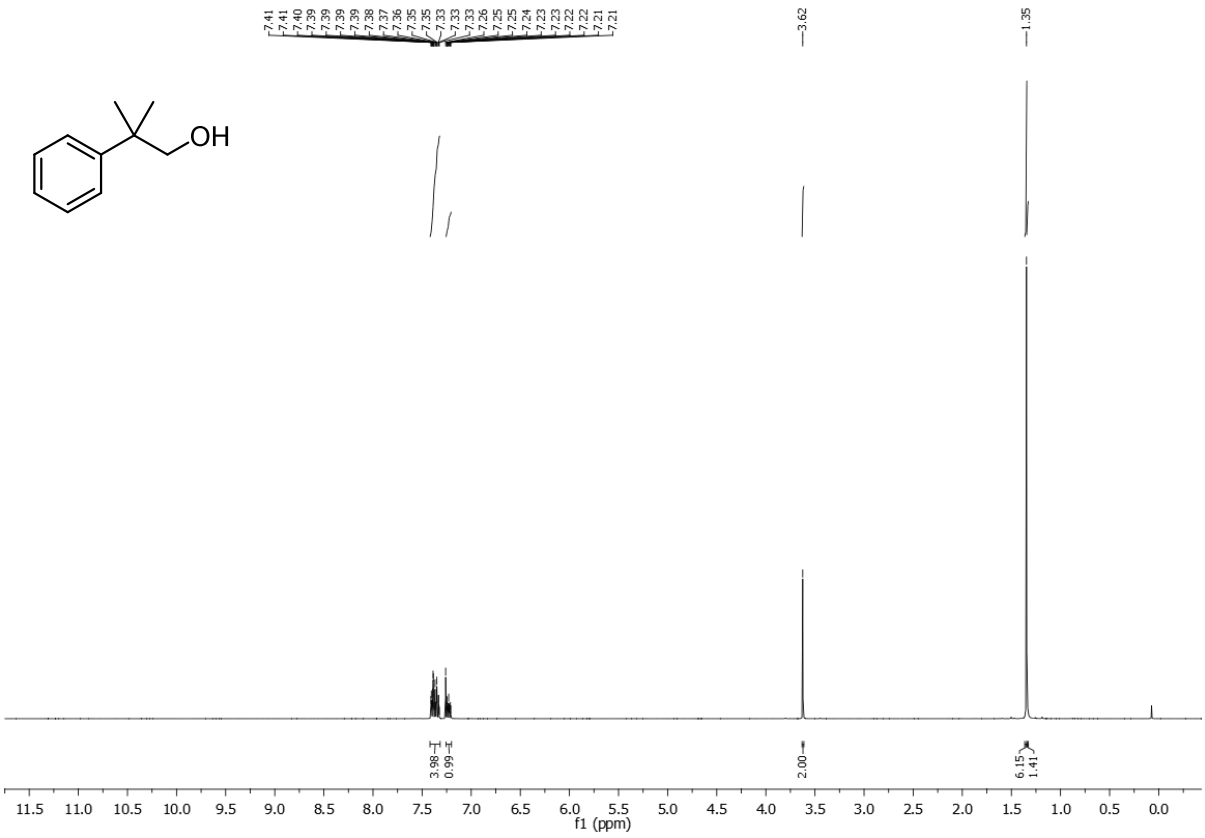
OH
7.41
7.41
7.40
7.39
7.39
7.39
7.39
7.38
7.37
7.36
7.35
7.35
7.33
7.33
7.33
7.26
7.25
7.25
7.24
7.23
7.23
7.22
7.22
7.21
7.21
3.62
1.35
3.98
0.99
2.00
6.15
1.41
f1 (ppm)

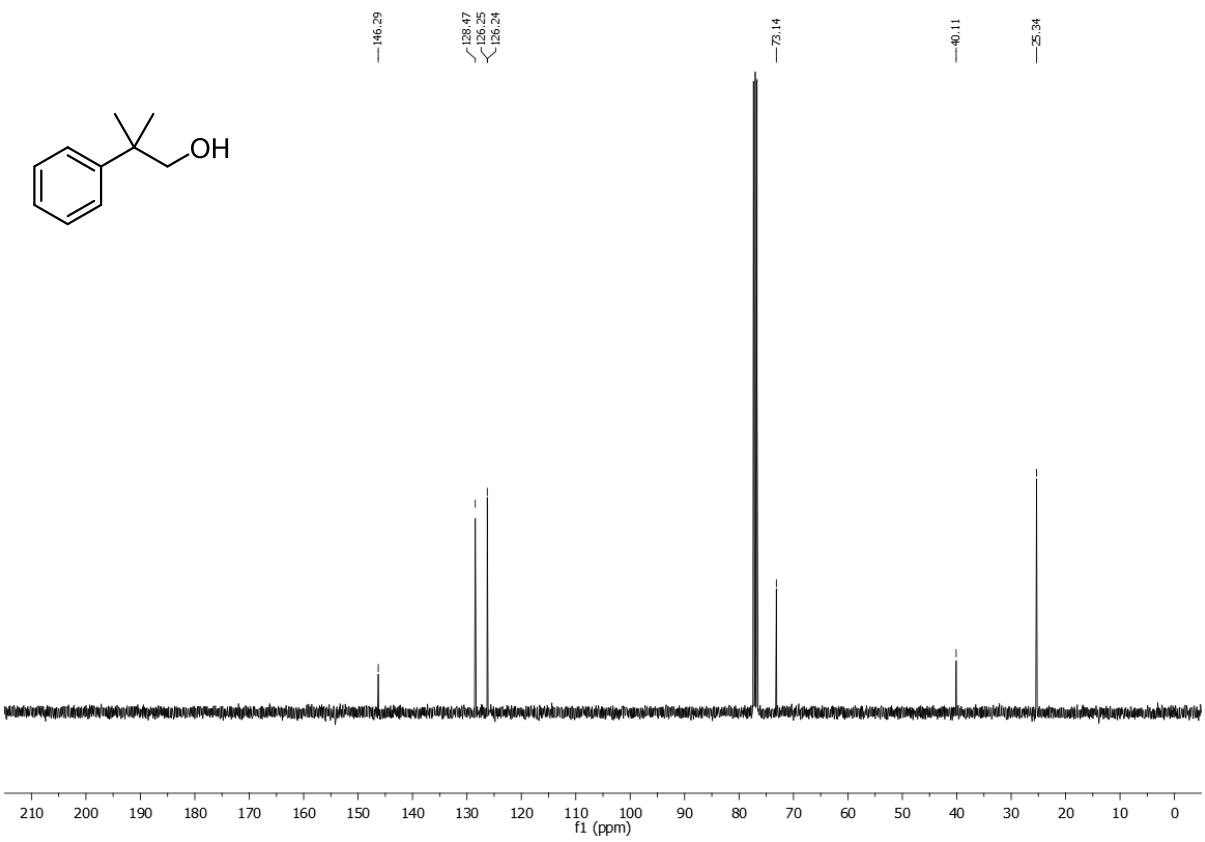
OH
146.29
128.47
126.25
126.24
73.14
40.11
25.34
f1 (ppm)

Procedure for the synthesis of 2-methyl-2-phenylpropyl acetate (26)

Following a literature procedure,[28] a solution of 2-methyl-2-phenylpropanol (3.1 mmol, 0.46 g, 1.0 equiv.) in pyridine (1.5 mL) was cooled to approximately 10 °C. Acetic anhydride (6.1 mmol, 0.58 mL, 2.0 equiv.) was added. The reaction mixture was kept at the given temperature and stirred until TLC control showed completion. Ethyl acetate (4 mL) and water (2 mL) were added to quench the reaction, after 30 minutes of stirring hydrochloric acid (10 mL, 3 M) was added. The organic layer was separated and washed with saturated aqueous Na_2CO_3 solution until a neutral *p*H was reached. The organic phase was dried over Na_2SO_4 und filtered. Evaporation of the solvent *in vacuo* afforded **26** as colorless oil (0.31 g, 53% yield).

2-methyl-2-phenylpropyl acetate (**26**)

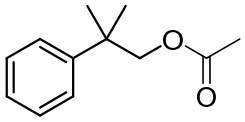

26

$C_{12}H_{16}O_2$ (192.26 g/mol)

***R*$_f$:** 0.39 (hexane/ethyl acetate 95:5)

m.p.: ambient temperature.

^{1}H-NMR (400 MHz, $CDCl_3$): δ_H/ppm= 7.32 – 7.22 (m, 4H, C$\underline{H}_{arom}$), 7.17 – 7.12 (m, 1H, C$\underline{H}_{arom}$), 4.06 (s, 2H, C$\underline{H}_2$O), 1.93 (s, 3H, C(O)C$\underline{H}_3$), 1.29 (s, 6H, C$\underline{H}_3$).

^{13}C-NMR (75 MHz, CDCl3): δ_C/ppm= 171.2, 146.2, 128.2, 126.2, 125.9, 73.0, 38.2, 25.9, 20.9.

GC-MS (EI): 192.1 (9, [$M^{+\bullet}$]), 132.1 (27, [$M^{+\bullet}$]-[AcO$^\bullet$]), 119.13 (100, [$M^{+\bullet}$]-[$AcOCH_2^\bullet$]), 103.1 (5, [$M^{+\bullet}$]-[$AcOCH_2^\bullet$]-[$CH_3^\bullet$]), 91.1 (43, [$M^{+\bullet}$]-[$AcOCH_2^\bullet$]-[$CH_3^\bullet$]-[$CH_3^\bullet$]).

The found analytical data were in accordance with the available literature data.[28]

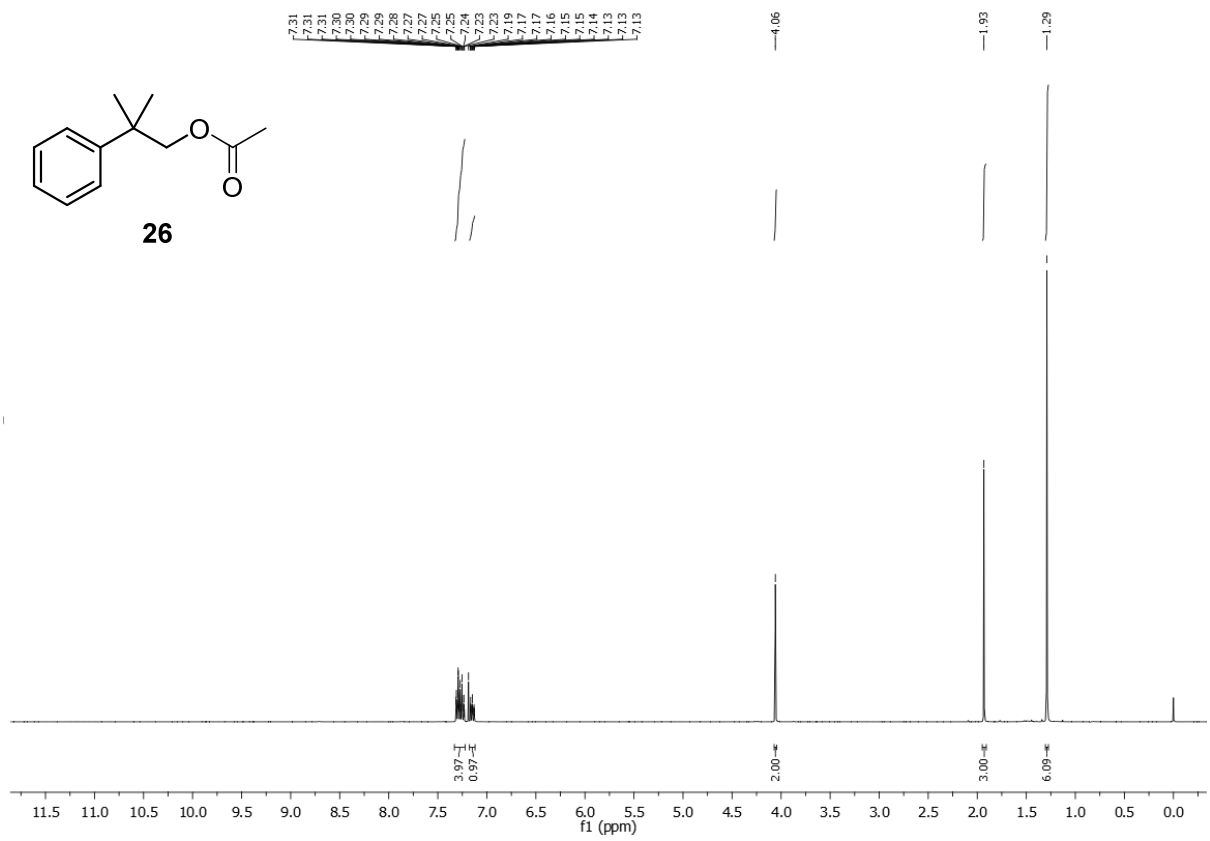
7.31
7.31
7.31
7.30
7.30
7.29
7.29
7.28
7.27
7.27
7.25
7.25
7.24
7.23
7.23
7.19
7.17
7.17
7.16
7.15
7.15
7.14
7.13
7.13
7.13
4.06
1.93
1.29
3.97
0.97
2.00
3.00
6.09
11.5 11.0 10.5 10.0 9.5 9.0 8.5 8.0 7.5 7.0 6.5 6.0 5.5 5.0 4.5 4.0 3.5 3.0 2.5 2.0 1.5 1.0 0.5 0.0
f1 (ppm)

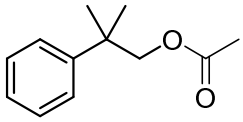

26

171.16
146.22
128.23
126.22
125.92
72.98
38.17
25.85
20.90
210 200 190 180 170 160 150 140 130 120 110 100 90 80 70 60 50 40 30 20 10 0
f1 (ppm)

26

6.7 Analytical data for products isolated from Pd-catalyzed transfer hydrogenolysis reactions

2-ethylnaphthalene (**35u**)

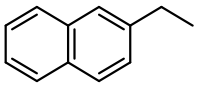

35u

Compound **35u** was isolated from the crude reaction mixture after evaporation of the solvent *via* kugelrohr distillation under reduced pressure as a colorless oil in 94% yield.

$C_{12}H_{12}$ (156.23 g/mol)

***R*$_f$:** 0.65 (cyclohexane/ethyl acetate 80:20).

m.p.: ambient temperature.

^{1}H-NMR (400 MHz, $CDCl_3$): δ_H/ppm= 7.86 – 7.78 (m, 3H, C$\underline{H}_{arom}$), 7.66 (bs, 1H, C$\underline{H}_{arom}$), 7.44 (m, 3H, C$\underline{H}_{arom}$), 2.85 (q, *J* = 7.6 Hz, 2H, C$\underline{H}_2$), 1.37 (t, *J* = 7.6 Hz, 3H, C$\underline{H}_3$).

^{13}C-NMR (101 MHz, $CDCl_3$):δ_C/ppm=141.8, 133.8, 132.0, 127.8, 127.6, 127.5, 127.1, 125.9, 125.6, 125.0, 29.1, 15.6.

GC-MS (EI): m/z = 156.1 (47, $[M^{+\bullet}]$), 141.1 (100, $[M^{+\bullet}]$-$[CH_3^{\bullet}]$), 128.1 (23, $[M^{+\bullet}]$-$[CH_2CH_3^{\bullet}]$), 115.1 (38, $[M^{+\bullet}]$-$[CCH_2CH_3^{\bullet}]$), 102.0 (6, $[M^{+\bullet}]$-$[CHCCH_2CH_3^{\bullet}]$).

The found analytical data were in accordance with the available literature data.[29]

1-ethylnaphthalene (**35t**)

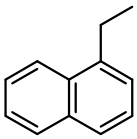

35t

Compound **35t** was isolated from the crude reaction mixture after evaporation of the solvent *via* kugelrohr distillation under reduced pressure as a colorless oil in 95% yield.

$C_{12}H_{12}$ (156.23 g/mol)

***R*$_f$:** 0.63 (cyclohexane/ethyl acetate 80:20).

m.p.: ambient temperature.

^{1}H-NMR (400 MHz, $CDCl_3$): δ_H/ppm = 8.08 (d, *J* = 8.3 Hz, 1H, C$\underline{H}_{arom}$), 7.89 – 7.85 (m, 1H, C$\underline{H}_{arom}$), 7.73 (d, *J* = 8.1 Hz, 1H, C$\underline{H}_{arom}$), 7.56 – 7.35 (m, 4H, C$\underline{H}_{arom}$), 3.14 (q, *J* = 7.5 Hz, 2H, C$\underline{H}_2$), 1.41 (t, *J* = 7.5 Hz, 3H, C$\underline{H}_3$).

^{13}C-NMR (75 MHz, $CDCl_3$): δ_C/ppm = 140.3, 133.9, 131.8, 128.8, 126.4, 125.7, 125.4, 124.9, 123.8, 25.9, 15.1.

GC-MS (EI): m/z = 156.1 (38, $[M^{+\bullet}]$), 141.1 (100, $[M^{+\bullet}]$-$[CH_3^{\bullet}]$), 128.1 (19, $[M^{+\bullet}]$-$[CH_2CH_3^{\bullet}]$).

The found analytical data were in accordance with the available literature data.[10]

triphenylmethane (**35α**)

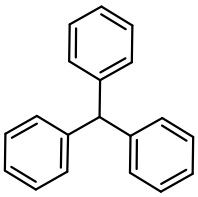

35α

Compound **35α** was isolated from the crude reaction mixture *via* column chromatography (petroleum ether 100%) as white crystals in quantitative yield.

$C_{19}H_{16}$ (244.34 g/mol)

***R*$_f$:** 0.60 (cyclohexane/ethyl acetate 80:20).

m.p.: 90.5 °C.

^{1}H-NMR (400 MHz, $CDCl_3$):δ_H/ppm = 7.32 – 7.25 (m, 6H, C<u>H</u>$_{arom}$), 7.25 – 7.18 (m, 3H, C<u>H</u>$_{arom}$), 7.12 (d, *J* = 7.4 Hz, 6H, C<u>H</u>$_{arom}$), 5.56 (s, 1H, C<u>H</u>).

^{13}C-NMR (75 MHz, $CDCl_3$): δ_C/ppm = 143.9, 129.5, 128.3, 126.3, 56.9.

GC-MS (EI): m/z = 244.2 (100, [$M^{+\bullet}$]), 167.1 (70, [$M^{+\bullet}$]-[$C_6H_5^{\bullet}$]).

The found analytical data were in accordance with the available literature data.[30]

4-ethyl-1,1'-biphenyl (**35l**)

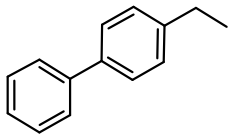

35l

Compound **35l** was isolated from the crude reaction mixture *via* column chromatography (petroleum ether 100%) as white crystals in 96% yield.

$C_{14}H_{14}$ (182.27 g/mol)

***R*$_f$:** 0.37 (petroleum ether).

m.p.: 45.4 °C.

^{1}H-NMR (400 MHz, $CDCl_3$):δ_H/ppm = 7.63 – 7.58 (m, 2H, C<u>H</u>$_{arom}$), 7.57 – 7.53 (m, 2H, C<u>H</u>$_{arom}$), 7.48 – 7.42 (m, 2H, C<u>H</u>$_{arom}$), 7.37 – 7.28 (m, 3H, C<u>H</u>$_{arom}$), 2.72 (q, *J* = 7.6 Hz, 2H, C<u>H</u>$_2$), 1.31 (t, *J* = 7.6 Hz, 3H, C<u>H</u>$_3$).

^{13}C-NMR (101 MHz, $CDCl_3$): δ_C/ppm = 143.4, 141.2, 138.7, 128.7, 128.3, 127.1, 127.0, 126.9, 28.6, 15.6.

GC-MS (EI): m/z = 182.2 (63, [$M^{+\bullet}$]), 167.2 (100, [$M^{+\bullet}$]-[$CH_3^\bullet$]), 153.1 (19, [$M^{+\bullet}$]-[$CH_2CH_3^\bullet$]).

The found analytical data were in accordance with the available literature data.[31]

6.8 NMR data for products isolated from deuterium-labelling experiments

The transfer hydrogenolysis of 1-(2-naphthyl)ethanol (**56**) was performed with different deuterated formic acid species following GP B (Scheme 6.1). The resultant 2-ethyl-naphthalenes **57a-d**, **57b-d** and **57c-d** were isolated and analyzed *via* ^{1}H- and ^{2}H-NMR spectroscopy.

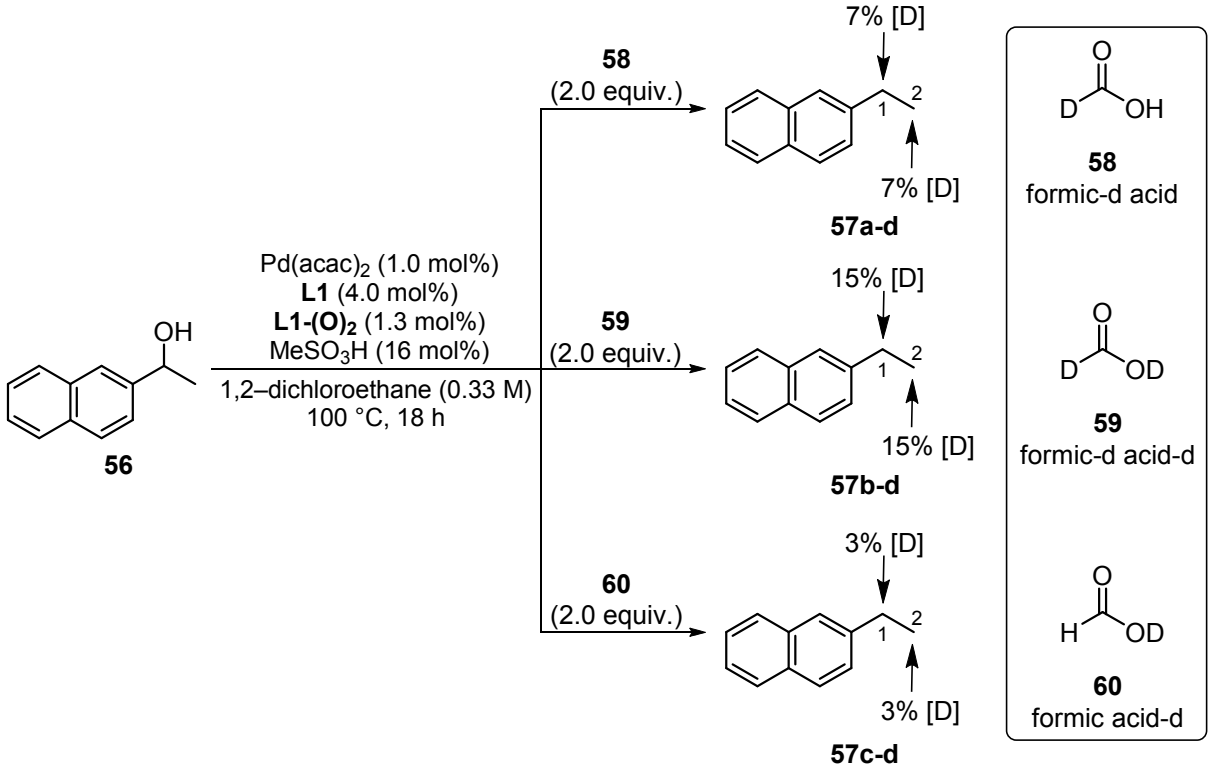

Scheme 6.1 **Isotope labelling experiments in the transfer hydrogenolysis of 1-(2-naphthyl)ethanol applying deuterated formic acid species (deuterium content determined *via* NMR analysis).**

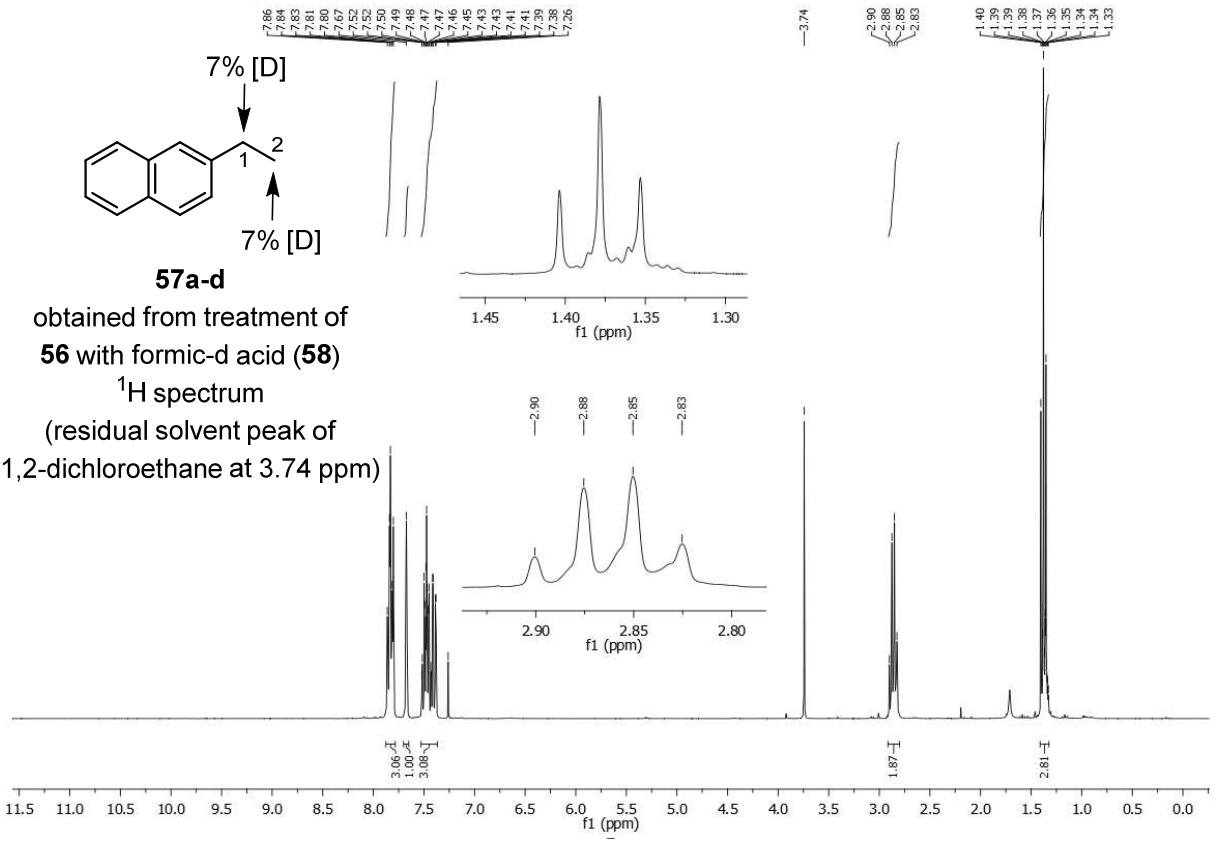

57a-d
obtained from treatment of
56 with formic-d acid (**58**)
^{1}H spectrum
(residual solvent peak of
1,2-dichloroethane at 3.74 ppm)

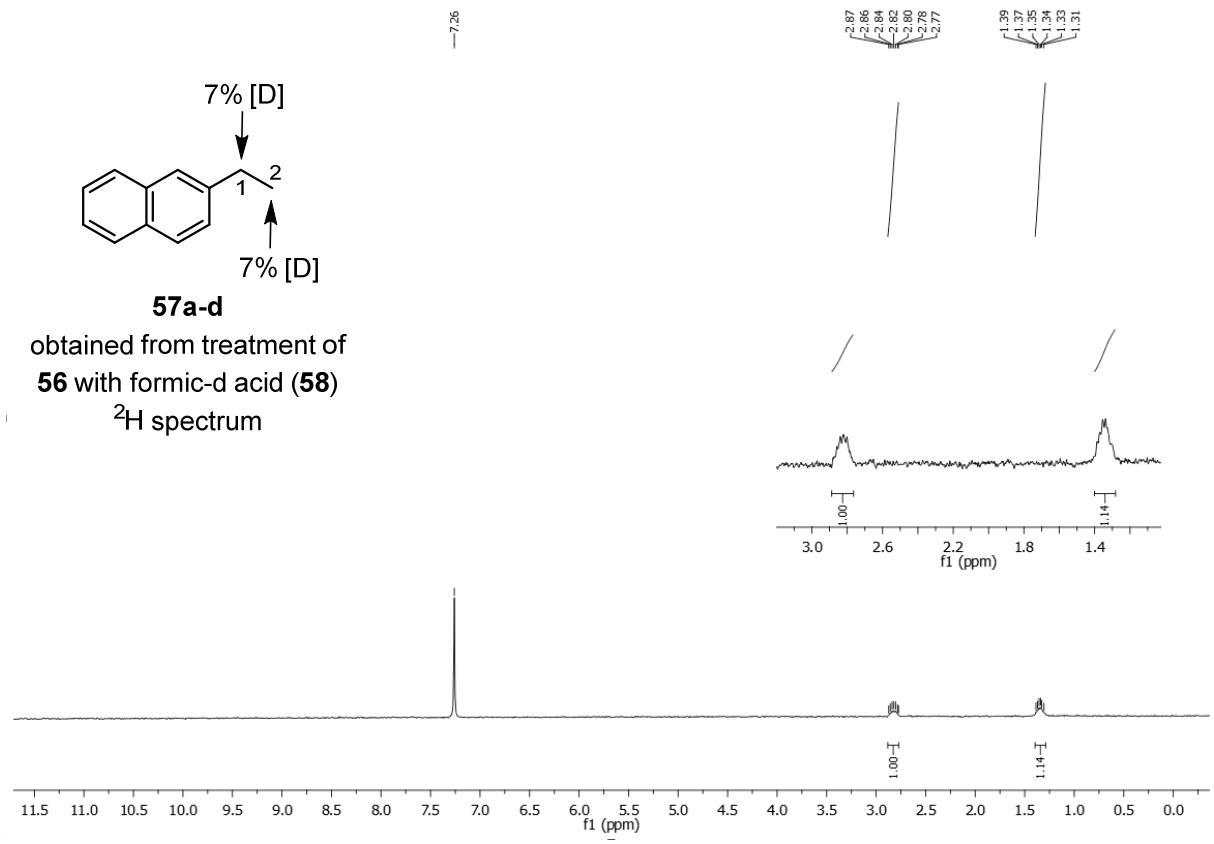

57a-d
obtained from treatment of
56 with formic-d acid (**58**)
^{2}H spectrum

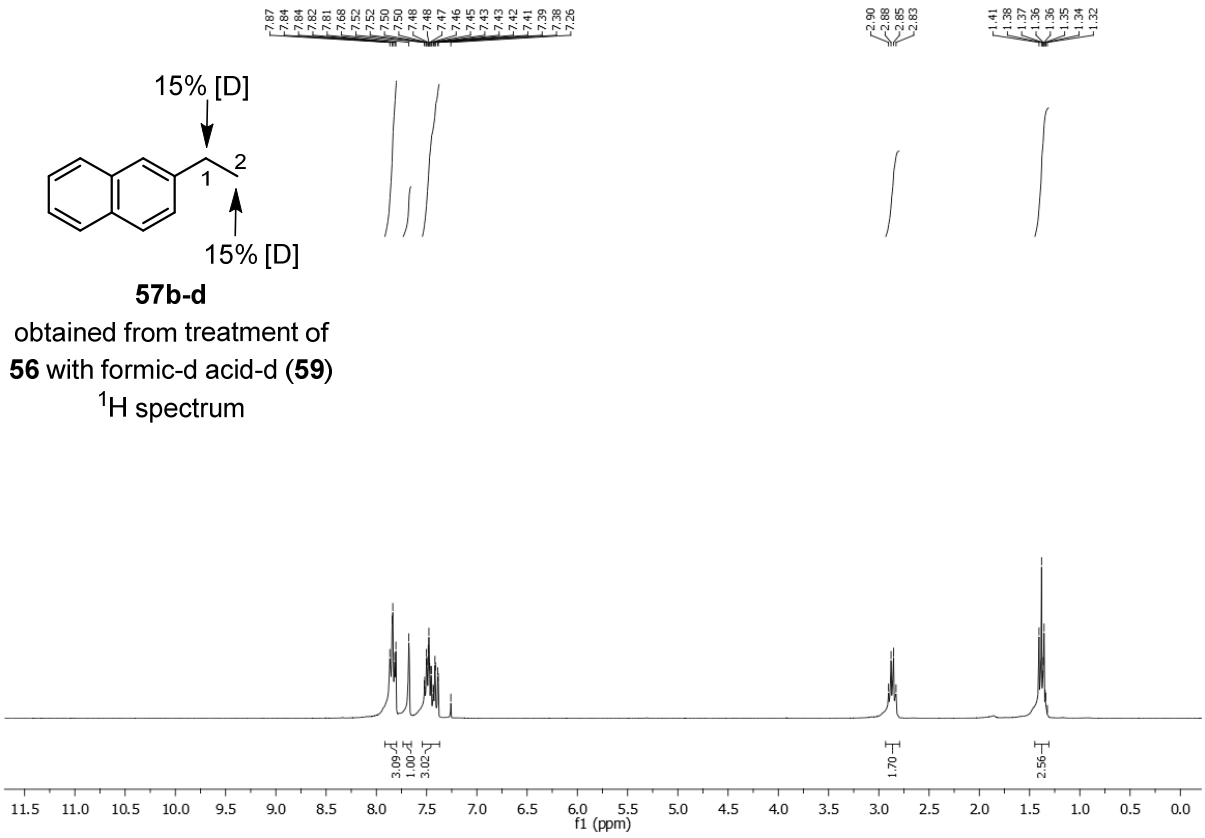

57b-d
obtained from treatment of
56 with formic-d acid-d (**59**)
^{1}H spectrum

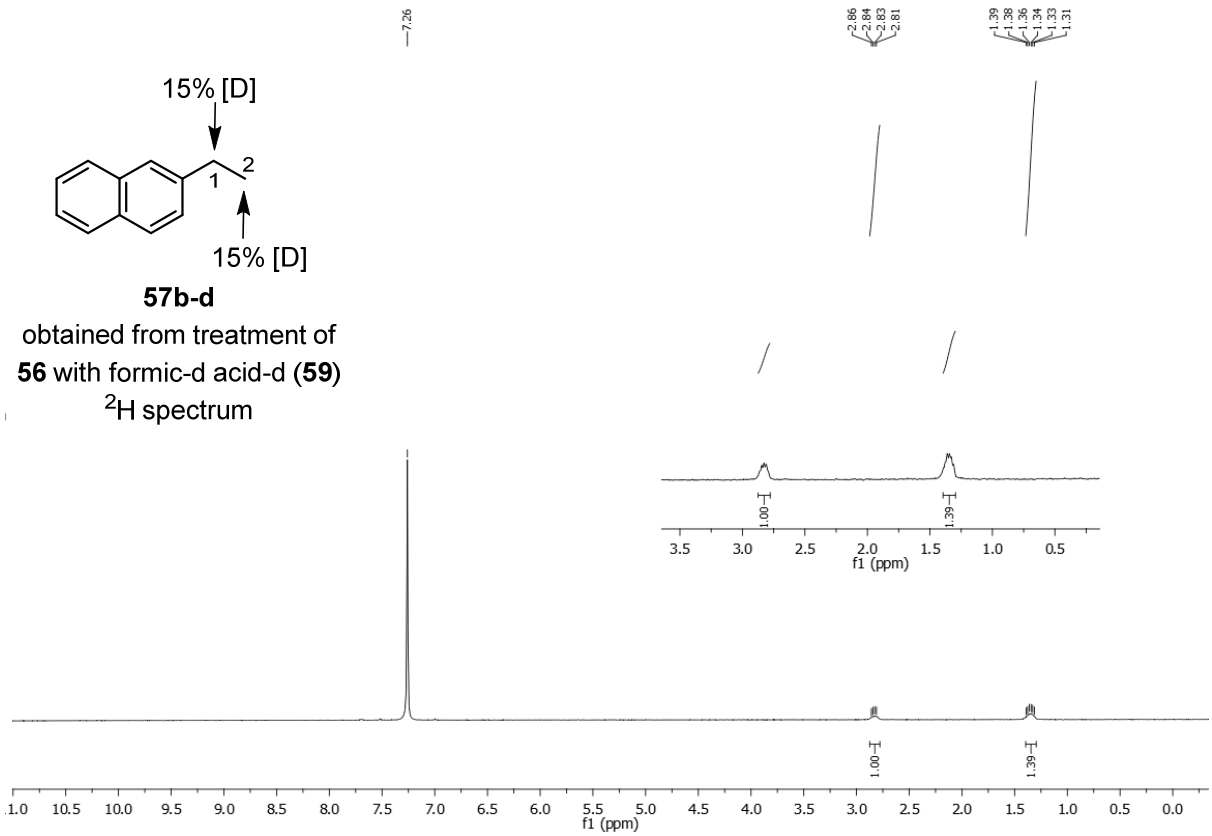

57b-d
obtained from treatment of
56 with formic-d acid-d (**59**)
^{2}H spectrum

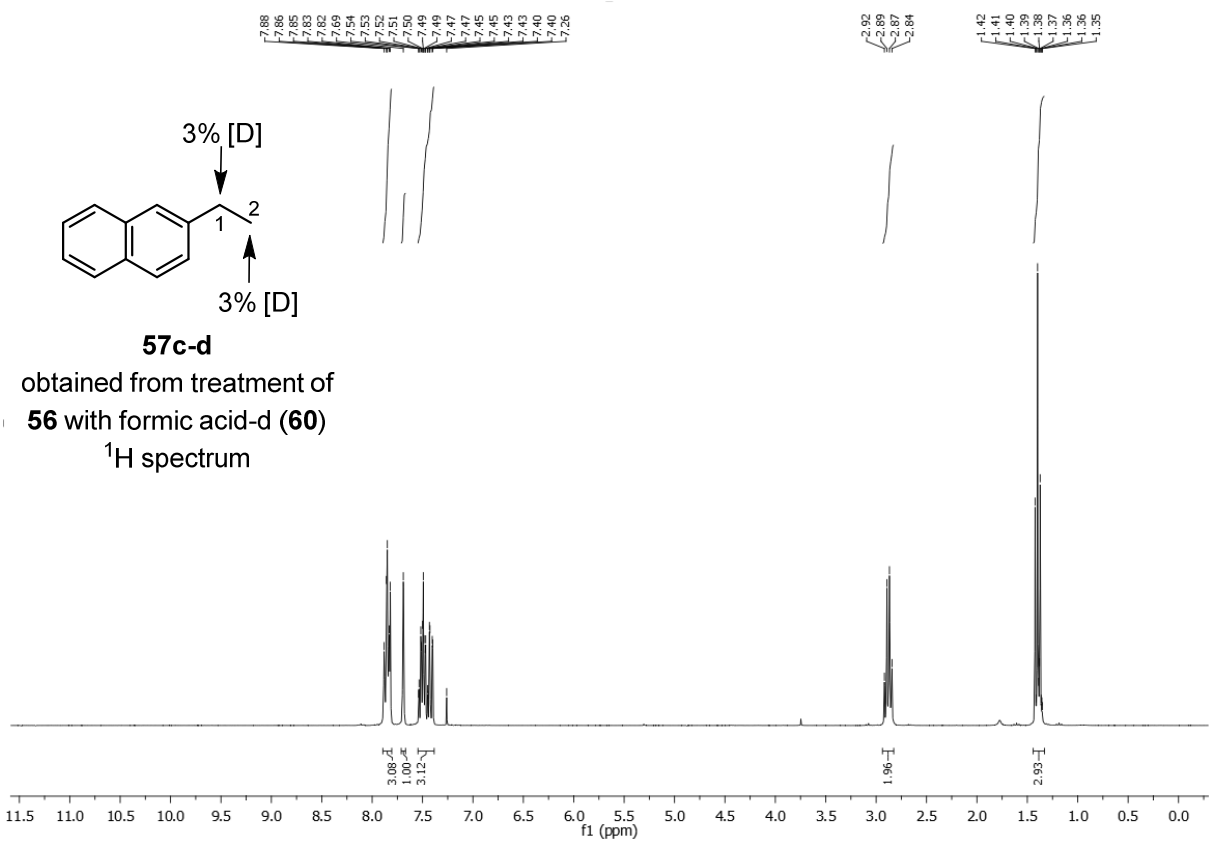
3% [D]
1
2
3% [D]
57c-d
obtained from treatment of
56 with formic acid-d (60)
1H spectrum
f1 (ppm)

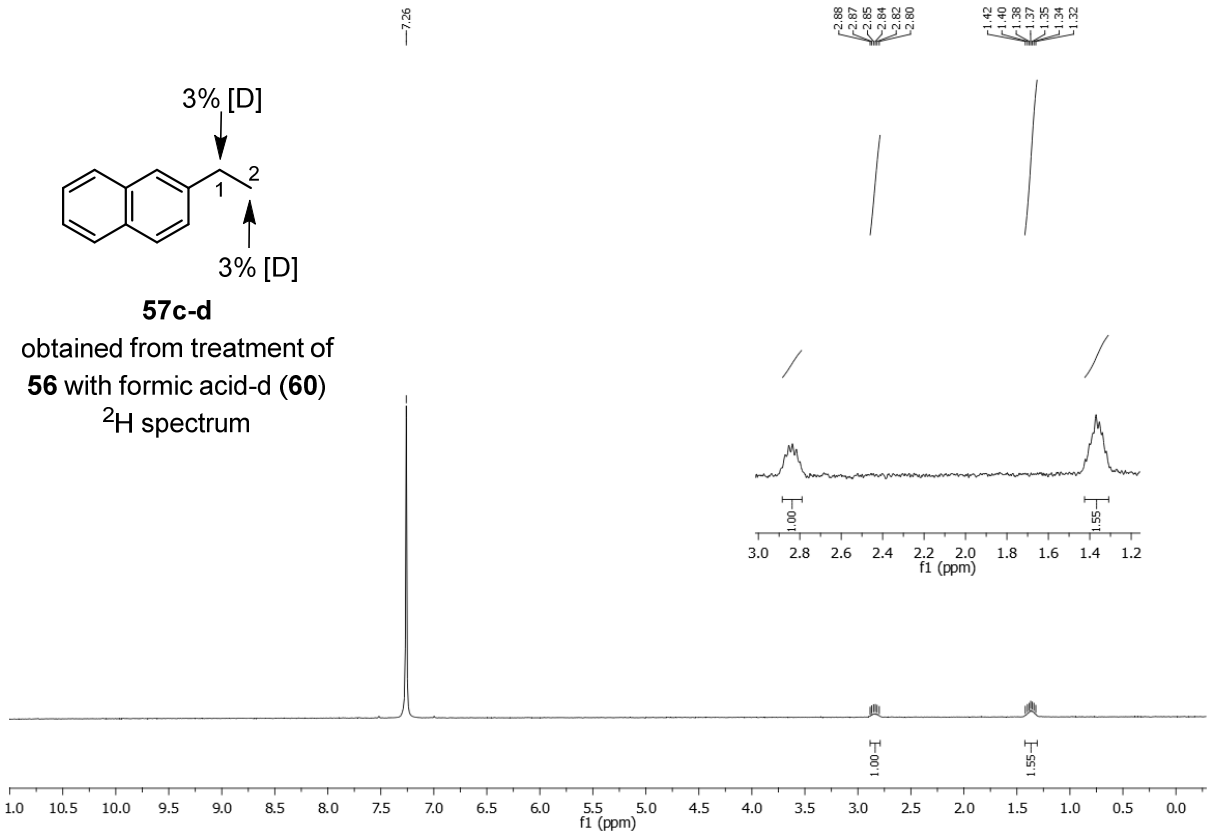
3% [D]
1
2
3% [D]
57c-d
obtained from treatment of
56 with formic acid-d (60)
2H spectrum
f1 (ppm)

To demonstrate a possible chain walking pathway of the palladium catalyst for the deuterium scrambling on the formed alkyl chains, 1-phenyl-1-propanol (**61**) was subjected to a transfer hydrogenolysis experiment applying formic-d acid-d (**59**) as reductant, following GP B (Scheme 6.2). The resultant propylbenzene (**62-d**) was isolated and analyzed *via* ^{1}H- and ^{2}H-NMR spectroscopy.

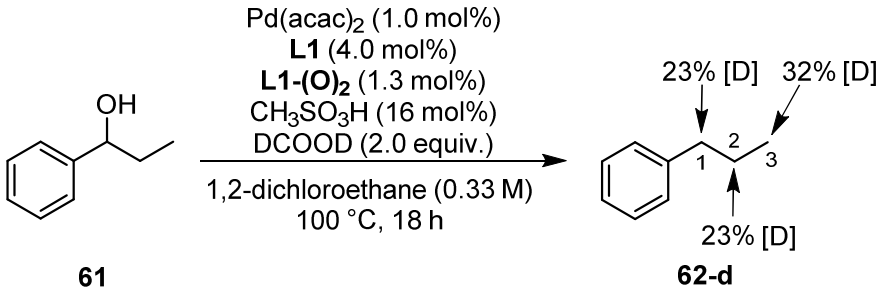

61 **62-d**

Scheme 6.2 **Isotope labelling experiments in the transfer hydrogenolysis of 1-phenylpropanol applying formic-d acid-d (deuterium content determined *via* NMR analysis).**

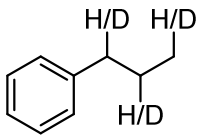

62-d
obtained from treatment of
61 with formic-d acid-d (**59**)
^{1}H spectrum
(residual solvent peak of
1,2-dichloroethane at 3.74 ppm)

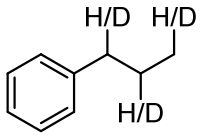

62-d
obtained from treatment of
61 with formic-d acid-d (**59**)
^{2}H spectrum
(residual solvent peak of
1,2-dichloroethane at 3.74 ppm)

In a competition experiment containing 1-(2-naphthyl)ethanol-d_3 (**56-d_3**) and 1-phenylethanol (**6**), the loss of deuterium from **56-d_3** as well as an intermolecular deuterium transfer to **6** was evaluated (Scheme 6.3). The resultant deoxygenated products **57d-d** and **7-d** were isolated and analyzed *via* ^{1}H-NMR spectroscopy.

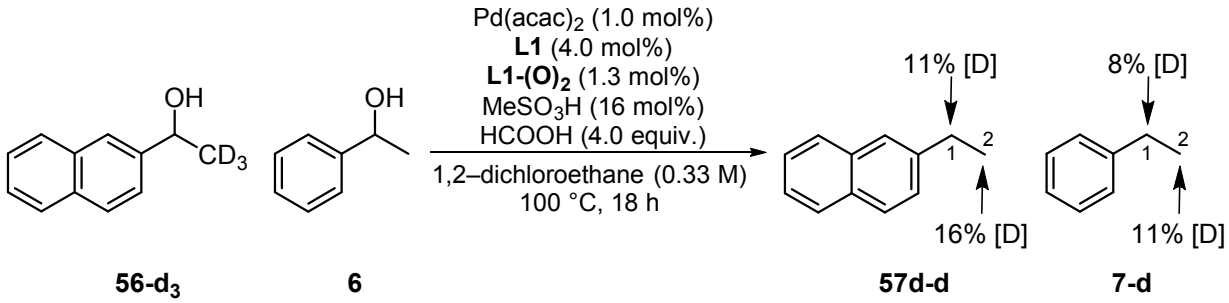

56-d_3 **6** **57d-d** **7-d**

Scheme 6.3 **Competition experiment for the transfer hydrogenolysis of 1-(2-naphthyl)ethanol-d_3 and 1-phenylethanol (deuterium content determined *via* NMR analysis).**

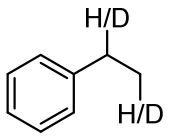

7-d
deuteration *via* D transfer
from **56-d$_3$**
^{1}H spectrum
(containing small amounts of **57d-d,**
residual solvent peak of
1,2-dichloroethane at 3.74 ppm)

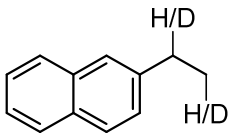

57d-d
loss of deuterium and
deuterium scrambling observed
^{1}H spectrum

6.9 Analytical data for products isolated from Pd-catalyzed reductive semipinacol-type rearrangement reactions

2-(1-naphthyl)ethyl acetate (**18**)

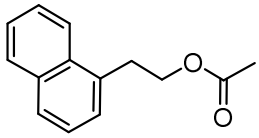

18

Compound **18** was isolated from the crude reaction mixture *via* column chromatography (hexane/ethyl acetate 9:1) as colorless oil in 92% yield.

$C_{14}H_{14}O_2$ (214.26 g/mol)

***R*$_f$:** 0.37 (hexane/ethyl acetate 9:1).

m.p.: ambient temperature.

^{1}H-NMR (400 MHz, $CDCl_3$):δ_H/ppm = 8.10 (d, *J* = 8.5 Hz, 1H, C$\underline{H}_{arom}$), 7.87 (dd, *J* = 8.3, 1.0 Hz, 1H, C$\underline{H}_{arom}$), 7.77 (d, *J* = 8.0 Hz, 1H, C$\underline{H}_{arom}$), 7.52 (dddd, *J* = 21.1, 8.0, 6.8, 1.3 Hz, 2H, C$\underline{H}_{arom}$), 7.45 – 7.35 (m, 2H, C$\underline{H}_{arom}$), 4.42 (t, *J* = 7.4 Hz, 2H, $CH_2C\underline{H}_2O$), 3.42 (t, *J* = 7.4 Hz, 2H, $C\underline{H}_2CH_2O$), 2.06 (s, 3H, $OC(O)C\underline{H}_3$).

^{13}C-NMR (101 MHz, $CDCl_3$): δ_C/ppm = 171.1, 133.9, 133.7, 132.1, 128.8, 127.5, 127.0, 126.2, 125.7, 125.5, 123.6, 64.5, 32.2, 21.0.

GC-MS (EI): m/z = 214.1 (5, $[M^{+\bullet}]$), 154.1 (100, $[M^{+\bullet}]$-$[CH_3C(O)O^{\bullet}]$), 141.1 (34, $[M^{+\bullet}]$-$[AcOCH_2^{\bullet}]$), 128.1 (6, $[M^{+\bullet}]$-$[AcOCH_2CH_2^{\bullet}]$), 115.1 (23, $[M^{+\bullet}]$-$[AcOCH_2CH_2C^{\bullet}]$).

The found analytical data were in accordance with the available literature data.[32]

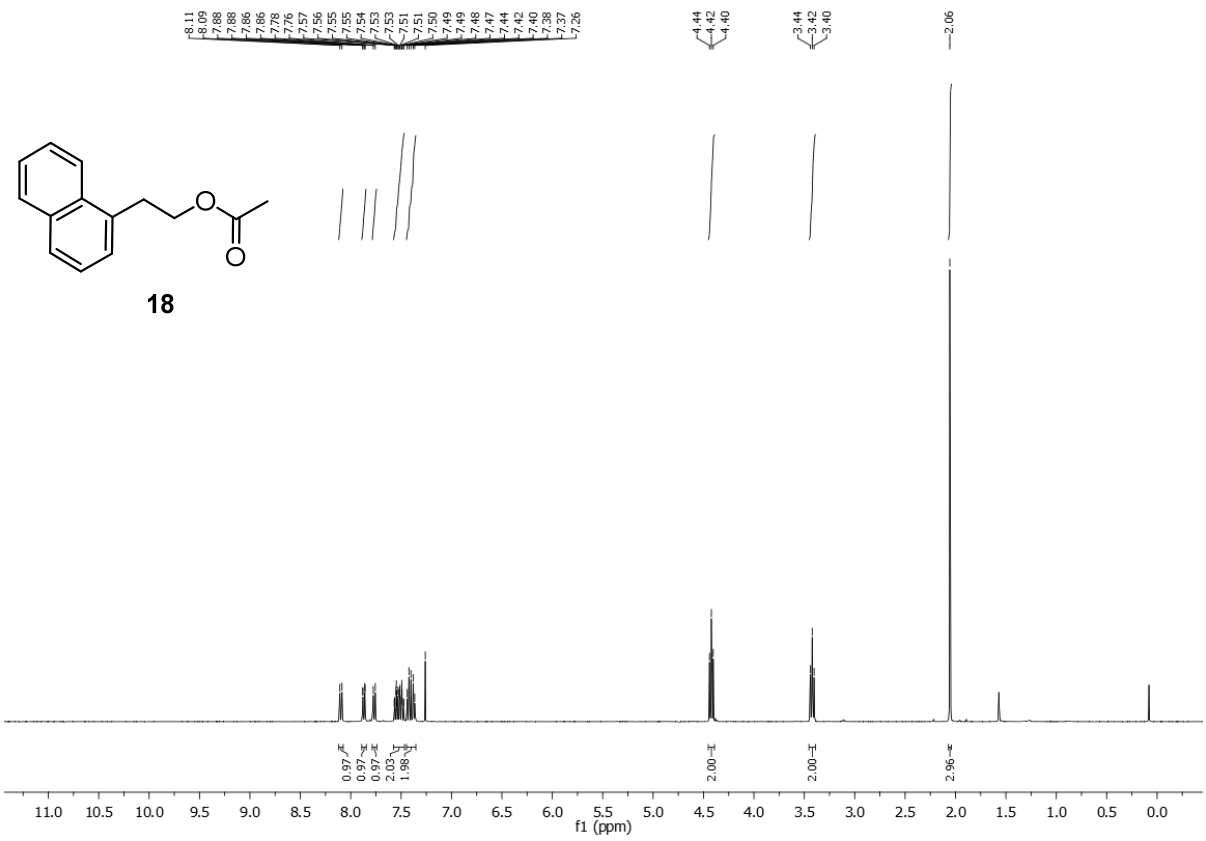
8.11
8.09
7.88
7.88
7.86
7.86
7.78
7.76
7.57
7.56
7.55
7.55
7.54
7.53
7.53
7.51
7.51
7.50
7.49
7.49
7.48
7.47
7.44
7.42
7.40
7.38
7.37
7.26
4.44
4.42
4.40
3.44
3.42
3.40
2.06
0.97
0.97
0.97
2.03
1.98
2.00
2.00
2.96
11.0 10.5 10.0 9.5 9.0 8.5 8.0 7.5 7.0 6.5 6.0 5.5 5.0 4.5 4.0 3.5 3.0 2.5 2.0 1.5 1.0 0.5 0.0
f1 (ppm)

18

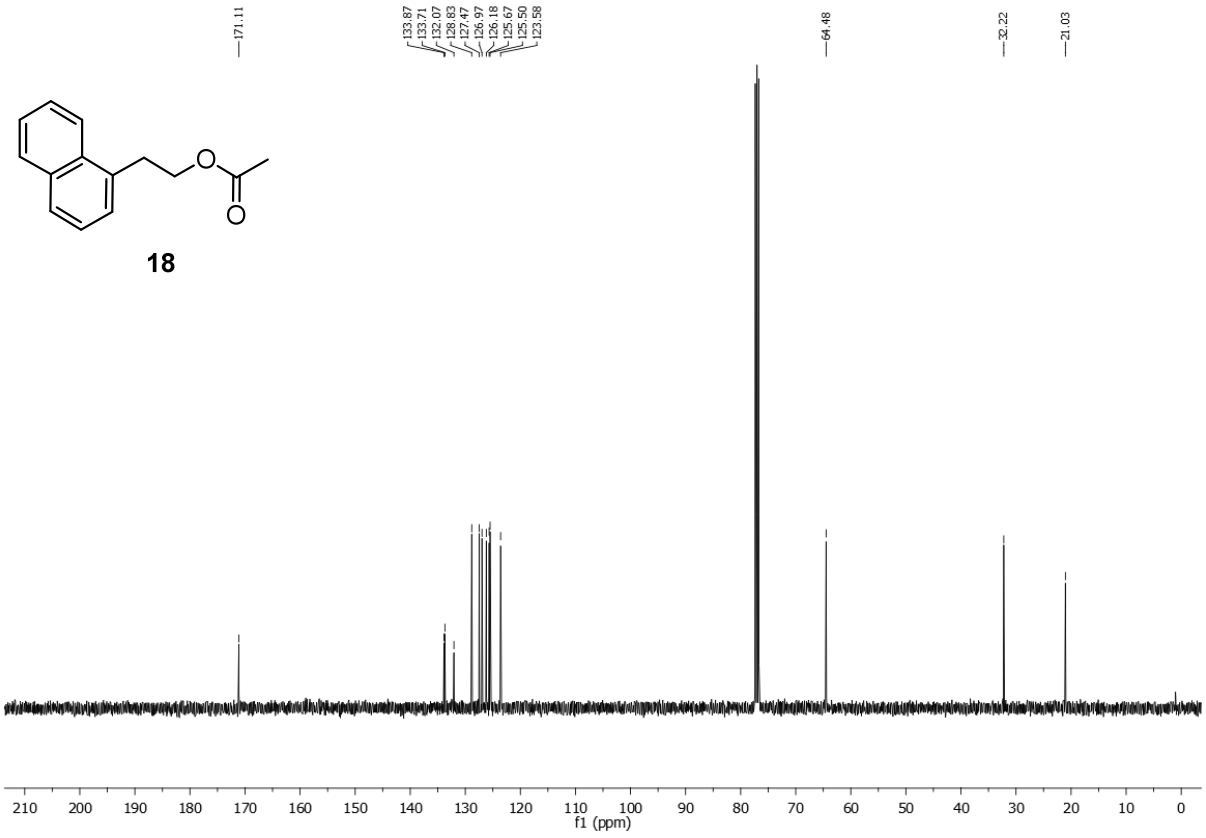
171.11
133.87
133.71
132.07
128.83
127.47
126.97
126.18
125.67
125.50
123.58
64.48
32.22
21.03
210 200 190 180 170 160 150 140 130 120 110 100 90 80 70 60 50 40 30 20 10 0
f1 (ppm)

18

2-(4-fluorophenyl)ethyl acetate (**20**)

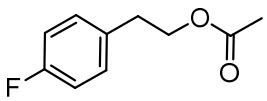

20

Compound **20** was isolated from the crude reaction mixture *via* column chromatography (hexane/ethyl acetate 93:7) as orange oil in 62% yield.

$C_{10}H_{11}FO_2$ (182.19 g/mol)

***R*$_f$:** 0.38 (hexane/ethyl acetate 93:7).

m.p.: ambient temperature.

^{1}H-NMR (400 MHz, $CDCl_3$): δ_H/ppm = 7.21 – 7.14 (m, 2H, C$\underline{H}_{arom}$), 7.02 – 6.95 (m, 2H, C$\underline{H}_{arom}$), 4.25 (t, *J* = 7.0 Hz, 2H, $CH_2C\underline{H}_2O$), 2.91 (t, *J* = 7.0 Hz, 2H, $C\underline{H}_2CH_2O$), 2.03 (s, 3H, $OC(O)C\underline{H}_3$).

^{13}C-NMR (101 MHz, $CDCl_3$): δ_C/ppm = 170.98, 161.72 (d, *J* = 244.5 Hz), 133.49 (d, *J* = 3.3 Hz), 130.30 (d, *J* = 7.9 Hz), 115.31 (d, *J* = 21.2 Hz), 64.83, 34.29, 20.94.

^{19}F-NMR (376 MHz, $CDCl_3$): δ_F/ppm = -116.6.

GC-MS (EI): m/z = 181.1 (1, [$M^{+\bullet}$]), 163.1 (2, [$M^{+\bullet}$]-[$F^{\bullet}$]), 139.1 (2, [$M^{+\bullet}$]-[$H_3CC(O)^{\bullet}$]), 123.2 (100, [$M^{+\bullet}$]-[$AcO^{\bullet}$]), 109.1 (24, [$M^{+\bullet}$]-[$AcOCH_2^{\bullet}$]), 96.1 (5, [$M^{+\bullet}$]-[$AcOCH_2CH_2^{\bullet}$]).

Although the compound is literature-known[33] and commercially accessible, no analytical data was available so far.

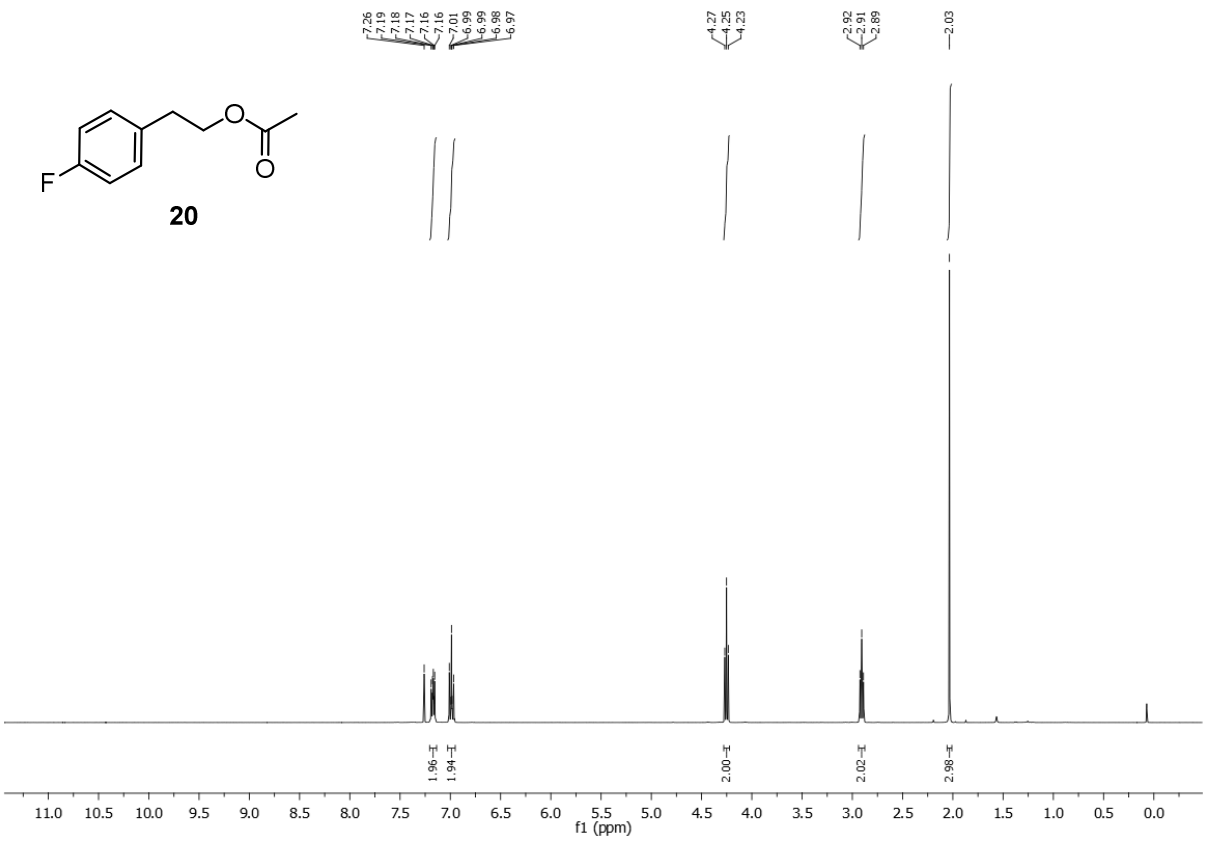
7.26
7.19
7.18
7.17
7.16
7.16
7.01
6.99
6.99
6.98
6.97
4.27
4.25
4.23
2.92
2.91
2.89
2.03
F
O
O
20
1.96
1.94
2.00
2.02
2.98
11.0 10.5 10.0 9.5 9.0 8.5 8.0 7.5 7.0 6.5 6.0 5.5 5.0 4.5 4.0 3.5 3.0 2.5 2.0 1.5 1.0 0.5 0.0
f1 (ppm)

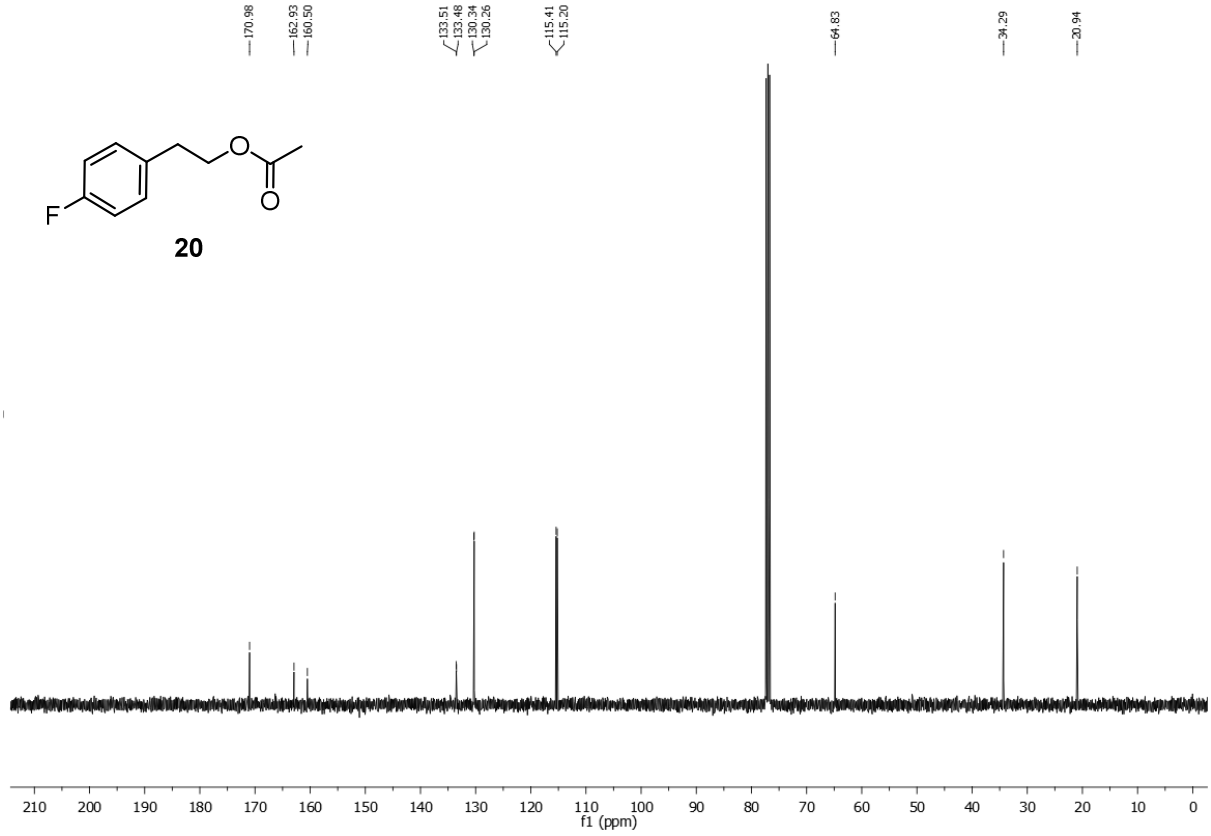
170.98
162.93
160.50
133.51
133.48
130.34
130.26
115.41
115.20
64.83
34.29
20.94
F
O
O
20
210 200 190 180 170 160 150 140 130 120 110 100 90 80 70 60 50 40 30 20 10 0
f1 (ppm)

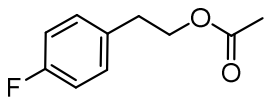

20

6.10 References

[1] J. Leonard, B. Lygo, G. Procter, *Advanced Practical Organic Chemistry*, CRC Press, **2013**.

[2] V. Goldbach, L. Falivene, L. Caporaso, L. Cavallo, S. Mecking, *ACS Catal.* **2016**, *6*, 8229-8238.

[3] R. Dyapa, L. T. Dockery, M. A. Walczak, *Org. & Biomol. Chem.* **2017**, *15*, 51-55.

[4] R. Soni, T. H. Hall, B. P. Mitchell, M. R. Owen, M. Wills, *J. Org. Chem.* **2015**, *80*, 6784-6793.

[5] T. D. Nixon, M. K. Whittlesey, J. M. J. Williams, *Tetrahedron Lett.* **2011**, *52*, 6652-6654.

[6] M. L. Clarke, M. B. Díaz-Valenzuela, A. M. Z. Slawin, *Organometallics* **2007**, *26*, 16-19.

[7] S. Enthaler, R. Jackstell, B. Hagemann, K. Junge, G. Erre, M. Beller, *J. Organomet. Chem.* **2006**, *691*, 4652-4659.

[8] T. Saito, Y. Nishimoto, M. Yasuda, A. Baba, *J. Org. Chem.* **2006**, *71*, 8516-8522.

[9] B. Martín-Matute, M. Edin, K. Bogár, F. B. Kaynak, J.-E. Bäckvall, *J. Am. Chem. Soc.* **2005**, *127*, 8817-8825.

[10] R. J. Rahaim, R. E. Maleczka, *Org. Lett.* **2011**, *13*, 584-587.

[11] V. Gauchot, W. Kroutil, A. R. Schmitzer, *Chem. Eur. J.* **2010**, *16*, 6748-6751.

[12] L. C. M. Castro, D. Bézier, J.-B. Sortais, C. Darcel, *Adv. Synth. Catal.* **2011**, *353*, 1279-1284.

[13] S. Liu, C. Wolf, *Org. Lett.* **2007**, *9*, 2965-2968.

[14] T. Itoh, Y. Matsushita, Y. Abe, S.-H. Han, S. Wada, S. Hayase, M. Kawatsura, S. Takai, M. Morimoto, Y. Hirose, *Chem. Eur. J.* **2006**, *12*, 9228-9237.
[15] C. Bosset, P. Angibaud, I. Stanfield, L. Meerpoel, D. Berthelot, A. Guérinot, J. Cossy, *J. Org. Chem.* **2015**, *80*, 12509-12525.
[16] A. Zvagulis, S. Bonollo, D. Lanari, F. Pizzo, L. Vaccaro, *Adv. Synth. Catal.* **2010**, *352*, 2489-2496.
[17] N. Luo, M. Wang, H. Li, J. Zhang, T. Hou, H. Chen, X. Zhang, J. Lu, F. Wang, *ACS Catal.* **2017**, *7*, 4571-4580.
[18] A.-L. Barthelemy, B. Tuccio, E. Magnier, G. Dagousset, *Angew. Chem. Int. Ed.* **2018**, *57*, 13790-13794.
[19] H. Luo, L. Wang, G. Li, S. Shang, Y. Lv, J. Niu, S. Gao, *ACS Sustain. Chem. Eng.* **2018**, *6*, 14188-14196.
[20] Y. M. Báez-Santos, S. J. Barraza, M. W. Wilson, M. P. Agius, A. M. Mielech, N. M. Davis, S. C. Baker, S. D. Larsen, A. D. Mesecar, *J. Med. Chem.* **2014**, *57*, 2393-2412.
[21] M. V. Galkin, S. Sawadjoon, V. Rohde, M. Dawange, J. S. M. Samec, *ChemCatChem* **2014**, *6*, 179-184.
[22] I. Kazuhiro, F. Kentarou, M. Teruaki, *Chem. Lett.* **2006**, *35*, 612-613.
[23] G. Sumrell, *J. Org. Chem.* **1954**, *19*, 817-819.
[24] H. Yu, Y. Xu, Y. Fang, R. Dong, *Eur. J. Org. Chem.* **2016**, *2016*, 5257-5262.
[25] T. C. Johnson, G. J. Clarkson, M. Wills, *Organometallics* **2011**, *30*, 1859-1868.
[26] M. Zhan, T. Zhang, H. Huang, Y. Xie, Y. Chen, *J. Label. Compd. Rad.* **2014**, *57*, 533-539.
[27] C. B. Kelly, K. M. Lambert, M. A. Mercadante, J. M. Ovian, W. F. Bailey, N. E. Leadbeater, *Angew. Chem. Int. Ed.* **2015**, *54*, 4241-4245.
[28] Z. Yu, W. Wang, L. Chen, *J. Label. Compd. Rad.* **2011**, *54*, 352-356.
[29] M. E. Sloan, A. Staubitz, K. Lee, I. Manners, *Eur. J. Org. Chem.* **2011**, *2011*, 672-675.
[30] J. J. Eisch, S. Dutta, *Organometallics* **2005**, *24*, 3355-3358.
[31] B. Karimi, D. Elhamifar, J. H. Clark, A. J. Hunt, *Chem. Eur. J.* **2010**, *16*, 8047-8053.
[32] V. H. Jadhav, J.-Y. Kim, D. Y. Chi, S. Lee, D. W. Kim, *Tetrahedron* **2014**, *70*, 533-542.
[33] S. de Burgh Norfolk, R. Taylor, *J. Chem. Soc., Perkin Trans. 2* **1976**, 280-285.

7 Appendix

7.1 List of abbreviations

Ac	acetyl	**m.p.**	melting point
acac	acetylacetonate	***m/z***	mass to charge ratio
aq	aqueous	**MS**	mass selective detector
Ar	aryl	**MsOH**	methanesulfonic acid
BINOL	1,1'-bi-2-naphthol	**NHC**	*N*–heterocyclic carbene
BTX	benzene, toluene, xylene	**NMR**	nuclear magnetic resonance
cat.	catalytic	**NP**	nanoparticle
COD	cyclooctadiene	**PMHS**	polymethylhydrosiloxane
conc.	concentration	**PMP**	*para*-methoxyphenyl
Cp*	pentamethylcyclopentadienyl	**R_f**	retention factor
CV	column volume	**TEM**	transmission electron microscopy
dba	dibenzylideneacetone	**TfOH**	trifluoromethanesulfonic acid
dct	dibenzo[*a,e*]cyclooctatetraene	**THF**	tetrahydrofurane
DDQ	2,3-dichloro-5,6-dicyano-1,4-benzoquinone	**TLC**	thin layer chromatography
DFT	density functional theory	**TOF**	turnover frequency
DMSO	dimethylsulfoxide	**TsOH**	*para*-toluenesulfonic acid
dtbpx	α,α'-bis(di-*tert*-butylphosphino)-*ortho*-xylene	***w/w***	mass fraction
equiv.	equivalents	**XAFS**	X-ray absorption fine structure
FID	flame ionization detector	**XANES**	X-ray absorption near edge structure
GC	gas chromatography	**xantphos**	4,5-bis(diphenylphosphino)-9,9-dimethylxanthene
H_2-TPR	hydrogen temperature programmed reduction	**XPS**	X-ray photoelectron spectroscopy
M	molar	**XRD**	X-ray diffraction

7.2 Acknowledgements

Als erstes möchte ich Frau Prof. Dr. Ivana Fleischer für die Gelegenheit danken, in ihrer Arbeitsgruppe ein solch spannendes, aber auch forderndes Thema zu bearbeiten. Die fachlichen Diskussionen waren nicht nur lehrreich, sondern führten oftmals auch zu neuen Ideen, um die jeweiligen Projekte voranzutreiben. Die mir dabei eingeräumte Freiheit, diese dann selbstständig weiter zu entwickeln, kam meiner Arbeit sehr zugute.

Weiter möchte ich Frau Prof. Dr. Doris Kunz für die Erstellung des Zweitgutachtens danken. Ebenso gilt mein Dank Frau Prof. Dr. Olga García Mancheño für ihre Teilnahme als Drittprüferin an meiner Promotionsprüfung und Herrn Prof. Dr. Bernd Speiser für die Übernahme des Vorsitzes der Prüfungskommission.

Ebenso bin ich der Deutschen Bundesstiftung Umwelt zum Dank verpflichtet, welche durch die Vergabe ihres Promotionsstipendiums an mich diese Dissertation erst ermöglicht hat. Neben der finanziellen Unterstützung sind hierbei auch die Stipendiatenseminare der DBU hervorzuheben, durch welche ich nicht nur Kontakte in andere Fachbereiche knüpfen durfte, sondern auch erfahren habe, wie wichtig ein Blick in andere Forschungsgebiete sowie die Fähigkeit, die eigene Tätigkeit fachfremden Wissenschaftlern zu vermitteln, sind.

Ein großer Dank gilt natürlich auch meinen ehemaligen und derzeitigen Kollegen am Arbeitskreis Fleischer für die gute Zusammenarbeit im allgemeinen Laborbetrieb und die allgemein freundliche Arbeitsatmosphäre, aber auch für die kurzweiligen Unternehmungen außerhalb des Labors: Paul Gehrtz, der stets zu inspirierendem fachlichen Austausch bereit war, sich aber auch auf fachfremde Diskussionen einließ und es dabei verstand, stets das preußisch-bayerische Gleichgewicht im Labor zu erhalten. Samuel Quintero-Duque, der für mich vor allem während meiner Masterarbeit eine große Hilfe bei der Einarbeitung in die Autoklavenchemie und den Umgang mit Druckgasen war. Sein von verschiedenen Kulturen gefärbter Humor und unser gutes Verhältnis auch nach seinem Ausscheiden aus dem Arbeitskreis lassen mich ihn besonders schätzen. Prasad Kathe danke ich für den mir gegebenen Einblick in die indische Kultur und die daraus stammenden Süßwaren sowie die stets angenehme Stimmung in unserer geteilten Laborzeile. Hier sind außerdem die gemeinsamen lauten Heavy-Metal-Abende zu später Stunde im Labor zu nennen. Valentin Geiger und Regina Oechsner als unsere Tübinger Nachwuchskräfte haben mich daran erinnert, dass es eine gewisse Euphorie braucht, um in der chemischen Forschung tätig zu sein, auch wenn diese mit der Zeit und durch unvermeidliche Rückschläge abnimmt. Eigene Erfahrungen an die "jüngere Generation" von Doktoranden und Masteranden weitergeben zu können, hat mich dabei besonders erfreut. Nicht zuletzt danke ich Tanno Schmidt, der im Rahmen seiner Masterarbeit mein letztes Projekt weiterführt und zu einem guten Ende

bringen wird. Es macht mich stolz zu sehen, dass von mir eröffnete Arbeitsfelder weiterhin beschritten werden und so hoffentlich zu neuen Projekten und Erkenntnissen führen.

Ich danke auch den Forschungspraktikanten und Bacheloranden Ulrike Wirth, Tobias Babl, Marvin Sindlinger, Regina Oechsner und Robin Scholl, die mich in Regensburg und Tübingen bei meinen Forschungsarbeiten unterstützt haben. Auch dem Arbeitskreis Jacobi von Wangelin sei gedankt für das gemeinsame Arbeitsgruppenseminar in Regensburg, den dringend benötigten Zugang zur instrumentellen Analytik sowie auch für die gemeinsamen Abende, etwa beim Grillen oder den Weihnachtsfeiern.

Auch die im Hintergrund arbeitenden Akteure seien hier erwähnt: Mein Dank geht an die Glasbläser sowie die Mitarbeiter der mechanischen Werkstätten und der zentralen Analytik-Abteilungen an den Universitäten Regensburg und Tübingen. Von mir benötigte Hilfe wurde stets bestmöglich geleistet, auch in Tübingen trotz meiner mangelnden Schwäbisch-Kenntnisse. Weiterhin danke ich Dr. Thomas Wendel vom Zentrum für angewandte Geowissenschaften für seine Unterstützung bei den Headspace-GC-Messungen.

Besonderer Dank gilt meinen Eltern, ohne deren Unterstützung mein Studium und die Promotion nicht so reibungslos hätten verlaufen können.

Abschließend möchte ich mich bei meiner Partnerin Dijana für ihr offenes Ohr, ihren Rückhalt und ihr Verständnis, gerade in der zweiten Hälfte der Promotion, bedanken. Sie hat mir nicht nur oftmals gute Ratschläge erteilt, sondern mir auch das Gefühl vermittelt, dass sich auch Menschen außerhalb des Labors für meine Arbeit interessieren.